SORPTION KINETICS OF HYDROPHOBIC ORGANIC COMPOUNDS ONTO ORGANIC MODIFIED SURFACES

by
James Edward Szecsödy

A Dissertation Submitted to the Faculty of the
DEPARTMENT OF HYDROLOGY AND WATER RESOURCES

In Partial Fulfillment of the Requirements
For the Degree of

DOCTOR OF PHILOSOPHY
WITH A MAJOR IN HYDROLOGY

In the Graduate College

THE UNIVERSITY OF ARIZONA

1 9 8 8

THE UNIVERSITY OF ARIZONA
GRADUATE COLLEGE

As members of the Final Examination Committee, we certify that we have read the dissertation prepared by James Edward Szecsody

entitled Sorption Kinetics of Hydrophobic Organic Compounds onto Organic modified Surfaces

and recommend that it be accepted as fulfilling the dissertation requirement for the Degree of Doctor of Philosophy.

Roger C. Bales	10/13/88 Date
Stanley N. Davis	10/13/88 Date
Daniel D. Evans	10/13/88 Date
Hinrich L. Bohn	10/13/88 Date
Arthur W. Warrick	10/13/88 Date

Final approval and acceptance of this dissertation is contingent upon the candidate's submission of the final copy of the dissertation to the Graduate College.

I hereby certify that I have read this dissertation prepared under my direction and recommend that it be accepted as fulfilling the dissertation requirement.

Dissertation Director Roger C. Bales — 10/13/88 Date

STATEMENT BY AUTHOR

This dissertation has been submitted in partial fulfillment of requirements for an advanced degree at The University of Arizona and is deposited in the University Library to be made available to borrowers under the rules of the Library.

Brief quotations from this dissertation are allowable without special permission, provided that accurate acknowledgment of source is made. Requests for permission for extended quotation from or reproduction of this manuscript in whole or in part may be granted by the copyright holder.

SIGNED: James Edward Szecsody

ACKNOWLEDGMENTS

I would like to thank those fellow graduate students with whom I have shared the glories of learning real water chemistry with: Thomas Whitehead, Adam Klein, David Kebler, and Robert Matzner. Each have given me greater insight, as true knowledge is gained one step at a time.

I would also like to express my very fond appreciation for the support and encouragement of my parents, Alex and Irene Szecsödy, throughout the years, and to my wife, Karen, for being by my side and providing valuable direction and purpose.

Lastly, I would like to acknowledge the guidance of Dr. Stanley Davis during the course of my studies. Dr. Roger Bales deserves special thanks for building up the water chemistry program in the Department of Hydrology and for providing technical direction for this research. Financial support was provided by Grant ECE-8504663 from the National Science Foundation, Grant R813179010 from the U.S. Environmental Protection Agency, and in part by the Petroleum Research Fund, administered by the American Chemical Society.

TABLE OF CONTENTS

LIST OF FIGURES

LIST OF TABLES

ABSTRACT

The sorption of five chlorinated benzenes and sixteen other organic solutes was investigated by determining the extent of sorption and the sorption rates in a series of 40 batch and 139 column experiments using surface-modified silica of known chemical composition. These surfaces were used to represent important functional groups in soil, and consisted of porous silica with patchy surface coatings of aliphatic chains (C_1, C_8, and C_{18}), and other substituent groups (phenyl, amine, alcoholic, and carboxylic). Three possible rate-limiting steps were examined: diffusion through immobile pore fluid, diffusion through bound organic matter, and the chemical binding and release rate.

First-order desorption rate coefficients were observed to be 10^{-1} to 10^{-2} s^{-1} on unbonded, and C_8, C_{18}, amine, and alcoholic modified surfaces, and 10^{-3} to 10^{-5} s^{-1} on C_1 and phenyl-polymer modified surfaces. Diffusion through immobile pore fluid had only a minor effect on the sorption rate, as evidenced by similar rates on organic-bound porous and solid particles. The diffusion rate through the bound organic layer is not rate limiting due to the small organic layer thickness. The observed slow desorption on the phenyl-polymer surface is consistent with the rate limiting step being the chemical binding and release rate. The changes in the rate with temperature and within a series of chlorinated benzenes support this conclusion.

The free energies for sorption onto the phenyl-polymer surface ranged from -4.0 kcal mol^{-1} for chlorobenzene to -6.9 kcal mol^{-1} for pentachlorobenzene, which are within the range expected for van der Waals interactions. The observed sorption energies are slightly stronger than predicted for hydrophobic surfaces, possibly reflecting strong binding due to multiple pi-pi electron interactions on the phenyl-polymer surface. Hydrophobic solute partitioning onto natural soils, as observed by others, is less than that observed on aliphatic and phenyl hydrophobic surfaces in this study, but greater than on amine or alcoholic modified surfaces. The sorption of di-, tri-, and tetra- chlorobenzenes onto the phenyl-polymer surface is apparently driven by the overall sorption enthalpy (ΔH° = -3.9 to -4.9 kcal mol^{-1}) and to a lesser extent by the entropy ($T\Delta S^\circ$ = 0.5 to 1.5 kcal mol^{-1}). As equilibrium of the reactions observed in this study are reached within hours, these reactions are important at small field scales where residence times are hundreds of hours or less.

CHAPTER 1
INTRODUCTION

In industrial nations, the mass of synthetically produced organic material is within an order of magnitude of that synthesized by nature [*Stumm et al., 1983*]. An understanding of the processes and interactions of organic solutes with the environment is important in order to control their spread in soil and in ground water systems. In many cases, by assuming that sorption of organic solutes onto surfaces is at equilibrium, their movement is overpredicted [*Valocchi, 1985*]. A more accurate description of the sorption process that includes kinetics can be used for better prediction of solute movement. The processes that cause slow sorption are examined in this research using model soils and laboratory scale transport systems.

1.1 Importance of Nonequilibrium Sorption

Nonequilibrium sorption and desorption in subsurface media arises when physical and chemical processes at the single pore level are slow relative to advection in the bulk media. Sorption and desorption in a porous media involves the physical and chemical rearrangement steps illustrated in Figure 1.1. In principle, any of these steps could limit the rate of the overall sorption process. In practice, bulk transport and boundary layer diffusion are generally not rate limiting in ground water media, as the distances and flow velocities involved are small.

Diffusion resistance inside a porous aggregate particle can be significant where pore sizes are small and aggregate sizes are large. Diffusion of molecules through organic material in subsurface media will be retarded relative to that in water due to the non-liquid nature of organic phases. The sorption binding step can be rate limited due to steric inhibition in reaching a binding site [*Jinno et al., 1985*] or to a high activation energy.

Models used to predict transport of solutes that assume equilibrium sorption [*Lapidus and Amundson, 1952*] can predict movement in most cases in large scale aquifers, where flow rates are slow. In cases of some degree of nonequilibrium sorption, equilibrium models can still be used, where the slow sorption/desorption process produces greater apparent dispersion [*VanGenuchten, 1985*]. In cases of considerable

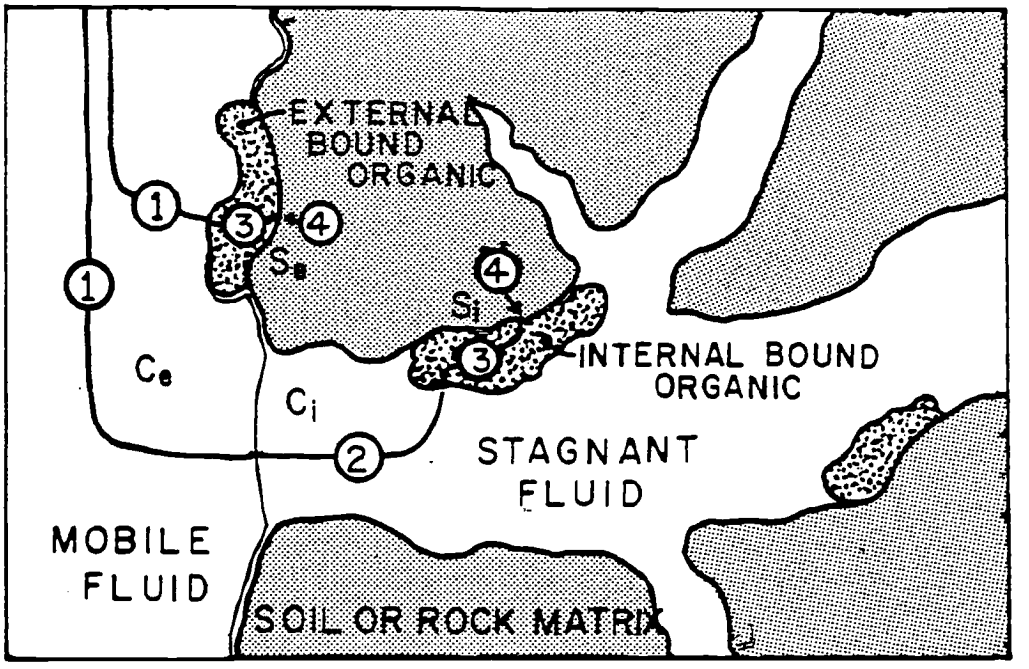

1. Advection and Dispersion in Mobile Fluid

Slow Rate Steps:

2. Diffusion through Immobile Pore Fluid
3. Diffusion through the Bound Organic Layer
4. Binding and Release

Figure 1.1 Conceptual model of microscale transport and sorption

nonequilibrium sorption, advection-dispersion models that assume equilibrium sorption cannot adequately describe the behavior.

The importance of nonequilibrium behavior for understanding and modeling contaminant transport has been illustrated for solute movement near pumping wells [*Valocchi, 1986*], in field soil experiments [*Leenheer and Ahlrichs, 1971; MacKay et al., 1986; Parker and VanGenuchten, 1984*], in laboratory soil columns [*VanGenuchten and Cleary, 1982; Schwarzenbach and Westall, 1981; Whitehead, 1987*], and in laboratory batch studies [*Wu and Gschwend, 1986; Karickhoff and Morris, 1985; Coates and Elzerman, 1986*].

1.2 Observations

1.2.1 Sorption

The predominance of natural organic matter in controlling the sorption of hydrophobic solutes in soil has been extensively documented [*Karickhoff, 1984*]. Partitioning of solutes between the sorbed phase (S in $\mu g\, g^{-1}$) and the aqueous phase (C in $\mu g\, cm^{-3}$) at low concentrations in many cases can be described by:

$$S = K_p\, C \tag{1}$$

where K_p is the partition coefficient between soil and water ($\mu g\, g^{-1}$ per $\mu g\, cm^{-3}$). In the carbon referenced sorption model:

$$K_p = f_{oc}\, K_{oc} \tag{2}$$

where f_{oc} is the fraction carbon by weight, and K_{oc} is the partition coefficient between water and a hypothetical soil that is 100 percent organic carbon ($cm^3\, g^{-1}$). K_{oc} values depend on solute properties, and not soil properties, reflecting nonspecific sorption of hydrophobic solutes to soil organic matter. Carbon referenced sorption is applicable to hydrophobic solutes at concentrations less than half their solubility [*Karickhoff, 1984*], where the number of sorbed sites is much smaller than the total number of sites, so the interaction energy can be considered to be the same at all sites. Deviations from this

linear relationship are caused by: 1) multiple sorption mechanisms (e.g. sorption onto mineral surfaces); and 2) non-equilibrium behavior (e.g. kinetic limitations on sorption). For many compounds, K_{oc} is related to the octanol-water partition coefficient (K_{ow}) with a linear free energy relation:

$$\log K_{oc} = \alpha \log K_{ow} + \beta \tag{3}$$

where α and β are emperical constants.

Retention of chlorinated benzenes onto natural soils was examined by *Schwarzenbach and Westall [1981]*, *Wu and Gschwend [1986]*, *Karickhoff et al., [1979]*, *Karickhoff [1984]*, *Klein [1986]*, and *Oliver [1985]*; data are shown in Table 1.1. The partition coefficients reflect differences in f_{oc} in different soils; however, the K_{oc} values reflect a linear trend of increasing sorption with molecular weight. Sorption from aqueous systems involves both a solvent effect energy [*Frank and Evans, 1945*], and the solute/surface interaction energy [*Sposito, 1984*]. The solvent effect includes a decrease in water structure upon solute removal from solution (positive entropy), and an increase in hydrogen bonding between water molecules (negative enthalpy). The interaction energy includes both the solute/surface reaction enthalpy and the negative entropy of moving the solute molecule from a liquid to a sorbed state. As the series of chlorinated benzenes in Table 1.1 have similar interaction energies with a surface, the increase in K_{oc} with molecular weight reflects mainly the solvent effect energy as a result of the increased hydrophobic surface area.

A slow approach to equilibrium has been observed in some cases, and is reported as the first-order desorption rate coefficient (k_b). Rates were on the order of 10^{-6} s^{-1} for di-, tri- and tetra-chlorobenzenes [*Wu and Gschwend, 1986*], and 10^{-6} to 10^{-7} s^{-1} for penta- and hexa-chlorobenzenes [*Karickhoff, 1984*]. Desorption rate coefficients on the order of 10^{-6} to 10^{-7} s^{-1} were observed for desorption of three polychlorinated biphenyls from river sediments [*Coates and Elzerman, 1986*]. These reported rates mean that the time to reach equilibrium took up to four weeks, which was observed in some of the

Table 1.1 Sorption of chlorinated benzenes onto soil

Solute Compound	C_o ($\mu g\ L^{-1}$)	Sorbent Name	f_{oc}	K_p	K_{oc}*	k_b (s^{-1})	Reference
Benzene	2000	GR	---	---	83.	---	9
CB	20	KSI	0.0073	1.2	164.	---	1
	20	KBIH	0.0008	0.4	500.	---	1
					Ave K_{oc}: 322 ± 237		
1,4-DCB	20	KSI	0.0073	4.4	603	---	1
	20	KBIH	0.0008	1.1	1380	---	1
	4.4	CR	0.170	87.0	512	1.2×10^{-2}	2
	1200	2V2 DB	0.0010	1.40	1500	---	3
	1200	102 SG	0.0010	3.33	3300	---	3
	1200	---	0.0009	0.42	477	---	3
		---	0.011	3.05	277	---	4
		---	0.012	0.51	280	---	5
	980	---	0.039	18.4	472	8×10^{-7}	6
					Ave K_{oc}: 609 ± 451		
1,2,4-TCB	20	KSI	0.0073	14.5	1990	---	1
	20	KBIH	0.0008	2.5	3125	---	1
	13.7	CR	0.170	265	1560	5.8×10^{-3}	2
					Ave K_{oc}: 2220 ± 809		
1,2,3,4-TECB	3.2	CR	0.170	1220	7180	1.6×10^{-3}	2
		IS	0.065	58	892	---	2
		NR	0.088	418	4750	---	2
					Ave K_{oc}: 4270 ± 3170		
1,2,4,5-TECB	40	KSI	0.0073	37.9	5192	---	1
		KBIH	0.0008	6.2	7750	---	1
					Ave K_{oc}: 6470 ± 1810		
PCB	2.3	CR	0.170	4690	27600	5.8×10^{-4}	2
	1.6	IS	0.065	239	3680	---	2
	0.4	NR	0.088	1560	17700	---	2
	3.5	13	---	7100	---	$1.0 - 3.5 \times 10^{-6}$	7,8
					Ave K_{oc}: 16300 ± 12000		
HCB	2.5	13	---	2800	---	$0.3 - 13 \times 10^{-6}$	7,8

*$K_{oc} = K_p/f_{oc}$.

[1]*Schwarzenbach and Westall, 1981.*

[2]*Wu and Gschwend, 1986.*

[3]*Keefer, 1986.*

[4]*Chiol et al., 1983.*

[5]*Southern and Hewer, 1986.*

[6]*Oliver, 1985.*

[7]*Karickhoff, 1984.*

[8]*Karickhoff and Morris, 1985.*

[9]*Karickhoff, 1979.*

laboratory experiments [*Karickhoff, 1980*].

The causes of the slow sorption of chlorinated benzenes on natural sediments were reported as diffusion through immobile pore fluid [*Wu and Gschwend, 1986*] and a series chemical reaction [*Karickhoff, 1984*]. In another study, the sorption of chlorinated phenols appeared to be controlled by the rate of penetration into the natural organic matter [*Isaacson and Frink, 1984*]. Earlier, sorption of carbaryl and parathion onto soil was reported to be limited by the rate of chemical binding and release [*Leenheer and Ahlrichs, 1971*].

The carbon-referenced-sorption model is observed to apply down to an f_{oc} value of 0.001. Below this value, sorption onto mineral surfaces is thought to be important. At low f_{oc} values, sorption can still be approximated from solute properties, as is illustrated for twelve chlorinated benzenes [*Schwarzenbach and Westall, 1981*]:

$$\log K_p = 0.4 \log K_{ow} + 0.29 \tag{4}$$

where less sorption onto mineral surfaces is observed compared to soils that contain organic matter. The lack of dependence on mineral surface properties may indicate that sorption of hydrophobic solutes is caused primarily by the solvent effect.

A weak dependence on the surface area of the soil, due to binding interactions, is observed with the sorption of 25 hydrophobic organic solutes to organic-free silica:

$$\log K_p = 0.16 \log K_{ow} + \log \frac{S_a}{200} \tag{5}$$

where S_a is the mineral surface area ($m^2\ g^{-1}$) [*McCarty et al., 1981*].

Data for the sorption of chlorinated benzenes onto mineral surfaces are shown in Table 1.2, where the partition coefficient is expressed per unit surface area. As with soils containing organic matter, sorption onto mineral surfaces increases linearly with solute molecular weight (or hydrophobic surface area), reflecting the solvent effect. Some difference in sorption is observed between silica and alumina, and sorption onto kaolinite is greater than either silica or alumina. This indicates that the binding

Table 1.2 Sorption of chlorinated benzenes onto mineral surfaces

Solute	Sorbent	S_a ($m^2 g^{-1}$)	K_p ($cm^3 g^{-1}$)	K_p ($cm^3/100\ m^2$)	Reference
Chlorobenzene	Kaolinite	12	0.6	5.0	1
	δ-Al_2O_3	120	0.6	0.5	1
	SiO_2	300	4.2	0.84	1
1,4-DCB	Kaolinite	12	1.1	9.2	1
	δ-Al_2O_3	120	0.9	0.75	1
	SiO_2	500	6.0	1.2	1
1,2-DCB	Sand (SiO_2)	---	7.63 ± 0.36	---	2
1,2,4-TCB	Kaolinite	12	2.4	20.0	1
	δ-Al_2O_3	120	1.5	1.25	1
	SiO_2	500	7.6	1.52	1
1,2,4,5-TECB	Kaolinite	12	4.9	41.0	1
	δ-Al_2O_3	120	2.2	1.8	1
	SiO_2	500	12.1	2.42	1

[1]Schwarzenbach and Westall, 1981.

[2]MacKay et al., 1986.

interaction energy cannot be completely ignored.

Slow sorption onto mineral surfaces was observed with trichloroethylene on clay [*Rogers, 1980*] and dichlorobenzene on sand [*Ball and Roberts, 1985*], where the slow approach to equilibrium is caused by immobile pore volume diffusion. Internal diffusion also caused slow exchange of Sr^{+2} for Ca^{+2} in 5-10 mm sand particles [*Jackman and Ng, 1986*]. No chemically caused slow sorption of hydrophobic solutes to mineral surfaces were reported in the literature.

1.2.2 Transport

A slow approach to sorption equilibrium for organic solutes can be significant in short-residence-time systems, such as aquifer cleanup sites or near pumping wells. In systems with longer residence times (i.e., slower velocities or longer distances), such as regional systems, an equilibrium description is usually adequate. In cases where non-equilibrium sorption is modeled with an equilibrium description, the lack of understanding of molecular level interactions will result in less accurate predictions, since sorption parameters (K_p, D) obtained at one velocity will not be the same at a different velocity.

Several different nonequilibrium models have been developed over the last few decades. A physical nonequilibrium model considering diffusion into immobile pore volume (no sorption) was developed [*Coates and Smith, 1964*], then modified to include sorption [*VanGenuchten and Wierenga, 1976*]. Other physical nonequilibrium models of diffusion into aggregate particles account for different aggregate geometries [*VanGenuchten, 1985*], or series diffusion processes [*Miller et al., 1987*].

Chemical nonequilibrium has been modeled as a first-order reversible reaction [*Leenheer and Ahlrichs, 1971; VanGenuchten, 1974*]. In many cases, more involved sorption reactions can be approximated with the first-order model. A model describing equilibrium sorption in parallel with first-order kinetic sorption [*Cameron and Klute, 1977*] provides one more parameter and can describe more involved sorption, as can series reactions [*Karickhoff, 1984*]. A model describing equilibrium sorption in parallel with different slow reactions [*Bahr and Rubin, 1987*] has also been formulated.

A model with three slow steps has been formulated [*Akratanakul et al., 1983*], but experimental determination of parameters is not feasible. In principle, physical and chemical measurements within individual pores are needed to determine parameters [*Davidson et al., 1981*]. The ability to formulate and numerically solve complex simulation models exceeds our ability to verify these models using the limited experimental data base presently available [*Rao et al., 1982*]. Experimentally, most cases that are described with more involved models can also be described with a simpler first-order model. This indicates that better experimental techniques are needed to obtain data that can distinguish cases of more involved slow sorption phenomena.

Even with the simple first-order sorption model, obtaining reliable sorption rates is difficult, as evidenced by the lack of rate data in the literature [*VanGenuchten and Cleary, 1982*]. A single experiment may not be conclusive to determine even the rate parameter, much less the sorption mechanism. Experiments run at certain velocities produce more accurate rate data [*Chu and Langer, 1985; Larsson et al., 1982*]. This technique is refined in this research for multiple experiments at different velocities.

Experimental methods are needed to distinguish slow sorption mechanisms. In one study, it was concluded that a physical or chemical slow sorption model could fit the data equally well [*Rao et al., 1979*]. This is to be expected since both models reduce to the same mathematical solution.

1.3 Purpose and Objectives

The purpose of this research is to develop an understanding of the sorption mechanism (equilibrium sense) of hydrophobic solutes in natural systems. The rates of sorption and desorption are controlled by one of three possible rate limiting steps (Figure 1.1): diffusion through immobile fluid, diffusion through organic matter, or chemical binding and release.

This is accomplished through a laboratory study of sorption onto model surfaces, which contain major functional groups found in natural soil. Use of model surfaces enables control of the solute-sorbent interactions and sorbent geometry. Experiments

with these model sorbents are designed to affect only one rate step at a time in order to determine the cause of slow sorption.

Diffusion through immobile pore fluid is examined with porous silica aggregates with internal porosity. Differences in particle diameter and internal pore size are used to change diffusion times. Diffusion through a bound organic layer is examined by changing the thickness or density of the organic matter, and by examination of the size and shape of the solute and sorbent molecules. The binding/release step is examined through the use of different bound functional groups, different solutes, and thermodynamics. Changes in the extent and rate of sorption with different compounds or at different temperatures are used to quantify the sorption energy and rate limiting step.

Model sorbents used in the experiments are made from silica and alumina. Silica has a negative surface charge, chemically resembling 2:1 clay surfaces. The silica is modified by covalently bonding organic compounds to the surface. Bound organic compounds include hydrophobic organic matter, and common functional groups found in soil. Sorption mechanisms on these modified surfaces are known in some cases [*Antle et al., 1985*]. Sorption mechanisms and rates may be applicable to natural systems, since sorbents used are portions of natural soil organic matter.

CHAPTER 2
BACKGROUND - SOLUTE SORPTION AND TRANSPORT

Organic solute transport and sorption are illustrated in Figure 1.1, where sorption is defined by three steps, any of which could be rate limiting. The chemical sorption processes and energies are discussed in Section 2.1, and the mathematical description of transport and sorption are discussed in Section 2.2.

2.1 Solute Sorption

The partitioning of an organic solute between water and a surface phase involves energy changes associated with cavity formation in the water (Figure 2.1) and the energy of interaction between the solute molecule and the surface phase [*Horvath et al., 1976*]. The total energy in bringing the solute molecule from the gas reference state to the surface phase [*Sinanoglu, 1968*] is similar to that shown in Figure 2.1, but with additional attractions to the surface. Sorption energy can be defined as the net energy gain in moving a solute molecule from solution to a surface [*Horvath and Melander, 1977*]. The net effect of the energy changes at the molecular scale is solute removal from solution. At a larger scale, sorption appears relatively simple and can be modeled with simple interactions.

2.1.1. Modeling Sorption

For simple single-site sorption of solute molecules, the sorption reaction can be described with:

$$\mathrm{A}(aq) + \mathrm{X} \Longleftrightarrow \mathrm{XA}(sorb) \qquad K' = \frac{[\mathrm{XA}(sorb)]}{[\mathrm{A}(aq)][\mathrm{X}]} = \frac{S}{(S_t - S)\,C} = \frac{k'_f}{k'_b} \tag{6}$$

where X represents a surface site; C is the solute concentration in solution ($\mu g\ cm^{-3}$), S_t is the total number of surface sites (maximum adsorption density; $\mu g\ g^{-1}$), S is the sorbed concentration ($\mu g\ g^{-1}$), and the forward and reverse rate constants are k'_f ($cm^3 \mu g^{-1} s^{-1}$) and k'_b (s^{-1}). Rearranging equation (6) to the form of a Langmuir isotherm gives:

$$\frac{S}{S_t} = \frac{K'C}{(1 + K'C)} \tag{7}$$

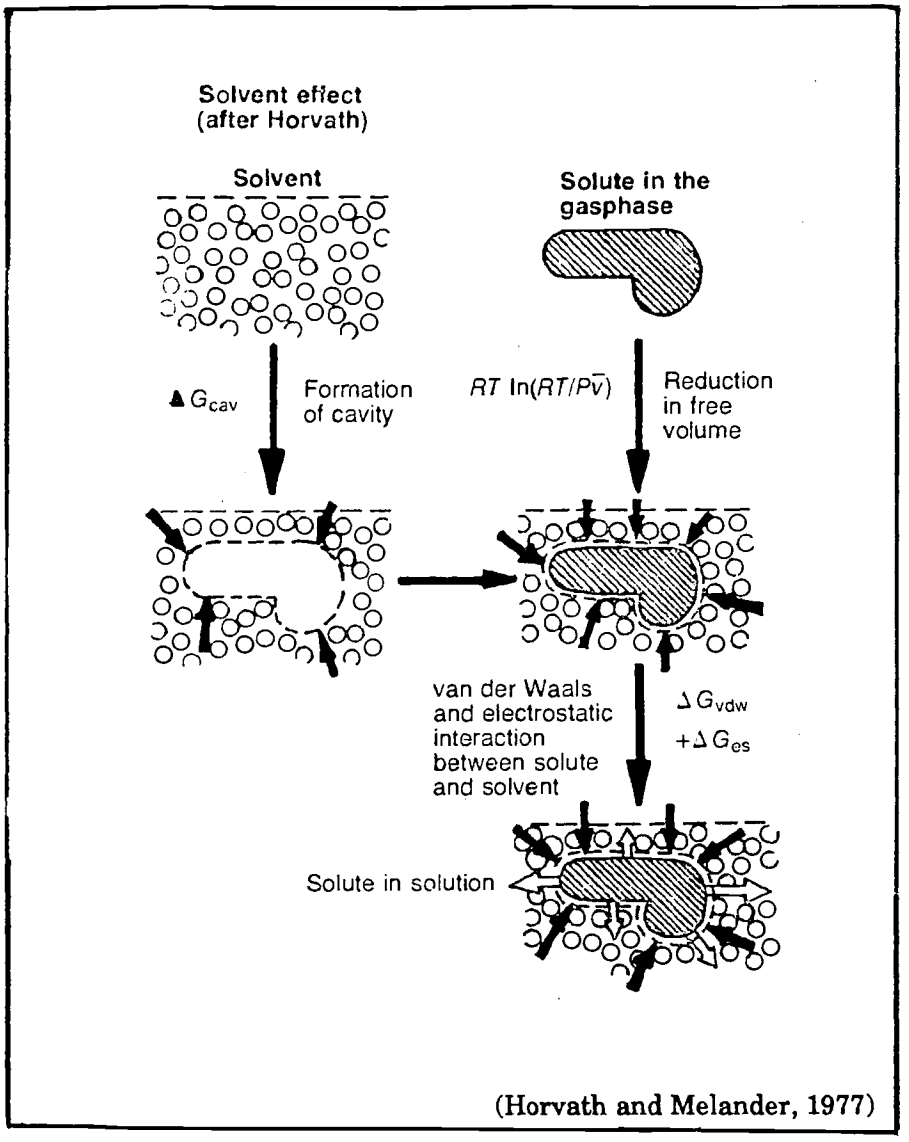

Figure 2.1 Energy of a solute molecule in solution

For organic solutes of limited solubility, the maximum adsorption density is not reached (K'C << 1), and equation (7) becomes a linear isotherm (equation 1). The Freundlich isotherm, which is empirically derived, is also used to describe nonlinear sorption:

$$S = K_p\, C^N \tag{8}$$

where N less than 1 can approximate a Langmuir isotherm over a small range. This form has advantages over the Langmuir isotherm for transport modeling (Section 2.2.7).

In this research, the total concentration of surface sites is much larger than the sorbed concentration. For example, if a DCB molecule sorbs to a single aromatic group on a phenyl-modified surface, then the number of occupied sites can be estimated. Assuming an f_{oc} of 1 percent on the surface, and one bonded benzene ring (6 carbons) per sorption site, the total number of sites is calculated at 1.9 x 10^{19} sites cm^{-3}. Dichlorobenzene at a concentration of 500 ppb (equivalent to 2.0 x 10^{-12} molecules g^{-1} in liquid) has an equilibrium partition coefficient (K_p = 60 $cm^3 g^{-1}$) equivalent to 1.2 x 10^{14} molecules g^{-1} sorbed. This corresponds to 1 site in 100,000 occupied for concentrations used in column experiments. At the solubility limit of DCB (89 mg L^{-1}), the number of occupied sites is 2.1 x 10^{16} g^{-1} or 1 site in 1000.

For S_t - S approximately equal to S_t, equation (6) simplifies to:

$$K'\, S_t = K_p = \frac{[\mathrm{XA}(sorb)]}{[\mathrm{A}(aq)]} = \frac{\rho_b}{\theta}\,\frac{k_f}{k_b} \tag{9}$$

where K_p is the partition coefficient, and the forward and reverse rate coefficients are k_f and k_b (s^{-1}), respectively. The thermodynamic K describes the partitioning between a pure organic phase ($\mu g / cm^3_{om}$) and water ($\mu g / cm^3_{aq}$), and is related to K_p by:

$$K = \frac{S\, f_c\, M_{om}\, [\mu g / cm^3_{om}]}{C\, f_{oc}\, V_{om}\, [\mu g / cm^3_{aq}]} = \frac{f_c\, M_{om}\, K_p}{f_{oc}\, V_{om}} \tag{10}$$

where f_c is the fraction carbon in the organic portion of the silane (Table 3.2), M_{om} is the molecular weight of the organic portion of the bound silane, f_{oc} is the mass fraction

of carbon based on total particle mass (Table 3.1), and V_{om} is the molar volume of the organic fraction (Table 3.2). The chromatographic capacity factor is equal to the partition coefficient (K_p) times the soil-to-water ratio (ρ_b/θ). The thermodynamic K is related to total sorption energy ($\Delta G°$):

$$\Delta G° = - RT \ln K \tag{11}$$

where R is the gas constant, and T is absolute temperature ($°K$).

Equation (9) can also be used to describe more involved reactions, if the pseudo-first-order reaction rates can adequately approximate the reaction. The first-order rate coefficients (k_f and k_b) can be used to calculate the time at which the reaction is half completed:

$$t_{1/2} = \frac{\ln 2}{k_b} \tag{12}$$

for comparison with the time scale of other processes.

Sorption reversibility is assumed in applying the above equations to this research, as it is in gas and liquid chromatographic systems [*Giddings, 1965*]. Hysteresis in isotherms [*VanGenuchten and Cleary, 1979*] can be due to a greater energy required for desorption as compared to sorption. This has been modeled as two components of sorption, a reversible fraction and an irreversible fraction [*Di Toro and Horzempa, 1982*].

2.1.2 Calculated Sorption Energies

The total energy of sorption from aqueous solution can be estimated with different empirical relationships. These include physically based relationships [*Yalkowsky, 1979*], the molecular connectivity model [*Kier and Hall, 1976*], and the solvophobic model [*Horvath and Melander, 1978*], among others.

The solubility and thus the partition coefficient of a hydrophobic solute is related to the molecule's total surface area. For the chlorinated benzenes used in this research, the molecular surface area increases almost linearly (Table 3.4) from chlorobenzene to

hexachlorobenzene. A relationship between the total molecular surface area and the solubility (mol L^{-1}) for 26 halobenzenes at 25°C is [*Yalkowsky et al., 1979*]:

$$S_w = -0.0103\, T_m - 0.04225\, S_a + 3.2970 \tag{13}$$

where T_m is the melting point (°K), and S_a is the surface area ($cm^3\,mol^{-1}$). *Hansch* [*1969*] first proposed a log-linear relationship between solubility and octanol-water partitioning (K_{ow}), and measured this relationship for many series of compounds over eight orders of magnitude of K_{ow}. *Hansch* [*1969*] also proposed that additional fragments and functional groups have an additive effect on K_{ow}. *Yalkowsky, Valvani, and MacKay* [1983] presented a log-linear relationship between solubility (mol L^{-1}) and K_{ow} for 162 aromatic compounds (including chlorinated benzenes) at 25°C:

$$\log S_w = -0.944 \log K_{ow} - 0.01\, T_m + 0.323 \quad (r^2{=}0.96) \tag{14}$$

Another relationship applicable to halogenated benzenes involves the measured supercooled liquid solubilities (S* in mol L^{-1}) of the solute and K_{ow} [*Chiou et al., 1982*] at 25°C:

$$\log K_{ow} = -0.862 \log S^* + 0.710 \quad (r = 0.994, n = 36) \tag{15}$$

Partitioning between octanol and water (K_{ow}) can then be related to the water-organic partition coefficient (K_{oc}), using equation (3):

$$\log K_{oc} = \alpha \log K_{ow} + \beta \tag{3}$$

For polycyclics α is 1.00 and β is -0.21 [*Karickhoff et al., 1979*], for 13 halo/methyl benzenes, α is 0.72 and β is 0.49 [*Schwarzenbach and Westall, 1981*], and for many low molecular weight hydrophobic compounds, α is 0.72 and β is 0.54 (compiled data from others) [*Schwarzenbach, 1983*].

The earliest use of this relationship was for estimation of hydrophobic bonding in biological systems [*Hansch, 1968*]. If organic surfaces are liquid-like, then partitioning may be similar to partitioning to octanol. Bound aliphatic chains shorter than four

methyl groups are relatively immobile, and partitioning is similar to solid surfaces [*Hunnicutt et al., 1986*]. Longer aliphatic chains resemble liquids with respect to sorption. Partitioning to more complex biological systems also may not be as simple as octanol-water partitioning [*Miller et al., 1985*]. The relationship between K_{ow} and K_{oc} does not apply at low K_{ow}'s where binding mechanisms other than van der Waals are present [*Karickhoff, 1984*].

The total sorption energy was calculated from measured solubilities (column 3 in Table 2.1; equations 3, 11, and 14) and from measured octanol-water partition coefficients (column 4; equations 3 and 11). The calculated energies with these two methods were similar, where energies increased with increased molecular weight.

The molecular connectivity theory uses index values that are based on electron and orbital counts [*Kier and Hall, 1976; 1986*]. Correlations between these structural parameters and a wide range of physicochemical parameters and activity parameters (such as sorption) are numerous. A relationship between solubility and the X_1 and X_2 molecular connectivity indices [*Kier and Hall, 1986*] for 35 halobenzenes is:

$$-log\ S_w = 0.890\,X_1 + 0.627\,X_2 + 0.00979\,T_m - 2.004 \qquad (16)$$

where T_m is the solute melting point and the indices are listed in Table 2.2. The total sorption energy was calculated from the molecular connectivity indices (column 2; equations 3, 11, 14, and 16). A difference in sorption energy for isomers is predicted with this method, but not for those calculated from measured values of K_{ow}, possibly reflecting less sensitivity in the K_{ow} technique. Values calculated from the molecular connectivity indices are larger for tetra-, penta-, and hexa- chlorobenzenes, compared to the energies calculated from solubility or K_{ow} data.

The solvophobic model was not used to estimate sorption energy. However, in an attempt to separate the energy due to solvent interactions from the sorbent/surface interaction energy, a simple model was assumed (Dr. S. Yalkowsky, Pharmaceutical Sciences, University of Arizona). Water, solute, and surface molecules are assumed to be

Table 2.1 Calculated sorption energies

Compound	ΔG^A from X_1 and X_2 (kcal/mole)	ΔG^B from S_w (kcal/mole)	ΔG^C from K_{ow} (kcal/mole)
Benzene	-2.74	-2.76	-2.77
CB	-3.25	-3.43	-3.49
1,2-DCB	-3.93	---	-4.17
1,3-DCB	-3.60	---	-4.17
1,4-DCB	-4.49	-4.21	-4.17
1,3,5-TCB	-5.03	---	-4.89
1,2,4-TCB	-4.94	-4.88	-4.89
1,2,3-TCB	-5.41	---	-4.89
1,2,3,5-TeCB	-5.90	---	-5.57
1,2,4,5-TeCB	-6.88	-5.60	-5.57
1,2,3,4-TeCB	-6.11	---	-5.57
PCB	-7.21	-6.31	-6.29
HCB	-9.60	---	-7.00

[A]from calculated indices, and equations 17, 19, and 21).
[B]From measured solubilities (Table 3.4) and equations 19 and 21.
[C]From measured K_{ow} and equation 21.

Table 2.2 Molecular connectivity indices for chlorinated benzenes

Compound	X_1	X_2
Benzene	3.00	1.500
CB	3.394	1.894
1,2-DCB	3.805	2.540
1,3-DCB	3.788	2.199
1,4-DCB	3.788	2.305
1,3,5-TCB	4.182	2.414
1,2,4-TCB	4.198	2.860
1,2,3-TCB	4.215	3.114
1,2,3,5-TeCB	4.609	3.343
1,2,4,5-TeCB	4.609	3.430
1,2,3,4-TeCB	4.626	3.702
PCB	5.037	4.197
HCB	5.464	4.976

(Sabljic, 1985)

the same size, and there is one interaction between each. The net energy in moving a hydrophobic solute molecule from a gas reference state into aqueous solution is equal to the gain of a water/solute interaction and the loss of a water/water interaction. The net energy in moving a hydrophobic solute molecule from a gas reference state to a surface site is equal to the gain of a solute/surface interaction, the gain of a water/water interaction (since a water molecule was displaced from the surface), and the loss of a water/surface interaction. Sorption energy is then defined as the net energy gain of a solute molecule moving from solution to a surface site [*McGuire and Suffet, 1979*].

For this approximation, four interactions were considered: water/water (dipole/dipole), water/solute (dipole/induced dipole), water/organic surface (dipole/induced dipole), and solute/organic surface (induced dipole/induced dipole). The dipole/dipole interaction between water molecules is strong and equal to 5.0 kcal mol^{-1} [*Porterfield, 1984*]. Dipole/induced dipole interactions are approximated with:

$$\Delta G_{di} = \frac{-1.44 \times 10^{13} \mu_1 \alpha_2}{r^6} \tag{17}$$

where r is the radius between molecules (3×10^{-8} cm), μ_1 is the dipole moment of water (1.7×10^{-18} esu) [*CRC, 1982*], and α_2 is the polarizability of the solute or surface-bound molecule (1×10^{-24} cm^3). Polarizability (α_2) can vary in the range of $0.2 - 1.0 \times 10^{-24}$ cm^3 for ions to large molecules. The units of ΔG_{di} are kcal mol^{-1}, where the constant includes a unit conversion.

The solute/surface interaction is calculated by assuming an induced dipole/induced dipole interaction with [*Porterfield, 1984*]:

$$\Delta G_{ii} = \frac{-1.44 \times 10^{13} \mu_1 \mu_2}{r^3} \tag{18}$$

where μ_1 and μ_2 are dipole moments. The dipole moment of 1,4-dichlorobenzene is 0.2×10^{-18} esu, chlorobenzene is 1.6×10^{-18} esu (Table 3.4), and the dipole moment of the surface is assumed to be 1.8×10^{-18} esu. If the sorption interaction is a dipole/dipole

interaction, then the energy is calculated with:

$$\Delta G_{dd} = \frac{-3 I' \alpha^2}{4 r^6} \tag{19}$$

where I' is the ionization potential of the solute molecule (461 kcal mol^{-1}) [*Porterfield, 1984*].

The calculated energy for a solute molecule sorbing onto a surface is the gain of a solute/surface interaction (0.19 to 1.5 kcal mol^{-1}, equation 19), the gain of a water/water interaction (5 kcal mol^{-1}), and the loss of a water/surface interaction (0.14 kcal mol^{-1}, equation 17). This net energy on the surface is -5.1 to -6.4 kcal mol^{-1}, where the range arises due to the value of dipole moment used for the surface (assuming a dipole/induced dipole interaction). Assuming a dipole/dipole interaction for the solute/surface energy, then the calculated solute/surface interaction energy is 0.47 kcal mol^{-1}, and the net energy is -5.5 kcal mol^{-1}. The solvent effect alone is the energy of placing a molecule in solution, which is equal to the loss of a water/water interaction (5 kcal mol^{-1}), and the gain of a water/solute interaction (0.14 kcal mol^{-1}; equation 17).

The net sorption energy is equal to the energy on the surface (-5.1 to -6.4 kcal mol^{-1}) minus the energy in solution (4.9 kcal mol^{-1}), totaling -9-9 to -11.2 kcal mol^{-1}. This shows that the solvent effect accounts for 40 to 50 percent of the net sorption energy. For the sorption of azobenzene [*Halicioglu and Sinanoglu, 1969*], the solvent effect accounts for one-fourth of the total sorption energy; for 1,4-dioxane, the solvent effect accounts for half the sorption energy [*McGuire and Suffet, 1979*]. Although the calculated energies are not accurate, this does provide an idea of the relative contributions of the solvent effect versus the interaction energy on the sorption from aqueous solution.

2.1.3 Temperature, Pressure, and Surface Tension effects on K_p

The effect of temperature on sorption is described by the van't Hoff equation [*Stumm and Morgan, 1981*]:

$$\ln K = -\frac{\Delta H^\circ}{RT} + \frac{\Delta S^\circ}{R} \tag{20}$$

where ΔH° is the reaction enthalpy (kcal mol^{-1}), ΔS° is the entropy of the overall sorption reaction (kcal mol^{-1} K^{-1}), and R is the gas constant. A plot of $1/T$ versus ln K yields a slope of $-\Delta H^\circ/R$ and an intercept of $\Delta S^\circ/R$ [*Melander et al., 1978*]. In order to calculate enthalpy and entropy, experiments are run at different temperatures. A non-linear plot could indicate a change in binding mechanism at different temperature. This was the case in one study [*Yang et al., 1987*], where more H-bonding and less van der Waals bonding is indicated at higher temperature.

Pressures for the column experiments in this research varied from less than 100 psi to over 4500 psi, which has an effect on the sorption energy. Assuming that the molar volume does not change over the pressure range, then the log of K_p increases with pressure [*Stumm and Morgan, 1981*]. This increase in ΔG° or (or K) with pressure has been confirmed experimentally [*Toyohide and Ishii, 1982*] for retention of aromatic compounds in aqueous solution sorbing to organic bound surfaces.

The change in sorption energy with ionic strength is expected since at higher ionic strength, there is an increase in surface tension, which increases the energy associated with the solvent effect. This increase in surface tension is about 3 percent for a 0.1 M solution of KCl, which is the highest concentration used in this research. Increasing the ionic strength then log-arithmetically increases retention [*Horvath and Melander, 1977*], shown with aromatic acids in Figure 2.2. This effect should be small for the small (< 3 percent) change in surface tension in this research. There is an exponential decrease in sorption upon the addition of a miscible cosolvent (such as methanol) to aqueous solution [*Horvath and Melander, 1977*; *Nkedi-Kizza et al., 1987*] due to the decrease in surface tension. The presence of an organic cosolvent such as methanol also

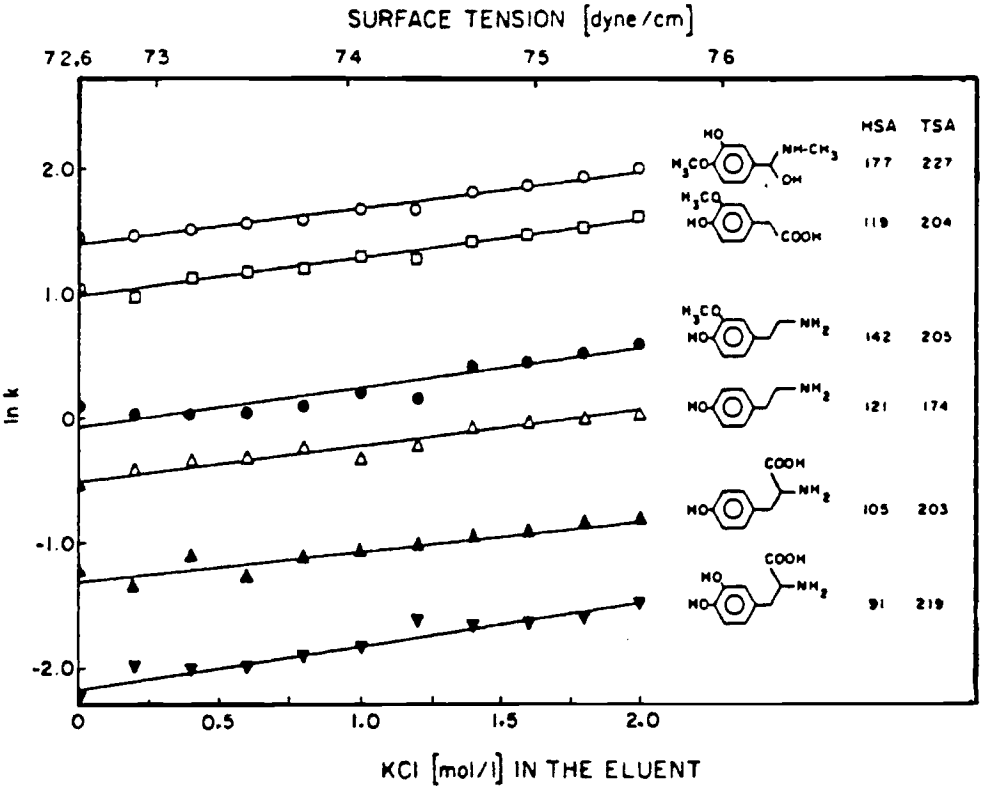

(Horvath and Melander, 1977)

Figure 2.2 ionic strength effect on sorption

appears to increase the sorption rate [*Nkedi-Kizza et al., 1987*].

Chromatography literature indicates no change in sorption with the presence of other solutes [*Snyder and Kirkland, 1979*]. Since the actual sorbent is heterogeneous, the most reactive and exposed sites are most likely involved in interactions, so there is some competition for sites. Competitive adsorption has been studied [*Weber, 1984*] and has been described when a solute with a stronger retention mechanism displaces a less strongly held solute. The breakthrough curve of a less strongly retained solute exhibits a peak that can exceed input concentration, as it is displaced by the more strongly retained solute [*Weber et al., 1987; Boast, 1973*]. Alternatively, sorption of a less strongly held solute in a system where a stronger solute is sorbed may show increased retention, provided there is no competition for sites and the first solute is attracted to the second solute. An S-type isotherm implies that successive sorbate molecules cooperate strongly in sorption of further sorbate sorption [*Isaacson and Frink, 1984*].

2.1.4 Sorption on Model Surfaces

In chromatography systems, hydrophobic interactions are more easily understood since some of the system complexity is reduced. Retention of hydrophobic compounds onto organic modified surfaces is in the following order (strongest first with a higher K_{oc}): C_{18} > C_8 > phenyl > C_1 > CN [*Antle et al., 1985*], where the aliphatic chain length is defined by the number of carbon atoms. The optimum van der Waals binding distance between methyl groups is 0.357 nm [*Bondi, 1964*].

Retention onto aliphatic chains depends on the number of electrons involved in the interaction, so longer chains have greater solute retention due to more van der Waals interactions, compared to shorter chains [*Hanai et al., 1984*]. Solutes with polar or ionic groups that H-bond with water are retained less. The binding strength of solutes on C_{18}-modified silica are in the following order (strongest first): aliphatic hydrocarbons, induced dipoles (CCl_4), dipoles ($CHCl_3$), weak Lewis bases (ethers, aldehydes, ketones), strong Lewis bases (amines), weak Lewis acids (alcohols, phenols), and strong Lewis acids (carboxylic acids) [*Macherey-Nagel, 1987*].

Retention of substituted benzenes onto a phenyl-modified surface is caused by the solvent effect and pi-electron to pi-electron van der Waals interactions [*Thus et al., 1985; Hanai et al., 1984; Jinno et al., 1985*]. The pi-electron attraction between aromatic groups are stronger than normal van der Waals attractions, as shown in Figure 2.3, where increased retention of aromatic compounds (compared to aliphatic compounds) on an aromatic (phenyl) surface is illustrated. Substituted aromatic solutes exhibit strong binding regardless of the functional groups, indicating that the interaction is with the pi-electrons in the benzene rings. Steric effects often account for breakdown in calculated sorption activity, especially in large molecular structures [*Tomlinson, 1975*].

This increased sorption energy between aromatic groups is on the order of: 1.2 times for chlorinated benzenes, 1.3 times for alkyl benzenes, and 1.5 times for polyaromatics. With the Hückel Molecular Orbital Theory [*Streuli and Orloff, 1971*], pi electron interaction energies are calculated at about 2 kcal mol^{-1} for benzene and chlorobenzene. Values are also experimentally reported varying from 1.7 to 2.2 kcal mol^{-1} for benzene, CB, DCB, and TCB [*Hanai and Hubert, 1984*]. The optimum binding distance between the aromatic solute and the aromatic sorbent is 0.32 nm [*Bondi, 1964*].

The observed sorption energies for chlorinated benzenes onto model sorbents are shown in Table 2.3. Sorption data on C_1-modified surfaces are from gas chromatography experiments, so does not include the solvent effect energy. Sorption in liquid systems onto the C_{18} or phenyl monomer surfaces are reported only in mixed liquids (water and acetonitrile), so K_{oc} values are normalized to 100 percent water, for comparison. Partitioning between octanol/water and fish fat/water are presented [*Opperhulzen et al., 1988*] with the reported values of entropy and enthalpy.

Fish fat to water partitioning differs from octanol/water partitioning (Table 2.3), with positive enthalpy values. Enthalpy for six aromatic acids sorbing to a C_{18} surface [*Horvath et al., 1978*] were negative, and about -3 kcal mol^{-1}, with the total sorption energy of 7 to 9 kcal mol^{-1}. Partitioning to fish fat is an entropy driven process (Table

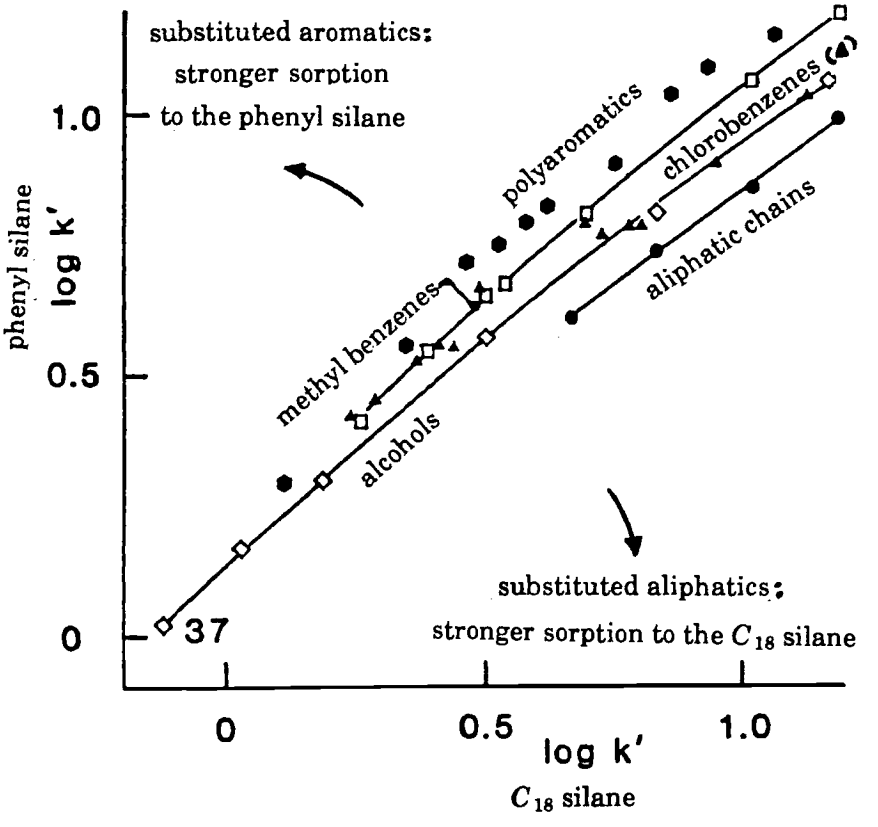

(Hanai and Hubert, 1984)

Figure 2.3 Selective retention on aromatic and aliphatic surfaces

Table 2.3 Sorption of chlorinated benzenes onto organic sorbents

Compound	Sorbent Type	f_{oc}	Solvent State	K_p	Retentention RI[2]	K'	K_{oc}	$K_{oc,n}$[3]	ΔG (Kcal/m)	ΔH (Kcal/m)	TΔS (Kcal/m)	Ref
Benzene	C_1	---	Gas	---	667	---	---	---	---	---	---	4
	C_{18}	0.195	Liq[1]	---	---	1.661	4.864	331.6	-3.44	---	---	5
	ØMono	0.0791	Liq[1]	---	---	0.750	5.415	369.1	-3.50	---	---	5
CB	C_{18}	0.195	Liq[1]	---	---	2.318	6.788	462.7	-3.63	---	---	5
	ØMono	0.0729	Liq[1]	---	---	0.888	6.412	437.1	-3.60	---	---	5
1,2-DCB	C_1	---	Gas	---	1006	---	---	---	---	---	---	4
	C_{18}	0.195	Liq[1]	---	---	3.180	9.312	634.8	-3.82	---	---	5
	ØMono	0.0791	Liq[1]	---	---	1.038	7.495	510.9	-3.69	---	---	5
1,3-DCB	C_1	---	Gas	---	964	---	---	---	---	---	---	4
	C_{18}	0.195	Liq[1]	---	---	3.791	11.10	756.6	-3.92	---	---	5
	ØMono	0.0791	Liq[1]	---	---	1.069	7.718	526.1	-3.71	---	---	5
	Fish	---	H_2O	---	---	---	---	---	-6.29	1.43	7.70	6
	Octanol	---	H_2O	3.55	---	---	---	---	-5.98	-3.59	2.39	6
1,4-DCB	C_1	---	Gas	---	970	---	---	---	---	---	---	4
	C_{18}	0.195	Liq[1]	---	---	3.471	10.16	692.6	---	---	---	5
	ØMono	0.0791	Liq[1]	---	---	1.069	7.718	526.1	---	---	---	5
1,2,3-TCB	C_1	---	N_2	---	1211	---	---	---	---	---	---	4
1,2,4-TCB	C_1	---	N_2	---	1177	---	---	---	---	---	---	4
	C_{18}	0.195	Liq[1]	---	---	5.440	15.93	1086.	---	---	---	5
	ØMono	0.0791	Liq[1]	---	---	1.264	9.126	622.1	---	---	---	5
1,3,5-TCB	C_1	---	N_2	---	1131	---	---	---	---	---	---	4
	C_{18}	0.195	Liq[1]	---	---	7.016	20.54	1400.	---	---	---	5
	ØMono	0.0791	Liq[1]	---	---	1.306	9.430	642.8	---	---	---	5
	Fish	---	H_2O	---	---	---	---	---	-7.05	2.51	9.56	6
	Octanol	---	H_2O	4.32	---	---	---	---	-7.05	-5.19	1.84	6
1,2,3,4-TeCB	C_1	---	Gas	---	1366	---	---	---	---	---	---	4
	C_{18}	0.195	Liq[1]	---	---	7.627	28.04	1502.	---	---	---	5
	ØMono	0.0791	Liq[1]	---	---	1.503	10.87	741.0	---	---	---	5
	Fish	---	H_2O	---	---	---	---	---	-7.58	3.23	10.8	6
	Octanol	---	H_2O	4.61	---	---	---	---	-7.41	-6.29	1.12	6
1,2,3,5-TeCB	C_1	---	Gas	---	1326	---	---	---	---	---	---	4
	C_{18}	0.195	Liq[1]	---	---	9.150	26.79	1826.	---	---	---	5
	ØMono	0.0791	Liq[1]	---	---	1.532	11.06	783.9	---	---	---	5
1,2,4,5-TeCB	C_1	---	N_2	---	1326	---	---	---	---	---	---	4
	C_{18}	0.195	Liq[1]	---	---	8.708	25.50	1738.	---	---	---	5
	ØMono	0.0791	Liq[1]	---	---	1.820	10.97	747.8	---	---	---	5
PCB	C_1	---	N_2	---	1496	---	---	---	---	---	---	4
	C_{18}	0.195	Liq[1]	---	---	12.88	37.72	2571.	---	---	---	5
	ØMono	0.0791	Liq[1]	---	---	1.851	13.36	910.7	---	---	---	5
	Fish	---	H_2O	---	---	---	---	---	-8.17	3.82	12.0	6
	Octanol	---	H_2O	---	---	---	---	---	-8.03	-7.56	0.67	6
HCB	C_1	---	Gas	---	1656	---	---	---	---	---	---	4
	C_{18}	0.195	Liq[1]	---	---	19.40	56.84	3875.	---	---	---	5
	ØMono	0.0791	Liq[1]	---	---	2.318	16.74	1141.	---	---	---	5
	Fish	---	H_2O	---	---	---	---	---	-8.75	4.28	13.0	6

[1]liquid solution; 30% water and 70% acetonitrile
[2]retention index
[3]$K_{oc,n}$ normalized to 1,4-DCB data from natural soil (K_{oc} x 609.3/8.939 = $K_{oc,n}$)
[4]Sabjlic, 1985
[5]Hanai and Hubert, 1984
[6]Opperhulzen et al., 1988

2.3), since the enthalpy values are positive, whereas partitioning to octanol (from water) is driven both by the positive entropy and the negative enthalpy. For the series of chlorinated benzenes, the total sorption energies on fish fat (Table 2.3) are slightly smaller than the calculated sorption energies on organic carbon (Table 2.1).

2.1.5 Sorption Mechanisms in Natural Soil

Interactions with natural soil are more diverse than with model systems, since the combined mineral and organic surface is heterogeneous. The mineral surface may include silica, alumina, and carbonates coated with iron and magnesium oxides [*Sposito, 1984*]. Soil organic matter appears to coat mineral surfaces in a thin layer, since in one case, the surface area was 50 percent coated with organic compounds even with a small f_{oc} (2 percent) [*Thurman, 1985*].

Natural organic matter has a heterogeneous structure, with portions that are hydrophobic (aliphatic chains and benzene rings), and portions with hydrophilic functional groups. In one study, terrestrial fulvic acid had 3 to 4 aromatic rings for every 60 carbon atoms [*Thurman, 1985*]. Marine organic matter has a greater fraction of aliphatic chains versus aromatic groups. The amounts of functional groups vary; one sample of terrestrial fulvic acid contained 9.1 meq g^{-1} of carboxylic groups, 3.6 meq g^{-1} of alcoholic groups, 3.3 meq g^{-1} of phenolic groups, and 3.1 meq g^{-1} of ketone groups [*Matsuda and Schnitzer, 1971*]. Minor functional groups include enolic hydrogen, quinone, ether, aldehyde, ester, lactone, and amide [*Thurman, 1985*]. Natural organic matter is generally sorbed to mineral surfaces through hydrogen bonds [*Karickhoff, 1980*], oriented with a higher percentage of carboxylic and ionic groups in contact with water, minimizing hydrophobic surface area [*Matsuda et al., 1971*].

Organic solutes are attracted to natural or model surfaces with the interactions summarized in Table 2.4. The total energy for sorption from aqueous solution results in part from solvent effects, along with the surface interactions. The overall process of removal from aqueous solution and binding to a surface is referred to as sorption when the mechanism(s) are unknown or complex. This ranges from adsorption, involving

Table 2.4 Sorption mechanisms

Functional Group	*Binding Mechanism*
Amines, ring NH, heterocyclic N	Cation exchange
Amines, heterocyclic N, carbonyl, carboxylate	Protonation
Carboxylate	Anion exchange
Amino, carboxylate, carbonyl, alcoholic OH	Water bridging
Carboxylate, amines, carbonyl, alcoholic OH	Cation bridging
carboxylate	Ligand exchange
Amines, carbonyl, carboxyl, phenyl hydroxyl	Hydrogen bonding
Uncharged, nonpolar organic functional groups	van der Waals Interactions

(*Sposito, 1985*)

chemical bonds for more strongly held solutes, to physical adsorption for hydrophobic solutes. The solvent effect is altered with some hydrophobic solutes (containing aliphatic chains) that fold over themselves, resulting in a more compact structure with greater water solubility [*Tomlinson, 1975*].

The sorption of highly ionizable organic compounds decreases with higher bound organic content [*Zierath et al., 1980*] reflecting the decrease in available mineral surface. Sorption of ionic groups onto a hydrophobic surface change as a function of pH. As the pH decreases lower than the pK_a, acidic groups become neutrally charged and hydrophobic sorption increases, whereas the sorption of basic groups increases at high pH. In some cases, hydrophobic and ionic components of sorption can be combined in a single partition coefficient [*Karickhoff, 1984*], with K_{oc} and K_{ionic} fractions. Sorption of pesticides may involve more than one type of interaction, but comparison between sorption and total clay, mineralogy, cation exchange capacity, or surface area [*Hassett et al., 1980; Kahn et al., 1979*] shows an insignificant correlation. Sorption mechanisms can change as a function of pH. For example, a decrease in pH caused a significant increase in aromatic amine sorption [*Means et al., 1987*] due to the ionic form having a higher binding energy. Adsorption of benzidine (4,4-diamino biphenyl) is significantly greater at pH greater than 5.3, above both the pK_a's of the surface and the solute (both ionized), indicating H-bonding [*Zierath et al., 1980*]. However, the sorption of naphthol on natural organic matter was mainly due to hydrophobic interactions and not H-bonding of the OH group [*Hassett, 1981*].

Interactions of noncovalent organic solutes include coulombic attraction of oppositely charged ionized groups, hydrogen bonding between suitable donors and acceptors and hydrophobic interactions of nonpolar groups [*Horvath and Melander, 1978*]. Dipole interactions arise from a slight permanent dipole [*Blevins, 1982*]. Dipoles arise from a significant difference in electronegativity (but not large enough to ionize). Induced dipole interactions arise from synchronous orbits of electrons causing instantaneous dipoles [*Fressenden et al., 1982*]; this energy is about 2 kcal mol^{-1} [*Blevins, 1982*].

Hydrogen bonding is an especially strong dipole interaction between H bonded to N, O, or F, with an energy of 5-10 kcal mol^{-1} [*Fressenden et al., 1982*]. Interactions with solutes with many functional groups are largely unexplained. Adsorption of phthalates was mainly through the phenolic groups for short alkyl chains, but for longer alkyl chains hydrophobic interactions were more significant [*Matsuda and Schnitzer, 1971*]. The pesticide DDT binds to humic material by unknown mechanism(s) where pH, calcium concentration, and ionic strength affect binding [*Carter et al., 1982*].

2.2 Solute Transport

2.2.1 General Sorption Model

Transport and sorption in a porous media at the grain scale involves the physical and chemical rearrangement steps illustrated in Figure 1.1. Any of steps 2 through 4 could cause the observed slow approach to equilibrium. Other researchers have considered up to four rate steps (film diffusion, intraparticle diffusion, physical adsorption, and chemical adsorption) [*Rubin, 1983*].

Diffusion through immobile pore fluid has been reported to cause rate-limited sorption [*Rao et al., 1979; Wu and Gschwend, 1986*], as has diffusion through a bound organic layer [*Isaacson and Frink, 1984*]. The chemical binding and release rate has also been reported to cause slow sorption [*Leenheer and Ahlrichs, 1971*].

In a one-dimensional transport situation, three rate limiting steps in a series can be replaced by a single rate (analogous to series resistors), which gives rise to considering the overall process as one single rate. If one step is significantly slower than the other steps, then this is a valid assumption. The governing equation for one-dimensional solute transport in a porous media with both mobile and immobile regions and sorption in both regions is [*van Genuchten et al., 1974*]:

$$\theta_e \frac{\partial C_e}{\partial t} + \theta_i \frac{\partial C_i}{dt} + f \rho_b \frac{\partial S_e}{\partial t} + (1-f)\rho_b \frac{\partial S_i}{\partial t} = \theta_e D \frac{\partial^2 C_e}{\partial Z^2} - v \theta_e \frac{\partial C_e}{\partial Z} \qquad (21)$$

where C_e and C_i are the solute concentrations ($\mu g\, cm^{-3}$) in the mobile and immobile regions, respectively; S_e and S_i are the respective bound concentrations ($\mu g\, g^{-1}$); θ_e and θ_i are the volume fractions of the immobile and immobile liquid regions, ρ_b is the dry bulk density ($g\, cm^{-3}$) of the porous media, f is the fraction of sorbent in the mobile region, D is the longitudinal hydrodynamic dispersion coefficient ($cm^2 s^{-1}$), and v is the average interstitial velocity ($cm\, s^{-1}$).

Diffusion through the immobile region is approximated by slow mass transfer between mobile and immobile water. The solute concentration in the two regions can be related by:

$$\theta_i \frac{\partial C_i}{\partial t} + \rho_b (1 - f) \frac{\partial S_i}{\partial t} = \alpha_e (C_e - C_i) \tag{22}$$

where α_e is the mass transfer coefficient (s^{-1}), which is dependent on the solute molecule size (changes the molecular diffusion coefficient) and the geometry of the immobile region (which alters the diffusion distance and tortuosity) [*Coates and Smith, 1964*]. This can also be formulated with diffusion coefficients for planar diffusion, rectangular diffusion, spherical diffusion, and cylindrical diffusion [*van Genuchten, 1985*].

Diffusion through a bound organic layer is approximated by:

$$\rho_b \frac{\partial S_i}{\partial t} = \alpha_i (K_p C_i - S_i) \tag{23}$$

where α_i is the mass transfer coefficient through the bound organic layer. For this process to be the rate limiting step, the organic layer must be thick enough compared to the solute molecule so that movement through it could be approximated by a diffusion process rather than considering individual molecular forces at each point.

For kinetically limited sorption and desorption, assuming a first-order reversible reaction, and a linear isotherm (equation 1), the governing equation is:

$$\rho_b \frac{\partial S_i}{\partial t} = k_f \theta_i C_i - k_b S_i \tag{24}$$

where k_f and k_b are the first-order forward and reverse rate coefficients (s^{-1}), respectively.

The lower (exit) boundary condition is:

$$\frac{\partial C_e}{\partial z}\,(Z = \infty, t\,) \;=\; 0 \tag{25}$$

which states zero concentration gradient in the semi-infinite domain. A finite domain boundary condition (z = L) is more difficult to solve and there is no evidence that the solution leads to a better description of the physical process [*van Genuchten, 1981*].

The initial condition at the upper boundary is a constant flux type and within the column:

$$v\,C_e - D\,\frac{\partial C_e}{\partial Z} \;=\; \begin{cases} v\;C_0 & 0 < t < t_1 \\ 0 & t_1 < t \end{cases} \quad , \qquad C_e = C_i = 0 \tag{26}$$

where t_1 is the duration of time that a solute with concentration C_o is injected into the column. A constant concentration initial condition, although simpler, can lead to mass balance errors which are significant with high velocities [*van Genuchten, 1981*].

A general solution to all the above equations for the boundary conditions in a column experiment is not available. In addition, since slow mass transfer rates and reaction rates are analogous to series resistances, a unique set of parameters would be difficult to determine experimentally. Solutions are presented in cases where a single step is rate limiting.

In this research, three cases based on this general sorption model are considered: 1) slow transfer between the mobile and immobile pore fluid regions, 2) slow transfer through the bound organic layer, and 3) first-order chemical kinetics. In addition, several cases of no advective flow with a rate-limiting step are considered.

Making the substitutions for the variables (C_e, C_i, z, and t, K_p, D, α_e, and f) listed in Table 2.5, equation (21) reduces to:

$$\beta R_f\;\frac{\partial C_1}{\partial T} + (1-\beta) R_f\;\frac{\partial C_2}{\partial T} = \frac{1}{P}\;\frac{\partial^2 C_1}{\partial Z^2} - \frac{\partial C_1}{\partial Z} \tag{27}$$

Table 2.5 Nondimensional parameters

Model	C_1	C_2	T	Z	P	R_f	ω	β
Equilibrium	$\frac{C}{C_o}$	—	$\frac{tv}{L}$	$\frac{x}{L}$	$\frac{vL}{D}$	$1+\frac{\rho_b K_p}{\theta}$	—	—
First-order kinetic	$\frac{C}{C_o}$	$\frac{S}{K_p C_o}$	$\frac{tv}{L}$	$\frac{x}{L}$	$\frac{vL}{D}$	$1+\frac{\rho_b K_p}{\theta}$	$\frac{k_b \rho_b K_p L}{\theta v}$	$\frac{1}{R}$
Bound-organic diffusion	$\frac{C}{C_o}$	$\frac{S}{K_p C_o}$	$\frac{tv}{L}$	$\frac{x}{L}$	$\frac{vL}{D}$	$1+\frac{\rho_b K_p}{\theta}$	$\frac{\alpha_i \rho_b K_p}{\theta v}$	$\frac{1}{R}$
Immobile-fluid diffusion	$\frac{C}{C_o}$	$\frac{C_i}{C_o}$	$\frac{tv\theta_e}{\theta L}$	$\frac{x}{L}$	$\frac{vL}{D}$	$1+\frac{\rho_b K_p}{\theta}$	$\frac{\alpha_e L}{\theta_e v}$	$\frac{\theta_e + f\rho_b K_p}{\theta+\rho_b K_p}$
Series or Parallel Reactions	$\frac{C}{C_o}$	$\frac{C_i}{C_o}$	$\frac{tv}{L}$	$\frac{x}{L}$	$\frac{vL}{D}$	$1+\frac{\rho_b K_p}{\theta}$	$\frac{k_b K_P L(1-X_1)}{v\theta}$	$\frac{\theta + X_1 \rho_b K_p}{\theta+\rho_b K_p}$

where the dimensionless model parameters are retardation factor (R_f), Peclet number (P), ω (or Damkohler number N_D), and beta (β, the fraction factor). A single rate step (of equations 22-24) can be reduced to a dimensionless form by making the substitutions listed in Table 2.5:

$$(1-\beta)R_f \frac{\partial C_2}{\partial T} = \omega(C_1 - C_2) \tag{28}$$

Each potential rate limiting mechanism is discussed individually in the following sections. The solution to the above dimensionless equations is available in analytical form where a linear isotherm is assumed (equation 1), or in numerical form where a Freundlich isotherm is assumed (equation 8).

A one-dimensional transport system is used to determine sorption parameters. In this research, all columns are fully saturated with water, and the velocity is held constant throughout the experiment. The average interstitial velocity is determined by the volume eluted over time (equation 62), using porosity experimentally determined from bulk and solids density (equation 63), and confirmed with a conservative tracer breakthrough.

A pore volume is then defined as the column volume times porosity. Unsorbed tracer breakthrough occurs at one pore volume, whereas sorbed tracer breakthrough is lagged since some of the mass is sorbed to the soil. The retardation factor is defined as the number of pore volumes required before the average mass breakthrough occurs. This is expressed as the relative velocity of water to solute, or in terms of the partition coefficient, with:

$$R_f = \frac{v}{v_{solute}} = \frac{\rho_b K_p}{\theta} + 1 \tag{29}$$

where a retardation factor greater than one is due to sorption [*Lapidus and Amundson, 1952*].

2.2.2 Batch Sorption Models

Batch experiments represent closed systems, eliminating velocity and the velocity-dependent mechanical dispersion in the general sorption model. In principle, a slow approach to equilibrium can be studied more easily in a batch system, as there are fewer variables. Three batch cases are considered in this research, a first-order reversible reaction, spherical diffusion, and planar diffusion.

The change in the solute concentration in the liquid and in sorbed phases for a first-order reversible reaction (equation 6) in a closed system are described by the following differential equations:

$$\frac{\partial C}{\partial t} = k_b S - k_f C \qquad \frac{\partial S}{\partial t} = k_f C - k_b S \tag{30}$$

Starting with initial solute concentration (C_0) and final concentration (C_∞) in a solution of limited volume, the solution is:

$$\ln\left[\frac{C - C_\infty}{C_0 - C_\infty}\right] = -(k_f + k_b)\, t = -\zeta t \tag{31}$$

where C is the solute concentration at time t [*Stumm and Morgan, 1981*]. Plotting the ln [normalized concentration] versus time produces a slope (ζ), which is used with equation (9) to determine the forward and reverse rates with:

$$k_f = \frac{\zeta}{[\theta / K_p\, \rho_b + 1]} \qquad k_b = \frac{\zeta}{[\rho_b\, K_p / \theta + 1]} \tag{32}$$

The resulting sorption and desorption curves are not symmetrical unless the final concentration (C / C_0) is 0.5.

A spherical diffusion model is used to quantify the diffusion rate into aggregate particles, which are assumed spherical. The governing equation is Fick's second law in radial coordinates:

$$\frac{\partial C}{\partial t} = D\left[\frac{\partial^2 C}{\partial r^2} + \frac{2}{r}\frac{\partial C}{\partial r}\right] \tag{33}$$

which is reduced to a linear partial differential equation and solved with boundary conditions of limited total mass [*Crank, 1956; Carslaw and Jaeger, 1959*]:

$$\frac{M_t}{M_\infty} = 1 - \sum_{n=1}^{\infty} \frac{6\,\alpha(\alpha+1)\exp(-D\,q_n^2\,t\,/a^2)}{9+9\alpha+q_n^2\,\alpha^2} \tag{34}$$

$$where:\ \ \alpha = \frac{\theta}{\rho_b\,K_p},\ \ \frac{M_\infty}{VC_o} = \frac{1}{1+\alpha},\ \ \tan q_n = \frac{3\,q_n}{3+\alpha q_n^2}$$

where the solution is approximated with the first six terms. Note that the solution is similar in form to the chemical reaction (i.e. log concentration versus time, equation 31), but with more terms. The spherical diffusion model [*Crank, 1985*] is used to estimate the time to reach equilibrium concentration in an aggregate particle (Table 2.6). For 100 μm particles, the equilibration time was about 1 minute; for 500 μm particles, the value increased to about 1 hour, and for 2 mm particles, the value is about 6 to 10 hours. Slower diffusion is possible when the aggregate pore size is on the same scale as the molecule [*Larsson et al., 1982*], and the molecules cannot exhibit random motion. A numerical solution of spherical diffusion considering a range of diffusivities was developed [*Wu and Gschwend, 1986*] but leads to a single parameter for fitting.

A planar diffusion model is used to simulate diffusion through the bound organic layer in a batch experiment. The governing differential equation is Fick's second law in rectangular coordinates, and the solution in a vial of limited volume is:

$$\frac{M_t}{M_\infty} = 1 - \sum_{n=1}^{\infty} \frac{2\alpha(1+\alpha)\exp(-Dq_n^2\,t\,/L^2)}{1+\alpha+\alpha^2 q_n^2} \tag{35}$$

$$where:\ \ \alpha = \frac{\theta}{\rho_b\,K_p},\ \ \frac{M_\infty}{2AC_o} = \frac{1}{1+\alpha},\ \ \tan q_n = -\alpha q_n$$

This is mathematically very similar to the spherical diffusion model, however, the planar diffusion model produces a steeper slope of time versus concentration during the slow approach to equilibrium sorption.

Table 2.6 Diffusion times into aggregate particles

Particle Dia. (μm)	Time to Concentration at Particle Center (C/Co) 0.50 KCl (sec)	0.50 DCB (sec)	0.90 KCl (sec)	0.90 DCB (sec)	0.95 KCl (sec)	0.95 DCB (sec)	0.99 KCl (min)	0.99 DCB (min)
20	0.011	0.027	0.024	0.058	0.031	0.073	0.048	0.114
100	0.28	0.66	0.61	1.44	0.77	1.82	1.20	2.84
500	2.00	16.6	15.2	36.1	19.2	45.6	30.0	71.0
2000	112.2	265	244	578	308	732	480	1134

Batch experiment results may not be comparable to column results due to several factors: the effect of partitioning into dissolved organic matter, the breakdown of particles moving in batch vials [*Wu and Gschwend, 1986*], and the pressure in column experiments.

2.2.3 Equilibrium Solute Transport Model

2.2.3.1 Description and Parameter Sensitivity

Using the general sorption model formulation (equations 21-24) and making the assumption that all of the rate processes are fast compared to the residence time in the flow system, the overall transport equation reduces to the equilibrium solute transport equation:

$$R_f \frac{\partial C}{\partial t} = \theta D \frac{\partial^2 C}{\partial Z^2} - \theta v \frac{\partial C}{\partial Z} \tag{36}$$

Sorption is described by the partition coefficient (equation 29). The equilibrium formulation of sorption is widely used in 2- and 3- dimensional models due to its simplicity [*Rao and Jessup, 1982*]. Making the nondimensional substitutions listed on Table 2.5 for the equilibrium model, and assuming N_D is 0 (no rate limitations), this dimensional equation reduces to equation (27) where N_D is 0, and β is 1.0.

This equilibrium model has two parameters, the partition coefficient (K_p) and the dispersion coefficient (D). The effect of the parameters on a breakthrough curve is illustrated in Figure 2.4A. The partition coefficient (or retardation factor) affects the time required before solute is eluted from the column (Figure 2.4A). The retardation factor is equal to the average mass breakthrough point, or the area in front of the breakthrough curve. Since concentration changes twice in the course of an experiment (from C / C_0 = 0.0 to 1.0 and back to 0.0), two separate retardation factors (and K_p's) can be obtained. For the breakthrough curve were R_f is 1, the two retardation factors are equal to area A and D in Figure 2.4A.

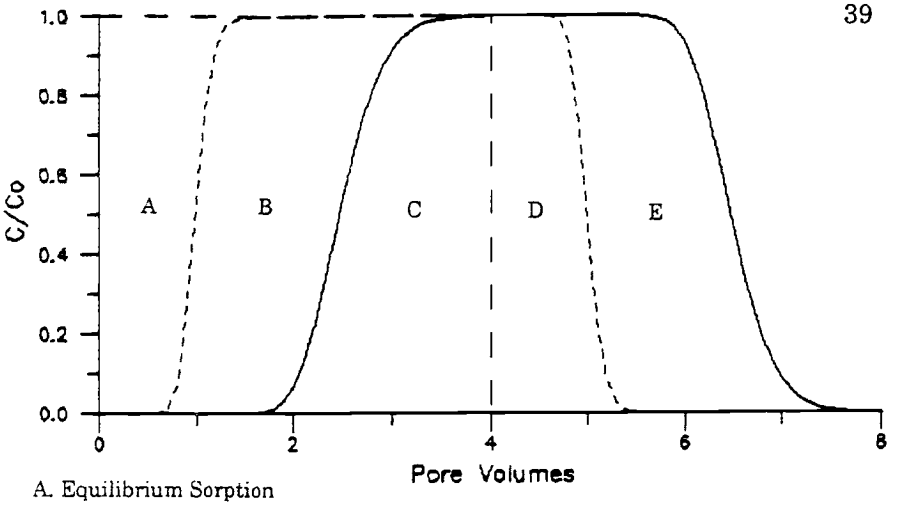

A. Equilibrium Sorption

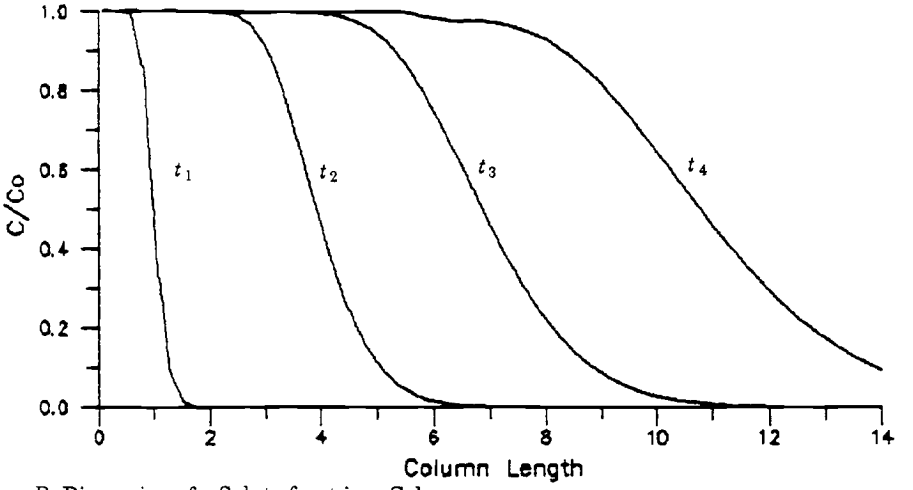

B. Dispersion of a Solute front in a Column

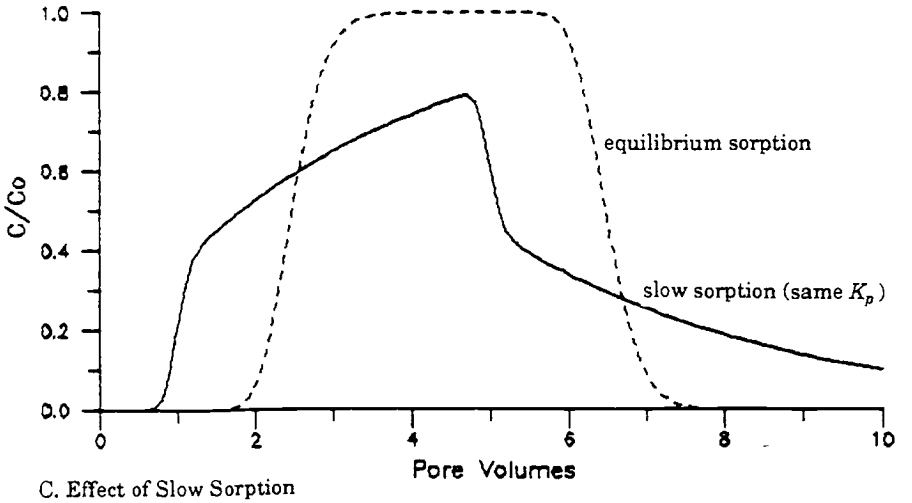

C. Effect of Slow Sorption

Figure 2.4 Solute breakthrough curves

Dispersion affects the spread of the solute in the column. In the absence of dispersion, breakthrough curves would instantly change concentration from 0 to 1 as governed by the partition coefficient. At any point in time, dispersion symmetrically spreads the sharp solute input (illustrated in Figure 2.4B). Dispersion is a function of time, so at later times, the observed spreading is greater. Therefore, solute elution from a column exhibits slightly asymmetrical breakthrough (Figure 2.4A), since there is more spreading at later elution times. This is analogous to the Doppler effect with sound waves. The slightly asymmetrical breakthrough curve produces a retardation factor that is not exactly equal to solute breakthrough at the 50 percent concentration point (C/C_0), but skewed past it. The breakthrough curves also are used to estimate sorption reversibility (or hysteresis) and the overall mass balance of the experiment. The sorption retardation factor (area A + B in Figure 2.4A) and the desorption retardation factor (area D + E) are equal for reversible sorption. The area under the sorption curve (area C + D + E) equals the injection area (A + B + C) when there is no mass loss in the system, including irreversible sorption.

Dispersion is not explicitly estimated in liquid chromatography, but reported in terms of a ratio of dispersion to retention, or plate height. Plate height is defined as the distance over which mobile phase solute and sorbed solute are in equilibrium [*Giddings, 1965*]:

$$H = \frac{w_{10}}{K'} \tag{37}$$

where dispersion is approximated by the peak width at 10 percent height (w_{10}). H is expressed in terms of a length and is about 20-100 μm for 5-10 μm particles, and is longer for larger particles [*Macherey-Nagel, 1987*]. In hydrologic terms, optimum peak height (minimum spreading) occurs at low velocity where mechanical dispersion is minimized, but not so slow that molecular diffusion becomes significant ($D/D_0 = 1$).

A slow rate process (or nonequilibrium) adds to the observed spreading, as shown in Figure 2.4C where increased spreading is due to incomplete sorption. The retardation factor is still equal to the mass-area in front of the solute breakthrough curve for sorption and desorption [*Jacobsen et al., 1984*]. The area under the breakthrough curve is still equivalent to the injected mass, demonstrated in Figure 2.5 for eight orders of magnitude of varying amounts of nonequilibrium. The dip in the breakthrough area shown in Figure 2.5 was caused by numerical error in calculating the breakthrough area, and can be eliminated.

The importance of nonequilibrium sorption on solute breakthrough is dependent on the transport time through the column. Assuming a first-order reversible reaction is the rate limiting step, the approximate ratio of residence time of a solute in the column to the reaction half-life is expressed as the Damkohler number [*Bahr and Rubin, 1987*]:

$$N_D = \frac{(L/v)(\rho_b K_p/\theta)}{1/k_b} \tag{38}$$

where (L/v) is a conservative tracer residence time, $(\rho_b K_p/\theta)$ is equal to v/v_{solute} (or R_f - 1; equation 29), so this product is the residence time of a solute, and $1/k_b$ is approximately the reaction half-life (equation 12). When N_D is 1.44, the solute residence time is exactly equal to reaction half-life.

2.2.3.2 Hydrodynamic Dispersion

Since both hydrodynamic dispersion and a slow rate process produce spreading of a breakthrough curve, in order to obtain an accurate estimate of the sorption rate, the hydrodynamic dispersion must be well defined. Solute molecules transported through a porous system are subject to molecular diffusion in solution and mechanical mixing due to the media geometry. Spreading caused by mechanical dispersion through a porous media can be due to: 1) velocity variation within a pore (zero velocity at walls), 2) tortuosity or difference in true path length, 3) difference in flow in pores of different size, 4) interconnected paths, 5) turbulence, and 6) immobile pore volume diffusion or eddys.

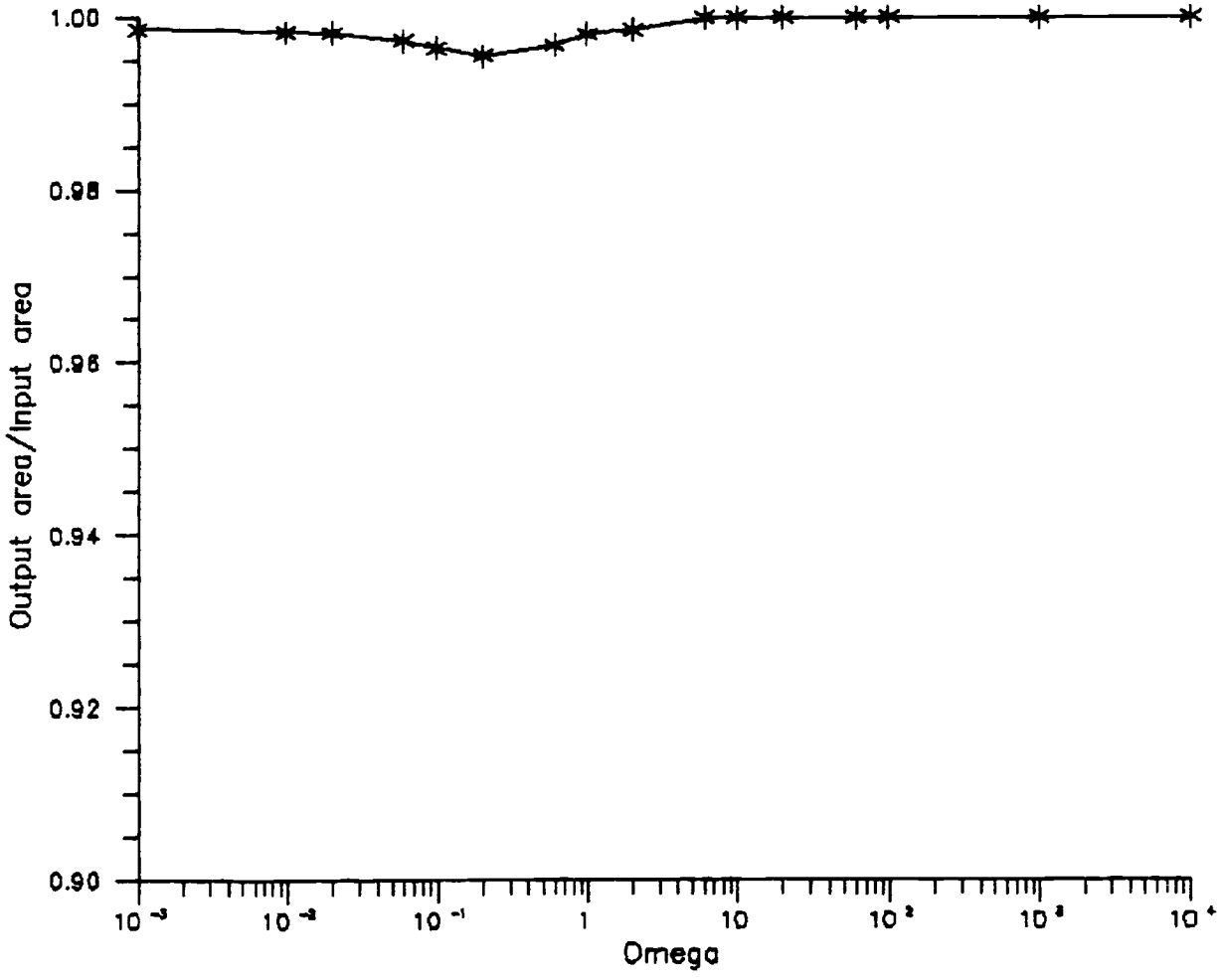

Figure 2.5 Mass balance at different reaction rates

At best, hydrodynamic dispersion is estimated with empirical relationships or by stochastic methods. Hydrodynamic dispersion is normalized with the Brenner number, or the previously defined column Peclet number ($P=vl/D$), where l is the column length [*Rose, 1977*]. Molecular diffusion is normalized with the Peclet number ($P^* = vd/D_o$), where d is the particle diameter.

The stagnant-phase slow mass transfer has been divided up into external film diffusion and internal immobile pore volume diffusion [*Snyder and Kirkland, 1979*] for modeling purposes. This is analogous to a two resistance diffusion model used in engineering [*Weber and Wang, 1987*]. Eddy viscosity is defined as turbulent transfer of momentum by eddies, giving rise to internal fluid friction; this is analogous to molecular viscosity in laminar flow, but at a much larger scale. The coefficient is about 10^{-4}, or 10^5 times the molecular kinematic viscosity [*CRC, 1980*]. Diffusion in internal pore volume is modeled with a simple diffusion equation with the modification of tortuosity factor (ratio of diffusion in porous medium/free liquid) which varies between 0.5 and 0.8 [*Bear, 1979*], and averages 0.66 [*Marshall and Homes, 1979*].

The turbulence effect on dispersion refers to the nonlaminar flow regime where different relationships exist describing spreading. The Reynolds number [*Bird et al., 1960*] describes the ratio of internal to viscous forces. When the Reynolds number is small (<10) flow is laminar and linear; when the Reynolds number is large ($10 < Nr < 100$) flow is laminar but nonlinear, and above 100, flow is turbulent. The Reynolds numbers for experiments in this research ranged from 0.002 to 0.24, and are thus within the linear, laminar range.

At intermediate velocities, pore-size variation and immobile phase diffusion processes produce the most spreading compared to other processes, whereas at high velocity, immobile phase diffusion is the largest portion of hydrodynamic dispersion [*Giddings, 1965*), based on empirical estimates of these processes.

Hydrodynamic dispersion increases non-linearly with temperature. Molecular diffusion increases with increasing temperature (equation 39); viscous shear forces and,

consequently slow mass transfer in stagnant fluids then decrease at increased temperature. Other researchers [*Wu and Gschwend, 1986*] predict an increase in hydrodynamic dispersion with increasing temperature. Dispersion increases with temperature when molecular diffusion is the largest term (low velocity) or in gas transport systems (gas chromatography) [*Conder and Young, 1979*] where molecular diffusion is five orders of magnitude greater than mechanical dispersion.

2.2.3.2.1 Molecular Diffusion

Molecules exhibit random motion as a function of internal energy (related to absolute temperature) and their ability to transfer this energy into motion (related to molecular size). This random motion can be described with a diffusion coefficient as defined by the Stokes-Einstein equation [*Bird et al., 1960*]. An approximation of the Stokes-Einstein equation for nonspherical molecules in liquid solution can be made with the Wilke-Chang equation:

$$D_o = \frac{5.062 x\ 10^{-7}\ T}{V_a^{0.6}} \tag{39}$$

where D_o is the molecular diffusion coefficient, T is temperature (°K), and V_a is the molar volume at normal boiling point. Constants for water are included in equation (39). Molar volumes are estimated by addition of fractions of molecules [*Welty et al., 1976*]. The accuracy of the Wilke-Chang equation is about 5 percent. This relationship shows that diffusion increases with molecular weight and temperature.

A case where diffusion into spherical particles is incorporated into hydrodynamic dispersion has been analytically solved [*van Genuchten, 1985*]:

$$D_{total} = \phi\ D_{mobile} + \frac{(1-\phi)\, a^2 v^2 R_{im}^2}{15 D_a\, [\phi R_m + (1-\phi) R_{im}^2]} \tag{40}$$

where D_{total} is the mobile phase hydrodynamic dispersion, D_{total} is the total spreading observed (in the mobile and immobile pore fluid regions), ϕ = fraction mobile porosity (θ_e/θ), R is retardation factor (R_f) in the immobile region (i) or mobile region (e), and

D_a is the diffusion coefficient in the porous particle ($D_o\,\tau$).

The effect of diffusion in the immobile pore space (equation 40) on hydrodynamic dispersion is shown in Table 2.7A. This illustrates several points; first, dispersion is theoretically different for molecules with a different molecular weight, since the ratio of dispersion coefficients is not equal to 1.0 in all cases (values range from 1.1 to 2.0). Secondly, the additional dispersion is greater with larger particles which require a longer time to reach equilibrium. For example, the D_{TeCB}/D_{KCl} ratio is 1.01 for 20-μm particles compared to 2.1 for 2-mm particles. Lastly, this effect is greater for solutes with a larger difference in diffusion coefficients, as shown with the D_{TeCB}/D_{KCl} ratios being larger than the D_{DCB}/D_{KCl} ratios.

Other aggregate geometries have also been solved analytically [*van Genuchten, 1985*] including rectangular, hollow cylindrical, and solid cylindrical cases. Diffusion in immobile pores assumes a monocontinuum [*Parker and Valocchi, 1986*], ignoring cases when the pore size is as small as the molecule, where a diffusion model fails to explain some observations at the molecular scale [*Davidson et al., 1981*]. In this research, the smallest pores could exclude some solute molecules.

2.2.3.2.2 Mechanical Dispersion

The processes of mechanical dispersion are combined with molecular diffusion to describe hydrodynamic dispersion in its most widely used form in transport models [*Freeze and Cherry, 1979; Bear, 1979*]:

$$D = D_o + D_l\, v^N \tag{41}$$

where D_o is the molecular diffusion, v is the average interstitial velocity, and D_l s the mechanical dispersion coefficient (or dispersivity), and N is an exponent generally equal to 1. As velocity increases, hydrodynamic dispersion increases, but mechanical dispersion in this case is assumed constant.

At typical ground water velocities, molecular diffusion is small compared to mechanical dispersion, and hydrodynamic dispersion is assumed linearly dependent on

Table 2.7 Calculated hydrodynamic dispersion

Particle Dia.(μm)	Calculated Dispersion						Dispersion Ratio				
	D_{KCl}	D_{CB}	D_{DCB}	D_{TCB}	D_{TeCB}	D_{PCB}	$\frac{D_{CB}}{D_{KCl}}$	$\frac{D_{DCB}}{D_{KCl}}$	$\frac{D_{TCB}}{D_{KCl}}$	$\frac{D_{TeCB}}{D_{KCl}}$	$\frac{D_{PCB}}{D_{KCl}}$
Table 2.7A. Hydrodynamic Dispersion with Spherical Diffusion[1]											
20	.0012	---	.0012	.0012	.0012	---	---	1.00	1.00	1.01	---
100	.0013	---	.0014	.0014	.0014	---	---	1.08	1.09	1.11	---
500	.0043	---	.0070	.0074	.0078	---	---	1.60	1.70	1.80	---
2000	.052	---	.094	.11	.11	---	---	1.80	1.95	2.06	---
Table 2.7B. Hydrodynamic Dispersion for Unsorbed Transport through Aggregates[2]											
20	.00015	.000071	.00023	.00024	.00025	.000095	1.18	1.51	1.58	1.64	1.33
100	.00014	.00063	.0024	.0025	.0026	.0013	1.64	1.76	1.85	1.94	2.03
500	.016	.0098	.032	.034	.036	.024	1.92	1.95	2.07	2.19	2.50
2000	0.17	0.13	0.36	0.40	0.41	0.35	2.04	2.11	2.26	2.40	2.70
Table 2.7C. Hydrodynamic Dispersion with Fast Sorption[3]											
20	.0011	.0011	.00098	.0023	.010	.017	0.58	0.89	2.14	9.32	14.3
100	.0023	.0016	.0031	.0045	.012	.017	0.95	1.36	1.96	5.38	9.07
500	.017	.011	.032	.034	.042	.046	1.78	1.88	1.96	2.42	2.75
2000	0.17	0.13	0.36	0.36	0.37	0.40	2.03	2.10	2.11	2.15	2.21
Table 2.7D. Hydrodynamic Dispersion with Slow Sorption[3]											
20	.0011	---	0.30	0.14	.050	---	---	267	127	45.1	---
100	.0023	---	0.30	0.14	.052	---	---	128	61.7	22.5	---
500	.017	---	0.33	0.17	.085	---	---	18.9	10.1	4.93	---
2000	0.17	---	0.66	0.53	0.46	---	---	3.80	3.06	2.67	---
Average for 100 μm Particles							1.3	1.5	1.9	3.7	5.6

[1]Using equation (52)[Parker and Valocchi, 1986]

[2]Using equation (54)[Horvath and Lin, 1976]

[3]Using equations (54) and (55)[Horvath and Lin, 1976 and 1978]

velocity. When modeling solute transport, the dispersive flux is considered to be linearly related to the concentration gradient, a form which is similar to Fick's Law describing a linear relationship between diffusive flux and the concentration gradient [*Kirkham and Powers, 1971*]. Dispersion is a scale-dependent parameter, because it averages different processes at different scales, and is not linearly related to concentration gradient. The similarity to Fick's Law is more or less accidental [*Scheidegger, 1960*], and is not accurate for all situations.

In a study of several hundred column experiments with natural soils [*Rose, 1977*], it was determined that hydrodynamic dispersion is better described with the exponent (N) equal to 1.0 to 1.5. Aggregate particles (359 experiments) had an average N of 1.11. Higher-order power-series expressions for hydrodynamic dispersion were developed for model particles, but it was concluded that for natural particles, equation (41) models the dispersion equally well. In addition, many of the parameters could not be determined for natural particles since they were not constant.

Chromatography researchers use porous aggregates and combine interparticle spreading processes into a single term, eddy diffusion, by assuming uniform pore sizes and path lengths, which is somewhat invalid even with chromatographic particles [*Snyder and Kirkland, 1979*]. Additional mechanical spreading is due to surface diffusion and diffusion within immobile pore fluid.

Spreading of unsorbed solutes is estimated by combining a series of empirical equations that describe molecular diffusion, eddy diffusion, surface (film) diffusion, and immobile-pore-volume diffusion [*Horvath and Lin, 1976 and 1978*]. This analysis assumes that processes are linear, so solutions are additive:

$$D = D_o + \frac{\lambda v\, d_p}{\gamma[1+w(v\, d_p/D_o)^{-1/3}]} + \frac{w\phi^2\theta_i\,(v\, d_p)^{5/3}}{9\gamma D_o^{2/3}(1+k_o)^2} + \frac{k_o\, v^2 d_p^2}{30\tau D_o\,(1+k_o)} \qquad (42)$$

where the terms account for molecular diffusion, eddy diffusion, film resistance, and intraparticle diffusion, respectively. The purpose of using this equation is to

demonstrate that different molecules have different characteristic dispersion coefficients in the same porous media. This equation accounts for more processes than just spherical diffusion (equation 40).

The eddy-diffusion term resulted from estimates by *van Deemter* and others [*1956*] where w is an obstruction factor (averaging 2.75), γ is an empirical parameter (0.6), λ is a spreading factor (1.0), and d_p is the effective particle diameter. Film resistance is based on a free-surface model [*Pfeffer et al., 1964*], where θ_i is the intraparticle porosity (0.46), θ_e is the interparticle porosity (0.40), k_o is a porosity factor ($\theta_i(1-\theta_e)/\theta_e=1.15$) [*Horvath and Lin, 1976*] and ϕ is the pore volume accessible to solute molecules (1.0). The intraparticle diffusion term is an empirical estimate of spherical diffusion where τ is the tortuosity.

Estimates of hydrodynamic dispersion are calculated with equation (42) for an ionic tracer and for chlorinated benzenes (Table 2.7B), using realistic values for real and empirical parameters. The calculated dispersion coefficients are larger for compounds with greater molecular weight, than for smaller compounds. The D_{solute}/D_{KCl} ratios (1.5 to 2.8) are larger than those in Table 2.7A where only immobile pore volume diffusion was considered (1.0 to 2.1). With larger particles, the D_{solute}/D_{KCl} ratio becomes larger (Table 2.7B), reflecting a greater amount of intraparticle diffusion. At this velocity, however, the eddy diffusion term was the largest.

2.2.3.2.3 Slow Rate Process and Dispersion

For some cases, slow rate process spreading can be included into dispersion, and transport could be modeled with an equilibrium transport model [*Parker and Valocchi, 1986*]. The purpose of including chemical kinetic spreading in dispersion is to demonstrate the effect a slow rate process has on a breakthrough curve, noting that for proper analysis of the processes, a slow intra-aggregate process must be separated from mobile-phase dispersion.

Assuming a first-order reversible reaction with a kinetic parameter, k_b, and partition coefficient, K_p, *Horvath and Lin (1978)* have developed an additional term accounting for spreading due to slow sorption:

$$D_{kinetic} = \frac{2[1 + (\rho_b K_p / \theta)]\, v^2}{(1 + k_o)(2 + \rho_b K_p / \theta)^2 k_b} \tag{43}$$

Two sets of calculated dispersion coefficients are presented in Table 2.7 which include sorption (combining equations 42 and 43). In Table 2.7C, a fast reaction is assumed (N_D = 100), and the D_{solute}/D_{KCl} ratios are approximately equal to the cases where sorption is not taken into account (Table 2.7B). Averaging the D_{solute}/D_{KCl} ratios from Table 2.7B and C for 100-μm particles results in 1.3 for chlorobenzene, 1.5 for dichlorobenzene, 1.9 for trichlorobenzene, 3.7 for tetrachlorobenzene, and 5.6 for pentachlorobenzene.

A case of sorbed solute dispersion where a slow reaction is assumed is presented in Table 2.7D (N_D = 1). The substantial increase in the dispersion of the solute is due to spreading caused by the slow reaction. These dispersion coefficients are about two orders of magnitude larger for solutes compared to other cases (Table 2.7A-C) that do not include the effect of a slow rate process. The D_{solute}/D_{KCl} ratios are also substantially greater for smaller particles, compared to cases where fast sorption was assumed (Table 2.7C). This analysis shows that if all of the spreading was modeled as dispersion (with an equilibrium transport model), the D_{solute}/D_{KCl} ratio can be used to evaluate the effect of the slow rate process. A substantial increase in the ratio of dispersion coefficients for a solute/ion ratio greater than about 1.5 can be attributed to kinetic effects. This approach has been qualitatively used for looking for cases of nonequilibrium [*Valocchi, 1985*].

The dispersion coefficient should include only hydrodynamic dispersion, but for a limited change in experimental conditions, a change in a slow kinetic rate has the same effect as a change in dispersion [*van Genuchten and Cleary, 1979*], as shown in Figure 2.4. Three cases of nonequilibrium sorption are quantitatively analyzed with an

equilibrium model in Figure 2.6. These cases are equilibrium sorption (N_D = 100), some slow sorption (N_D = 10), and slow sorption (N_D = 1.0). The three cases are equivalent to a single slow sorption process in which velocity is increased an order of magnitude in successive cases. The equilibrium model fits some of the data well (N_D = 100 and 10), but does not fit the slow sorption data (where N_D = 1.0).

In the case of considerable nonequilibrium sorption, the equilibrium model cannot account for the behavior, and more importantly, cannot predict this phenomena. The case of considerable nonequilibrium (N_D = 1.0) cannot be fit with the equilibrium model by changing dispersion (model fit 3), or even by altering K_p (model fit 4). The partition coefficient is a constant for a soil/solute combination and does not change at different velocities. This example shows that an equilibrium sorption model cannot be used for accurate prediction of solute breakthrough when a slow rate process is involved.

2.2.4 First Order Model

2.2.4.1 Chemical Kinetics

If a reversible first-order reaction (equation 6) is the only rate limiting step (no diffusional limitations), then the general sorption model equations (21) and (24) reduce to:

$$\theta_e \frac{\partial C_e}{\partial t} + \rho_b \frac{\partial S_e}{\partial t} = \theta_e D \frac{\partial^2 C_e}{\partial Z^2} - v \theta_e \frac{\partial C_e}{\partial Z} \tag{44}$$

$$\rho_b \frac{\partial S_e}{\partial t} = k_b \rho_b [K_p C_e - S_e] \tag{45}$$

These equations reduce to the nondimensional equations (27) and (28) by making the substitutions for the parameters (C_e, C_i, z, t, K_p, D, and k_b) listed in Table 2.5. Omega (ω) in this model is equivalent to Damkohler number (equation 38).

This model has three parameters, where hydrodynamic dispersion (D) produces spreading and K_p produces a lag in the solute breakthrough time. The third parameter, k_b, produces a time-related spreading phenomena, more intuitively described with the dimensionless Damkohler number. When the Damkohler number is large (N_D > 100),

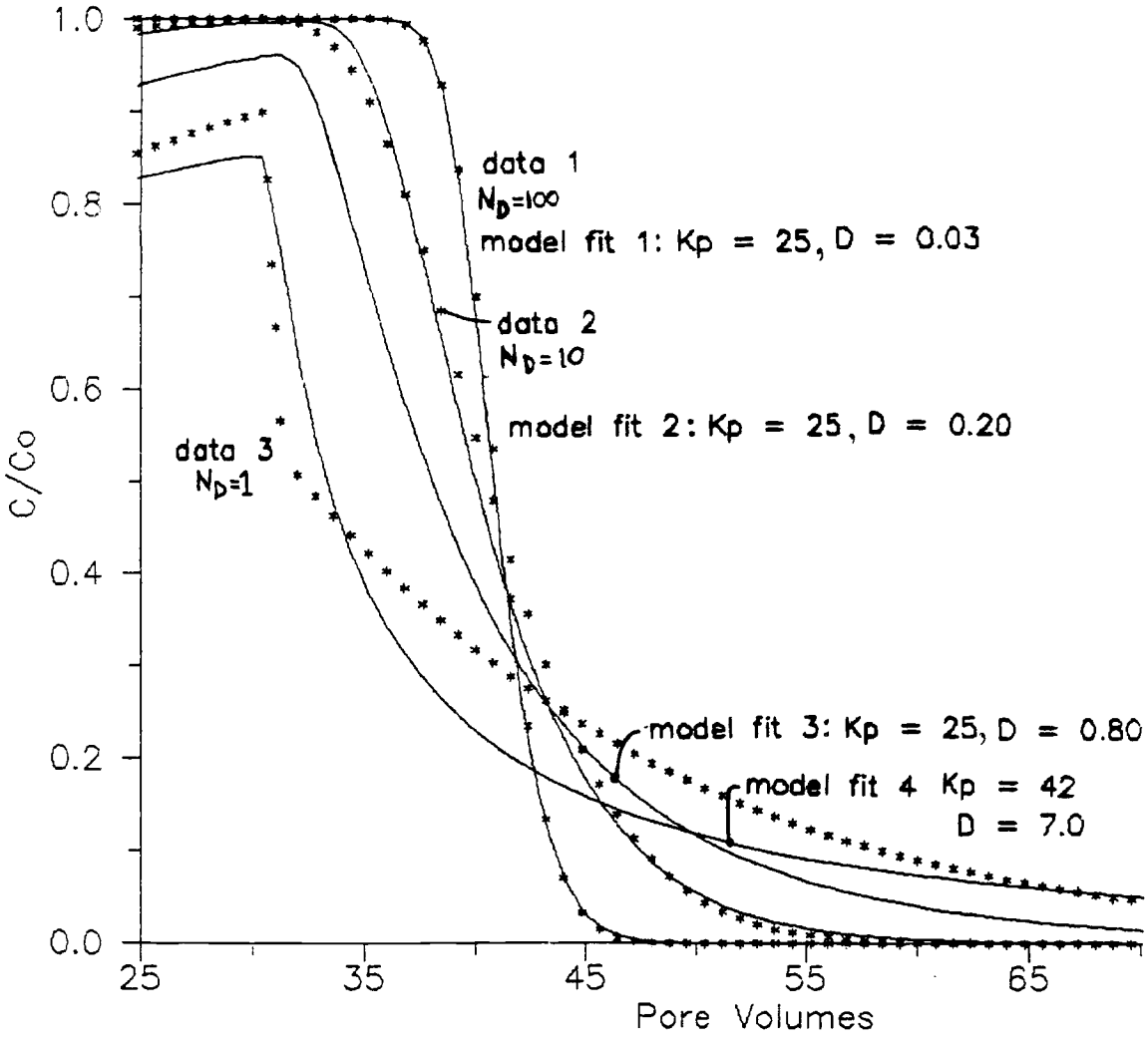

Figure 2.6 Equilibrium model fit to simulated nonequilibrium data

the reaction time is two orders of magnitude faster than residence time and the reaction is near equilibrium, as shown in Figure 2.7. When the reaction rate and residence time are about equal (N_D near 1.0), then only some of the solute reacts with the surface, and additional spreading results in the breakthrough curve. When the reaction is two or more orders of magnitude slower than the residence time ($N_D < 0.01$), then only a small portion of the solute reacts with the surface and the breakthrough curve is almost like that for a conservative tracer.

The first-order model parameters are also used to define the amount of observed nonequilibrium, as defined by Valocchi [*1985*] with the second central moment (E_2):

$$E_2 = \frac{v^2}{Dk_b} \left[\frac{\rho_b K_p / \theta}{[1+\rho_b K_p / \theta]^2}\right] \tag{46}$$

where $E_2 > 100$ indicates nonequilibrium (additional spreading). Skewness of a breakthrough curve indicates hysteresis and can be defined in terms of the third central moment (E_3) using first-order model parameters [*Valocchi, 1985*]:

$$E_3 = E_2 \left[1 + \frac{v^2}{Dk_b} \frac{1}{[2+2\rho_b K_p / \theta]}\right] \tag{47}$$

First-order model rates can also be determined with a plot of retardation factor versus plate height (equation 37) for cases of varying velocity. Increased spreading (and plate height) and the decreased retardation factor are used to define the reaction rate [*Chu and Langer, 1985*].

2.2.4.2 Diffusion through the Bound Organic Layer

If the slow mass transfer through a bound organic layer is the only rate limiting step, then the general sorption model equations (21) and (23) reduce to:

$$\theta_e \frac{\partial C_e}{\partial t} + \rho_b \frac{\partial S_e}{\partial t} = \theta_e D \frac{\partial^2 C_e}{\partial z} - v\theta_e \frac{\partial C_e}{\partial z} \tag{48}$$

$$\rho_b \frac{\partial S_e}{\partial t} = \alpha_i [K_p C_e - S_e] \tag{49}$$

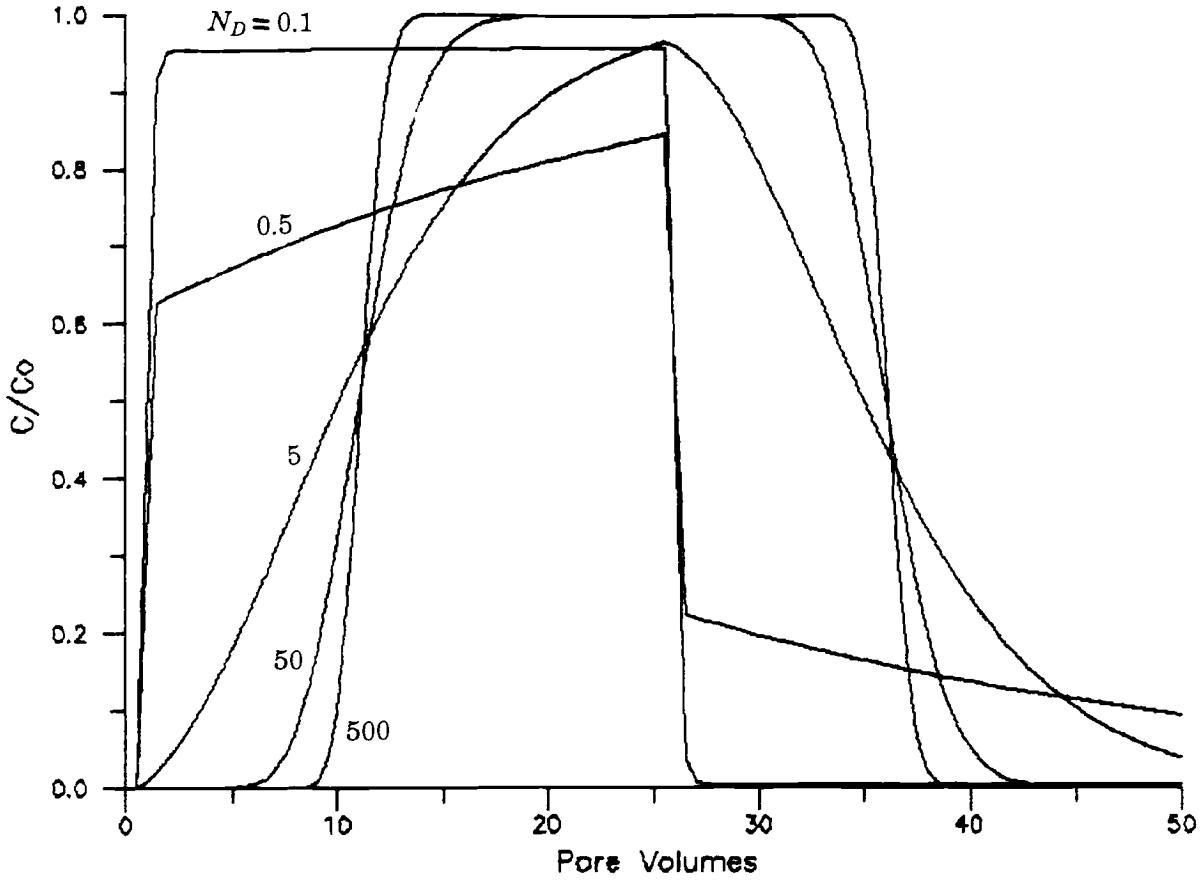

Figure 2.7 First-order model rate parameter effect on a breakthrough curve

where α_i is the mass transfer coefficient between liquid and sorbed phases. These equations are reduced to the general dimensionless equations (27) and (28) by making the substitutions listed in Table 2.5 (where $\beta = 1/R_f$). The solution is analytical with a linear isotherm (Section 2.2.6) or numerical with a Freundlich isotherm (Section 2.2.7). This model has three parameters (D, K_p, and α_i), where dispersion (D) controls the physical spreading, K_p controls the relative position in time of the breakthrough curve, and the additional term α_i (or dimensionless rate ω) produces a time-dependent spreading.

This model formulation is mathematically equivalent to the first-order chemical model where α_i is $\rho_b\ k_b$, so the effect of changing α_i is also illustrated in Figure 2.7. When the diffusion rate is on the same time scale as residence time, a large amount of spreading is observed ($N_D = 1$), whereas when the diffusion time is small compared to the residence time ($N_D = 100$), equilibrium sorption is observed.

2.2.4.3 Parameter Sensitivity and Estimation

The effect of changing the three parameters in the first-order model is illustrated in Figure 2.4 and Figure 2.7. Estimating the three parameters from a breakthrough curve may not produce a unique set of parameters. Independent determination of hydrodynamic dispersion must be made in order to properly separate dispersion from a slow rate process. The partition coefficient can be determined by integration of the area in front of the solute breakthrough curve, regardless of the extent of nonequilibrium, but is more accurate when near equilibrium (sharper breakthrough curve). This corresponds to an experiment run at low velocity. The first-order model fit produces a K_p assuming a linear isotherm with no hysteresis in sorption (no irreversible sorption), whereas the K_p determined from the area in front of a breakthrough curve does not assume an isotherm.

The observed spreading in the breakthrough curve must be separated into hydrodynamic dispersion and a slow rate process. The D_{solute}/D_{KCl} ratio (Table 2.7) is used

for this purpose, where the dispersion for the solute is fixed at a factor times D_{KCl}. Dispersion in the model fit now represents hydrodynamic dispersion and additional spreading is due to the slow rate process.

The third parameter, k_b, is best determined at a sufficiently high velocity such that the slow rate process has the greatest effect on the breakthrough curve (approximately N_D = 1). The sensitivity of the rate parameter (N_D) is illustrated in Figure 2.8 in a plot of average N_D versus the area between two N_D values. This shows the maximum area difference (greatest parameter sensitivity and lowest error in fit) occurs when N_D is equal to 1.44. This is where the solute residence time is equal to reaction half life (equation 38). Experimentally, the maximum effect of the slow sorption process is obtained by varying the velocity with the same sorbent/sorbate combination. Obtaining rate data from single experiments at different velocities are only accurate to 2 to 3 fold under the best conditions [*Chu and Langer, 1985*]. Multiple experiments run at different velocities are used to obtain a single rate parameter (in Section 5.3.3), which should provide more accurate rate data.

2.2.5 Two Region Model

The two-region model represents a case of slow diffusion through immobile pore fluid, and is mathematically equivalent to parallel or series reactions where one reaction is slow. This model has four parameters, including K_p, D, a rate parameter, and a fraction parameter.

2.2.5.1 Diffusion through Immobile Pore Fluid

Assuming that diffusion through immobile pore fluid is the only rate limiting step, the general sorption model (equations 21 and 22) reduces to:

$$[\theta_e + f\,\rho_b\,K_p]\,\frac{\partial C_e}{\partial t} + [\theta_i + (1-f)\,\rho_b\,K_p]\,\frac{\partial C_i}{\partial t} = \theta_e D\,\frac{\partial^2 C_e}{\partial z^2} - v\,\theta_e\,\frac{\partial C_e}{\partial z} \qquad (50)$$

$$[\theta_i + (1-f)\,\rho_b\,K_p]\,\frac{\partial C_i}{\partial t} = \alpha_e\,(C_e - C_i) \qquad (51)$$

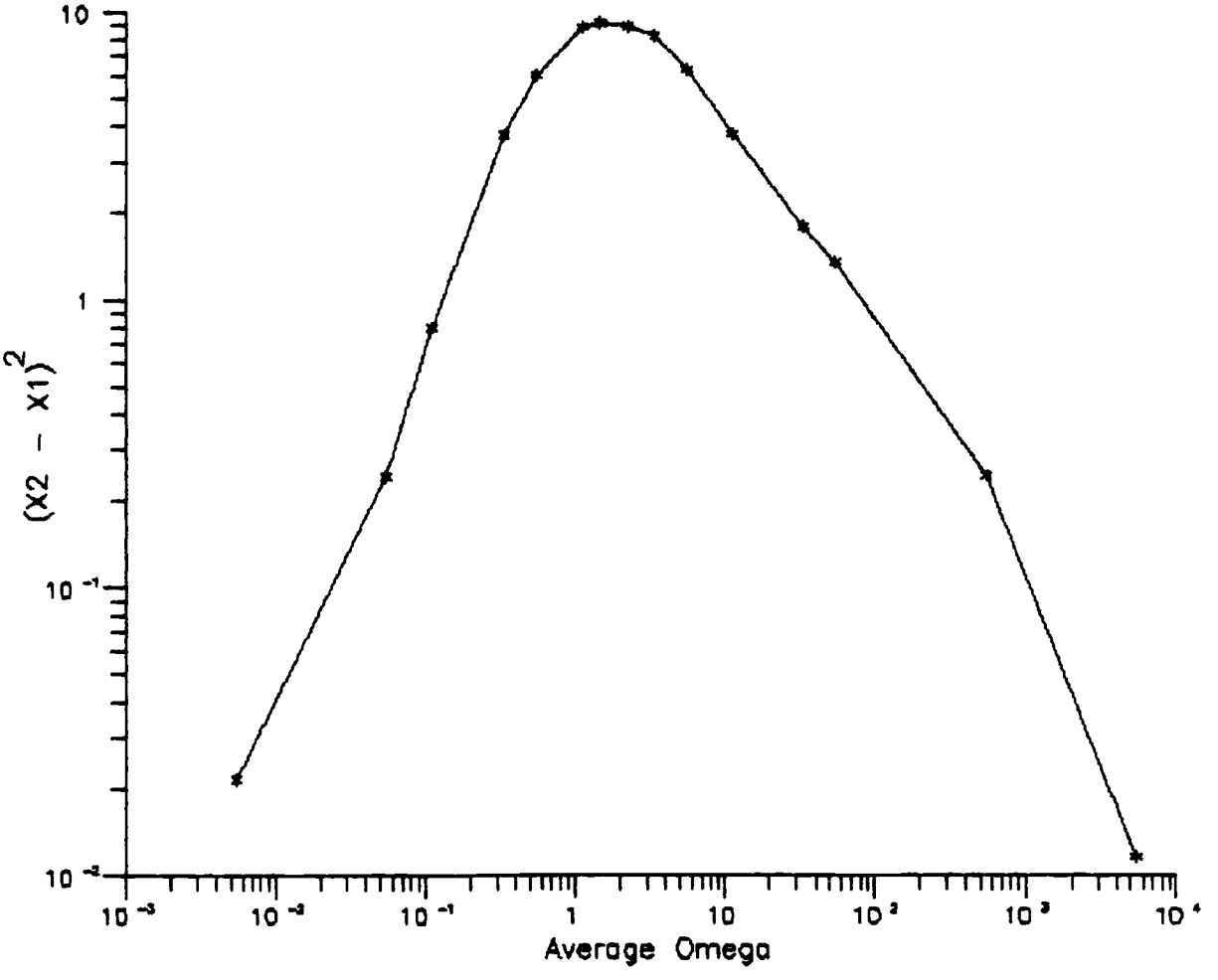

Figure 2.8 Rate Parameter sensitivity at different velocity

If the substitutions listed for a mobile/immobile model in Table 2.5 are made, the four model parameters are nondimensionalized into retardation factor (R_f), Peclet number (P), omega (ω), and beta (β), and equations (50) and (51) are reduced to dimensionless equations (27) and (28). This model was first formulated by *Coates and Smith [1964]* with no sorption, and by *van Genuchten and Wierenga [1974]* to account for diffusion through aggregate particles with sorption in mobile and immobile regions.

The parameters in this model differ from the previous model in that porosity is divided into mobile porosity (θ_e) and immobile porosity (θ_i), and D and α_e are calculated using mobile porosity rather than the total porosity. The fourth parameter, the fraction mobile sites (f), adds to the model ability to fit a breakthrough curve, compared to a first-order model. This model has been successfully used to model transport in cracked soil and in soil containing macropores where a large fraction of immobile region is present, and sorption occurs in mobile and immobile regions [*van Genuchten, 1981*].

The nondimensional equations (27 and 28) can also represent cases of diffusion through immobile fluid, where geometries of the aggregate particle can include spherical [*Parker and Valocchi, 1986*], planar, rectangular, hollow cylindrical, and solid cylindrical [*van Genuchten, 1985*]. Diffusion into spherical aggregates can be reduced from this two-region model to an equilibrium model where the slow rate process is included in the dispersion term (equation 40) [*Parker and Valocchi, 1986*].

2.2.5.2 Multiple Reactions

A case of an equilibrium reaction in parallel with a first-order reversible reaction:

$$S_1 \;<=>\; C \;\underset{k_b}{\overset{k_f}{\rightleftharpoons}}\; S_2 \qquad (52)$$

can be represented by the two-region model (equations 27 and 28) with the substitutions for the parameters listed in Table 2.5. The total sorbed concentration, S, is the sum of S_1 and S_2. In this case, K_p and D are as previously defined, k_b is the desorption rate coefficient for the slow reaction, and X_1 (the fraction parameter) represents the fraction

of fast reaction sites (that sorb to S_1). Formulation of equilibrium sorption in parallel with one or more kinetically influenced terms was made by *Bahr and Rubin [1987]*, where the nonequilibrium effects are also described in terms of a dimensionless rate parameter. Parallel reversible and irreversible reactions can be modeled with a first-order model and zeroeth order mass loss term [*Di Toro et al., 1982*].

A case of an equilibrium reaction occurring in series followed by a first-order reversible reaction:

$$C \;<=>\; S_1 \underset{k_b}{\overset{k_f}{\rightleftharpoons}} S_2 \tag{53}$$

is also solved with the two-region model making the substitutions indicated in Table 2.5. This model was formulated by *Karickhoff [1984]*. In this case, the total sorbed concentration (S) is the sum of S_1 and S_2, and the K_p for fast sorption sites is equal to 1. The parameters are the same as the parallel reaction case.

2.2.5.3 Parameter Sensitivity and Estimation

The two-region model has four parameters, K_p, D, a rate parameter, and a fraction parameter (f). The effects of dispersion and the partition coefficient on breakthrough curves are discussed with other models (Figure 2.4). The rate parameter has a similar effect to that of the first-order-model rate parameter (Figure 2.7). An example of the effect of varying ω, when f is 0.5, is shown in Figure 2.9A. The maximum sensitivity (or the fastest change) of the rate parameter occurs when ω is 1.44, as discussed earlier with the first-order model (Figure 2.7).

The fourth parameter, f, is the fraction of sorption sites in the mobile region and (1-f) is the fraction of sites in the immobile region. At a fixed value of f, variation of α_e is analogous to a first-order model where:

$$k_b' = \frac{\alpha_e}{\rho_b K_p} \tag{54}$$

Varying f (Figure 2.9B) shows little sensitivity, but mathematically when f is 0, this

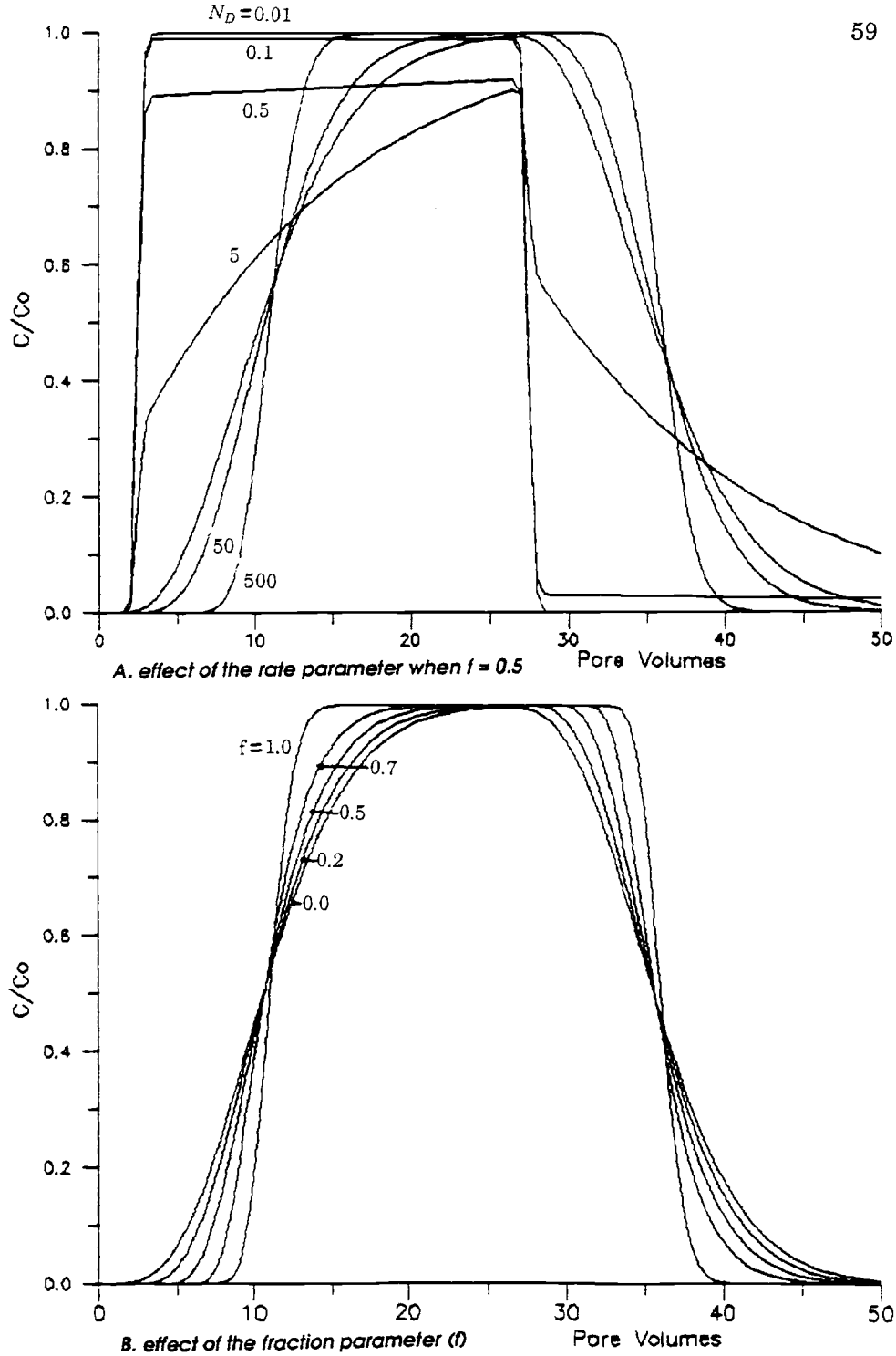

Figure 2.9 Two region model rate and fraction parameters

solution reduces to a first-order model, and when f is 1, this solution reduces to the equilibrium model.

Particles used in this research have an interparticle porosity (θ_e) of 0.40 and an intraparticle porosity (θ_i) of 0.46. Assuming that the sites are evenly distributed over the surface area, and noting that the external surface area is 1 percent of total surface area), then f is 0.01. If the bound organic material preferentially binds to the exterior of particles, then f may be larger than this value. If all of the organic material binds to the particle exterior, then f is 1.0. Since the distribution of the bound organic material on the surfaces used in this research is not known, f is used as a fitting parameter.

Since f can affect the breakthrough curve spreading, it should be independently determined. If the best estimate of f is small (near 0.0), then the first-order model can be used [*van Genuchten, 1985*]. If f is known, then t should be fixed, allowing α_e to be the only parameter that varies, since if both f and α_e are allowed to vary, a unique fit will not be determined. Reduction of this two-region model to a first-order model has been solved analytically [*van Genuchten, 1985; Parker and Valocchi, 1986*].

Since this two-region model can represent both physical and chemical slow approach to equilibrium, a single experiment cannot distinguish between these two cases [*Rao et al., 1979*], but rather experiments must be designed to alter the diffusion rate or chemical rate separately.

2.2.6 Analytical Solution - CFITIM

An analytical solution to the general sorption model (equations 27 and 28) with the listed boundary and initial conditions (equations 25 and 26) is available with a nonlinear-least-squares parameter-estimation routine (CFITIM; *van Genuchten, 1981*). A second program is also available with a more efficient routine for parameter estimation (CXTFIT; *Parker and van Genuchten, 1984*). Two boundary conditions are available, which lead to different solutions at fast velocities where the first boundary type leads to mass balance errors. The constant flux boundary condition (second type) is

used in this research. The analytical solution is accurate as long as the Peclet number is not too small (dispersion becomes large), as defined by:

$$P > \frac{5 + 5D\ vt}{l\ R_f} \tag{55}$$

For cases of smaller column Peclet numbers (0.1), the solution is only slightly in error.

The curve-fitting routine is designed to accept fixed values of the transport parameters or allow them to be altered iteratively to obtain a better fit. The goodness of fit is described by the sum of the squares of the difference between each data point and the model point (*ssq*).

Van Genuchten [1981] recommends using a small number of data points (15-30) to reduce the model iteration time, with an upper limit of 90 points. This does, however, require the subjective removal of data points. All points are treated with equal weight in the curve-fitting routine, so if fitting a portion of the breakthrough curve is more important, then the number of points in other portions of the breakthrough curve should be reduced. The curve-fitting routine may not converge to a solution if poor estimates of parameters are chosen, or may converge to a wrong solution. The best technique is to fix as many parameters as possible that can be independently determined, as discussed earlier.

2.2.7 Numerical Solution - MOB2

A finite-difference solution of the general sorption equations (27 and 28) is available with the listed boundary and initial conditions (equations 25 and 26), but with a Freundlich isotherm (equation 8) [*van Genuchten, 1979*]. This central-in-time finite difference solution was used with 100 nodes, each with a length of length 0.14 cm, to define a total column length of 14 cm. The finite difference stability condition:

$$\frac{D\,\Delta t}{(\Delta x)^2} < 0.5 \tag{56}$$

indicates that the time step could be as large as 4.0 sec; 1.0 sec is used in order to not

violate the Peclet and Courant conditions:

$$\frac{v\,\Delta t}{D} < 10 \tag{57}$$

$$\frac{v\,\Delta t}{\Delta x} < 1 \tag{58}$$

where the Courant number [*Daus et al., 1985*] defines the accuracy of the finite difference scheme. This leads to a large number of time steps (28,758) to simulate a breakthrough curve.

The finite difference solution (Freundlich exponent = 1) is compared to the analytical solution in Figure 2.10 where five cases of different Peclet numbers are simulated. At large Peclet numbers (300, 170, 100) where the analytical solution is slightly more accurate, the analytical and numerical solutions diverge. This may reflect a difference in the definition of the input variables. At small Peclet numbers (P = 10, 1) the solutions converged.

This model has an additional parameter, the Freundlich isotherm exponent (N). The effect of a nonlinear isotherm ($0.7 < N < 1.3$) on a breakthrough curve that exhibits slow sorption ($\alpha_e = 4 \times 10^{-4}\ s^{-1}$) is shown in Figure 2.11. When the exponent is smaller than 1.0, then at higher concentrations, less solute is sorbed. This situation is found when the number of sorption sites is limited. This case of less retardation of a solute at higher concentrations (N = 0.7) produces a steeper ascent of the breakthrough curve compared to the case for which N is 1. On the desorption part of the curve, more sorption at lower concentration leads to tailing. When N is greater than 1.0, then the greater sorption at higher concentrations leads to a less steep sorption curve. During desorption, less sorption at lower concentration leads to a steeper slope.

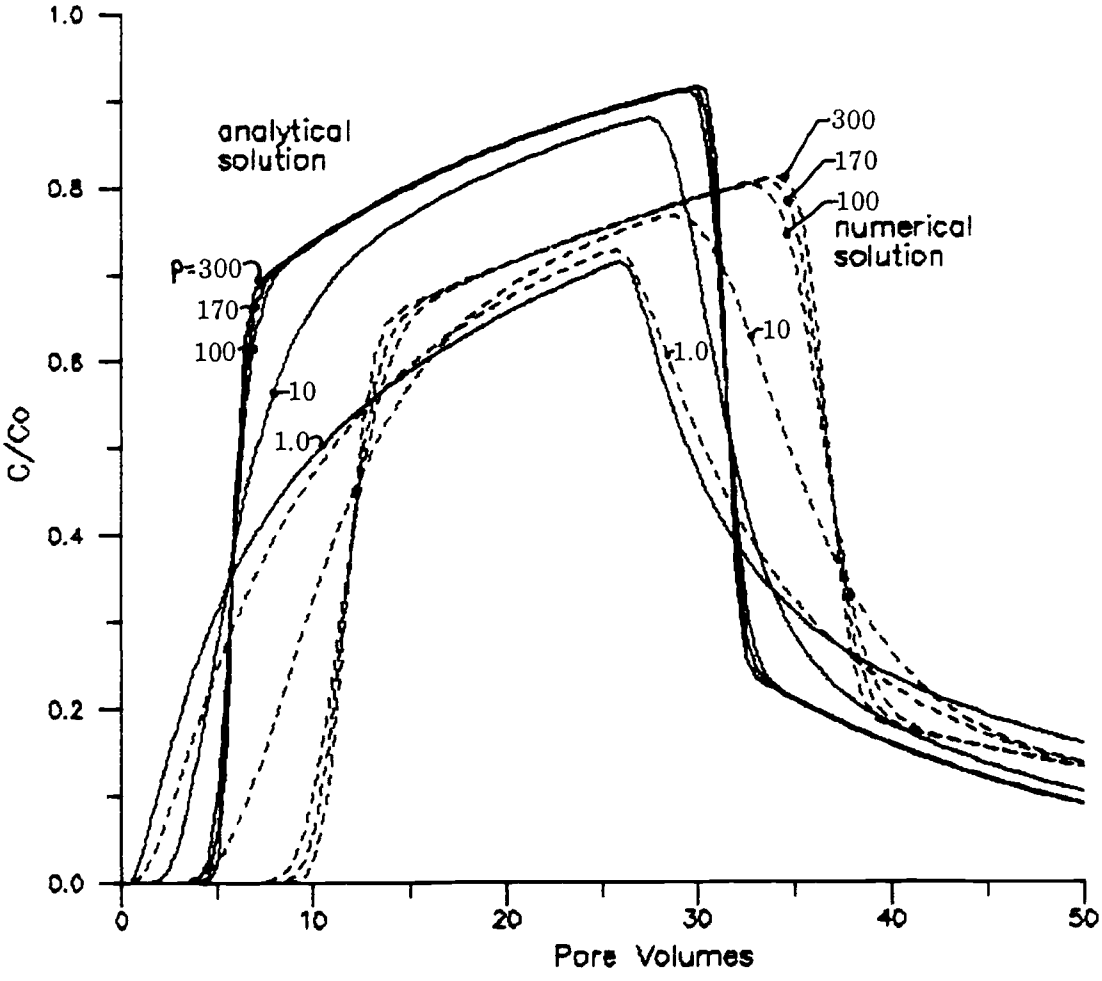

Figure 2.10 Comparison of analytic and numerical solutions

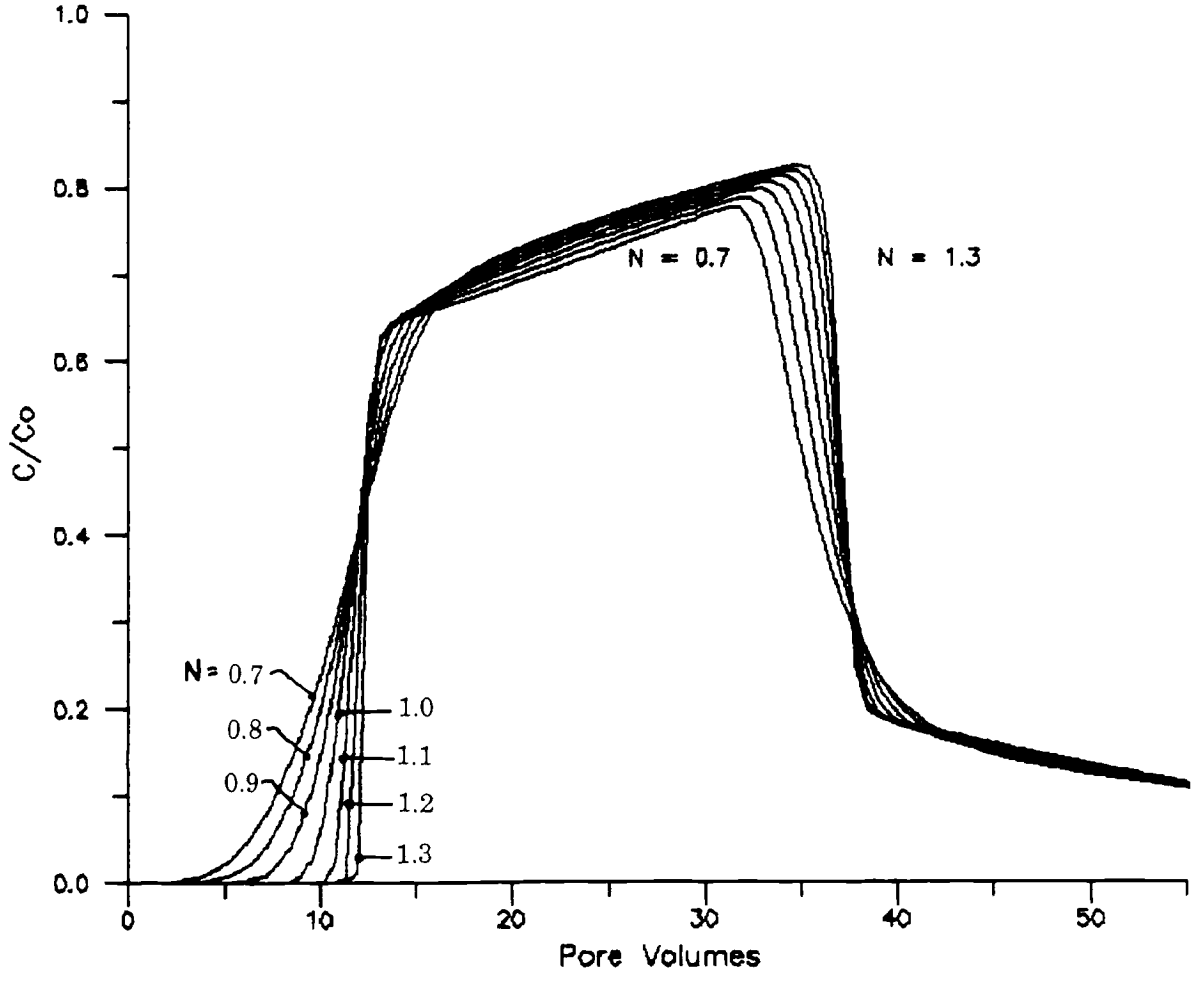

Figure 2.11 Effect of a nonlinear isotherm on a breakthrough curve

CHAPTER 3
MATERIALS AND METHODS

3.1 Experimental Approach

The observed slow sorption and desorption of solutes is considered to be caused by one of three possible rate limiting steps: diffusion through immobile pore fluid, diffusion through the bound organic layer, and the chemical binding and release step. Experiments performed in this research are designed to vary conditions that will affect only one of these steps in order to determine which is causing the observed slow sorption. Batch experiments are used primarily for screening for sorbent/sorbate combinations that exhibit slow sorption. Additionally, batch experiments are used to develop isotherms, and in some cases, determine sorption rates. Column experiments consist of passing a contaminant solution through a column packed with bonded silica until contaminant breakthrough occurs, then flushing the column with a contaminant-free solution. The resulting breakthrough curves were then evaluated using the models developed in Chapter 2 to estimate sorption parameters. Column experiments are performed with chlorinated benzenes, and batch experiments with a broader range of organic solutes.

Sorbents used in this research are made from porous aggregates of silica and alumina, which in most cases are partially coated with an aliphatic or aromatic organic compound. Organic modifiers simulate portions of natural organic matter that are important in the sorption of the hydrophobic compounds. The organic modifiers are either hydrophobic organic matter (aliphatic chains or phenyl groups), or common functional groups found in natural organic matter (carboxylic, amine, or alcoholic).

Particles with differing geometry and dimensions are used to examine the rate of diffusion through immobile pore fluid. This was done with the use of porous silica aggregates that have a different particle size to simulate a change in diffusion path length, or particles with different internal pore dimensions to simulate a change in tortuosity. Solid particles are used to eliminate all immobile pore volume. The diffusion rate through the bound organic layer is examined by changing the thickness or surface density of the organic layer. In addition, examination of the molecular size and shape of

the solute and sorbate is done to determine if diffusion through the organic layer is a rate-limiting step. The chemical binding and release step is examined by altering the surface functional group. In addition, column experiments are run at different temperatures to determine if the rate limiting step is caused by a physical or chemical process. The change in the sorption rate over a homologous series of compounds of increasing molecular weight is also used to separate physical and chemical processes.

3.2 Batch Experiments

Batch experiments were used for screening sorbent/sorbate combinations that exhibited slow sorption. Most experiments resulted in partition coefficients and qualitative sorption and desorption rates. A total of 47 separate batch experiments were completed from August, 1985 to December, 1986 (20-40 vials each) with 38 successful experiments using 16 different compounds.

3.2.1 Experimental Procedure

Batch experiments consisted of adding 0.1-10 g of sorbent, 1.5-40 mL of water and solute to a borosilicate vial with a teflon-lined cap, without head space. Bottles were rotary mixed (10 rpm) for times ranging from seconds to 14 days. A typical experiment consisted of 20-40 vials. Bottles were then centrifuged at 3000 rpm for 15 minutes, and then the solute concentration remaining in the liquid was analyzed. Short-time-scale samples were not centrifuged, but were withdrawn with a syringe and passed through a 0.22-μm polycarbonate filter before analysis.

Pentane extraction involved transferring 0.2-1.0 mL of liquid centrate (filtrate) into a second vial and adding 0.5 mL of pentane. After 50 shakes of the vial, 3 μL of the pentane was injected into a gas chromatograph (GC); most of the hydrophobic solutes partition into the pentane. A Varian 3760 packed column GC or a Hewlett Packard 3890 capillary column GC were used. The separation column consisted of a 3 percent SP-2250 on an activated carbon support (Supelco, Inc., Bellefonte, PA), or OV-1 on a diatomaceous earth support, or OV-1 on a glass capillary column. Detection was with an electron capture detector in all cases.

Liquid chromatography analysis was used with some substituted aromatic compounds and was performed on a Spectra-Physics 8100 (Spectra-Physics, Santa Clara, CA), using an RP-18 column (Millipore, Bedford, MA), a flow rate of 1.0 mL min^{-1}, a mixed methanol-water mobile phase, and an ultraviolet (UV) detector. Blanks and standards were made in identical sample bottles and treated in the same manner as samples. Some standards were analyzed at the end of the experiment to account for any losses of mass. Substituted benzenes were found not to absorb to glass.

The reaction rates obtained from batch experiments may be different from column experiments since flow in columns forces some advective flow through porous particles [*Antle et al., 1985*]. Particles in batch reactors are subject to shear forces that break particles apart [*Wu and Gschwend, 1986*]. Partitioning in batch systems may be altered due to colloid partitioning [*Gschwend and Wu, 1985*]. In addition, in batch experiments, as each bottle is a different sorbent sample, more sampling variability may result compared to column experiments, where all samples sorb to the same mass of sorbent. As a result, batch experiments generally show more variability, less sorption, and faster sorption than column experiments.

3.2.2 Modeling Batch Experiment Data

Batch-experiment partition coefficients were calculated from the fraction solute remaining in solution (f_l):

$$K_p = \frac{(1-f_l)}{f_l}\,\frac{V_{liquid}}{M_{solid}} = \frac{1-f_l}{f_l\, r_{sw}} \tag{59}$$

where r_{sw} is the solid/liquid ratio ($Mass_{solid}/Volume_{liquid}$). Data for long time scales (weeks) is accurate to within 2 percent, based on the standard deviation in K_p for six experiments. Data are less reliable for smaller vials where the surface tension of water makes separation of water from solids more difficult.

Desorption experiments required calculation of the solute mass remaining in the vial with:

$$C_{or} = C_o[1 - f_l(1 - \frac{\Delta V_{liquid}}{V_{liquid}})] \tag{60}$$

where C_{or} is the total mass of solute remaining expressed in terms of a liquid concentration, ΔV_{liquid} is the volume of water removed from the system, and V_{liquid} is the total volume of water. The fraction solute (f_1) remaining in solution was then calculated using the calculated initial concentration remaining in solution (C_{or}). The desorption data showed more scatter due to a greater number of sample handling steps; a similar observation has been made by other researchers [*Karickhoff, 1980*]. The sorbed concentration for sorption and desorption experiments was calculated with:

$$S = \frac{(C_o - C)}{r_{sw}} \tag{61}$$

Rate data were modeled with planar and spherical diffusion models, and a first-order chemical model. The models required two points to fit experimental data; the time to reach equilibrium sorption and a 50 percent sorption point were used. Shorter time scale data (<2 minutes) were considered inaccurate and were not used. Where sorption rates were not calculated, the values shown represent the time to reach a point within 2 percent of equilibrium.

Kinetic data at shorter time scales are less reliable since proper mixing and centrifugation required ten minutes. Filtering out solids worked only with particles of diameter greater than 100 μm, and could be performed within a minute. Slow mixing of the soil with water and solute before extracting liquid was another source of error in short-time-scale samples. Less sorption was observed in experiments where no mixing was performed. As a result, the short-time-scale rate data are unreliable (±15 percent) for times less than 1 minute, and somewhat unreliable (±5 percent) for times of 1-5 minutes.

A loss in mass of a solute in solution caused by mechanisms other than sorption occurs in natural systems, but can be controlled to a greater extent in laboratory

systems. Mass loss occurs by volatilization, biodegradation, sorption onto dissolved organic matter, and irreversible sorption.

Biodegradation of organic solutes in natural soils has been observed for a wide variety of compounds [*Graham-Bryce, 1981*]. Di-, tri-, and tetra-chlorinated benzene biodegradation has been reported in soil [*McCarty et al., 1981*] even at low concentration [*Kobayashi et al., 1982*]. Biodegradation of 1,2 dichlorobenzene in the laboratory and field has been reported [*Wilson et al., 1987*] after 9-12 weeks.

Mass loss due to partitioning of solutes to colloidal organic matter decreases the observed partition coefficient between soil and water [*Gschwend and Wu, 1985; McBath et al., 1987; Capel et al., 1987*]. Sorption is less at higher solid/liquid ratios where colloidal organic matter increases, and is more significant in batch experiment systems than in column systems. Dissolved organic matter is not significant with the model soil used, where organic compounds are covalently bound to the surface, but is a factor in natural soils, where dissolved organic matter averages 3 mg L^{-1} [*Thurman, 1985*].

3.3 Column Experiments

3.3.1 Apparatus Description and Procedure

Column experiments consisted of feeding a KCl solution containing an organic solute into a 1.0-cm diameter by 5- to 25-cm long column until solute breakthrough occurred, then feeding a lower conductivity, solute-free solution until all of the organic solute was removed from the column (Figure 3.1). To collect column inlet and exit samples, a 200-μL volume was isolated in a liquid chromatograph (HPLC) sample-injection valve; and when 700 μL of pentane was injected into the valve, water and pentane were flushed into a 1.5-mL vial with teflon-lined septa cap. This procedure is reproducible (± 1 percent), accomplishing sample removal and pentane extraction all within 30 seconds. Extraction and analysis was the same as for batch experiments.

Discrete samples (200 μL) represented 1.3 to 6.3 percent of the column volume, thus output concentrations were averaged over only a short time. Experiments with

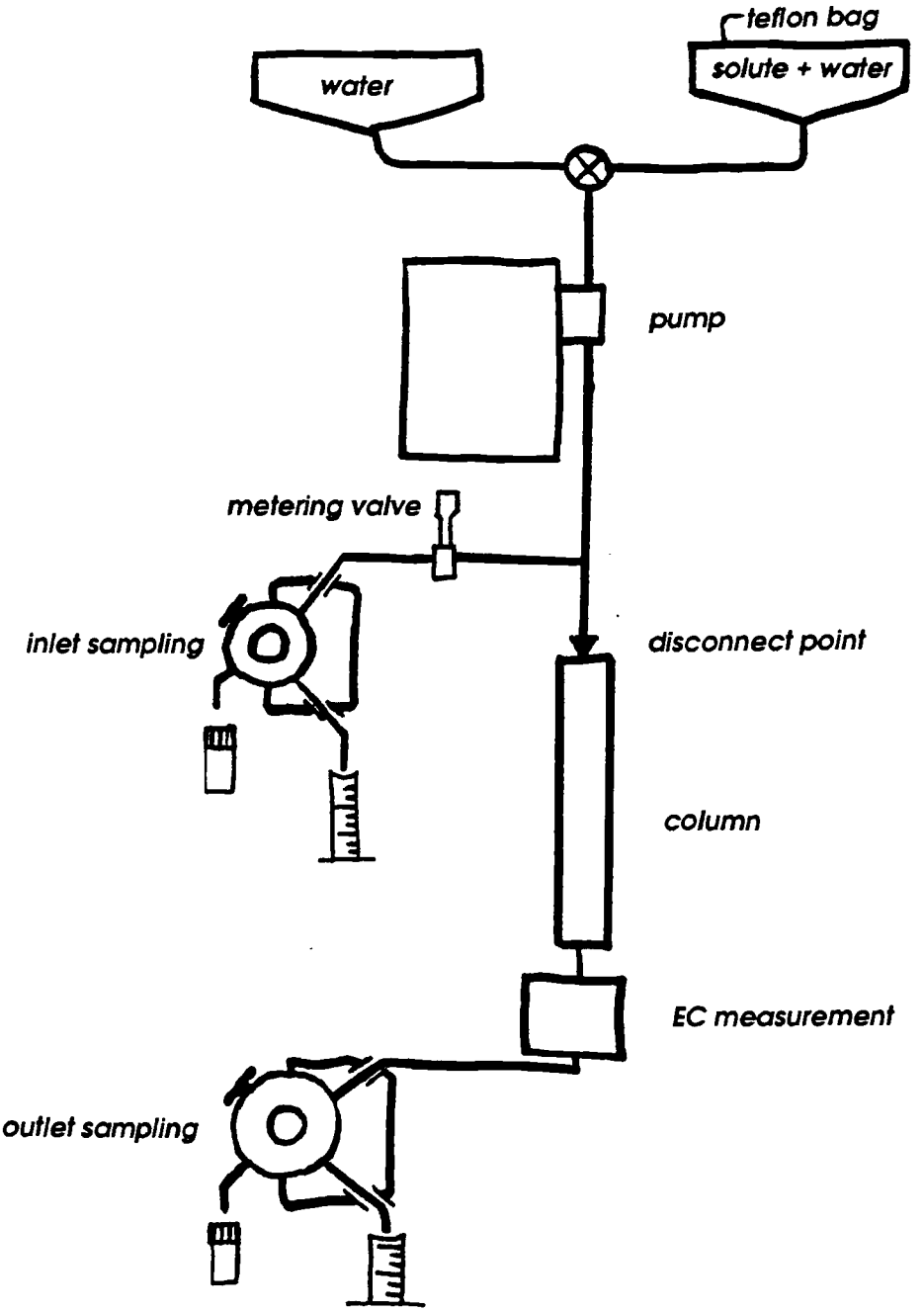

Figure 3.1 Column experimental apparatus

very short columns (sample volume was 6.3 percent of column volume) that were run at very high velocities (up to 2 pore volumes per minute) were subject to large jumps in concentration by a combination of the sample averaging effect and the time needed to sample. Stainless-steel tubing used in the apparatus was the smallest obtainable (0.013-cm internal diameter) to minimize dead volume between the column and the detector. Extra column volume after the column was 0.216 mL, including a 0.200-mL sampling loop, so the sample was considered to represent the concentration at the column exit. Sampling precision was 0.3 percent, based on 300 of the 15,000 samples analyzed. Another measure of the sampling precision is the average of the solute inlet concentration, which was 0.9996 ± 0.026 ($n = 150$).

A flexible teflon bag was used as the feed-solution reservoir. It was necessary to fill the bag several days before an experiment, since some initial solute mass loss occurred. Constant flow was accomplished with an HPLC pump (Eldex Laboratories, San Carlos, CA or Beckman Instruments, Santa Ana, CA). A pulse damper was not used since it added undesirable volume to the apparatus, and its removal added only a fixed amount of dispersion. All parts in contact with the solute were stainless steel, glass (piston), or teflon.

A lack of mass balance in breakthrough curves could indicate irreversible sorption or mass loss in the apparatus. The average ratio of the solute mass fed into the column to the amount detected for the 92 column experiments was 1.026 ± 0.106, with six experiments showing large mass imbalances. Upon removal of these six experiments, the mass balance becomes 1.011 ± 0.043, showing that the apparatus was capable of no mass losses.

Two KCl solutions (0.01 and 0.02 M) were used in the solute feed water and blank feed water to identify system dispersion; the high ionic strength was necessary to minimize the effect of anion exclusion. The column retention volume (and porosity) was calculated from particle and solids density (equation 63) and verified with the KCl breakthrough. Electrical conductivity was measured with a Wescan 2540 conductivity

meter and micro-cell.

Several experiments were run at temperatures from 3 to 48°C. Temperature control was accomplished by placing the entire apparatus inside a refrigerator and wrapping copper tubing around the solute feed reservoir, pump head, column, and sampling valves; water from an external constant temperature bath was circulated through the tubing. Insulation was also wrapped around the apparatus, exposing only the sampling valves. The refrigerator was opened only when sampling. The reported experiment temperature is an average for the solute reservoir and the column.

Six different columns were used with diameters of 0.9 or 1.0 cm and lengths of 5.0, 11.0, 14.0, or 25.0 cm. They were sized to accommodate a small amount of sorbent for large retention (K_p large) or large columns for small retention. The velocity dependence of dispersion was different for each column and was determined experimentally (Section 4.3.1). Prior to use, columns and 0.45-μm frits were washed in methanol, then dried at 105°C overnight.

Sorbent was packed dry with the "tap-fill" method [*Snyder and Kirkland, 1979*]; 30 pore volumes of water were then run through the column. The column inlet was opened and examined for additional void volume caused by grain rearrangement, and then the column was repacked if necessary. Electrical conductivity was monitored during the process to check for stability.

Packed columns were stored for up to 65 days (long-term sorption experiments) with only one case of bacterial growth observed. Columns could withstand high pressure (6000 psi) and were used for several experiments before clogging; one column was used for over 11,000 pore volumes. It was not determined, however, if the bonded organic content, or particle size changed. Column clogging was minimized by filtering liquid input into column and minimizing exposure to high pH or heat.

3.3.2 Modeling Column-Experiment Data

Column experiments were analyzed for mass balance, breakthrough curve symmetry, and model parameters. For each experiment, column dimensions, sorbent properties, and solute concentration were noted. Velocity was calculated from the volume per unit time of fluid transported through the column:

$$v = \frac{Q}{A\,\theta} \tag{62}$$

where Q is the volumetric discharge, A is the cross-sectional area, and θ is the total porosity. All columns were fully saturated with water and pumping rate held constant throughout the experiment.

Breakthrough curves were planimetered to calculate the retardation factors for sorption and desorption, and the mass eluted. Mass eluted divided by mass injected was used as a measure of the mass balance. Partition coefficients were calculated from planimetered retardation factors using equation (29). Some error was introduced when sorption did not reach C/C_o of 1.0, or desorption did not reach 0.0, as it was necessary to extrapolate the curve in order to planimeter the area. The ratio of sorption K_p to desorption K_p (K_{ps}/K_{pd}) was used as a measure of sorption reversibility.

Dispersion (D) for a conservative tracer was determined by fitting the KCl breakthrough curve to an equilibrium model; the fitted parameters were K_p and D, with injection pulse fixed. If the model fit to KCl data was poor ($ssq > 0.20$), then dispersion was calculated from the velocity/dispersion data (see Section 4.3.1). The measure of total error in the model fit is the sum of the squares of the deviation between model and data (ssq in Appendix B).

Solute breakthrough data were first modeled with the equilibrium model, fixing only the injection pulse; fitted parameters were K_p and D. The resulting dispersion coefficient in this case was used as an indicator of nonequilibrium. Data were also fit to the first-order and two-region models, fixing D at the ionic-tracer dispersion value times

a factor. This factor was 1.3 for chlorobenzene, 1.5 for dichlorobenzene, 1.9 for trichlorobenzene, 3.7 for tetrachlorobenzene, and 5.6 for pentachlorobenzene, as developed in Section 2.2.2.1. Nonequilibrium models were run fixing K_p at the planimetered value in one run, and allowing K_p to vary in another run. Allowing K_p to vary resulted in a substantially better fit in some cases, even if K_p did not change more than 10 percent. Other researchers [*Nkedi-Kizza et al., 1987*] have found a 20 percent variation in determining K_p by various methods.

Experiments were also modeled fixing the solute dispersion (D) value at that of the ionic tracer. In some cases, a third fit was performed, letting dispersion vary. In all cases, the planimetered K_p was used as the initial guess, or K_p was fixed at that value. Allowing K_p to vary resulted in a better fit. Parameters not fixed were determined by a nonlinear least squares fit to data [*van Genuchten, 1981*], which included sorption rate (k_b) for the first-order model, and mass transfer rate (α_e) and fraction mobile sites (f) for the two-region model.

In one case (experiment G-2), dispersion for DCB was fixed at 1.0, 1.3, 1.7, and 3.0 times the KCl dispersion coefficient. This surface (phenyl polymer) exhibited slow sorption of DCB in all breakthrough curves. Varying the dispersion value from 1.0 to 3.0 made little difference in the fit (only a slight increase in *ssq*). However, as dispersion increased, the rate parameter (ω) also increased (i.e. a faster reaction), as more of the observed spreading was included in hydrodynamic dispersion (and less included in a slow rate process). For a breakthrough curve exhibiting fast sorption (experiment B-1), the fitted curve was very sensitive to the value of dispersion, and the best model fit was obtained when dispersion was fixed at 1.5 times the KCl dispersion, similar to the calculated value. Apparently, when the dispersion coefficient was too large, the model curve exhibited greater spreading than the experimental data, and the resulting error (*ssq*) increased substantially.

Allowing the injection pulse (volume of solute-containing water injected) to vary can result in a substantially better fit for cases where K_p for sorption and desorption

differ. Varying the pulse compensates for apparent hysteresis in sorption by equalizing the K_p's. However, fitted values of K_p and the rate parameter have little meaning in this case; for meaningful results, sorption and desorption portions of breakthrough curves should be modeled separately. Therefore, an understanding of each parameter in the model is necessary to obtain meaningful data, because obtaining a better model fit by curve fitting does not necessarily reflect any understanding of the processes.

3.4 Sorbent Properties

Sorbents used in this research are made from porous and solid silica and alumina. The porous mineral surfaces used are commercially available with a wide range of geometrical structure. This difference in structure was used to alter the diffusion time through the immobile pore fluid. The silica used for many experiments was modified with an organosilane, which is covalently bound to the surface and provides a variety of accessible organic functional groups.

3.4.1 Unbonded Mineral Surfaces

Porous sodium silicate used in this research was a commercial product donated by manufacturers (Table 3.1). Some nonporous silica was also used, as well as porous alumina. Most experiments were performed with porous silica from a single manufacturer (PQ Corporation), to minimize the difference in surface properties. Particles used ranged in diameter from 2-μm (nonporous) to 600-μm (porous) particles, and had internal pore diameters of 11-27 nm.

3.4.1.1 Structure

Porous silica and alumina are prepared by the manufacturer by coagulating nanometer sized primary particles into aggregates, which are then crushed and sized. The pore size is controlled by the primary particle size. A larger range in pore size is caused by using primary particles with varying diameter. Other mineral surfaces used in chromatography include alumina, diatomaceous earth, styrene divinyl benzene and carbon [*Blevins, 1982*].

Table 3.1 Surfaces used in experiments

Name	Lab Name	Manufacturer	Diam.[1] (μm)	Surf. Area ($m^2 g^{-1}$)	Frac. Area Reduced	Pore Diam. (nm)	Bulk Density ($g cm^{-3}$)	Poro-sity	Bound organic	F_{oc}	Frac. organic Coverage	Frac. silane Coverage
K	AC-A	Analytichem	40	313.4	---	---	---	---	none	---	---	---
L	AC-B	Analytichem	40	500.0	---	---	---	---	C_1-Poly	0.0430	1.074	2.331
AA	AC-C	Analytichem	40	500.0	---	---	---	---	C_2-Poly	0.0432	0.525	0.763
M	AC-D	Analytichem	40	500.0	---	---	---	---	C_8-Poly	0.1162	0.363	0.518
N	AC-E	Analytichem	40	500.0	---	---	---	---	C_{18}-Poly	0.1818	0.252	0.375
AB	AC-F	Analytichem	40	500.0	---	---	---	---	AMIN-Poly	0.1200	1.501	3.786
AC	DEG-A	Degussa OX50	0.040	38.83	---	none	---	---	none	---	---	---
AD	DEG-B	Degussa Al203	0.015	94.13	---	none	---	---	---			
AE	MIN-A	PGS minusil 30	8.8	1.624	---	none	---	---	---			
J	MIN-B	PGS minisil 5	1.9	6.351	---	none	--	--	none	---	---	---
A	PQ-A	PQ Corp CD-807	100	182.6	0.902	27.5	0.3489	0.858	C_1-Poly	0.0143	0.893	1.091
B	PQ-B	PQ Corp CD-807	100	203.4	1.005	27.5	0.3627	0.852	C_8-Poly	0.0068	0.053	0.054
C	PQ-C	PQ Corp CD-807	100	191.5	0.946	27.5	-.3555	0.855	C_{18}-Poly	0.0105	0.036	0.037
D	PQ-D	PQ Corp CD-807	100	224.7	1.110	27.5	0.3520	0.856	PHE-Mono	0.0016	0.012	0.013
E	PQ-E	PQ Corp CD-807	100	195.2	0.964	27.5	0.3614	0.852	PHE-Poly	0.0137	0.143	0.149
AF	PQ-F	PQ Corp CD-807	100	215.6	1.065	27.5	0.3597	0.853	Carboxylic	0.0085	0.088	0.138
R	PQ-G	PQ Corp CD-807	100	209.7	1.036	27.5	0.3383	0.862	DIOL-Poly	0.0087	0.091	0.093
S	PQ-H	PGS minisol 30	8.8	1.631	1.004	none	---	---	PHE-Poly	0.0004	0.521	0.522
F	PQ-I	PQ Corp CD-803	20	345.5	0.858	11.0	0.3536	0.856	PHE-Poly	0.0111	0.058	0.060
G	PQ-J	PQ Corp CD-807	20	190.7	0.896	27.5	0.2905	0.881	PHE-Poly	0.0101	0.105	0.109
T	PQ-K	PQ Corp CD-807	100	199.1	0.983	27.5	0.3415	0.861	AMIN-Poly	0.0081	0.084	0.177
H	PQ-L	PQ Corp XG-10	425	387.8	0.887	10.0	0.4185	0.829	PHE-Poly	0.0106	0.055	0.057
AG	PQ-M	PQ Corp XG-10	135	401.0	0.917	10.0	0.4342	0.823	PHE-Poly	0.0092	0.048	0.049
I	PQ-N	PQ Corp CD-807	100	202.5	---	27.5	0.3300	0.865	none	---	---	---
W	PQ-O	PQ Corp CD-803	20	402.5	---	27.5	0.2776	0.887	none	---	---	---
X	PQ-P	PQ Corp CD-807	100	207.7	1.026	27.5	0.3632	0.852	.473 C_{18}-Poly	0.0060	0.021	0.021
			100	207.7	1.026	27.5	0.3632	0.852	.527 PHE-Poly	0.0066	0.069	0.070
AH	PQ-Q	PGS min-u-sil 5	1.9	6.515	1.026	none	0.9400	0.616	C_1-Poly S	0.0142	0.293	0.298
O	PQ-R	PGS min-u-sil 5	1.9	5.816	0.916	none	0.8978	0.634	C_1-Poly S	0.0022	0.045	0.039
AI	PQ-S	PQ Corp CD-807	100	211.6	1.043	27.5	0.3576	0.85	PHE-Poly	0.0093	0.097	0.100
Q	PQ-T	PQ Corp CD-807	100	201.2	0.994	27.5	0.3510	0.857	PHE-Mono	0.0075	0.059	0.059
U	PQ-U	PGS min-u-sil 5	1.9	5.923	0.933	none	0.8748	0.643	PHE-Poly S	0.0044	1.514	1.536
V	PQ-V	PQ Corp XG-10	425	437.1	---	10.0	0.4372	0.822	none	---	---	---
AJ	PQ-W	PQ Corp CD-807	20	212.9	---	27.5	0.3544	0.855	none	---	---	---
AK	SCM-A	Smith Corona G600	4.7	325.0	---	13.5	---	---	C_1-Poly	---	---	---
AL	SCM-B	Smith Corona G600	4.7	325.0	---	13.5	---	---	C_8-Poly	---	---	---
AM	SCM-C	Smith Corona G600	4.7	325.0	---	13.5	---	---	C_{18}-Poly	---	---	---
AN	SCM-D	Smith Corona G600	4.7	325.0	---	13.5	---	---	PHE-Mono	---	---	---
AO	SCM-E	Smith Corona G600	4.7	325.0	---	13.5	---	---	PHE-Poly	---	---	---
AP	SCM-F	Smith Corona G600	4.7	325.0	---	13.5	---	---	Carboxylic	---	---	---
AQ	SCM-G	Smith Corona G600	4.7	325.0	---	13.5	---	---	DIOL-Poly	---	---	---
AR	SCM-H	Smith Corona G900	8.5	493.5	---	2.6	---	---	none	---	---	---
P	SCM-I	Smith Corona G604	13.5	247.1	---	13.5	---	---	none	---	---	---
AS	ZEO-A	Huber ZEOSYL110SD	13.0	140.0	---	---	---	---	C_{18}-Poly	0.0068	0.034	0.034
AT	ZEO-B	Huber ZEOSYL110SD	13.0	140.0	---	---	---	---	C_{18}-Poly	0.0117	0.058	0.059
AU	ZEO-C	Huber ZEOSYL110SD	13.0	140.0	---	---	---	---	C_{18}-Poly	0.0194	0.096	0.100
AV	ZEO-D	Huber ZEOSYL110SD	13.0	84.29	---	---	---	---	none	---	---	---
Y	AL-A	ALCOA CS4712-A2	236	314.6	---	4.0	0.7205	0.788	none	---	---	---
Z	AL-B	ALCOA CS4713-B2	236	122.1	---	10.0	0.6775	0.801	none	---	---	---
AW	AL-C	ALCOA CS4712-A1	483	316.7	---	4.0	0.6556	0.807	none	---	---	---
AX	AL-D	ALCOA CS4713-B1	483	128.0	---	10.0	---	---	none	---	---	---

[1]Average particle diameter between sieves.
[2]By single point N_2 adsorption.
[3]Surface area/unbonded surface area.
[4]Measured.
[5]Calculated with equation (76); ρ_s = 2.45 (silica), 3.40 (alumina).
[6]Calculated with equation 84 and Table 3.1.

The porous silica used in this research is formed by homogeneous nucleation of amorphous silica particles from silicic acid molecules, continued growth of these nanometer sized silica beads which are then "melted" together with acid or heat [*Fleming, 1986*], forming irregular aggregates with internal void space. The average coordination number of primary particles is 4 (tetrahedral structure) [*Drake et al., 1986*]. Primary particles range from 1 to 10 nm in diameter; secondary particle structure is around 100 nm, and final particles are about a centimeter in diameter. Particles are crushed and sieved to a desired size; they are angular and edges break when packed into columns [*Horvath et al., 1977*]. Secondary particles are round agglomerates of primary particles. Growth of secondary particles to large diameters is possible, but expensive. These have been made [*Macherey Nagel, 1987*] with particle sizes from 3 to 70 μm with seven pore diameters from 5 to 400 nm.

The interparticle porosity averages 0.40 [*Iler, 1979*] for the angular particles used in this research, with an intraparticle porosity about 0.46 [*PQ Corporation, 1986*]. Total porosity for silicas used in this research ranged from 0.35 (nonporous) to 0.88 (porous). Porosity was calculated from bulk density and solids density:

$$\theta = 1 - \frac{\rho_b}{\rho_s} \tag{63}$$

where ρ_b is the dry bulk density, and ρ_s the solids density. Bulk density was calculated with the measured mass and volume of sorbent packed into a 10 to 30 cm^3 graduated cylinder. The solids density is 2.45 for silica (PQ Corporation, 1986), and 3.40 for alumina [*Iler, 1979*]. The porosity was also determined from the breakthrough curve of a conservative (KCl) tracer at high ionic strength.

Other commercially available porous silicas [*Merck*] have porosities ranging from 0.59 to 0.73 [*Drake et al, 1986*]. Determination of total porosity can also be done by weighing a packed column with different density fluids in it [*Blevins, 1982*], or injecting a conservative, nonsorbing tracer such as $CaNO_3$ [*Yang and Gilpin, 1987*].

Fractal models can be used for calculating particle internal geometry [*Avnir, 1986; Drake et al., 1986; Keefer, 1986*] and are useful because the absolute surface topology depends on the method used to probe the surface. Fractal analysis indicates a probe of 0.3 nm is needed to characterize the surface; a larger size would not characterize all the surface structure. This is equal to the spacing between oxygens on the silica surface (0.30 nm) [*Miller et al., 1985*]. The surface area can be measured by nitrogen adsorption only where pores or surface roughness are greater than 1.2 nm [*Drake et al., 1986*].

The aggregate particles packed into a column provide for tremendous reactive surface area, but create additional dispersion by immobile pore fluid diffusion [*Rose, 1977*]. Irregularities in interparticle porosity have been demonstrated mathematically to result in asymmetrical breakthrough curves [*Yeroshenkova et al., 1983*], even assuming no immobile pore volume.

Researchers [*Snyder et al., 1979*] believe that there is advective transport around and through porous particles with only a minor amount of immobile internal pore space. The amount of immobile pore space may be a function of pressure, so it could be greater for batch (low pressure) experiments. Gaseous diffusion of water vapor through porous silica is in the range of 10^{-6} to 10^{-10} cm s^{-1}, whereas diffusivities of ions in aqueous solution are on the order of 10^{-5} to 10^{-6} cm s^{-1} [*Andersson et al., 1985*]. Gas diffusion of water vapor into 50-μm particles reached equilibrium within 30 minutes.

3.4.1.2 Properties

Single-point nitrogen adsorption was determined on the sorbents used in this research, and is reported in Table 3.1. This technique (Quantisorb, Bristol, PA) consisted of a flow-through cell containing the sorbent, and the means to measure the difference in mass of nitrogen flowing in and out of the cell. The cell holder containing the sorbent was placed in liquid nitrogen, liquefing gaseous nitrogen that is flowing past the sorbent. Assuming monolayer coverage of liquid nitrogen, the total mass of nitrogen adsorbed to the particle surface is proportional to the sorbent surface area. Desorbing the liquid nitrogen from the sorbent surface is done with water (25°C), and results in a

mass gain to the system that is also proportional to the surface area.

A minimum of three adsorption/desorption cycles were done on each surface with duplicates for 10 percent of the samples. Precision was about ± 1 percent, although accuracy between samples of the same surface was ± 3 percent. The manufacturer suggests an accuracy of 5 percent. Measured surface areas ranged from 5 to 500 $m^2 g^{-1}$.

The pore-size distributions for some of the silicas used in this research were supplied by the manufacturer (Figure 3.2) [*PQ, 1986*]. These were determined from multipoint nitrogen adsorption data, and calculated by assuming a BET isotherm and cylindrical geometry. The distributions are narrow; the 27.5 nm pore silica (surfaces A through E) had a pore size range of 15-36 nm (99.5 percent).

The porous silica used is somewhat amorphous [*Iler, 1979*], but the structure is generally silica tetrahedra with the distance between the silicon and oxygen atoms of 0.187 nm, an angle between oxygens (O-Si-O) of 109 degrees, and a distance between oxygens of 0.299 nm [*Miller et al., 1985*]. The pH_{iep} of silica is 2.0 ± 0.5 [*Iler, 1979*], indicating that the surface has a net negative charge at neutral pH. The pK_a for proton dissociation from of the silica surface is 7.1 to 9.5 [*Miller et al., 1985*], accounting for silica stability in the 1 to 9 pH range [*Karch et al., 1976*]. Silica dissolution increases dramatically at $pH > 9.5$ and at elevated temperatures.

Hydroxyl groups chemisorbed on the silica surface are oriented with the OH groups parallel to the surface [*Urban et al., 1985*]. The surface is considered chemically heterogeneous [*Hunnicutt, 1986*], with an average silanol (SiOH) distribution of 8 $\mu molm^{-2}$. Researchers estimate that 50 to 75 percent of the silanol groups can be brought to reaction [*Bein et al., 1984*]; the calculated maximum site density is 4.5 to 8.0 nm^{-2} [*Blevins, 1982*].

Magnetic resonance has been used to determine the relative fractions of surface groups [*Fyfe et al., 1985*]. Silica gel has 60 percent siloxane bonds (Si-O-Si), 32 percent lone bonds (SiOH), and 8 percent geminal bonds ($Si(OH)_2$). It was also determined that

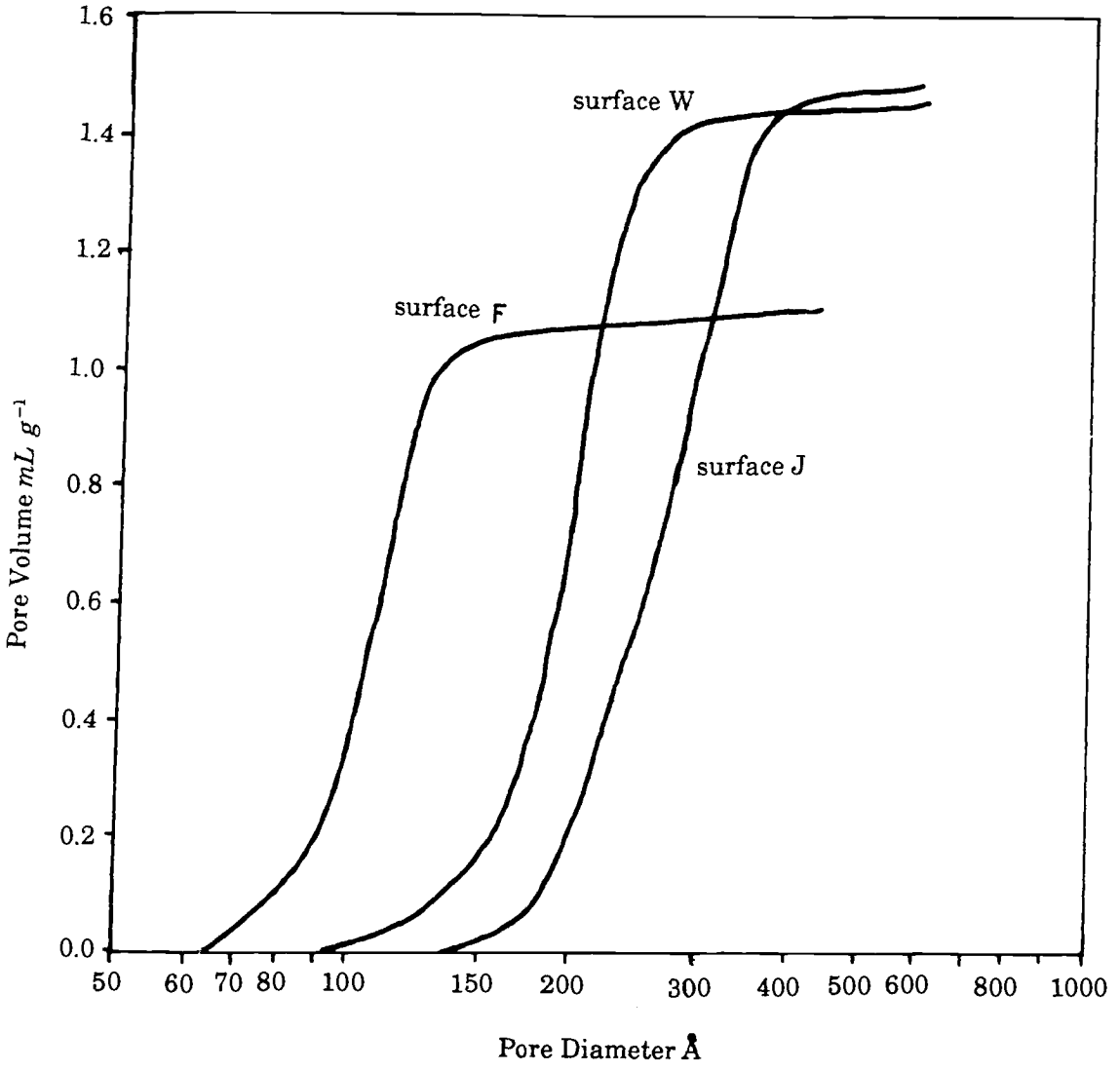

(PQ Corporation, 1986)

Figure 3.2 Pore size distribution of unbonded silica

all of the geminal sites and only some of the lone sites reacted (20 percent of the total number of sites) when a silane was bound to the surface. Hydrogen bonding between adjacent lone sites [*Miller et al., 1985*] is observed and causes greater activity. Glass beads are reported to have a greater percentage of reactive sites (35 percent) compared to the sodium silicate. The nature of the silica surface does affect partitioning since bonded phases from different manufacturers react differently, possibly caused by trace elements in the amorphous silica.

3.4.2 Organic Modified Surfaces

3.4.2.1 Sorbents Used

Organic molecules are bound to silica particles to simulate some of the functional groups found in natural soil organic matter. Silica was modified with aliphatic chains, phenyl groups, and aliphatic chains with alcoholic, amine, or carboxylic groups for this purpose, as indicated on Table 3.1. The most extensive use was made of the nonpolar modifiers (phenyl groups and aliphatic chains), since sorption of the solutes of interest is predominantly through van der Waals attractions between nonpolar groups. Properties of the organic modifiers are shown in Table 3.2.

The organic modifiers are bonded to the surface in clumps, with the mass fraction of bound carbon being about one percent, to simulate distribution found in natural soils. Natural soils have a range of bound carbon of 0.01 - 5 percent [*Karickhoff, 1984*].

Organic-modified silica was introduced in 1952 by Howard and Martin [*Blevins, 1982*]. The first organic modified liquid chromatographic (LC) stationary phase was a C_{18}-modified silica developed in 1966 [*Horvath et al., 1977*]. Bonded phases are used for chromatographic separation, reaction catalysis, waterproofing, and specialized coating. Surface modification can be made with alcoholic groups (Si-O-C bonds), primary or secondary amines (Si-N-C bond), or with a chlorosilane (Si-O-Si-C bond); these are listed in order of increasing stability against hydrolysis [*Karch et al., 1976*]. Bonded phases now represent over 80 percent of LC columns [*Horvath et al., 1978*].

Table 3.2 Silane properties

Name	M_t Total Molecular Weight ($g\ m^{-1}$)	f_{ct} Fraction Carbon of Total Silane (g/g)	M_{om} [1] Organic Fraction Molecular Weight ($g\ m^{-1}$)	f_c Fraction Carbon of Organic Fraction (g/g)	V_{om} [2] Volume of the Organic Fraction ($cm^3\ m^{-1}$)	Thickness (length) from Surface (nm)
C_1	149.5	0.08	15	0.800	13.6	0.5
C_8	247.5	0.388	113	0.850	85.1	1.6
C_{18}	387.5	0.557	253	0.854	187	2.5
Phenyl-Monomer	170.5	0.563	107	0.897	75.7	1.1
Phenyl-Polymer	211.5	0.340	77	0.935	44.9	1.1
Carboxylic	217.5	0.221	144	0.500	85.7	---
Dialcoholic	235.0	0.306	121	0.496	84.3	---
Amine	221.5	0.163	44	0.545	34.2	---

[1]Molecular weight of organic fraction of silane; excludes Si, Cl, and O.

[2]Bondi, 1964.

Chloro- or methoxy- (OCH_3) silanes are most commonly used due to great binding strength on silica and alumina, and the extensive availability of bonded phases (Petrarch Systems, Bristol, PA). The general silane formula $R_NSiX_{(4-N)}$ can be subdivided into:

C_1–Si–R_3 trifunctional and monomer

C_2–Si–R_2 difunctional and dimer forming

C_3–Si–R_1 monofunctional and polymer forming

Chlorosilanes (monomers) bind in monolayers on the surface and trichlorosilanes (polymers) bind to the surface in polymer clumps. Attachment to the silica surface is by removal of chlorine from the silane and hydrogen from the surface to form a Si-O-Si covalent bond [*Hunnicutt et al., 1986*]. Silanes can also be bound to an alumina surface, and metals including aluminum, silicon, tin, titanium, copper, iron, gold, and zinc [*Petrarch Systems, 1987*].

Functional group(s) are generally hydrophobic, but can also be polar groups. Commonly used functional groups include: 1) aliphatic chains (C_1, C_2, C_4, C_6, C_8, C_{18}, C_{24}); 2) aromatic groups; 3) polynuclear groups; and 4) silanes with specific functional groups. Aliphatic chains (C_{18}) and monofunctional phenyl silanes are the most common.

Phenyl silanes are of particular interest in this research and are available as mono-, di-, or tri-phenyl silanes [monomers; *Jinno et al., 1985*], penta-phenyl functional silane [*Chen et al., 1986*], phenyl polymer (Petrarch Systems, Bristol, PA), and phenyl groups attached to aliphatic chains of varying length [*Blevins, 1982; Den et al., 1985*]. Polyaromatic (napthyl and pyrene) silanes are also available [*Takana et al., 1982*] as well as heterocyclics (hexyl and hexanol). Phenyldimethylchlorosilane is used as a catalyst and in a variety of industrial reactions; triphenylchlorosilane is used as a GC column deactivator and in some LC columns [*Okamoto et al., 1985*], and phenyltrichlorosilane (polymerizing) is used for hole filling on silica surfaces, wear coating on magnetic recording surfaces, and waterproofing [*Matzen et al., 1986*].

From mono- to di- to tri- phenyl silanes, as the bulkiness of the bonded group increases, steric exclusion of the silane from the smaller pore silica is observed [*Okamoto et al., 1985*], and some pore clogging is observed by the reduction in surface area. Trichlorophenyl silane is observed to polymerize in water to a molecular weight of 1.2×10^6 in an organic solution [*Dianippon Chemicals, Inc., 1984*].

Silanes with polar or ionic functional groups can also be attached to a silica surface but require deactivation of the group before binding, then reactivation of the functional group. Silanes with alcoholic, amine, and carboxylic groups were used in this research. Using carbonyl dimidaxole (CDI) instead of a silane, virtually any ligand can be bound to a silica surface [*Hearn, 1983; Larsson et al., 1982*].

3.4.2.2 Preparation

The procedure used in this research to bind silanes is designed to obtain only a partial (< 3 percent) and lumpy coating, in order to simulate the distribution of soil organic matter coatings on mineral surfaces. This procedure was developed with the advice of Dr. M. Burke (personal communication) in the Chemistry Department at the University of Arizona. Silane polymers were used to make a lumpy coating. Polymers do not increase the thickness of the silane since they polymerize laterally [*Hunnicutt et al., 1980*]. Silanes bound on surfaces are not observed with more than monolayer coverage. The presence of water with a multichlorosilane will produce a silane polymer in solution [*Karch et al., 1976*], which can then be bound to the surface. Adding the silane to a water and a silica slurry allows for some polymerization but silane is still able to diffuse into pores. Polymerization is also controlled by the solid-liquid ratio and rate of evaporation of water during condensation.

Prior to use, the silica was washed with methanol and 0.1 N HCl, then dried at 200°C overnight. The silane was added into a silica-water slurry (10 g of silica and 200 mL of water) and mixed for 2-12 hours (for polymerization), then dried at 105°C overnight (binding to the silica surface), and finally rinsing with carbon tetrachloride, hexane, methanol, hydrochloric acid, and finally water prior to use. Note that after packing

into a column, silica was rinsed further (30 pore volumes) before experimentation.

The binding reaction of monomeric groups are made from chlorosilanes with methyl side groups is:

$$>SiOH + Cl(CH_3)_2SiR \longrightarrow Si{-}O{-}Si(CH_3)_2R \tag{64}$$

where R is an organic functional group (C_1, C_8, C_{18}, or phenyl), and >SiOH refers to a surface silanol site. The phenyl silane used was phenyldimethylchlorosilane (Petrarch P0160) from Petrarch Systems [*Bristol, Pa.*]. Properties of the silanes used in this research are listed in Table 3.2.

Polymer surfaces are made from trichlorosilanes with the following reaction:

$$RSiCl_3 \xrightarrow[H_20]{hydrolysis} RSi(OH)_3 \xrightarrow{poly-merize} -O(RSiOH)-O-(RSiOH)O- \tag{65}$$

$$\xrightarrow[surface]{H-bond} -O-(RSiOH_2OSi<)-O-(RSiOH_2OSi<)-O-$$

$$\xrightarrow[\Delta, -H_20]{covalent\ bond} -(>SiOR)-O-(>SiOR)-$$

where the phenyl silane used was phenyltrichlorosilane (Petrarch P0280). A carboxylic functional group is bound to silica with a 2-(carbomethoxy)ethyltrichlorosilane (Petrarch C2905):

$$>SiOH + Cl_3SiCH_2CH_2(C{=}O)CH_3 \xrightarrow[H^+]{\Delta} >Si{-}O{-}SiCH_2CH_2(C{=}O)OH \tag{66}$$

An alcoholic functional group is bound to silica with 3-glycidoxypropyltrimethoxysilane (Petrarch G6720):

$$>SiO(-OCH_3)_2Si(CH_2)_3OCH_2\text{-}\underset{\diagdown O \diagup}{CH}\text{-}CH_2 \longrightarrow \tag{67}$$

$$>Si{-}O{-}Si(CH_2)_3{-}OCH_2CH(OH){-}CH_2OH$$

An amine monomer is bound to silica with 3-aminopropyldimethylethoxysilane (Petrarch A0735) and with the same reaction conditions as the aliphatic chain monomer

binding reaction:

$$>SiOH + ClSi(CH_3)_2CH_2CH_2NH_2 \longrightarrow >Si\text{–}O\text{–}Si(CH_3)_2CH_2CH_2NH_2 \qquad (68)$$

where the surface is washed with carbon tetrachloride and methanol after binding. An amine polymer is bound to silica with 3-aminopropyltriethoxy silane (Petrarch A0750) with the following reaction:

$$>SiOH + Si(OCH_3)_3CH_2CH_2NH_2 \xrightarrow[H^+]{2\,hrs} \xrightarrow[\Delta]{6\,hrs} \qquad (69)$$

$$>SiOSi(O\text{–})_2CH_2CH_2NH_2$$

Amine modified silicas were also modified to produce carboxylic and ketone groups bound to an aliphatic chain [*Zerda et al., 1985*] with the following reaction:

$$>SiOSi(O\text{–})_2CH_2CH_2NH_2 + C(=O)(CH_2\text{–})OC(=O)(CH_2\text{–}) \xrightarrow[pH=6]{H_20} \qquad (70)$$

$$SiOSi(O\text{–})_2CH_2CH_2OC(=O)CH_2CH_2C(=O)OH$$

A list of thirty modified silicas with chemical and physical properties made in this research is presented in Table 3.1. The bound silane is covalently bonded to the surface, and is thus stable over a wide range of pH and temperatures up to 220°C [*Karch et al., 1976*]. The bound silane thickness varies from 0.5 nm for C_1 to 2.5 nm for C_{18} [*PQ Corp., 1986*], to 1.1 nm for phenyl. The silane binds on surfaces in pores, and will bridge across pores if the silane molecule is large enough (more common for polymers).

The procedure used to bind silanes for chromatography purposes are designed for complete coverage of the silica surface [*Antle et al., 1985*]. About half of the 4.8 groups nm^{-2} are sterically able to react with C_1 [*Blevins, 1982*]. Longer chains lie flat on the surface, covering unbound silanol groups. Silanes longer than C_8 have less access to the reactive surface. The rate of silane binding is slow compared to reagent transport [*Hunnicutt et al., 1986*]. From fastest to slowest, the silation reaction rate is: short aliphatics > long chain aliphatics > phenyl > amine > alcoholic silanes.

The typical chromatography binding procedure is to clean and dry the silica (absence of water), apply 2 to 5 percent of the silane in toluene, reflux for 12 hours, add an acid scavenger (pyridine), end cap with a C_1 polymer, then rinse with toluene and methanol [*Kingston et al., 1976*]. Analysis of 21 variables in the reaction [*Jones, 1987*], indicated that six factors are very significant to achieve complete coverage. These are the nature of the silane, silanizing twice, using a large excess of silane (5 equivalents), end capping (C_1 silane), using a trifunctional silane, and using an acid scavenger. Silanization can also be done in situ [*Gilpin et al., 1976*] which additionally coats the inside of the column. Even chromatographers admit, however, that the binding procedure is unique and the organic coated silica produced varies from batch to batch, so the bound silica still represents unique set of variables.

3.4.2.3 Properties

The mass of bound organic carbon was determined by elemental pyrolysis, giving percent carbon by total mass with a lower limit of 0.0002 ± 0.0001. Unbound silica was also measured to account for the inorganic carbon. Bound particles made in this research had a fraction carbon by mass (f_{oc}) ranging from 0.04 to 1.94 percent (Table 3.1). The amount of surface area coverage of organic matter (X_{om}) based on the mass of carbon was calculated with:

$$X_{om} = \frac{1}{[(f_c / f_{oc} - 1) M_{om} F S_a]} \tag{71}$$

where f_{oc} is the fraction organic carbon in the sorbent, f_c is the fraction carbon in the organic portion of the silane, M_{om} is the molecular weight of the organic portion of the silane (Table 3.2), F is the surface site density (6.67×10^{-6} mol m^{-2} for silica) and S_a is the silica surface area ($m^2\ g^{-1}$). The fraction organic coverage ranged from 0.9 to over 100 percent (Table 3.1), and represents the area (and volume) where most hydrophobic organic compounds sorb.

The fraction silane coverage (X_s) was calculated with equation (71), making the substitutions of the total bound silane molecular weight (M_t) from Table 3.2, and the fraction carbon of the silane (f_{ct}). This fraction silane coverage represents the mole fraction of total material added to the unbonded silica. As shown in Table 3.1, the fraction coverage is slightly greater than the fraction organic matter coverage, as expected.

The maximum mass of bound silane varies with silane size; for a C_1 monomer, f_{oc} is 3.3 percent, for a C_8 monomer, f_{oc} is 12 percent, for a C_{18} polymer, f_{oc} is 19 percent, and for phenyl monomer, f_{oc} is 7 percent [*Karch et al., 1976; Bein-Vogelsand et al., 1984*]. Maximum coverage is one molecule per 0.18 nm^2 (C_1), 0.49 nm^2 (C_{18}) [*Karch et al., 1976*], and 0.52 nm^2 (phenyl monomer) [*Okamoto et al., 1985*]. Most porous surfaces used in this research averaged 1 percent carbon by mass, which covered 1 to 15 percent of the surface sites. Nonporous silica coverage by bound organic matter was calculated at 50 to 150 percent of the silica sites, possibly indicating some coverage greater than monolayer.

Binding silanes reduces the amount of available silanol surface. The unreacted surface area was determined experimentally by nitrogen adsorption, and sodium hydroxide titration. Single-point nitrogen adsorption was performed on the unbound and bound silicas used in this study; the reduction in surface area for bound silicas was 10 percent or less, since only a small mass of silane was bound. Solid particles did not show a reduction in surface area even with a high fraction coating.

Internal porosity (and surface area) is reduced when silane polymers are large enough to bridge across pores, as observed with C_{18} polymers (PQ Corporation, 1986). Surface-area reduction is not observed with C_1, C_8, and C_{18} monomers [*Hunnicutt et al., 1986*].

Multipoint nitrogen adsorption can be used to examine pore clogging. In a study where different phenyl silanes were bound to silica [*Okamoto et al., 1985*], the unbound silica had a pore diameter of 9.5 nm. Binding a monophenyl silane to the silica (f_{oc} =

0.0445) produced an average pore diameter of 8.6 nm; binding a diphenyl silane (f_{oc} = 0.0592) changed the average pore diameter to 8.5 nm, and binding a triphenyl silane (f_{oc} = 0.0518) changed the pore diameter to 8.5 nm. The pore distributions, however, show most of the decrease is in the percentage of pores smaller than 2.0 nm.

Silanol surface activity can also be determined by titrating the surface to high pH [*Sears, 1956*] with the following reaction:

$$>SiOH + OH^- <==> >SiO^- + H_20 \tag{72}$$

The mass of eluted hydrogen ions depends on the total surface area of the silica surface and can be correlated to nitrogen surface area.

The titrations were done under a nitrogen atmosphere (eliminating the effect of carbon dioxide in the air), and with an autotitrator. This provided accurate pH control, records of acid or base addition and the surface area. In addition, the rate to reach equilibrium was noted. The rate depends on the diffusion rate of hydrogen ions out of the porous particles. The apparatus requires 10 to 20 seconds to stabilize pH, so faster rates are not observable.

The procedure involved first cleaning the silica, adding 1.5 g of silica and 30 g of sodium chloride to 100 mL of water, stabilizing the pH at 4.00 for 30 minutes, then changing the pH to 9.00 quickly and measuring the amount of base needed to maintain that pH. Surface area (S_a) is determined from linear regression between surface area and volume of NaOH added (V):

$$S_a = 32V - 25 \tag{73}$$

Thirteen titrations were performed on six different surfaces, where five were modified with bound organic compounds (Figure 3.3). The steps in the curves reflect the apparatus resolution where 0.10 pH unit is 1 percent of the surface area. Unbound silica showed a surface area of 102 $m^2\ g^{-1}$ (compared to 200 $m^2\ g^{-1}$ on Table 3.1). Silane-modified surfaces generally showed a reduction in surface area compared to unbound;

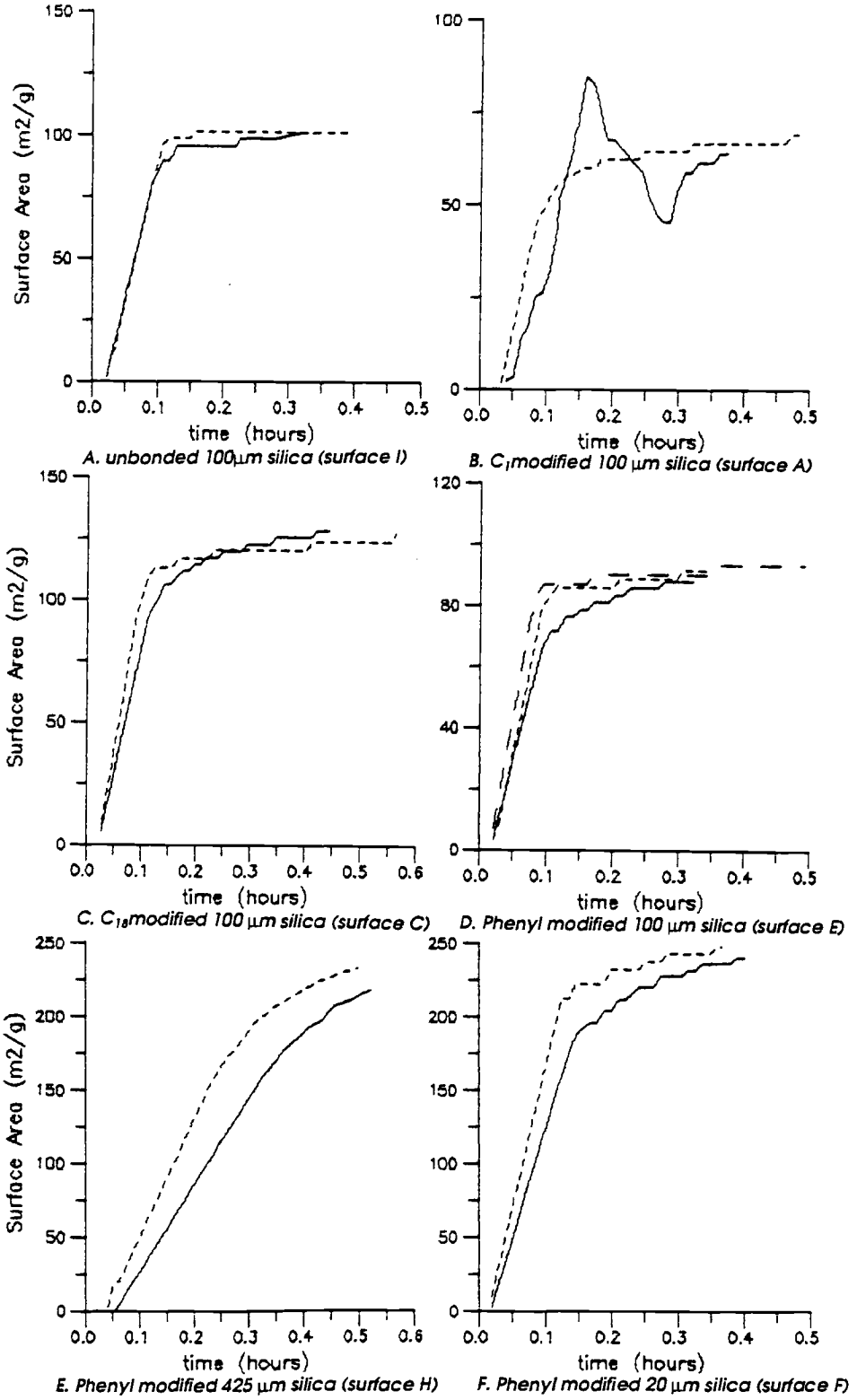

Figure 3.3 Surface area determination by NaOH titration

the C_1 surface had an area 65 percent that of unbound silica, the C_{18} surface had greater surface area (128 percent), and the phenyl-modified silica had a surface area that was 89 percent of unbound silica. Nitrogen adsorption surface area did not show as much reduction. Two other phenyl-polymer modified silicas (Figure 3.3E and F) also showed less surface area when compared to respective unbound silica.

Fast sorption (within 15 minutes) is observed for the unbonded silica, and the 100-μm organic-bound particles; the rate shown at very short times is controlled by the apparatus pH adjustment rate. Slower sorption is observed for the 425-μm phenyl-polymer-bound silica in Figure 3.3E where equilibrium is reached within 1.5 hours.

Two additional methods can be used to characterize the bonded-silica surface. Methyl red complexes with the unreacted silanol sites, turning them red [*Karch et al., 1976*]. A copper amine complex is also adsorbed to silanol sites but is best used for determination of external activity, since adsorption to internal sites can take up to 80 days [*Jennings and Brownlee, 1986*].

The length of the aliphatic chain has an effect on the motion of the silane, and its accessibility to solute molecules. Chains shorter than 4 methyl groups are relatively rigid, and longer chains are flexible. The motion of the longer aliphatic chains [*Beaufils et al., 1985*] causes the silane to occupy a larger volume in water than should occupy. This motion increases mass transfer (sorption) and the bound surface is liquid-like [*Antle et al., 1986*]. On the other hand, if a short organic compound, such as trichloro-phenylsilane, is bound to a surface, it exists as hydrated crystal clumps due to restriction in motion imposed by the absence of an alkyl chain [*El-Hassan et al., 1986*]. This also hinders the mass transfer of solute molecules to surface sites.

X-ray photoelectron spectroscopy can be used to measure the external and internal surface composition. A C_{18} monomer modified silica [*Hunnicutt et al., 1986*] showed no difference with depth, indicating an evenly distributed coating. Magnetic resonance spectra of an unbound and C_1 bound silica [*Fyfe et al., 1985*] showed that all 9 percent of the $Si(OH)_2$ sites and about a fifth of the available SiOH sites reacted.

3.5 Sorbate Properties

Sorbates used in this study were chosen to be relatively simple molecules that may exhibit slow sorption and are of environmental concern. Substituted benzenes with 1-3 chloro- groups and nine batch experiment solutes are priority pollutants [*Keith et al., 1979*]. Sixteen compounds were used in batch studies (data in Table 3.3), but only chlorinated benzenes were used in column experiments (data in Table 3.4). Physical properties such as molecular volume, radius, and area were calculated from x-ray diffraction data [*Bondi, 1964*]. Structure - activity relationships were used to calculate some physicochemical data [*Kier and Hall, 1986*] and experimental data are included where noted. For the series of chlorinated benzenes, the molecule volume doubled, but the properties changed considerably. The octanol-water partition coefficient increased four orders of magnitude, molecular diffusion decreased 40 percent, and the vapor pressure decreased six orders of magnitude.

Table 3.3 Sorbents used in batch experiments

Compound	Molecular Weight	Melting Point (°C)	Boiling Point (°C)	Solubility in Water (mg/l)	Log K_{ow}	Vapor Pressure (mm)	K_H (ATM m^2/M)	D_o^1 (cm^2/s)
1,2-Dichloroethane	98.96	-110.	76.12	11,000	1.458	107.2	1.39×10^{-3}	1.15×10^{-5}
1,3-Dichloropropene	111.0	-100.	109.2	8532.	1.603	31.20	5.87×10^{-4}	1.03×10^{-5}
Trichloroethane	133.4	-88.0	108.1	3220.	2.051	28.81	1.73×10^{-3}	9.85×10^{-6}
Trichloroethene	131.4	-89.0	119.1	1814.	2.267	20.72	2.17×10^{-3}	9.85×10^{-6}
Perchloroethene	165.8	-69.0	148.1	326.8	3.020	6.04	4.44×10^{-3}	8.704×10^{-6}
Toluene	92.14	15.92	118.8	328.2	2.791	17.62	7.16×10^{-3}	1.023×10^{-5}
Nitrobenzene	123.1	97.87	189.3	867.0	1.885	.362	7.45×10^{-5}	9.00×10^{-6}
Nitrotoluene	137.14	95.16	204.6	191.8	2.534	.164	1.70×10^{-4}	8.34×10^{-6}

[1]Estimated with the Stokes-Einstein Equation (51)

Table 3.4 Chlorinated benzene data

Compound	Volume[1]		Surface Area[1]		Dimensions[2]			Dipole[3]	T_m[3]	T_b[3]	M	S_w	K_H	log K_{ow}[4]	log K_{oc}[5]	D_o[6]	P_i
	(cm^3/M)	(A^3/atom)	(cm^2/M)	(A^3/atom)	(A)	(A)	(A)	μ (esu)	(°C)	(°C)	(g/M)	(mg/L)	(ATMm^3/M)			(cm^2/s)	(mm)
Benzene	48.36	80.31	5.33	109.5	3.54	8.29	8.29	-	5.52	93.31	78.11	1490.3	0.00395	2.142	2.032	1.00×10^{-5}	52.01
CB	57.84	96.05	7.14	127.1	3.54	8.29	9.07	1.55	-4.8	132.0	112.6	339.8	0.00177	2.855	2.546	8.82×10^{-6}	3.69
1,2-DCB	67.32	111.8	8.95	142.7	3.54	8.29	9.83	2.05	-17	180.5	147.00	---	---	3.523	3.027	8.08×10^{-6}	--
1,3-DCB	67.32	111.8	8.95	144.7	3.54	8.29	9.83	1.36	-25	173.0	147.00	---	---	3.568	3.059	8.08×10^{-6}	---
1,4-DCB	67.32	111.8	8.95	144.7	3.54	8.29	9.83	0.20	3.6	174.0	147.00	79.1	0.00164	3.568	3.059	8.08×10^{-6}	0.286
1,2,3-TCB	76.80	127.5	10.76	158.3	3.54	9.07	9.83	--	52.7	218.0	181.45	---	---	4.281	3.572	7.49×10^{-6}	--
1,2,4-TCB	76.80	127.5	10.76	160.2	3.54	9.07	9.83	--	25.0	233.9	181.45	13.71	0.00140	4.2811	3.572	7.49×10^{-6}	0.0730
1,3,5-TCB	76.80	127.5	10.76	162.2	3.54	9.07	9.83	0	63.2	208.0	181.45	---	---	4.281	3.572	7.49×10^{-6}	--
1,2,3,4-TeCB	86.28	143.3	12.57	173.8	3.54	9.07	9.83	-	46.9	254.0	215.9	---	---	4.994	4.086	7.00×10^{-6}	--
1,2,3,5-TeCB	86.28	143.3	12.57	175.8	3.54	9.07	9.83	-	50.8	216.0	215.9	---	---	4.994	4.086	7.00×10^{-6}	--
1,2,4,5-TeCB	86.28	143.3	12.57	175.8	3.54	9.07	9.83	-	139.1	267.4	215.9	0.188	0.00134	4.994	4.086	7.00×10^{-6}	0.00081
PCB	95.76	159.0	14.38	189.4	3.54	9.47	9.83	-	84.6	298.0	250.3	0.118	0.000288	5.107	4.599	6.58×10^{-6}	9.4×10^{-5}
HCB	105.2	174.8	16.19	203.0	3.54	9.83	9.83	0.63	228.0	322.0	285.8	---	---	6.438	5.125	6.16×10^{-6}	--

[1][*Bondi, 1964, Miller et al., 1984*]

[2][*Bondi, 1964, Kier and Hall, 1986*]

[3][*Miller et al., 1984*]

[4][*Schwarzenbach and Westall, 1981, Hanai and Hubert, 1984*]

[5]Calculated with equation (21)

[6]Calculated with equation (51)

CHAPTER 4
RESULTS

Batch and column experiments were used to examine the sorption of hydrophobic compounds from aqueous solution to surfaces. Batch experiments were used primarily for screening of sorbate/sorbent combinations that exhibited slow sorption, and for developing isotherms. Column experiments were used to determine sorption parameters while simulating one-dimensional ground water flow.

4.1 Batch Experiments

4.1.1 Batch Screening for Slow Sorption Combinations

Results of batch experiment indicate the relative time necessary for various sorbate-sorbent combinations to reach equilibrium. Sorption of dichloroethane (DCA) and trichloroethylene (TCE) onto unbonded porous and nonporous silica reached equilibrium within minutes. Sorption of TCE onto high-f_{oc} organic-coated silica (C_1, C_8, and C_{18}) reached equilibrium within 30 minutes (Table 4.1), indicating some observable kinetic effects. However, tetrachloroethylene (PCE) sorption and desorption on a C_1 coated silica took longer; on the order of 10 and 50 hours, respectively. Experiments of sorption of TCE onto the high-f_{oc} organic-coated silica were performed with a cosolvent, methanol, in order to be able to wet the sorbent. This cosolvent lowers the K_p (see Section 2.1.3), and may cause faster sorption and desorption rates [*Nkedi-Kizza et al., 1987*].

Sorption of 1,4-dichlorobenzene (DCB) and nitrotoluene onto unbonded porous silica (Table 4.2) reached equilibrium in 10 hours. The substituted aromatic compounds investigated generally exhibited slower desorption than sorption from organic-coated silicas. Vials for desorption experiments were equilibrated for 1-2 weeks before starting experiments. Toluene sorption and desorption on a high-f_{oc} C_{18} silica was relatively fast, and reached equilibrium in 30 minutes. Nitrobenzene and nitrotoluene sorption onto C_{18} silica also reached equilibrium in 30 minutes, but desorption took about 100 hours. Sorbate/sorbent combinations that exhibited the slowest behavior were DCB, 1,2,4-trichlorobenzene (TCB), and 1,2,4,5-tetrachlorobenzene (TeCB) onto phenyl and

Table 4.1 Batch results with aliphatic sorbents

Solute		Sorbent[1]		r_{sw}	K_p	Time Scale[2]	
	($\mu g\ cm^{-3}$)	ident	type	($g\ cm^{-3}$)	($cm^3 g^{-1}$)	sorb(hr)	des(hr)
dichloroethane	0.217	J	unb	0.29	3.16	1.0	---
dichloropropene	0.185	J	unb	0.36	0.46	0.5	---
trichloroethane	0.211	J	unb	0.36	0.78	1.0	---
trichloroethane	0.303	J	unb	0.34	0.95	1.0	---
trichloroethene	0.210	J	unb	0.34	0.60	2.0	---
trichloroethene	0.187	AC	unb	0.19	3.17	1.0	---
trichloroethene	0.176	AD	unb	0.25	3.59	20.0	---
trichloroethene	0.176	K	unb	0.094	13.4	2.0	---
trichloroethene[3]	0.149	L	C_1	0.023	42.3	1.0	1.0
trichloroethene[3]	0.199	L	C_1	0.023	48.8	1.0	---
trichloroethene[3]	0.201	AA	C_2	0.031	94.5	2.0	---
trichloroethene[3]	0.225	M	C_8	0.0094	132.	0.5	---
trichloroethene[3]	0.199	M	C_8	0.032	90.3	1.0	---
trichloroethene[c]	0.185	N	C_{18}	0.031	260	1.0	1.0
trichloroethene[c]	0.209	N	C_{18}	0.026	274	1.0	---
trichloroethene	0.145	AT	C_{18}	0.026	2.75	1.0	---
trichloroethene	0.198	AB	amine	0.095	5.65	1.0	---
perchloroethene	0.199	L	C_1	0.022	118	10.0	50.0
perchloroethene	0.200	N	C_{18}	0.034	937	1.0	2.0
perchloroethene	0.192	J	unb	0.31	2.65	2.0	---

[1]See Table 3.1.
[2]Time after which no change in $K_p \pm 2$ percent.
[3]Methanol used as a cosolvent.

Table 4.2 Batch results with aromatic sorbents

Solute		Sorbent[1]		r_{sw}	K_p	Time Scale[2]	
	($\mu g\ cm^{-3}$)	ident	type	($g\ cm^{-3}$)	($cm^3 g^{-1}$)	sorb(hr)	des(hr)
toluene	5.620	N	C_{18}	0.029	33.8	1.0	1.0
nitrobenzene	0.971	AU	C_{18}	0.056	7.65	1.0	100
nitrotoluene	1.005	I	unb	0.118	4.78	0.2	---
nitrotoluene	1.005	W	unb	0.118	9.86	0.2	---
nitrotoluene	1.005	AJ	unb	0.118	1.62	0.5	---
nitrotoluene	1.005	AR	unb	0.118	2825	2.0	---
nitrotoluene	1.005	P	unb	0.118	5.67	0.5	---
nitrotoluene	1.005	AU	C_{18}	0.056	9.53	0.5	100
1,4-DCB	6.000	AE	unb	0.056	3.86	10.0	---
1,4-DCB	0.810	AE	unb	0.056	2.74	5.0	---
1,4-DCB	0.506	N	C_{18}	0.29	1073	0.2	0.5
1,4-DCB	3.785	AT	C_{18}	0.056	21.6	1.0	20.0
1,4-DCB	10.40	AT	C_{18}	0.056	11.5	0.5	1.0
1,4-DCB	0.483	C	C_{18}	0.056	17.3	1.0	22.0
1,4-DCB	0.393	E	PhP	0.111	19.9	2.0	---
1,4-DCB	0.548	H	PhP	0.111	10.7	1.0	22.0
1,2,4-TCB	0.320	H	PhP	0.111	89.9	21.0	50.0
1,2,4,5-TeCB	0.245	C	C_{18}	0.056	111	20.0	21.0
1,2,4,5-TeCB	0.105	H	PhP	0.111	36.0	23.0	100
PCB	0.030	P	unb	0.056	25.8	1.0	---

[1]See Table 3.1.
[2]Time after which no change in $K_p \pm 2$ percent.

C_{18} coated silica. The first-order rate coefficients were on the order of 10^{-3} s^{-1} for sorption and 10^{-3} to 10^{-4} for desorption.

In most cases, diffusion or chemical models were not fit to data because only an estimate of the time scale for equilibration was needed. Batch screening indicated that substituted aromatics showed the slowest sorption and desorption. Two surfaces were examined further in batch experiments, the C_{18}-modified silica, and phenyl-polymer modified silica.

4.1.2 Batch Results of Chlorinated Benzenes and C_{18} Silica

DCB sorption onto a high-f_{oc} C_{18}-coated silica was examined in detail with planar and spherical diffusion and first-order chemical models (Figure 4.1). The data show faster sorption (within 1 hour) than desorption (up to 20 hours).

With a single diffusion parameter, the spherical diffusion model (equation 33) gave a relatively good fit to the sorption data, but a poor fit to the desorption data (case 1 on Figure 4.1). In case 2, the desorption data were fit using a diffusion constant 3-fold smaller; the point at 20 hours was used for the fit. The sorption data, however, cannot be fit with the diffusion constant obtained in case 2.

A planar diffusion model is mathematically similar to the spherical diffusion model, but with a slightly steeper slope before reaching equilibrium. The model fit to the sorption data is good (case 3), but the model fit to the desorption data is poor. Using parameter α in the model ($\theta/\rho_b K_p$) as a fitting parameter rather than fixing it at the appropriate value, a change in slope can be made that results in a better fit to the desorption data (case 4). This corresponds to a K_p of 154 $cm^3 g^{-1}$, or 7 times larger than indicated by the equilibrium K_p from the desorption data.

The best model fit is obtained with either a planar or a spherical diffusion model using the observed K_p with the sorption data, and using a seven-fold higher K_p with the desorption data. Spherical diffusion is probably closer to the actual diffusional geometry of the particle, however, planar diffusion is appropriate for diffusion into the surface

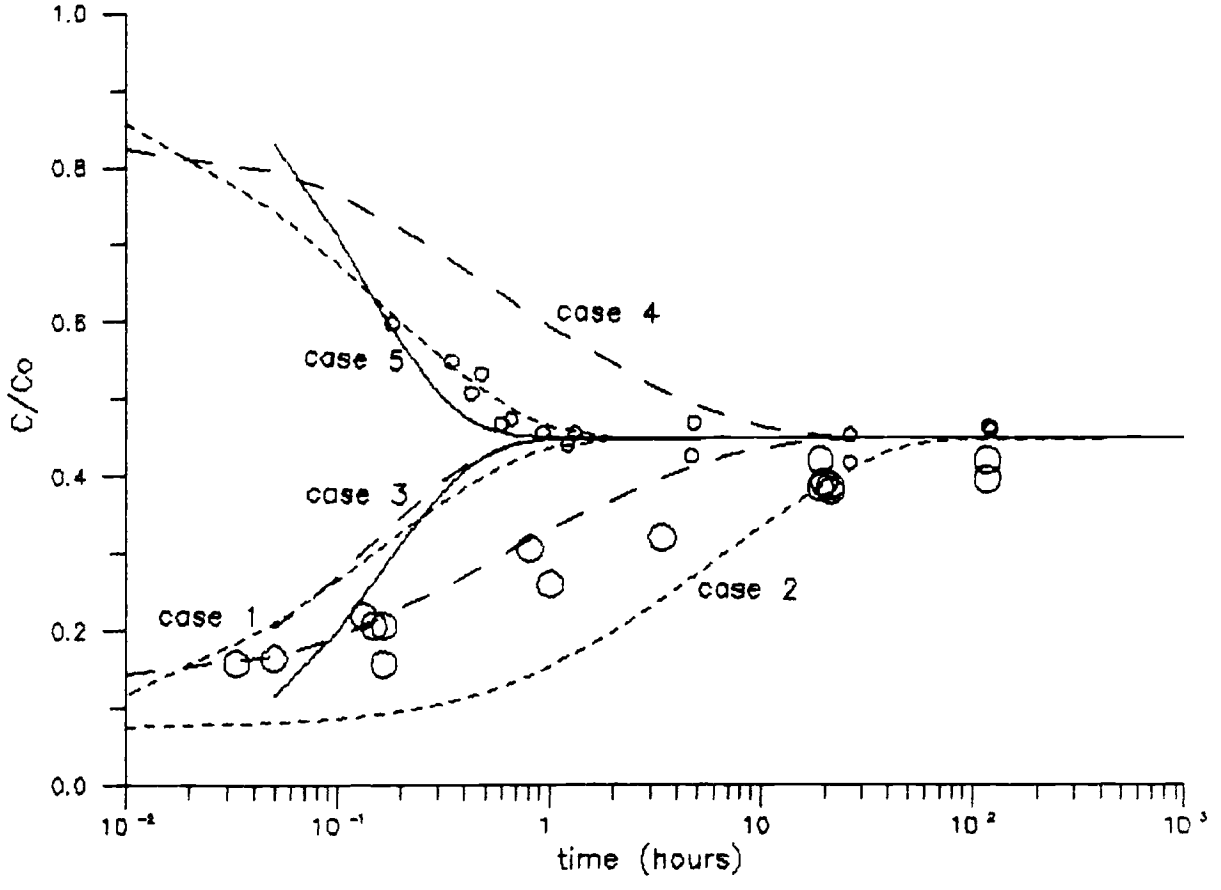

Case 1: Spherical Diffusion (D = 5.5 x 10^{-5} s^{-1})
Case 2: Spherical Diffusion (D = 1.8 x 10^{-5} s^{-1})
Case 3: Planar Diffusion (D = 6.3 x 10^{-5} s^{-1})
Case 4: Planar Diffusion (D = 1.2 x 10^{-6} s^{-1}, K_p = 154 $cm^3 g^{-1}$)
Case 5: First-order Reaction (K_p = 22 $cm^3 g^{-1}$, k_f = 1.5 x 10^{-3} s^{-1}, k_b = 1.4 x 10^{-4} s^{-1})

Figure 4.1 Sorption/desorption of 1,4-DCB onto C_{18} modified silica

organic layer (which is not very thick). However, since different model parameters are needed for sorption and desorption, diffusion alone is not causing the observed slow approach to equilibrium; the desorption tailing must be caused by the chemical nature of the sorbent.

A first-order chemical model (equation 30) was fit to the data in case 5 (Figure 4.1). As with the diffusion models, a better model fit was obtained with the sorption data compared to the model fit to the desorption data. Note that the first-order model does allow for a difference in rate of approach to equilibrium between sorption and desorption. The desorption data were modeled with a slightly smaller coefficient than the sorption data. The sorption rate was on the order of 2×10^{-3} s^{-1} and desorption rate 1×10^{-3} s^{-1}, although the model fit to the desorption data was poor. This surface was a porous silica that was not well characterized, so additional experiments were done on well characterized silica modified with C_{18} polymer (sorbent C).

The first-order model fit to DCB sorption onto the C_{18}-modified surface (Figure 4.2A) gave a good fit with $k_f = 1.1 \times 10^{-3}$ s^{-1}, and the desorption data fit with $k_b = 3.8 \times 10^{-4}$ s^{-1}. The first-order model fit of TeCB sorption onto the C_{18} surface (Figure 4.2B) gave a good fit with $k_f = 2.8 \times 10^{-3}$ s^{-1} and desorption with $k_b = 6.3 \times 10^{-5}$ s^{-1}. Note that as sorption increases from DCB to TeCB, the ratio of k_f/k_b increases, corresponding to a slight increase in k_f and a large decrease in k_b. The model fit was made with equations (31) and (32).

4.1.3 Batch Results of Chlorinated Benzenes and Phenyl-Silica

Sorption and desorption rates of DCB, TCB, and TeCB on a phenyl-polymer modified silica (surface H) were examined with batch experiments and modeled with a first-order chemical model as shown in Figure 4.3. Dichlorobenzene sorption ($k_f = 9.0 \times 10^{-4}$ s^{-1}) and desorption ($k_b = 5.0 \times 10^{-4}$ s^{-1}) again showed a good fit to the sorption data and a fair fit to the desorption data. Desorption appeared to proceed as fast as sorption when far from equilibrium, but near equilibrium, the rate was slower (Figure 4.3A).

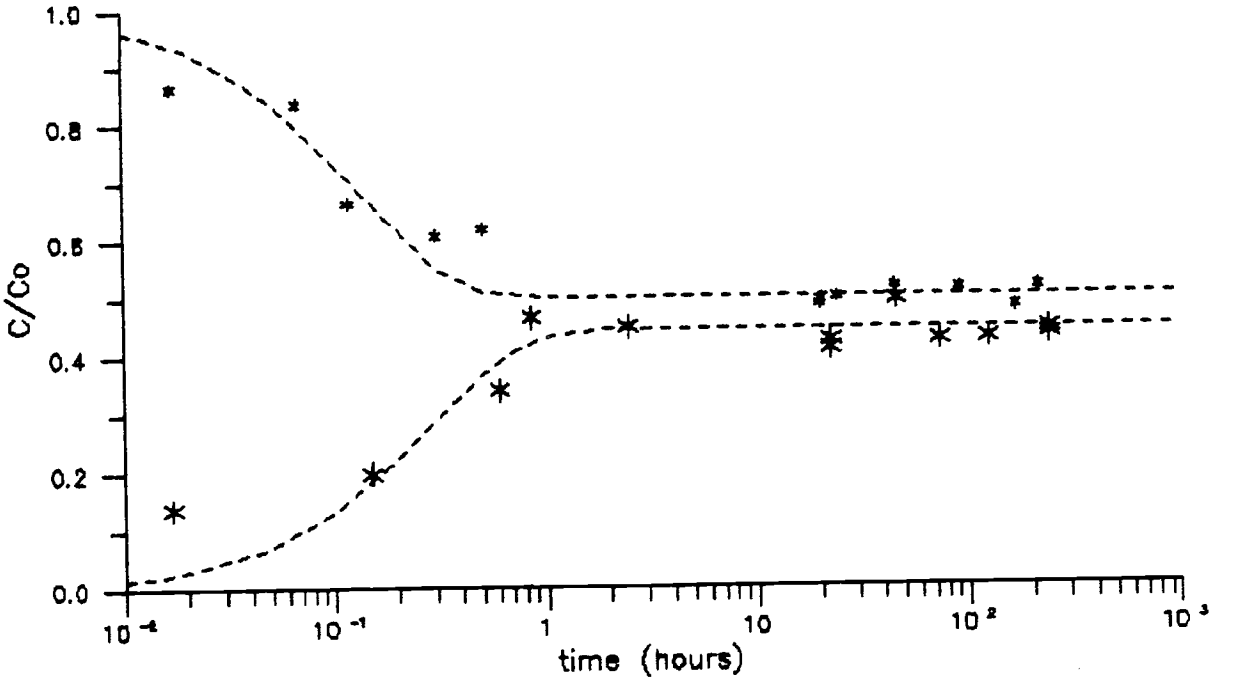

A. 1,4-Dichlorobenzene

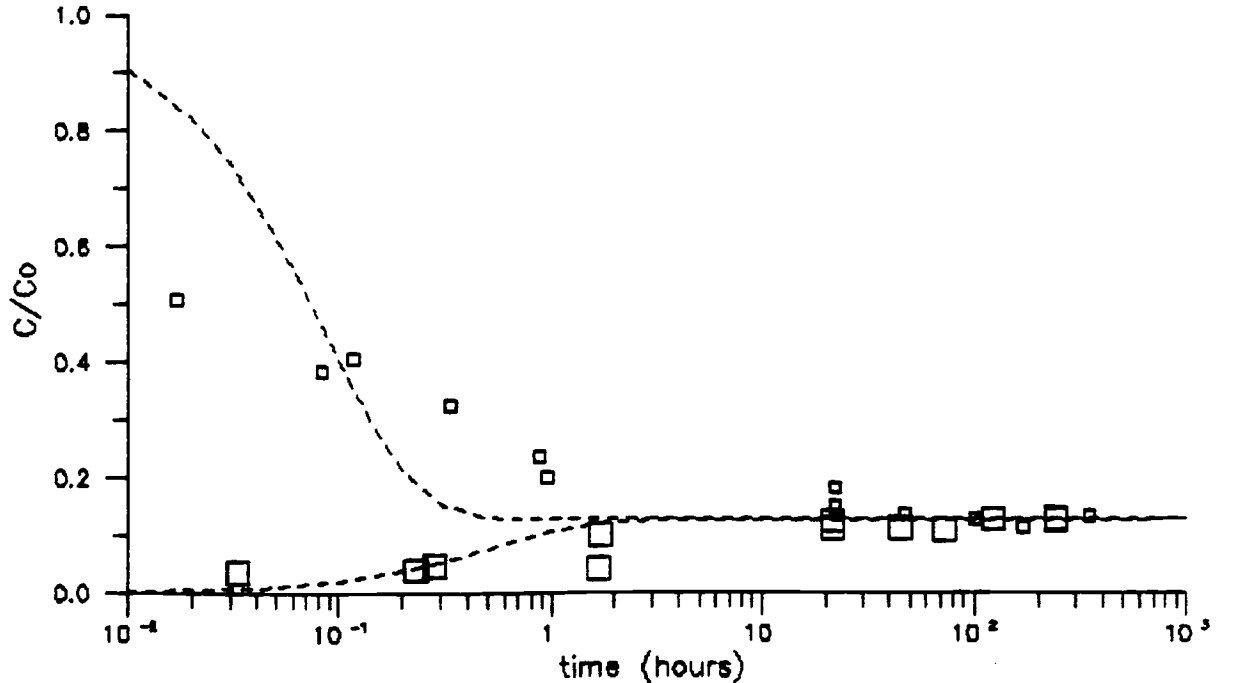

B. 1,2,4,5-Tetrachlorobenzene

Figure 4.2 Batch sorption/desorption onto C_{18} modified silica

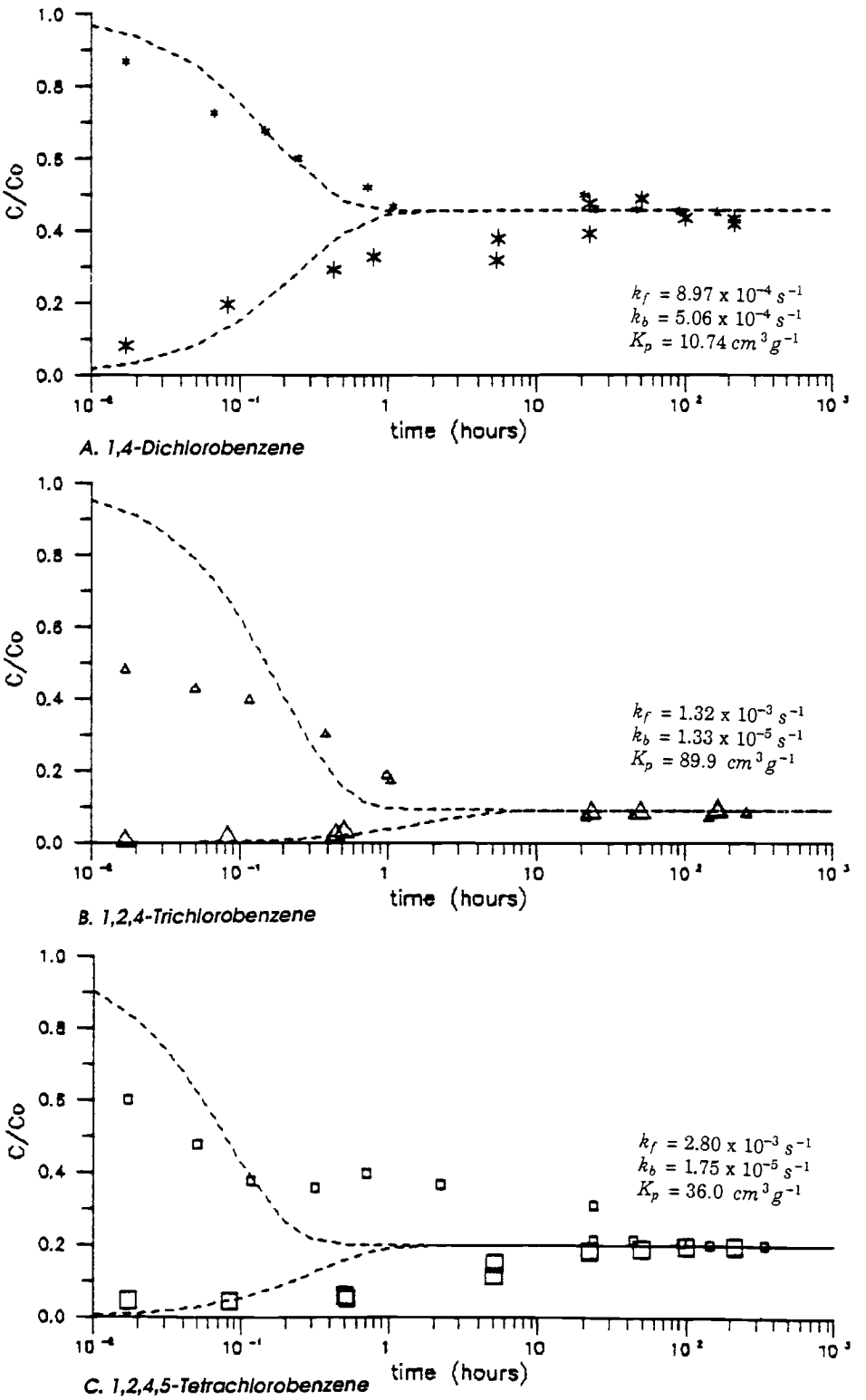

Figure 4.3 Batch sorption/desorption onto phenyl polymer modified silica (surface E)

Sorption of TCB (k_f = 1.3 x 10^{-3} s^{-1}) exhibited about the same rate as DCB, but desorption was slower (k_b = 1.3 x 10^{-5} s^{-1}). The model fit to the desorption data was uncertain due to small f_l at equilibrium (Figure 4.3B). Sorption of TeCB (k_f = 2.8 x 10^{-3} s^{-1}) was slightly faster than other chlorinated benzenes (Figure 4.3C), and desorption was slower (k_b = 1.8 x 10^{-5} s^{-1}) by 1.5 orders of magnitude compared to DCB. As discussed in the Section 3.2, the sorption data are more accurate (± 2 percent) than the desorption data (± 5 percent) due to more steps in the procedure for desorption experiments.

Note that the sorption and desorption of DCB appeared to have almost identical rates for both C_{18} and phenyl modified surfaces (same diameter particles), whereas the desorption rate of the TeCB data was half an order of magnitude slower than indicated by the phenyl silica data. With the sampling procedure used, accurate samples cannot be obtained in less than one minute. The lack of difference in the reaction rates may be caused by this experimental limitation, where the actual rate may be faster. Column experiments were used to determine faster sorption rates.

4.1.4 Isotherms of DCB Sorption Onto Phenyl Modified Silica

Equilibrium partitioning of 1,4-dichlorobenzene on a phenyl modified silica (surface F) was examined, with concentrations ranging from 10 $ng\,cm^{-3}$ to the solubility limit (87 $\mu g\,cm^{-3}$). The lower limit was 20 times the minimum detection limit, so is subject to error with even a small amount of contamination or analytical error. A total of 60 vials were analyzed for this isotherm at sixteen different concentrations (Figure 4.4A), with an average K_p of 39 ± 16 $cm^3\,g^{-1}$.

A power-series fit to the full data set (Figure 4.4A) gave an exponent of 0.92 (r^2 = 0.961), indicating virtually no decrease in partitioning even at the solubility limit; justifying the claim that the number of available sorption sites is large compared to the number of sorbed sites. The calculated number of sites occupied is 1/100,000 at a concentration of 500 $\mu g\,L^{-1}$ (most experiments).

Column experiments are generally run at concentrations lower than 1.0 mg L^{-1}, so an isotherm of all partitioning data below this limit has a power series exponent of 1.08 (r^2 = 0.894), which indicates slightly greater sorption above 500 µg L^{-1}. The slope of the low-concentration data is not significantly different from 1.00 at the 90 percent confidence level, so a linear isotherm was used in modeling data from the column experiments. A trend of slight decrease in K_p at higher concentrations is shown in Figure 4.4B, with considerable variation at very low concentrations. A nonlinear isotherm has some effect on the breakthrough curve shape (Section 2.2.7), but with exponential values of 1.08, there is essentially no noticeable effect, and a linear isotherm is assumed for modeling column experiments.

Isotherms were also developed from column experiments to test the linearity of sorption and desorption (Section 4.4.4.2). A sorption isotherm was also calculated from a single column experiment (equation 76), assuming the sorption reaction is at equilibrium at all times.

4.2 Ionic Tracer Breakthrough

4.2.1 Ion Exclusion

The breakthrough curve for a nonsorbing tracer, KCl, was used as an independent estimate of the void volume in the column. Experiments were performed to determine the ionic strength range where anion exclusion would be minimized so that KCl breakthrough could be considered conservative. Premature breakthrough of anions caused by the exclusion produces a pore volume (and porosity) value smaller than the total. Since chromatographic silica has a large amount of surface area, and exclusion is a near surface phenomena, a large amount of exclusion is possible. A total of forty KCl breakthrough experiments were performed; results are shown in Appendix A. The total porosity of 100-µm porous silica when packed into columns is about 0.86, of which intraparticle porosity is 0.46, and interparticle porosity is 0.40 [*Iler, 1979*]. Porosities are calculated from KCl breakthrough experiments, where the initial (in the column) and final

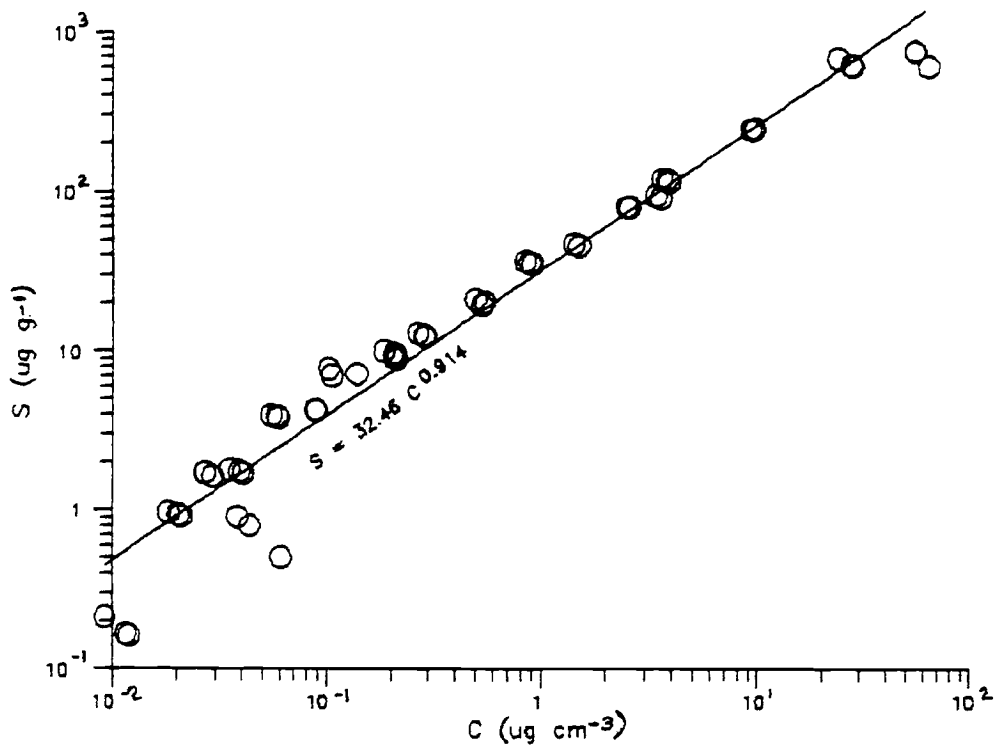

A. Sorption Isotherm of 1,4-DCB on surface F

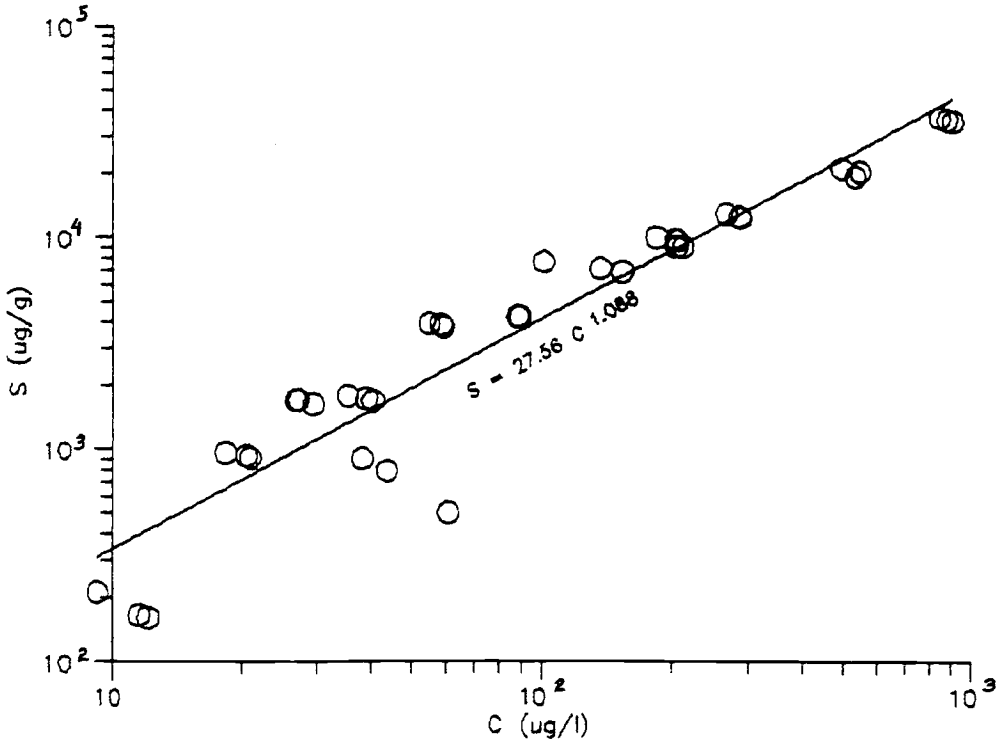

B. Sorption Isotherm for concentrations less than 1.0 ppm DCB

Figure 4.4 Sorption isotherm of DCB

(breakthrough) ionic strength are similar (Figure 4.5A). In these experiments, the initial and final ionic strength differed by two fold (0.01 M and 0.02 M, for example). The data show that the calculated porosity is reduced by anion exclusion from near surface pore space at an ionic strength below 10^{-3} M.

The distance from the surface over which anions are excluded is approximately equal to the double diffuse layer thickness. For a monovalent electrolyte at 25°C, this distance ($1/\kappa$ in nm) is given by [*Stumm and Morgan, 1981*]:

$$\frac{1}{\kappa} = 0.28\, I^{-1/2} \tag{74}$$

where I is the ionic strength (M). An analysis used in soil systems substitutes a step function for the actual exponential decrease of anions (and increase of cations) near charged surfaces [*Krupp et al., 1972*]:

$$d_s = 0.448\, I^{-1/2} - 0.0566 \tag{75}$$

where d_s is the exclusion distance (nm), and constants for silica have been included in the two coefficients.

The change in the calculated porosity of KCl at different ionic strengths (Figure 4.5A) shows up to 50 percent exclusion (all intraparticle volume) at 10^{-4} M ionic strength, and no effect at 10^{-3} M. This narrow ionic strength range is due to the narrow pore size distribution.

The magnitude and direction of the step change in ionic strength also affects the amount of anion exclusion (and the calculated porosity). Eleven experiments were run varying only the initial KCl concentration from 10^{-5} to 1 M, and keeping the final concentration at 10^{-5} M for maximum effect (Figure 4.5B). Up to a 60 percent decrease in calculated porosity is observed at concentrations below 10^{-4} M. In addition, six experiments were done in which the final ionic strength was varied (Figure 4.5C). These showed exclusion at concentrations below 10^{-2} M. Experiments in which the final ionic strength was varied did not show as much exclusion as varying the initial ionic

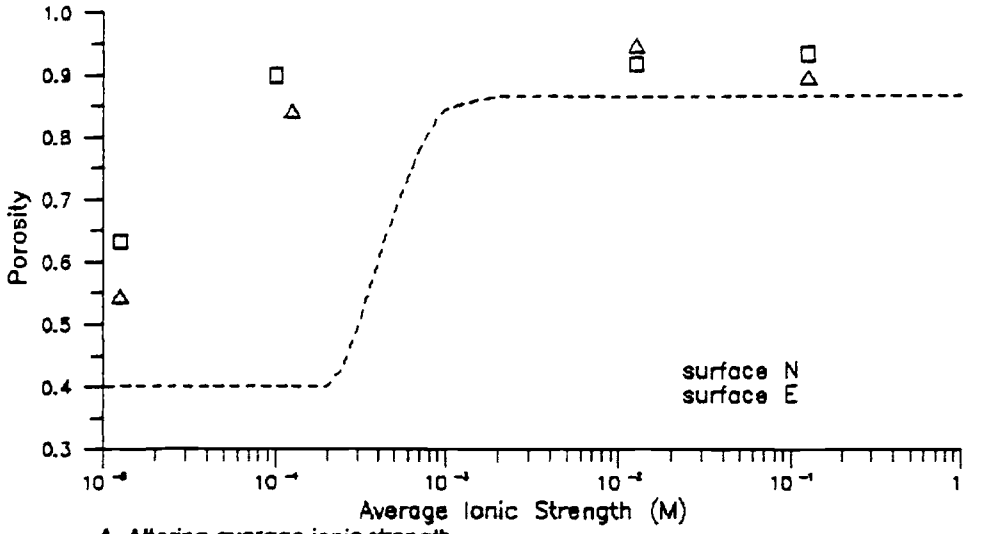

A. Altering average ionic strength

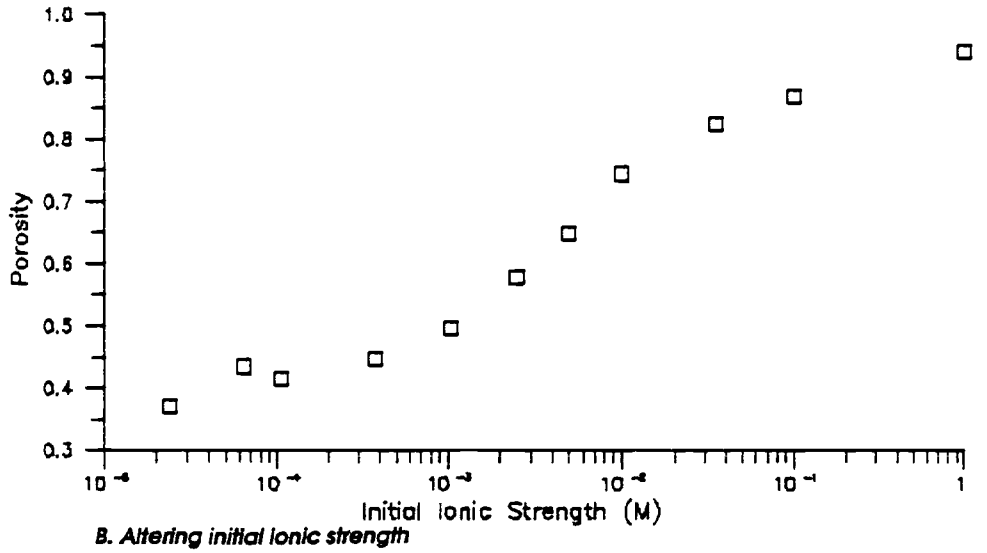

B. Altering initial ionic strength

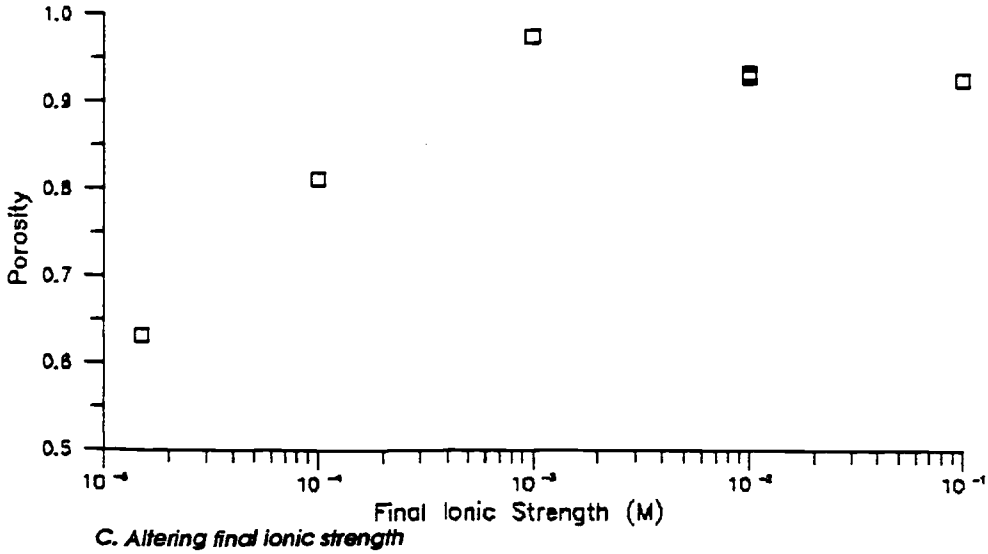

C. Altering final ionic strength

Figure 4.5 ionic strength effect on porosity

strength, since at a KCl concentration of 10^{-5} M, exclusion was only about 30 percent (varying final ionic strength), compared to 60 percent when varying initial ionic strength.

Results show that the exclusion process is dynamic, which is not indicated with the static exclusion models. In the frontal analysis of breakthrough curves [*Jacobson et al., 1984*], the porosity is calculated based on the final solute concentration, so in effect, the porosity is considered independent of the initial ionic strength [*Horvath and Lin, 1976*]. The average porosity in a column could be estimated using a numerical simulation to describe changing porosity during ion breakthrough. If the kinetics of reaching anion sorption equilibrium are important, then the calculated porosity would be more dependent on initial ionic strength. This conclusion is likely, since varying initial ionic strength had more effect on the calculated porosity.

4.2.2 Dispersion of the Ionic Tracer

In order to separate spreading of solute due to a slow interaggregate process from hydrodynamic dispersion, the effects of velocity, column diameter and length, and repacking on dispersion were investigated. Results from eleven different sorbate/column groups were correlated with velocity (Table 4.3). As expected, there was no correlation between column length or diameter and dispersion. Many results have a large error due to the small number of experiments. The larger particles generally showed greater dispersion than the smaller particles. This is expected as interparticle diffusion is greater for the larger aggregate particles (Table 2.7).

Considering data from all the column experiments (n = 139) produces the relation between velocity and dispersion illustrated in Figure 4.6A (r^2 = 0.851). The spread in the data is due to repacking the same sorbent into a column, dissolution of the sorbent, or grain rearrangement due to the pressure in the column. Running experiments with a single column (not repacked) produces a better correlation between velocity and dispersion (Figure 4.6B, r^2 = 0.995), with the relationship being similar to the overall trend shown in Figure 4.6A (all experiments). The power series relationship of Figure 4.6B (D

Table 4.3 Hydrodynamic dispersion of an ionic tracer

Sorbate Dia.(μm)	Name	Column Dia.x Length (cm)	Number of exp.	Power Series Fit	r^2
2 μm Solid	AH,O,U	1.0 x 5.0	3	$D = 0.119\ v^{0.755}$	
20 μm	F	0.9 x 14	3	$D = 2.61 \times 10^{-12}\ v^{-6.74}$	
	G	1.0 x 14	3	$D = 5.18 \times 10^{6}\ v^{6.38}$	
100 μm Phenyl	E	0.9 x 5.0	19	$D = 0.859\ v^{1.66}$	
	E	1.0 x 14	4	$D = 12.4\ v^{1.57}$	
100 μm Unbonded	I,D	0.9 x 5.0	11	$D = 5.23 \times 10^{7}\ v^{7.23}$	
100 μm Aliphatic	I,B,C	1.0 x 14	42	$D = 0.150\ v^{1.10}$	
All 100 μm	I,B,C X,R,T	0.9 x 14	16	$D = 0.465\ v^{1.17}$	
100 μm Unbonded	I	0.9 x 14	7	$D = 0.267\ v^{1.303}$	0.984[1]
236 μm	Y,Z	1.0 x 10.5	3	$D = 7.39\ v^{2.23}$	
425 μm	V	0.9 x 25	3	$D = 6.28\ v^{1.83}$	
	H	1.0 x 14	3	$D = 5.5 \times 10^{-30}\ v^{-19.2}$	
All Sizes	All	All	139	$D = 0.210\ v^{1.137}$	0.851[2]

[1]Shown in Figure 4.6B.

[2]Shown in Figure 4.6A.

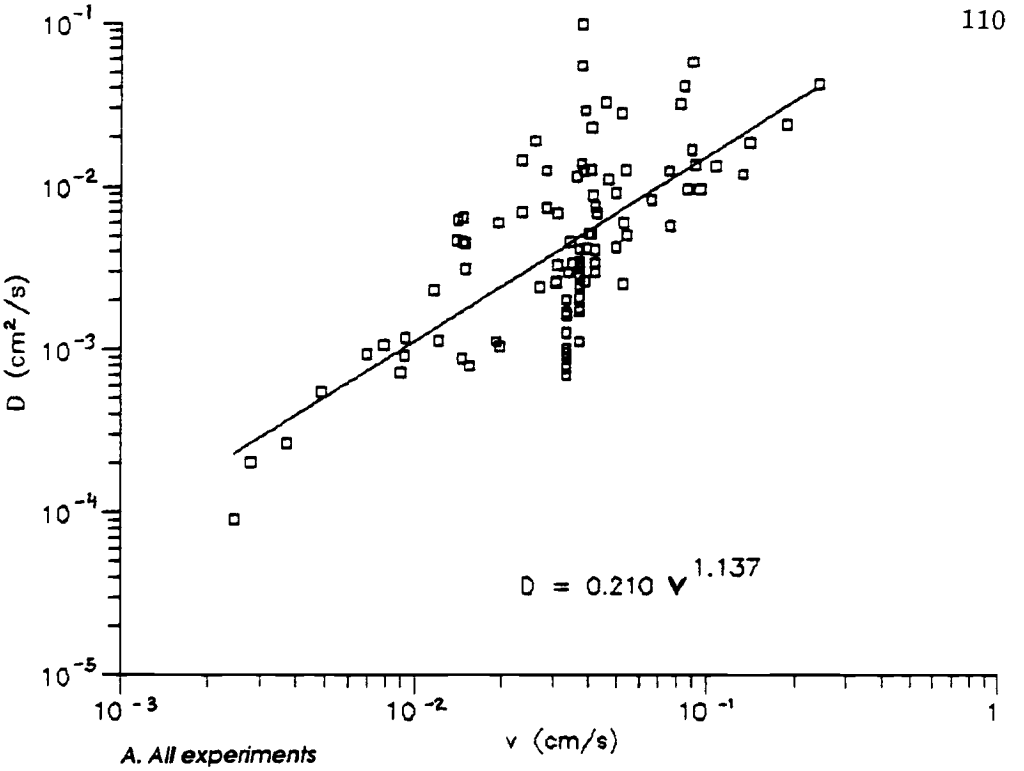

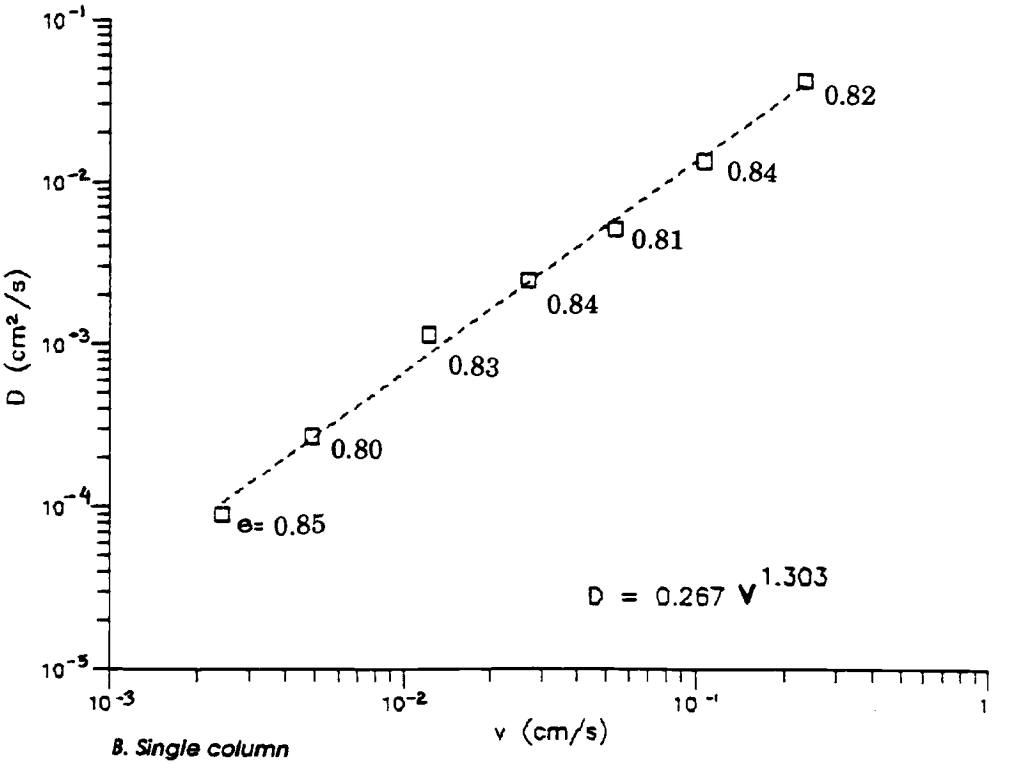

Figure 4.6 Velocity dependence of dispersion

= 0.267 $v^{1.31}$) was used to estimate KCl dispersion for subsequent experiments in the few cases where a good KCl breakthrough curve was not obtained.

The pressure in the column changes from < 100 psi at low velocities (0.0017 cm s^{-1} in Figure 4.6B) to over 3000 psi for 0.15 cm s^{-1}. As indicated by the porosities shown next to points in Figure 4.6B, there is no correlation of porosity with pressure.

4.3 Solute Sorption Onto Unbonded Mineral Surfaces

An acidic surface (silica) and a basic surface (alumina) were used in experiments to determine the extent of partitioning of chlorinated benzenes to unbonded surfaces. Sorption was fast in all cases, with little evidence of nonequilibrium behavior.

4.3.1 Silica

Six column experiments using two unbonded silicas were performed with sorption of DCB, two with TCB, and two with TeCB. All experiments are shown in Appendix C-1, with modeling results in Table 4.4. Sorption of DCB onto 100-μm porous silica (surface I; shown in Figure 4.7A) had an average K_p of 4.05 ± 0.95 (Table 4.4), which was fast and reversible sorption. Sorption of DCB onto 425-μm porous silica (surface V) had a K_p of 3.01 (higher surface area) and was also fast and reversible. The K_p for sorption divided by the K_p for desorption (K_{ps}/K_{pd}) was slightly greater than 1.0 in both cases (1.32 ± 0.49 for surface I and 1.17 ± 0.27 for surface V). Since four of the experiments on the 100-μm surface were the earliest experiments when the experimental procedure was still being refined, the error was larger, possibly accounting for this discrepancy.

The equilibrium model fits to the data suggest that DCB breakthrough was near equilibrium since the D_{DCB}/D_{KCl} ratio was 2.17 ± 0.81 for the 100-μm silica and 3.11 for the single experiment on the 425-μm silica. Calculated ratios (Table 2.7) are on the order of 1.4 for the 100-μm and 1.9 for the 500-μm particles. Equilibrium sorption is also indicated by the first-order model fits, which give large ω's (> 60). The best estimate of the first-order model k_b (Table 4.4) is 0.024 s^{-1} for 100-μm silica and 0.013 s^{-1} for 425-μm silica. This indicates that the time scale of the sorption reaction (defined by

Table 4.4 Sorption onto unbonded surfaces

					Equilibrium Model			First Order Model				Two Region Model				
Exp.	Sorbent	Solute	D_{KC} (cm^2/s)	K_{pS}[1] K_{pD}[2] rev. (cm^3/g)	K_p (cm^3/g)	D (cm^2/s)	D/D_{KC} ssq	K_p (cm^3/g)	N_D	k_b (s^{-1})	ssq	K_p (cm^3/g)	N_D	α_e (s^{-1})	f	ssq
I-6 Y	PQ-N	DCB	0.0033	--- --- ---	0.005	0.0261	7.84 0.7230	---	---	---	---	---	---	---	---	---
I-7 Z			0.00688	5.731 4.304 1.332	3.555	0.00856	1.24 0.2700	---	---	---	---	---	---	---	---	---
I-8 ZZ			0.00744	5.235 2.479 2.112	1.659	0.00121	1.63 0.1885	---	---	---	---	---	---	---	---	---
I-9 ZB			0.00106	3.346 2.300 1.455	3.552	0.00275	2.59 0.2422	---	---	---	---	---	---	---	---	---
I-1 ZC			0.000925	4.220 4.782 0.882	4.037	0.00248	2.68 0.1375	3.848	63.90	0.0288	0.1625	4.20	0.7011	0.000186	1.098	0.1153
ave.				4.050 ± 0.945 1.317 ± 0.493			2.173 ± 0.806									
I-2 SF	PQ-V	DCB	0.00508	3.013 3.001 1.004	5.193	0.0158	3.11 0.1415	5.122	68.09	0.0422	0.1397	---	---	---	---	---
I-3 SG	AL-A		0.00794	0.565 0.234 2.415	0.906	0.0996	12.54 0.5044	0.614	10^3	268.0	0.6114	0.400	55992	33.70	1.934	0.7020
I-4 SH	AL-B		0.00267	0.355 0.336 1.057	0.412	0.00605	2.27 0.292	0.345	10.44	0.0553	0.1102	0.345	160.5	0.0993	1.622	0.0999
I-5 SI	AL-B		0.00119	0.252 0.412 0.612	0.341	0.00128	1.08 0.3824	---	---	---	---	---	---	---	---	---
I-2 SF	PQ-V	TCB	0.00508	4.772 5.080 0.939	8.542	0.0231	4.55 0.1566	8.402	53.43	0.0202	0.1527	---	---	---	---	---
I-10 SD	PQ-V		0.00941	10.47 11.31 0.926	9.660	0.0321	3.41 0.1329	9.457	285.1	0.154	0.1327	9.46	409.1	0.445	0.097	0.1326
ave.				7.91 ± 3.46 0.933 ± 0.009			3.98 ± 0.80									
I-3 SG	AL-A	TCB	0.00794	2.018 2.000 1.009	1.904	0.0398	5.01 0.1090	---	---	---	---	---	---	---	---	---
I-4 SH	AL-B		0.00267	1.166 1.246 0.936	1.259	0.0304	11.4 0.0365	---	---	---	---	---	---	---	---	---
I-2 SF	PQ-V	TeCB	0.00508	8.493 9.001 0.944	14.96	0.0267	5.26 0.1031	14.60	119.6	0.0260	0.1094	---	---	---	---	---
I-10 SD	PQ-V		0.00941	15.76 16.01 0.984	14.77	0.0382	4.06 0.0962	14.45	138.8	0.0491	0.0966	14.42	4195.2	4.56	0.585	0.0936
ave.				12.32 ± 4.13 0.964			4.65 ± 0.846									
I-3 SG	AL-A	TeCB	0.00794	7.354 7.320 1.005	6.919	0.0453	5.71 0.1257	---	---	---	---	---	---	---	---	---
I-4 SH	AL-B		0.00267	4.232 4.512 0.938	4.486	0.0711	26.6 0.1087	---	---	---	---	---	---	---	---	---

[1]From sorption portion of breakthrough curve. [2]From desorption portion of breakthrough curve. [3]Parameter fixed at this value.

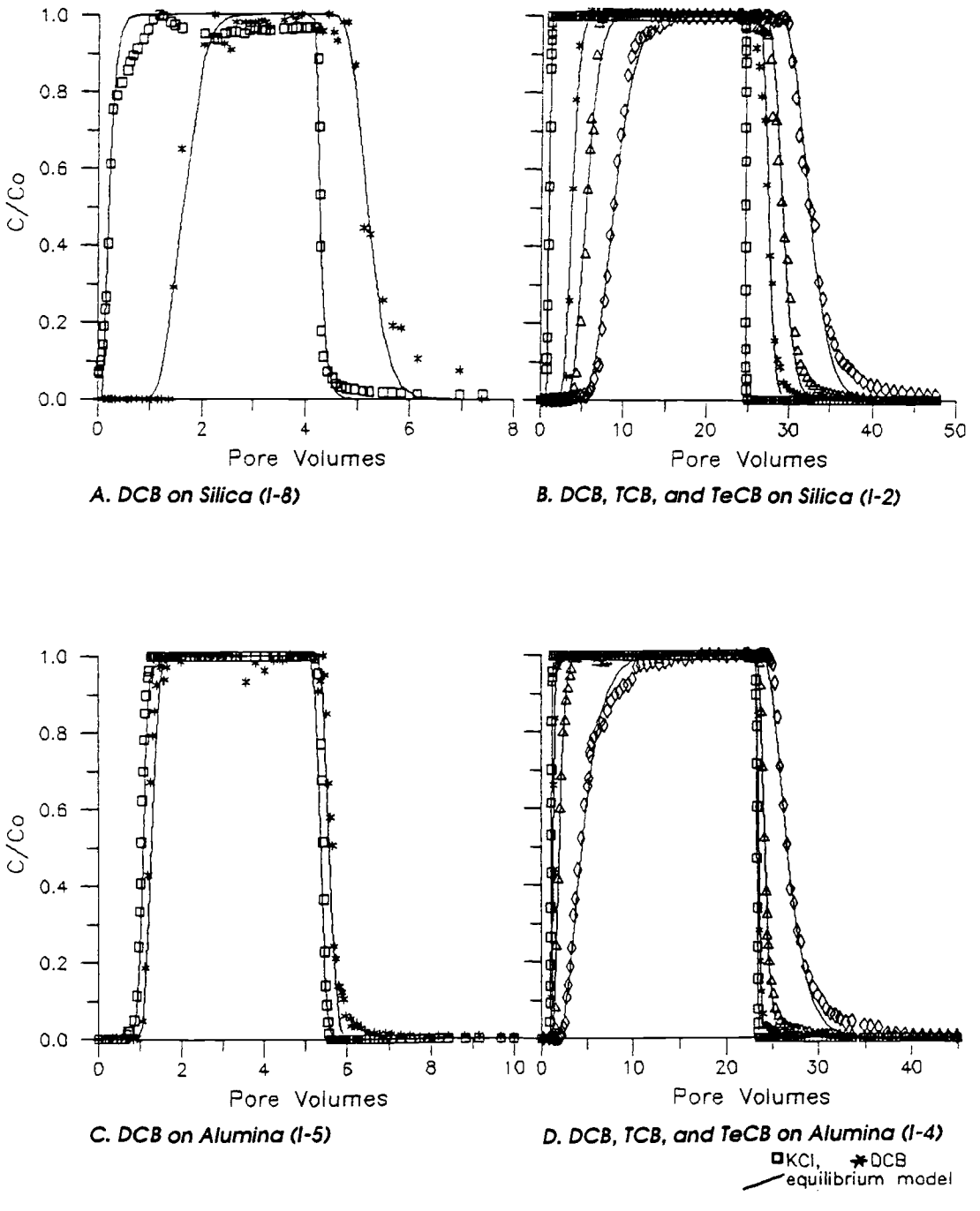

Figure 4.7 Sorption onto mineral surfaces

reaction half-life) is less than a minute for both surfaces. Two experiments with DCB (Figure 4.7A and B) show little tailing of breakthrough curves, where the residence time in the column is on the order of an hour or longer.

Sorption of TCB onto 425-μm silica (two experiments) had an average K_p of 7.91 ± 3.46 (surface V). Sorption was reversible (K_{ps}/K_{pd} = 0.93 ± 0.01) and fast as indicated by large ω's (> 50) and rates (k_b = 2 x 10^{-2} s^{-1}; Table 4.4) using the first-order model. The D_{DCB}/D_{KCl} ratio averaged 3.98, indicating little nonequilibrium, as can be observed in Figure 4.7B with a TCB breakthrough curve.

Sorption of TeCB onto 425-μm silica (two experiments) had an average K_p of 12.3 ± 4.1 which was reversible (K_{ps}/K_{pd} = 0.96 ± 0.03). The equilibrium model D_{DCB}/D_{KCl} ratio averaged 4.66 ± 0.85, which showed greater dispersion for DCB. This is expected since the molecular diffusion coefficient is smaller (Table 2.7) for DCB. The first-order model fit gave a large ω with a k_b of 4 x 10^{-2} s^{-1}. Even with large differences in model fits, generally, smaller ω's are observed with TeCB than DCB as expected, apparently reflecting slower diffusion or exchange at the surface.

Four experiments were done injecting multiple solutes onto unbonded surfaces; DCB, TCB, and TeCB were sorbed to silica (Figure 4.7B). The partition coefficients were similar to those obtained from single solute experiments. The number of silica adsorption sites is very large compared to the number of sorbed sites, so sorption should be independent of additional solutes in solution. Chromatography researchers [*Snyder and Kirkland, 1979*] use silica for separation of hydrophobic solutes and assume no difference in partitioning when multiple solutes are present.

4.3.2 Alumina

Three experiments of chlorinated benzenes sorption were performed on two different porous aluminas (Appendix C-2). Sorption of DCB onto surface Y (4.0-nm pore) produced a K_p of 0.35 $cm^3 g^{-1}$, substantially less than on silica. As the hydrogen atoms on hydrophobic compounds represent a slightly positive pole [*Thurman, 1985*], these

compounds should be attracted to a surface which has a negative charge, such as silica at neutral pH. Alumina at neutral pH has a slight positive charge, and thus should exhibit less sorption than onto the negatively charged silica.

Sorption of DCB onto alumina surface Z (11-nm pore) produced a K_p of 0.34 $cm^3 g^{-1}$ (Figure 4.7C), similar to the other porous alumina (surface Y) even though the surface area is reduced three fold. Sorption reversibility (K_{ps}/K_{pd}) was high for surface Y (2.42), but reversible for surface Z (0.84 ± 0.32). Variability may be due to the small K_p values. Sorption was fast, as indicated by the D_{DCB}/D_{KCl} ratio, which was 12.6 for surface Y and 1.17 for surface Z. A first-order model fit to one experiment indicated some slow sorption (some tailing is observed), although the k_b was relatively fast (5 x 10^{-2} s^{-1}).

Sorption of TCB onto the 4-nm pore alumina (Y) produced a K_p of 1.00, and a K_p of 0.95 $cm^3 g^{-1}$ onto the 11-nm pore alumina (Z). Surface area decreased three fold from surface Y to Z (315 $m^2 g^{-1}$ for Y, 122 $m^2 g^{-1}$ for Z), but K_p did not reflect this change. This indicates that sorption was only weakly dependent on the surface interactions. The K_{ps}/K_{pd} ratio indicated that sorption was reversible (1.01 for surface Y; 0.94 for surface Z), and relatively fast as indicated by the D_{TCB}/D_{KCl} ratio (0.40 for surface Y and 1.14 for surface Z).

Sorption of TeCB onto the 4-nm pore alumina produced a K_p of 7.34, and a K_p of 4.37 on the 11-nm pore alumina (Table 4.4). This solute did not show a decrease in K_p as the surface area decreased 3-fold from surface Y to Z. Sorption was reversible (K_{ps}/K_{pd} = 1.01 and 0.94, respectively), but slightly slower than TCB as indicated by D_{TeCB}/D_{KCl} ratio (0.46 for surface Y and 2.66 for surface Z). Slight desorption tailing was observed for the chlorinated benzenes when sorbed onto alumina, as shown in Figure 4.7D.

A comparison of sorption of chlorinated benzenes onto silica (Figure 4.7B) and alumina (Figure 4.7D) shows less sorption onto alumina, but both appear to sorb at the

same rate. None of the experiments show a large amount of slow sorption even with varying pore size (27-nm silica, and 11 or 4-nm alumina) or diameter (100-μm or 236-μm). The pore size is large compared to solute size (1.1 nm), so tortuosity should not affect diffusion. The calculated diffusion times into porous particles (Table 2.6) of this size are on the order of several seconds. Since the column residence time is on the order of minutes or greater, sorption will appear fast.

4.4 Solute Sorption onto Aliphatic Chain Modified Silica

4.4.1 C_1 Modified Silicas

Three C_1-polymer modified silicas were made in this research; one bound to a 100-μm porous silica (surface A), and two bound to 1.9-μm nonporous silica (surfaces AH and O). The C_1 polymer was bound to the solid particles to eliminate any slow sorption that may be caused by diffusion through immobile pore fluid. Column experiments are shown in Appendix C-3, and model results are presented in Table 4.5.

Four experiments were performed with C_1-modified surface (two are shown in Figure 4.8A and B), where K_p averaged 326 ± 137 $cm^3 g^{-1}$, showing considerable variation. Some of this variation may be due to running the experiments at high velocities. The average K_{oc} of 23,000 is an order of magnitude larger than other organic modified surfaces studied, and is also large compared to natural organic matter (610 from Table 1.1) and chromatographic materials (650 from Table 2.3). This indicates a stronger binding mechanism on the C_1-polymer modified surface than other surfaces studied. The sorption K_p was about 30 percent smaller than desorption K_p (K_{ps}/K_{pd} averaged 0.68 ± 0.36).

The D_{DCB}/D_{KCl} ratio was 3.21, which indicates little additional solute spreading from a slow sorption process. The large number of pore volumes required to reach equilibrium sorption (Appendix C-3) are probably caused by the large K_p. The first-order model fit to the best data (Figure 4.8A) indicates slow sorption with an ω of 8.3 and a k_b = 4.1 x 10^{-4} s^{-1}. This is about two orders of magnitude slower than the k_b on

Table 4.5 DCB sorption onto aliphatic chain modified silica

Exp.	Sorbent[1]	D_{KCl}	Equilibrium Model						First Order Model				Two Region Model					
			K_{pS}	K_{pD}[2]	rev.	K_p	D	D/D_{KCl}	ssq	K_p	N_D	k_b	ssq	K_p	N_D	α_c	f	ssq
		(cm^2/s)	(cm^3/g)			(cm^3/g)	(cm^2/s)			(cm^3/g)		(s^{-1})		(cm^3/g)		(s^{-1})		
A-3 QA	PQ-A C_1-Poly	0.0188	152.8	329.1	0.464	165.5	0.0587	3.12	0.3637	---	---	---	---	---	---	---	---	---
A-4 QB	PQ-A C_1-Poly	0.0242	126.8	304.3	0.417	175.7	1.21	50.0	0.8062	232.4	6.720	0.000950	0.4644	---	---	---	---	---
A-1 RF	PQ-A C_1-Poly	0.0113	498.7	414.7	1.203	479.4	0.0545	4.82	0.8062	407.6	8.275	440.0	0.1715	453.1	0.968	0.00362	0.593	0.0705
A-2 RJ	PQ-A C_1-Poly	0.0290	300.6	477.6	0.629	355.5	0.0465	1.60	0.5230	335.7	208.2	0.0158	1.0459	337.8	106000	0.0440	0.304	0.9893
ave.			326 ± 137		0.678 ± 0.362			3.21 ± 10.4				0.00071						
O-2 RV	PQ-Q C_1-PolyS	0.345	89.01	95.96	0.928	106.4	0.0511	12.2	1.0610	56.21	2.289	0.000232	2.6990	58.66	2.157	0.00749	0.046	2.6870
O-1 SA	PQ-R C_1-PolyS	0.164	45.99	60.26	0.763	77.82	0.0378	9.04	0.3224	71.82	7.780	0.000628	0.3948	77.35	1.057	0.00347	0.592	0.2961
B-2 QC	PQ-B C_8-Poly	0.0171	23.91	28.28	0.845	23.80	0.0324	1.89	0.1083	30.32	207.1	0.103	0.8971	30.28	238.4	0.611	0.036	0.8946
B-3 QD	PQ-B C_8-Poly	0.00853	18.86	27.53	0.685	23.87	0.0150	1.76	0.0861	24.86	87.54	0.0168	0.3770	25.00	2.427	0.00197	0.876	0.3766
B-5 QF	PQ-B C_8-Poly	0.000729	27.18	28.71	0.947	29.67	0.00474	6.50	0.1481	---	---	---	---	---	---	---	---	---
B-4 QH	PQ-B C_8-Poly	0.00612	28.58	27.73	1.031	32.58	0.0105	1.72	0.1740	29.55	30.44	0.00363	0.3103	87.62	0.0925	0.0000514	0.344	0.2175
B-1 RK	PQ-B C_8-Poly	0.0140	26.45	27.08	0.977	28.37	0.0187	1.34	0.0801	26.83	526.1	0.123	0.0872	26.76	6724.1	7.20	0.323	0.0720
ave.			25.86 ± 5.39		0.874 ± 0.143			1.51 ± 2.44				0.085						
B-6[3] SO	PQ-B C_8-Poly	0.0296	15.31	16.03	0.955	15.67	0.0200	0.68	0.0170	15.02	710.2	0.308	0.0176	15.01	238.5	0.264	1.039	0.0173
B-7[4] TC	PQ-B C_8-Poly	0.0337	26.73	39.57	0.676	27.09	0.0461	1.37	0.1496	23.11	471267	156.0	0.2158	23.19	68509	72.30	1.021	0.2890
C-2 QJ	PQ-C C_{18}-Poly	0.0127	23.08	24.61	0.938	24.21	0.0858	6.76	0.0168	22.89	13.00	0.00735	0.0239	23.22	3.748	0.00807	0.518	0.1493
C-1 QK	PQ-C C_{18}-Poly	0.000947	25.89	23.01	1.125	26.47	0.00282	2.98	0.1057	24.93	49.74	0.00239	>10	27.36	6724.0	1.34	0.32	0.0719
C-3 QL	PQ-C C_{18}-Poly	0.109	18.28	21.39	0.855	21.74	0.0133	1.22	0.0509	---	---	---	---	---	---	---	---	---
ave.			23.00 ± 1.61		0.973 ± 0.138			3.97± 2.44				0.0065						

[1]Bound on 100 µm diameter, 27 nm pore - silica except RV and SA which are 2 µm nonporous silica. [2]By planimeter. [3]Loosely packed column (see text). [4]With diffusion column (see text).

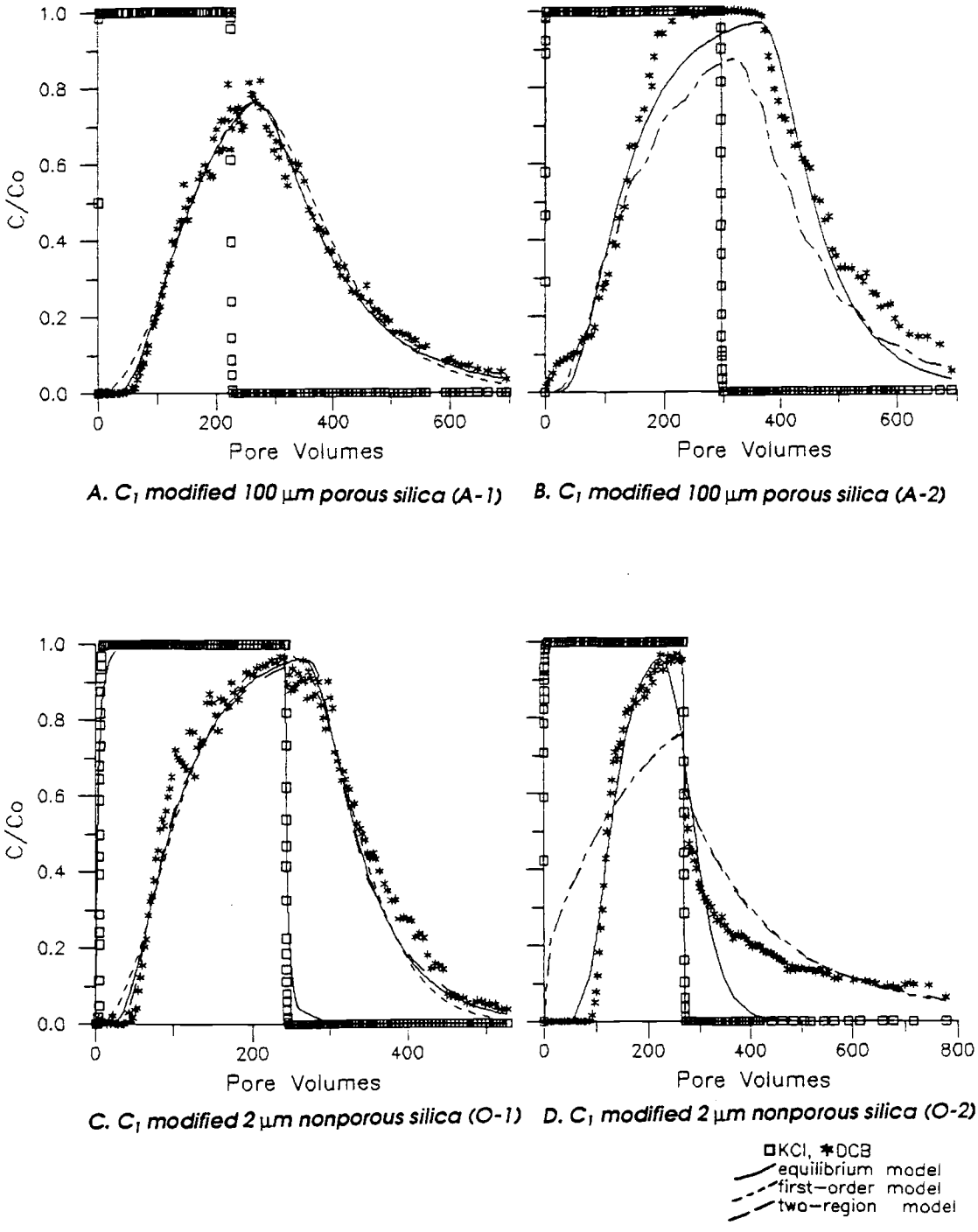

A. C_1 modified 100 μm porous silica (A-1) *B. C_1 modified 100 μm porous silica (A-2)*

C. C_1 modified 2 μm nonporous silica (O-1) *D. C_1 modified 2 μm nonporous silica (O-2)*

Figure 4.8 DCB Sorption onto C_1 modified surfaces

unbonded silica of the same diameter and pore dimensions (surface I). A two region model fit gave an α_e of 7.76 x 10^{-4} s^{-1} with an f of 0.592. The fraction of mobile sites (f) was found to vary considerably between model fits, and was relatively insensitive.

One C_1-polymer modified solid surface (AH) had the same mass fraction organic coating (f_{oc}) as the C_1-modified porous silica (surface A), whereas a second C_1-modified solid surface (O) had much lower f_{oc}. DCB sorption onto surface AH (Figure 4.8D) had a K_p of 92.5 $cm^3 g^{-1}$ and a K_{oc} of 6510. This surface (see Table 3.1) has the equivalent organic monolayer coverage of 30 percent; at this high coverage, slow sorption could be caused by thicker polymer layer on the surface. Sorption reversibility (K_{ps}/K_{pd}) of DCB on surface AH was 0.93 (Table 4.4). The first-order model fit to the data had a small ω (2.3), with the desorption rate (k_b = 2.3 x 10^{-4} s^{-1}) virtually identical to the C_1-modified porous surface (A).

Since the C_1-modified solid surface (AH) may have had more than monolayer coverage, a second C_1-modified nonporous surface was made (O). Sorption of DCB onto this surface (Figure 4.8C) had an average K_p = 53.1 $cm^3 g^{-1}$, and a K_{ps}/K_{pd} of 0.76, which may indicate some irreversible sorption. The K_{oc} was 24,000, which is the same as the C_1-modified 100-μm porous surface. The equivalent organic monolayer coverage for surface O is about 4 percent. An equilibrium model fit gave a D_{DCB}/D_{KCl} ratio of 9.04, compared to 4.8 for the C_1 porous silica (A). A first-order model fit also indicated non-equilibrium sorption with an ω of 7.8 and a k_b of 8.5 x 10^{-4} s^{-1}.

This C_1 polymer bound on a solid surface had a k_b only twice as large as the C_1 porous silica. The additional slow sorption onto the 100-μm porous particle may be caused by diffusion into the particle. Since both rates are still two orders of magnitude slower than the rate on the unbonded surface (or C_8 surface), this indicates that the presence and nature of the organic layer is related to the slow sorption.

The two-region model (Table 4.5) shows virtually identical fits for the C_1 solid surface as the C_1-porous silica, with the fraction mobile sites (f) varying between 0.3 and

0.6, and similar mass transfer rates through the immobile fluid (averaging 4.5 x 10^{-3} s^{-1}). Desorption of DCB after 26 days (experiment A-4) had the same sorption and desorption K_p as those experiments immediately desorbed, indicating no very slow reactions or development of stronger binding mechanisms.

4.4.2 C_8 Modified Surfaces

4.4.2.1 C_8 Column Experiments

Different chain length silanes were bound to silica to examine the rate of diffusion through the bound organic layer. Seven experiments with a C_8 polymer surface (B) had an average K_p of 25.9 ± 5.4 $cm^3 g^{-1}$ (Appendix C-4 and Table 4.5). Sorption was reversible (K_{ps}/K_{pd} = 0.87 ± 0.14) and fast (D_{DCB}/D_{KCl} ratio averaged 1.51). Sorption was 10-fold smaller than on the C_1 surfaces, with K_{oc} averaging 3800 for the C_8 surface. Two experiments are shown in Figure 4.9A and B; both show little tailing, indicating fast sorption and desorption.

An isotherm can be developed from a single column experiment if sorption equilibrium is assumed at all points in the breakthrough curve with [*Gleuckauf, 1947*]:

$$S(c) = \frac{C_o \theta \rho_s}{\rho_b} \int_0^{C_a} PV(c)\,dc = \frac{C_o \theta \rho_s}{\rho_b} A_r \qquad (76)$$

where $PV(c)$ is the retention time (in pore volumes), and A_r is the retention volume of a solute (concentrations from 0 to C_a) [*Conder and Young, 1979*]. Two isotherms were calculated from experiment B-1 (Figure 4.10), where C_o was 0.5 ppm. The sorption isotherm (S = 96.7 $C^{1.40}$) and the desorption isotherm (S = 77.0 $C^{0.95}$) differed, but both exhibited a near-linear trend that is similar to the isotherm on the phenyl surface (exponent = 1.09, Figure 4.4B). Isotherms were also calculated from the equilibrium model fit, where the sorption and desorption isotherm exponents (1.09 and 0.93, respectively) were close to the value of 1.0 that is assumed in the model.

A first-order model was fit to several C_8 experiments (Table 4.5) with an average k_b of 8.5 x 10^{-2} s^{-1}. This rate corresponds to a reaction half-life of 8 seconds, compared

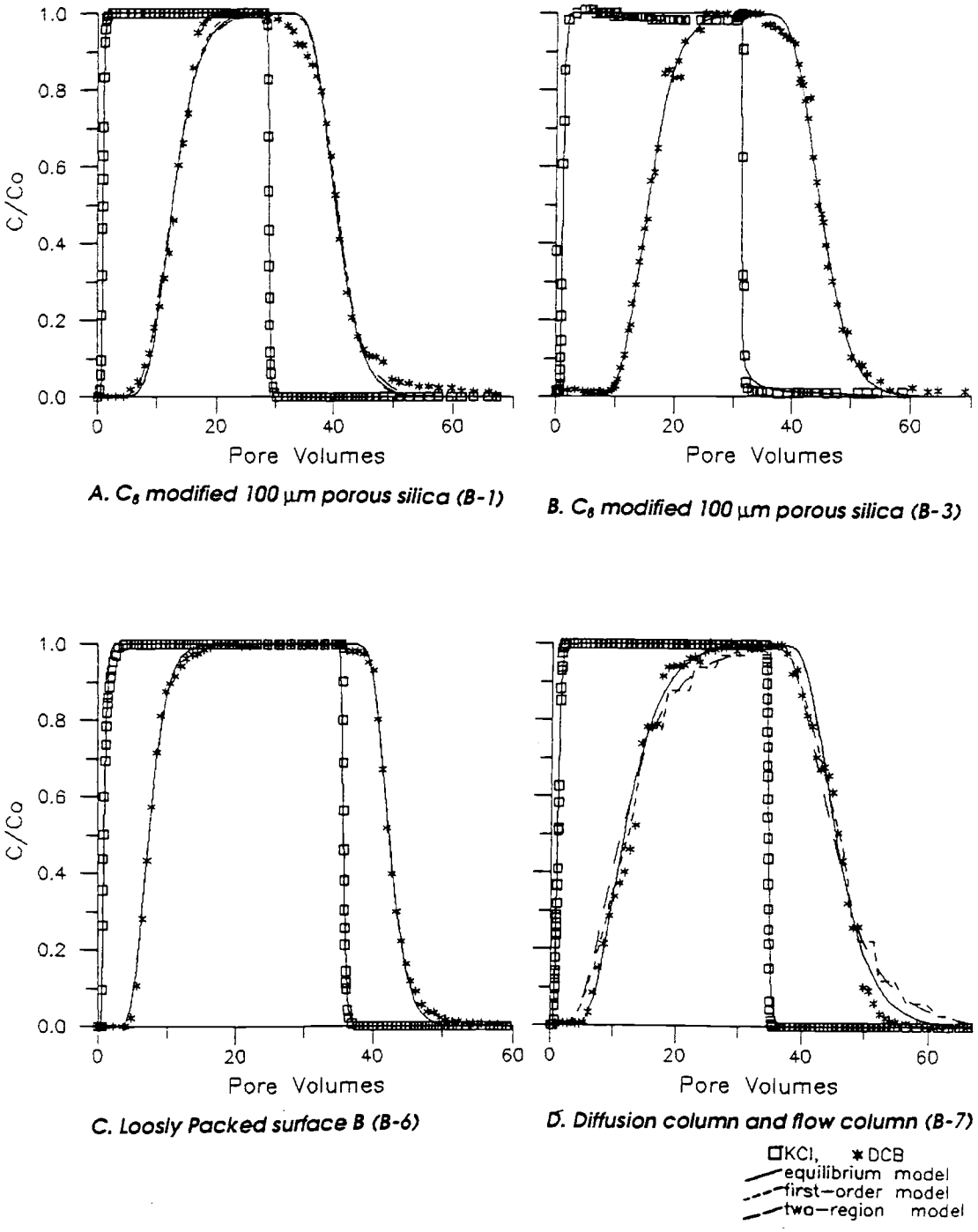

Figure 4.9 DCB sorption onto C_8 modified silica

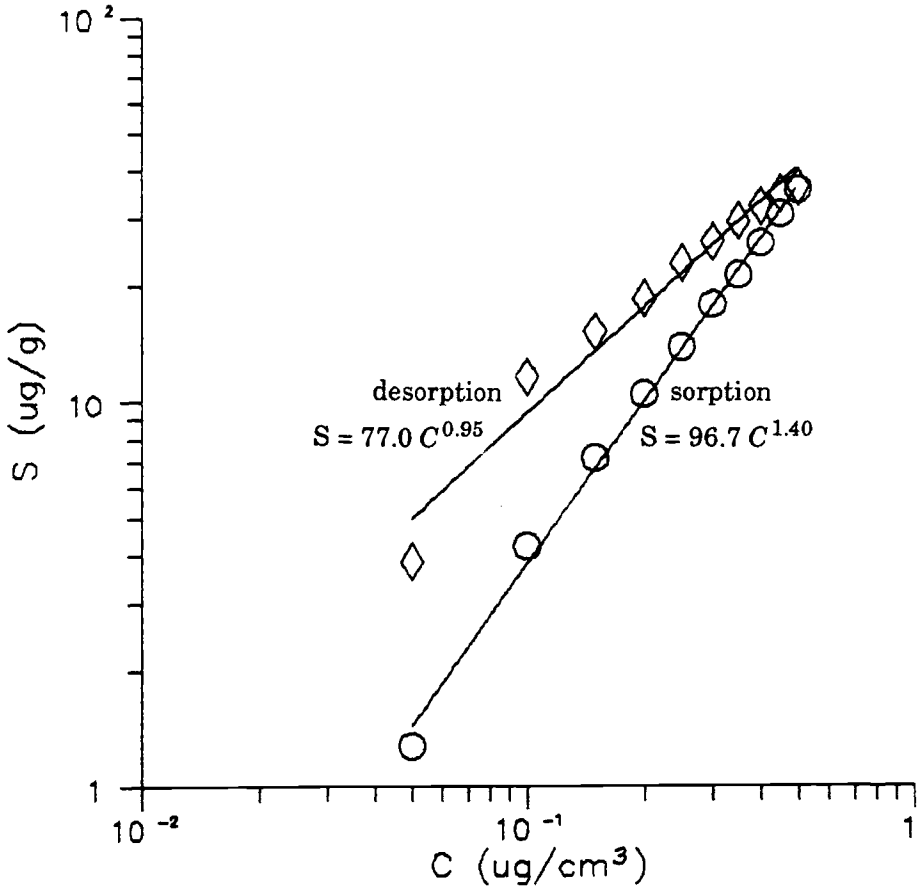

Figure 4.10 Isotherm calculated from a breakthrough curve (B-1)

to a column residence time of 50 minutes, so the reaction can be considered at equilibrium. Note that there is much uncertainly in determining k_b when the breakthrough curve is near equilibrium (Figure 2.7). All other first-order model fits to C_8 breakthrough curves also gave large ω's and fast rates. The two-region model fit also gave a large α_e (15.3), which was four orders of magnitude larger than for the C_1 surface. The ratio of solute residence time to mass transfer time (ω) varied from 30 to 500.

If the C_8 polymer was evenly coated on both external and internal surfaces of the porous silica, then sorption should be uniformly distributed. The sorption rate would be equal to or slower than on the unbonded silica, which is thought to be diffusion controlled. Slower sorption for a C_8 surface could indicate diffusion through the C_8 polymer to a binding site, or that the C_8 polymer clogs some of the internal pore space. The C_8 polymer is 1.3-nm long, so is unlikely to affect the pores (27-nm average width). Sorption on the C_8 surface was faster than on the unbonded silica, however. If the C_8 polymer was coated mainly on the outer surface, then sorption should be faster, since most diffusion into the porous particle is eliminated. The C_8 polymer was calculated to cover 5 percent of the surface (Table 3.1); as the external surface is about 1 percent of the total surface area, it is possible that the C_8 polymer could be preferentially bound near the surface.

The surface area (Table 3.1) measured by nitrogen adsorption was not reduced for the C_8 modified surface compared to the unbonded surface, indicating no clogging of the pores. This also implies that the C_8 silane is not bound entirely on the outer surface, where a coating this dense could lead to pore clogging (and surface area reduction), but more distribution throughout the particle.

Desorption of DCB from the C_8 surface after 20 days (Figure 4.9B) had a larger K_p than for sorption, but this was not different from the immediate desorption K_p (Figure 4.9A), indicating that no stronger binding developed with time.

4.4.2.2 Induced Slow Sorption with C_8 Modified Silica

Two experiments were designed to induce additional dispersion with the C_8 surface in order to confirm that the slow sorption observed on other surfaces can be related to the nature of the sorbent.

One experiment (B-6) was performed with a column only partially packed with C_8 modified silica (other half water). This magnifies the formation of additional pore space in the column as a result of grain rearrangement, which is observed with some columns. This experiment showed (Figure 4.9C) a lower K_p (15.7 $cm^3 g^{-1}$), which is expected with about 50 percent loss of sorbent mass. The dispersion of both KCl and DCB increased, but the D_{DCB}/D_{KCl} ratio did not. The first-order model fit indicated a fast reaction (ω = 710, k_b = 0.31 s^{-1}), which was similar to the C_8 experiments with fully packed columns. This indicates that loose column packing will lead to variation in K_p and additional dispersion but should not affect the sorption rate if the D_{DCB}/D_{KCl} ratio is used to calculate D in the nonequilibrium models.

The column apparatus was then modified so that a fully packed C_8-silica column was in line, and an additional column without packing was installed at a right angle into the exit of the C_8 column (experiment B-7 in Figure 4.9D). This diffusion column was filled with water, and as there is no advective flow through this column, solute mass can only slowly diffuse into it. The diffusion column volume was 15 cm^3 and column volume was 7.5 cm^3. With this apparatus, both KCl and DCB dispersion should increase, not just DCB, when there is a slow sorption process.

Results of the diffusion column experiment (Table 4.5) show an increase of about three fold for both KCl and DCB dispersion. The equilibrium model D_{DCB}/D_{KCl} ratio is still small (1.37), indicating no change in the observed nonequilibrium. A first-order model fit does show a smaller ω compared to other C_8 experiments, indicating a slow process. The two-region model would accurately represent this case where the immobile pore space in the diffusion column is used to calculate the immobile and mobile porosity.

The two-region model fit had an f of 0.8 to 1.0, and an α_e of 2 x 10^{-4}. The KCl breakthrough data also show increased dispersion, which could be modeled with a two-region mobile-immobile model.

Therefore, a system which exhibits increased tailing can be created, but only by increasing the tailing of both the conservative and sorbed tracer. The extent of tailing in this case is still insignificant compared to other experiments. The effectiveness of the diffusion column could be improved by packing the column with sorbent to increase the mass of solute that can be transferred into the diffusion column.

4.4.3 C_{18} Modified Surfaces

C_{18} modified silica is the most commonly used chromatographic sorbent. It is used because of its large sorption capacity, and fast, reversible sorption properties. One C_{18} modified silica was made in this research (surface C) which was 1.05 percent carbon by mass, and had an estimated monolayer surface coverage (equation 71) of 3.6 percent. A total of three column experiments were performed (Appendix C-5 and Table 4.5), which exhibited very reproducible sorption (K_p = 23.0 ± 1.6) and reversible sorption (K_{ps}/K_{pd} = 0.97 ± 0.14). Two experiments are shown in Figure 4.11. The K_{oc} for C_{18}-modified silica (2190) is similar to that for C_8 (K_{oc} = 3800), but much smaller than for C_1 surfaces (23,000).

Desorption of DCB from C_{18} silica was made after 62 days in one experiment (Figure 4.11B), and did not show any difference in K_p compared to immediate desorption (Figure 4.11A), indicating no strong binding with time.

The equilibrium model D_{DCB}/D_{KCl} ratio averaged 3.97 ± 2.44, indicating some additional spreading due to the C_{18} chain, compared to the C_8 modified silica. As the C_8 chain showed faster sorption than unbonded silica, one could conclude that in this case the slower approach to equilibrium may be caused by slower diffusion through the C_{18} mass. A first-order model fit to the C_{18} experiments also indicates about 1.5 orders of magnitude slower sorption than for C_8 experiments (Table 4.5), with ω ranging from 13

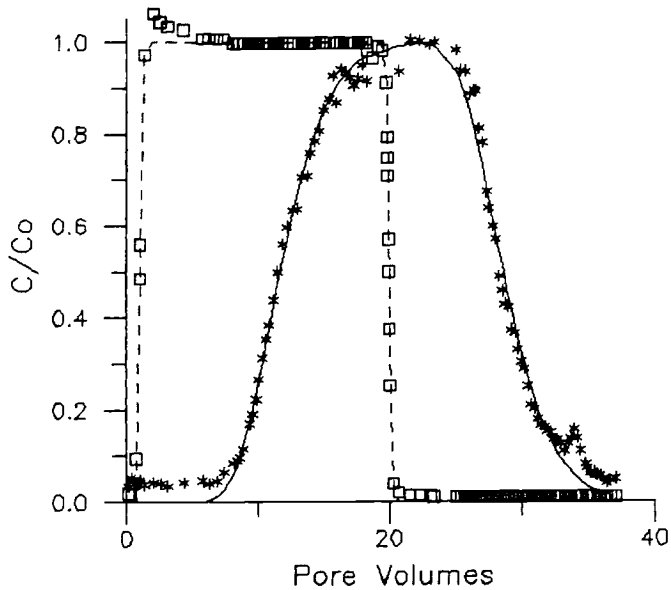

A. Immediate desorption (C-1)

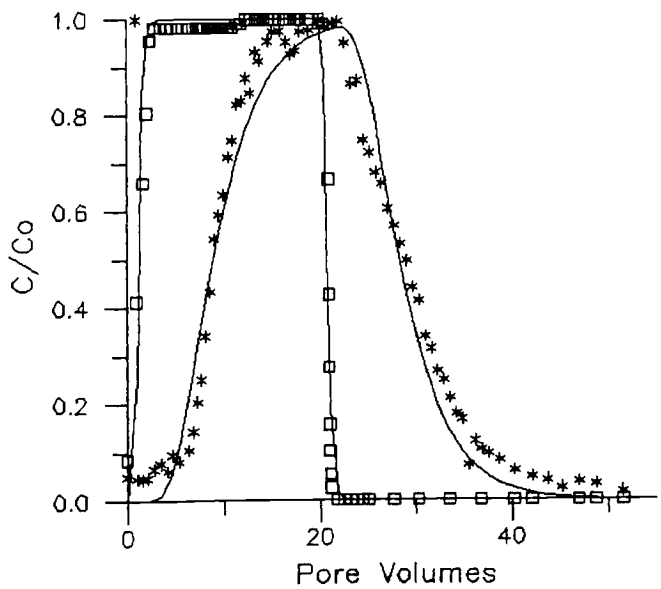

B. Desorption after 62 days (C-3)

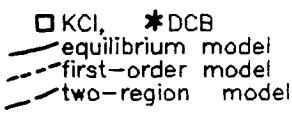

Figure 4.11 DCB sorption onto C_{18} modified silica

to 50 and k_b averaging 6.5 x 10^{-3} s^{-1}.

4.5 Phenyl Modified Surfaces

Phenyl monomer and polymer silanes were bound to various porous and solid silicas. These eleven surfaces were made to examine various rate-limiting mechanisms.

4.5.1 Phenyl Monomer on 100 μm Porous Silica

Two surfaces were made with a phenyl monomer bound onto 100-μm silica (surfaces D and Q). The reaction covalently binding the phenyl monomer onto silica proceeds slowly, so apparently little was bound during the two hours used in making the first surface (D), where f_{oc} was 0.0016, and during the 12 hours used in making the second surface (Q), where f_{oc} was 0.0075.

Six column experiments were performed (Appendix C-6) on these surfaces with results shown in Table 4.6. The K_p averaged 4.1 ± 1.1 for surface D and 5.2 ± 1.6 for surface Q; these small K_p values are essentially equal to that of unmodified silica. As a consequence, sorption at the silica surface undoubtedly played the major role in sorption. Sorption onto surface D (Figure 4.12A) and surface Q (Figure 4.12B) showed fast sorption and desorption. The K_{oc} values for surface Q (690) and surface D (2560) were small, and sorption was reversible (K_{ps}/K_{pd} = 0.85).

The D_{DCB}/D_{KCl} ratio averaged 1.3 (Table 4.6), indicating little slow sorption. The first-order model fits also indicated fast sorption, with an average k_b of 1.2 x 10^{-2} s^{-1} (surface D) and 1.2 s^{-1} (surface Q). The two-region model fits also indicated a fast process with an α_e of 4.1. All six breakthrough curves showed little tailing.

4.5.2 Phenyl Polymer Bound to 100 μm Porous Silica

Eighteen experiments with 100-μm porous silica with phenyl polymer bound to the surface (E) were performed with five different chlorinated benzenes (CB, DCB, TCB, TeCB, and PCB) and at six different temperatures. Sorption of DCB is discussed in the first section, various chlorinated benzenes in the second section, and sorption at different temperatures in the third section.

Table 4.6 DCB sorption onto phenyl monomer modified silica

Exp.	Sorbent[1]	D_{KCl}	K_{pS}	K_{pD}	rev.	Equilibrium Model K_p	D	D/D_{KCl}	ssq	First Order Model K_p	N_D	k_b	ssq	Two Region Model K_p	N_D	α_s	f	ssq
		(cm^2/s)	(cm^3/g)			(cm^3/g)		(cm^2s)		(cm^3/g)		(s^{-1})			(cm^3/g)	(s^{-1})		
D-3 QM	PQ-D PHEmono	0.000266	6.106	5.564	1.097	5.997	0.000743	2.79	0.1866	---	---	---	---	---	---	---	---	---
D-4 QN	PQ-D PHEmono	0.00232	4.472	---	---	3.981	0.00645	2.78	0.1790	---	---	---	---	---	---	---	---	---
D-1 RL	PQ-D PHEmono	0.000714	3.334	2.828	1.179	3.473	0.00294	4.14	0.0924	3.349	18.32	0.0115	0.1047	3.743	0.3109	0.000108	1.114	0.0379
D-2 RM	PQ-D PHEmono	0.000752	2.186	4.621	0.473	2.896	0.00319	4.24	0.0809	2.843	16.10	0.0126	0.0884	3.147	0.3562	0.000130	1.166	0.0526
ave.			4.1 ± 1.1		0.845			3.49				0.012						
Q-2 SM	PQ-T PHEmono	0.000339	3.773	5.479	0.689	3.975	0.000447	1.32	0.1380	3.904	14355	12.30	0.1176	3.899	0.0193	0.0000106	1.334	0.1378
Q-1 SN	PQ-T PHEmono	0.000203	2.792	3.551	0.786	3.863	0.000241	1.19	0.0485	3.762	2229	1.28	0.0536	3.794	5273.4	1.87	0.357	0.0489
ave.			5.2 ± 1.6					1.26				1.2						

[1]Bound to 100 μm porous silica.

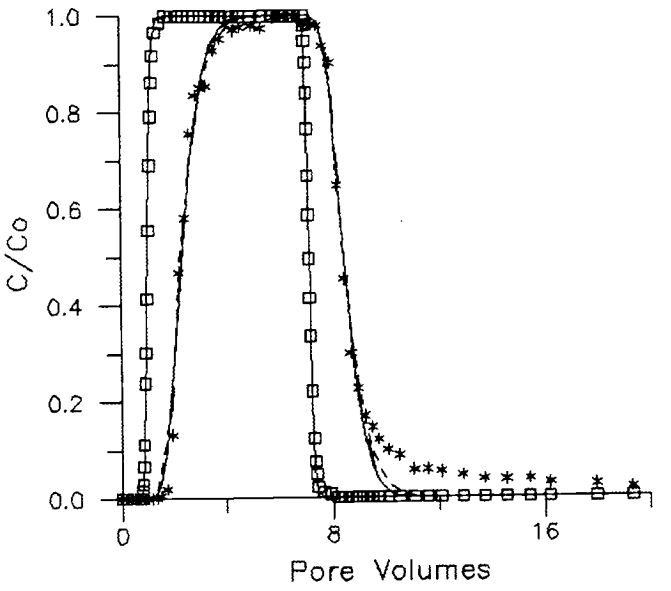

A. Surface D (D-1)

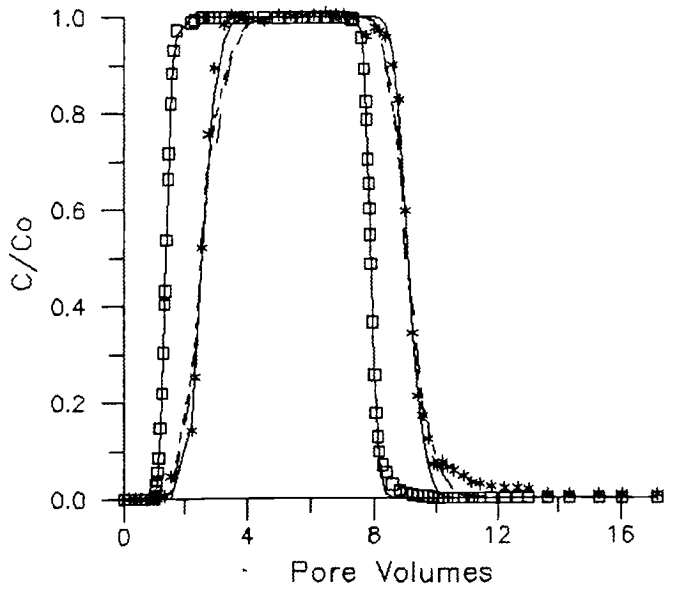

B. Surface Q (Q-1)

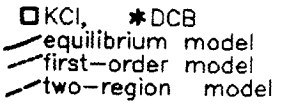

Figure 4.12 DCB sorption onto phenyl monomer modified silica

4.5.2.1 DCB and Phenyl Polymer Surface E at 25°C

Six column experiments of DCB sorption performed on the phenyl-polymer modified 100-μm silica (E) at 25°C exhibited considerable slow sorption (Appendix C-8); model results are shown in Table 4.7. The results of two experiments (Figure 4.13A and B) illustrate the considerable tailing, where sorption and desorption took from 30 to 100 pore volumes. Experiments exhibiting fast sorption, such as that observed with the phenyl monomer surface (Figure 4.12) reach equilibrium within 3 pore volumes. The average K_p on the phenyl polymer surface is 60.6 ± 41.9 $cm^3 g^{-1}$, which showed considerable variation between experiments. The K_p was consistent within experiments, with K_{ps}/K_{pd} equal to 0.96 ± 0.21, based on eleven experiments (including those run at different temperatures).

The equilibrium-model D_{DCB}/D_{KCl} averaged 32 ± 8.3, indicating slow sorption is causing much of the observed DCB spreading. The first-order model fit to data in these six experiments produced an average k_b of 3.8×10^{-4} s^{-1}, which is two orders of magnitude smaller than for a C_8 surface bound on the same porous silica and with a similar f_{oc}. This indicates that the slow process depends on the nature of the bound organic matter.

The two-region model α_e averaged 3.4×10^{-3} s^{-1}, and was relatively consistent between experiments even with f varying from 0.14 to 0.45. This rate coefficient can be dimensionally compared to the first-order rate coefficient with equation (54); the average $\alpha_e/\rho_b K_p$ is 1.5×10^{-4} s^{-1}, or about 40 percent of k_b.

The solvophobic model indicates a small increase in K_p with increasing ionic strength, since surface tension is greater at higher ionic strength, and K_p is dependent on surface tension. The ionic strengths used in experiment E-3 were 10^{-5} and 2×10^{-5} M where the resulting K_p is 64.6 $cm^3 g^{-1}$, compared to an average of 60.6 $cm^3 g^{-1}$ for experiments run at 10^{-2} M. There is too much variability in the data to make a definite conclusion regarding the change in K_p with ionic strength.

Table 4.7 Sorption onto phenyl polymer modified silica at 25°C

			Equilibrium Model						First Order Model				Two Region Model				
Exp.	Solute	D_{KCl}	K_{pS}[1]	K_{pD}[2]	rev.	K_p	D	D/D_{KCl}	ssq	K_p	N_D	k_b	ssq	K_p	N_D	α_e	f	ssq
		(cm^2/s)	(cm^3/g)			(cm^3/g)		(cm^2s)		(cm^3/g)		(s^{-1})		(cm^3/g)		(s^{-1})		
E-17 RT	CB	0.00106	4.873	13.96	0.349	7.267	0.0557	56	0.2561	7.616	1.982	0.00243	0.4440	7.713	1.666	0.00263	0.225	0.4390
E-18 RW		0.000800	11.32	1.652	6.852	6.943	0.00607	7.6	0.5301	3.889	1.065	0.00201	1.0590	4.432	0.671	0.000835	0.401	1.0200
ave.			7.95 ± 5.68									0.0020						
E-5 QP	DCB	0.858	8.015	9.949	0.806	11.810	0.517	60.3	0.1348	8.98	2.195	0.00417	0.1377	8.983	2.593	0.00750	0.024	0.1160
E-1 QQ		0.00629	18.23	28.78	0.633	18.777	0.140	222.0	0.2124	14.57	2.701	0.000439	0.5534	19.08	0.578	0.000232	4.51	0.3220
E-2 RN		0.000889	59.45	53.24	1.117	54.00	0.0251	282.0	0.0592	45.97	3.608	0.000542	0.2864	53.65	1.119	0.00131	0.408	0.1030
E-3 SR		0.00501	72.38	56.85	1.273	84.82	0.0448	8.94	0.2512	63.86	3.259	0.000385	0.5854	77.81	1.143	0.00146	0.352	0.3319
E-4 TD		0.00114	98.41	92.39	1.065	109.1	0.0635	55.7	0.2720	82.42	2.840	0.000312	0.4635	85.48	2.121	0.00326	0.142	0.4655
E-9 SS		0.0139	105.5	115.6	0.913	88.13	0.594	42.7	0.6544	62.64	2.045	0.00142	0.7633	71.20	1.124	0.00826	0.189	0.6582
ave.			60.6 ± 41.9					32 ± 8.3				0.00038				0.0037		
E-12 RX	TCB	0.00611	81.42	85.17	0.956	82.54	0.151	24.7	0.0855	64.97	2.394	0.000919	0.4114	77.30	0.609	0.00258	0.393	0.2110
E-13 RZ		0.0128	84.61	90.41	0.936	90.16	0.213	16.6	0.1256	67.92	2.691	0.00100	0.3724	82.16	0.470	0.00202	0.371	0.1076
E-14 SB		0.0120	138.7	88.19	1.573	89.71	2.01	167.0	0.4840	87.21	0.793	0.000568	0.3578	91.23	0.685	0.0359	0.028	0.3354
E-15 SC		0.00586	203.8	116.1	1.755	242.5	0.535	91.3	0.4098	137.1	2.255	0.000592	0.9937	134.6	2.335	0.0176	0.004	0.9301
E-9 SS		0.0139	262.1	202.6	1.294	268.1	0.521	37.5	1.7400	179.3	3.071	0.000742	1.6076	159.9	0.646	0.00394	0.394	0.6302
ave.			135 ± 65		1.256			54.1				0.00070						
E-14 SB	TeCB	0.0120	135.3	144.3	0.938	158.0	0.758	63.2	0.2444	102.4	2.222	0.00136	0.2956	108.0	1.946	0.0206	0.028	0.2920
E-15 SC		0.00586	438.0	536.9	0.816	624.6	0.436	74.4	0.2531	344.6	2.877	0.000300	0.7706	541.8	0.857	0.00523		
E-9 SS		0.0139	563.6	563.6	1.000	801.2	0.605	46.8	1.5710	385.2	3.731	0.000420	1.6542	377.1	3.566	0.0262	0.047	1.6560
ave.			397 ± 204		1.083			63.5				0.00050						
E-16 SE	PCB	0.00976	858.3	755.2	1.137	754.4	0.189	19.4	0.4716	566.2	6.758	0.000541	0.7276	774.8	0.7693	0.00591	0.473	0.3664
E-9 SS		0.0139	987.9	1269.1	0.778	1278.5	0.324	23.3	1.1770	813.5	4.444	0.000237	1.3752	867.8	2.454	0.0776	0.188	1.2891
ave.			968 ± 222		0.958			21.3				0.00030						

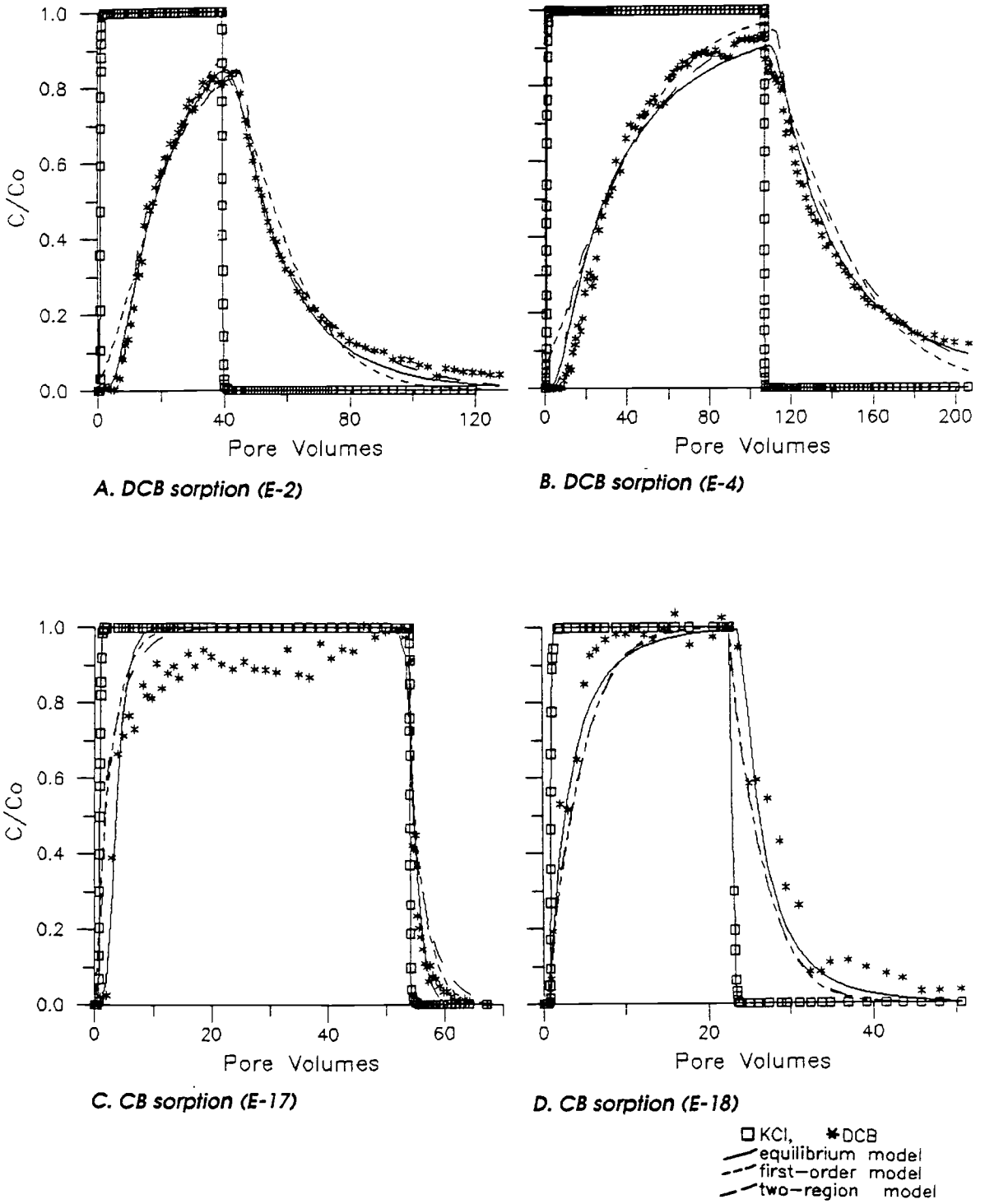

Figure 4.13 DCB and CB sorption onto phenyl polymer surface E

The partition coefficient is more accurately determined at low velocity, but since the shape of the breakthrough curve changes at different velocities, K_p can appear to change. There was no correlation of K_p with velocity with the six experiments over velocities ranging from 0.02 to 0.2 cm s^{-1}.

4.5.2.2 Other Chlorinated Benzenes

Four additional chlorinated benzenes were sorbed and desorbed onto the phenyl polymer modified 100-µm silica.

Two experiments were performed with chlorobenzene (Figure 4.13C and D), with considerable variation in results (Table 4.7). Chlorobenzene is not easily detected with an electron capture detector on the gas chromatograph, so higher concentrations were used (2.6 and 3.2 ppm). The average K_p for both sorption and desorption for two experiments was 8.0 ± 5.7 with one experiment showing a larger desorption K_p and one a larger sorption K_p. Experiment E-17 (Figure 4.13D) had better solute mass balance, and this experiment showed the desorption K_p three times the sorption K_p. The equilibrium model D_{DCB}/D_{KCl} ratios for the two experiments were 52 and 7.6, indicating some slow sorption. The first-order model produced ω's of 1-2, and k_b's of 1-3 x 10^{-3} s^{-1}.

Five column experiments of TCB sorption were performed on the phenyl-polymer modified 100-µm silica (surface E) at 25°C (Appendix C-10), with results presented in Table 4.7. The K_p averaged 135 ± 65 $cm^3 g^{-1}$, with larger values for sorption (K_{ps}/K_{pd} = 1.26 ± 0.43), although most of the 11 experiments showed completely reversible sorption. Two experiments are shown in Figure 4.14A and B. The K_{oc} for TCB is 9880, five times that for DCB on the same surface. A significant amount of tailing is seen with TCB, as shown by the average equilibrium model D_{TCB}/D_{KCl} ratio, which was 54.1. Values of D_{TCB}/D_{KCl} larger than 2.0 (Table 2.7) indicate slow sorption. The first-order model fits gave ω's of 0.8 to 3.0, with an average k_b of 7 x 10^{-4} s^{-1}; the model fits were only fair (*ssq* = 0.2 - 1.0). The poor fit to the breakthrough curve tailing could indicate a more complex sorption process. The two-region model did provide a better fit to the data,

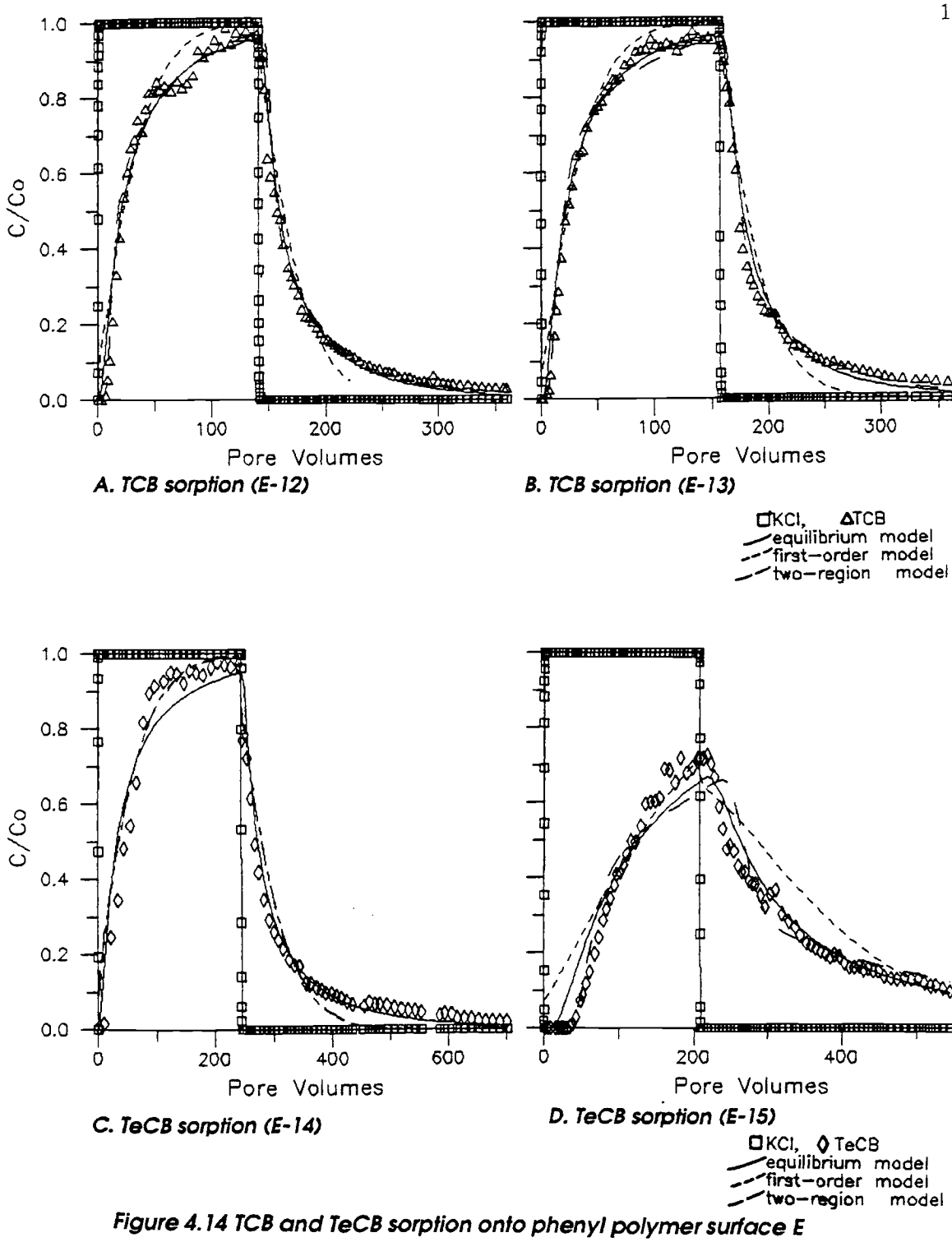

Figure 4.14 TCB and TeCB sorption onto phenyl polymer surface E

where α_e averaged 2 x 10^{-3} s^{-1} and f ranged from 0.004 to 0.4. The average value for $\alpha_e/\rho_b K_p$ (equation 54) was 4 x 10^{-5} s^{-1}.

Three column experiments were performed with the sorption of TeCB onto the phenyl-polymer modified 100-μm silica at 25°C (Appendix C-12 and Figure 4.14C and D) with results in Table 4.7. Sorption was reversible (K_{ps}/K_{pd} = 1.08 ± 0.38 for 8 experiments) where the average K_p was 397 ± 204 $cm^3 g^{-1}$. Tailing was significant for these experiments; the D_{TeCB}/D_{KCl} ratio averaged 63.5, as compared to a calculated value of 5.4 for fast sorption (Table 2.7). The first-order model fits gave ω's of 2 to 4, with a k_b averaging 5 x 10^{-4} s^{-1}, and fair model fits (ssq = 0.3 to 2.0). The two-region model fits were better in some cases, with α_e ranging from 0.005 to 0.02 s^{-1}, and fraction mobile sites (f) ranging from 0.02 to 0.5. The $\alpha_e/\rho_b K_p$ averaged 1.8 x 10^{-3} s^{-1}. The non-equilibrium model fits are only fair even though the data are not scattered, which may indicate the sorption process is not adequately described. With the large K_p's, experiments were run at high velocity, which created more dispersion and possibly preferential flow channels in the column. This could change the shape of the breakthrough curves.

Two experiments of pentachlorobenzene sorption were performed on the phenyl-polymer modified 100-μm silica (shown in Figure 4.15A and B), with results in Table 4.7. The K_p averaged 968 ± 222 $cm^3 g^{-1}$, and sorption was reversible (K_{ps}/K_{pd} = 0.96). The large K_p required a large number of pore volumes to be eluted (over 3000 pore volumes for experiment E-9), and a high velocity. The equilibrium model dispersion of PCB was only 2.3 to 19 greater than the KCl dispersion, indicating only a small amount of non-equilibrium sorption. The first-order model fits to thethe data also indicated some non-equilibrium with an ω of 4-5 and a k_b of 3 x 10^{-4} s^{-1}. The first-order model fits were poor (ssq = 0.7-1.7), but the two-region model fits were better (ssq = 0.4-1.4), where α_e averaged 0.6-1.0 x 10^{-2} s^{-1} and f ranged from 0.2 to 0.5. The $\alpha_e/\rho_b K_p$ averaged 2.3 x 10^{-5} s^{-1}, which is an order of magnitude slower than first-order rate coefficient.

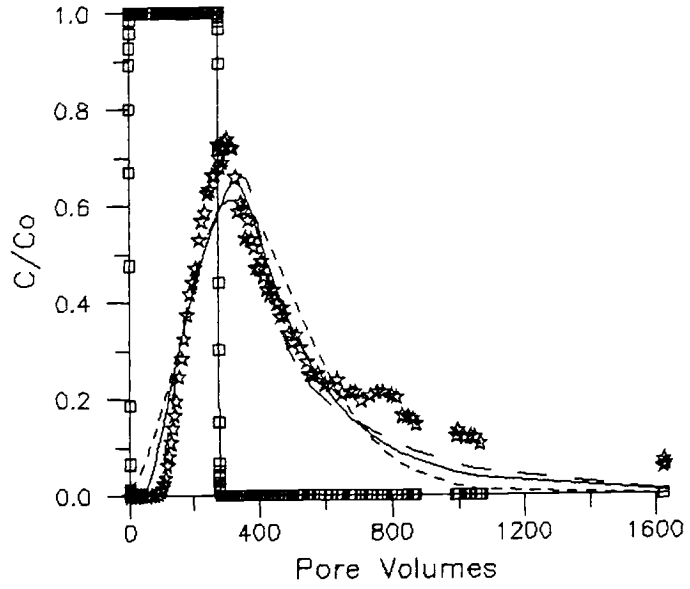

A. Experiment E-16

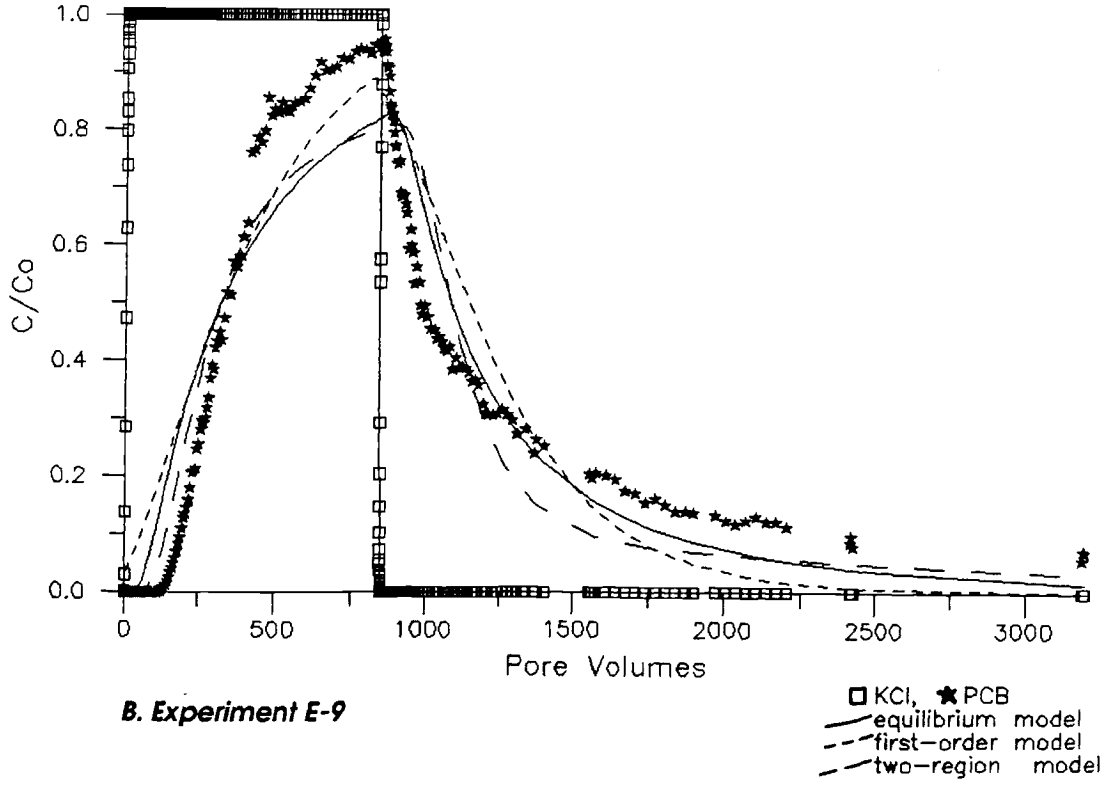

B. Experiment E-9

Figure 4.15 PCB sorption onto phenyl polymer surface E

For eight of the experiments, from two to four chlorinated benzenes were fed simultaneously through columns packed with the phenyl-polymer surface E. Experiment E-9 is shown in Figure 4.16 with breakthrough curves for KCl, DCB, TCB, TeCB, and PCB. These K_p's for all solutes were from 40 to 190 percent greater than K_p's obtained from single solute experiments (Table 4.8). Most experiments have consistent K_p's between sorption and desorption, but there is much a wider variation of K_p's between experiments. Even with this variation, in all cases, multiple solute experiments exhibited larger K_p's than single solute experiments.

Increased sorption could be due to sorption onto another sorbate (cosorption). For example, sorbed PCB could be considered additional bound organic phase for DCB to sorb to. This trend is not reported in chromatography literature [*Antle et al., 1985*] where multiple solute injections are made routinely, although low injection masses of solutes are generally used.

4.5.2.3 Sorption at Different Temperatures

Five experiments with DCB, TCB, and TeCB were performed on a single column (surface E) at temperatures from 3 to 48°C; breakthrough curves are shown in Figure 4.17A-F and Appendix C-9, C-11, and C-13, with the modeling results in Table 4.9. Temperature was equilibrated at least 12 hours before running each experiment.

The change in K_p at different temperatures can be seen more clearly in Figures 4.18A, B, and C, for DCB, TCB, and TeCB, respectively. Each solute shows decreased retention at higher temperature; using the van't Hoff equation (20), $\Delta H°$ can be determined. The sorption rate is generally faster at higher temperature; the Arrhenius equation (77) is used to determine the activation energy.

4.5.2.3.1 Partition Coefficient

The partition coefficients of three chlorinated benzenes decreased as temperature increased (Figure 4.18). The partition coefficients from first-order model fits are plotted against $1/T$ in Figure 4.19. Visually, the slopes are similar, corresponding to a similar

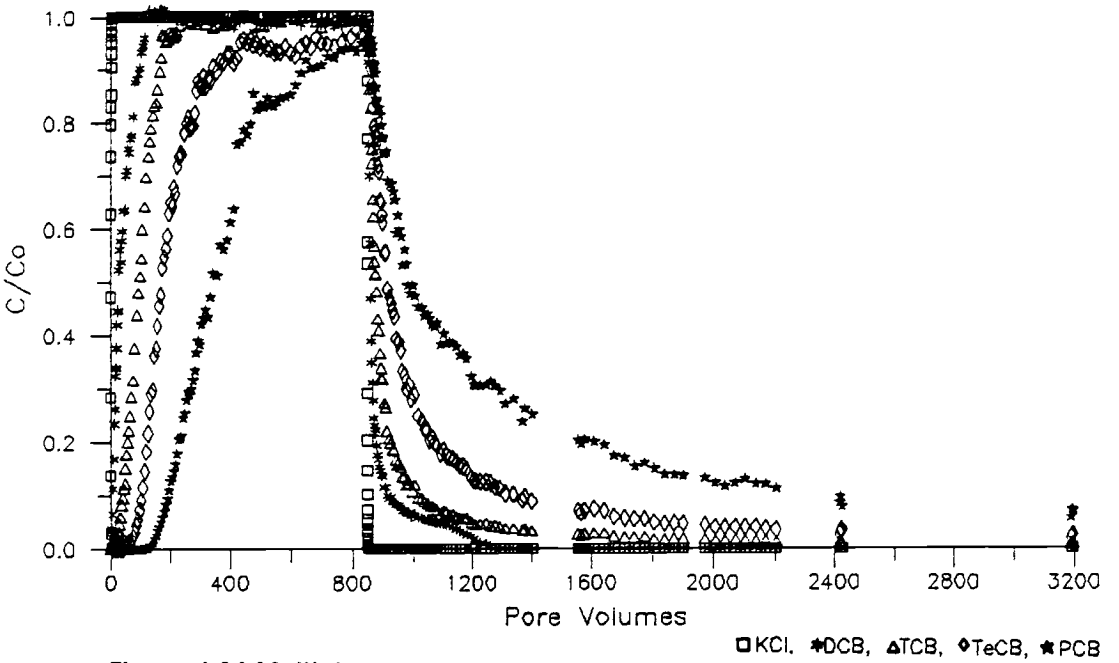

Figure 4.16 Multiple solute breakthrough (E-9)

Table 4.8 Effect of multiple solutes on partitioning

Solute	Single Solute		Multiple Solute			Percent
	K_p	Ave K_p	N	K_p	Ave K_p	Increase
DCB	8.98					
	23.5					
	56.3	49.8	4	111	111	120
	64.6					
	95.4					
	19.9*					
TCB	83.3		4	232		
	87.4	85.3	2	113	169	94
	89.9		2	160		
TeCB	136*		4	564		
			2	140	397	190
			2	487		
PCB	808		4	1130	1130	40

*Batch experiment.

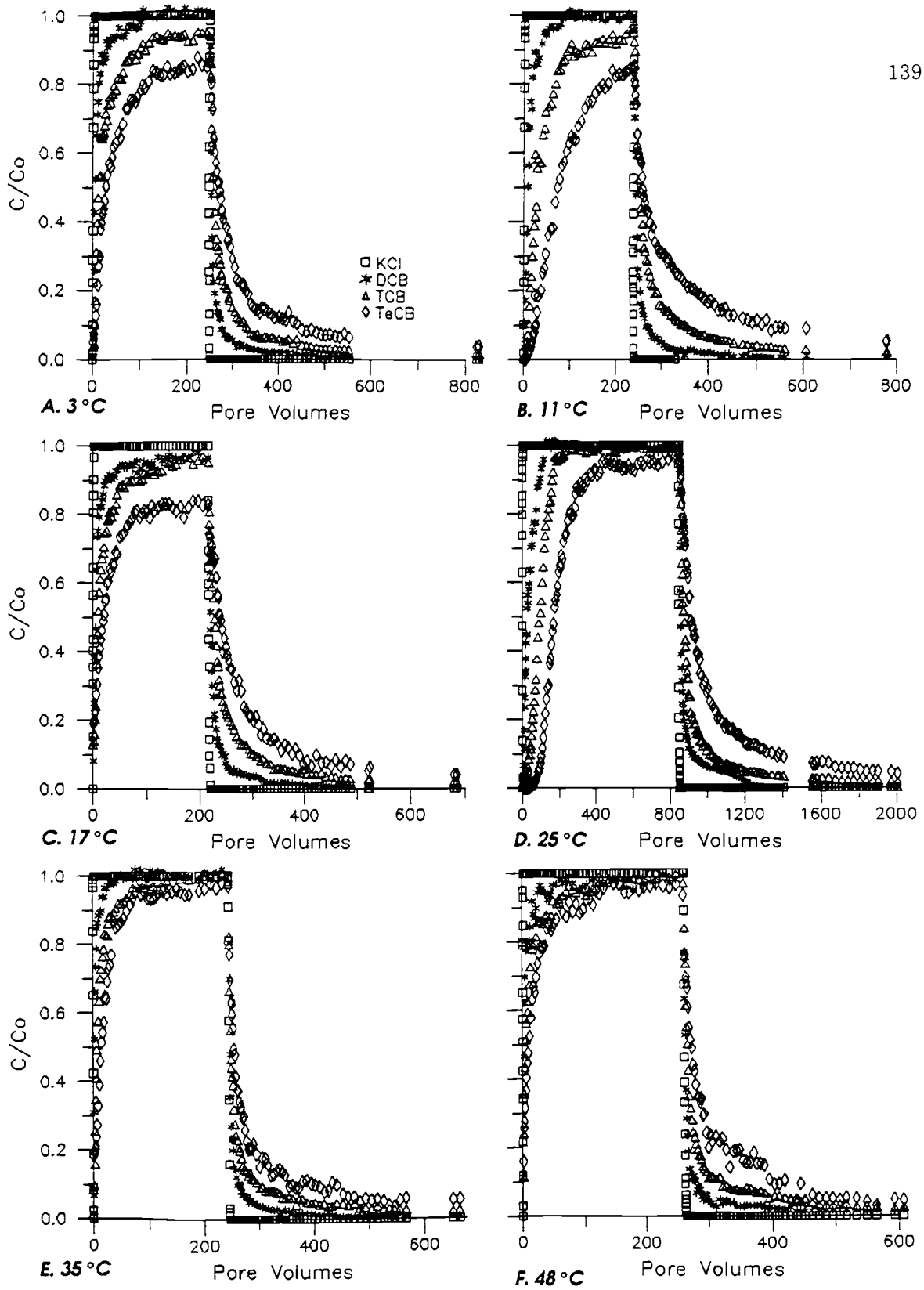

Figure 4.17 Sorption at different temperatures

Table 4.9 Sorption onto surface E at different temperatures

								Equilibrium Model			First Order Model				Two Region Model				
Exp.	Solute	T	D_{KCl}	K_{pS}[1]	K_{pD}[3]	rev.	K_p	D	D/D_{KCl}	ssq	K_p	N_D	k_b	ssq	K_p	N_D	α_e	f	ssq
		(°C)	(cm^2/s)	(cm^3/g)			(cm^3/g)		(cm^2/s)		(cm^3/g)		(s^{-1})		(cm^3/g)		(s^{-1})		
E-6	SY	DCB	3	0.0426	26.43	28.15	0.939	22.94	0.463	10.87	0.0691	16.84	1.809	0.00431	0.2518	21.15	0.532	0.00362	0.336	0.0756
E-7	SX		11	0.0329	31.86	38.70	0.823	28.01	0.245	7.447	0.1404	21.05	3.622	0.00667	0.2179	24.07	0.636	0.00418	0.484	0.1580
E-8	SZ		17	0.469	46.00	35.49	1.296	23.81	0.645	1.375	0.0829	14.96	1.429	0.00346	0.2085	14.97	1.420	0.00870	0.086	0.2085
E-9	SS		25	0.0139	105.5	115.6	0.913	88.13	0.549	42.73	0.6544	62.64	2.045	0.00142	0.7633	71.20	1.124	0.00826	0.189	0.6582
E-10	TA		35	0.00984	12.74	14.73	0.865	11.39	0.647	65.75	0.1103	8.128	0.926	0.00467	0.1894	8.586	0.793	0.00551	0.183	0.1810
E-11	TB		48	0.0592	32.64	39.08	0.835	15.96	1.26	21.28	0.0882	7.932	0.639	0.00342	0.1836	11.71	0.272	0.00196	0.262	0.1011
E-6	SY	TCB	3	0.0426	108.2	52.53	2.060	96.93	1.10	25.82	0.0499	45.22	1.849	0.00164	0.4928	61.28	0.239	0.00162	0.328	0.0571
E-7	SX		11	0.0329	131.6	101.9	1.291	164.6	0.873	26.54	0.4363	63.86	3.011	0.00183	0.8200	207.9	0.166	0.00109	0.234	0.3019
E-8	SZ		17	0.469	73.18	67.17	1.089	79.07	1.04	2.217	0.1226	40.64	1.442	0.00128	0.2798	42.01	0.453	0.00277	0.289	0.2044
E-9	SS		25	0.0139	262.1	202.6	1.294	268.1	0.521	37.48	1.7400	179.3	3.071	0.000742	1.6076	168.9	3.165	0.0233	0.044	1.5990
E-10	TA		35	0.00984	44.16	52.46	0.842	45.36	1.17	118.9	0.2134	24.00	1.329	0.00227	0.3504	25.52	0.796	0.00553	0.207	0.3254
E-11	TB		48	0.0592	47.34	61.97	0.764	53.82	1.78	30.07	0.0448	22.61	1.126	0.00212	0.2355	26.08	0.210	0.00151	0.290	0.0902
E-6	SY	TeCB	3	0.0426	288.4	201.7	1.430	296.7	1.50	35.21	0.0624	110.9	1.550	0.000560	0.5669	135.1	0.349	0.00237	0.311	0.1012
E-7	SX		11	0.0329	308.1	221.1	1.393	698.5	1.39	42.25	0.3846	198.8	2.370	0.000462	1.0640	333.9	0.406	0.00266	0.312	0.3946
E-8	SZ		17	0.469	260.5	153.6	1.696	251.7	1.45	3.092	0.4845	101.3	1.254	0.000448	0.3383	78.58	1.340	0.00821	0.017	0.3025
E-9	SS		25	0.0139	563.6	563.6	1.000	801.2	0.605	43.53	1.5710	385.2	3.731	0.000420	1.6542	377.1	3.566	0.0262	0.096	1.6560
E-10	TA		35	0.00984	75.34	115.3	0.653	101.1	1.32	134.1	0.2982	45.57	1.509	0.00136	0.3310	44.10	1.545	0.0107	0.026	0.3273
E-11	TB		48	0.0592	76.02	103.1	0.737	110.5	1.82	30.74	0.3183	49.59	1.157	0.000991	0.3588	42.14	0.479	0.00345	0.213	0.2976

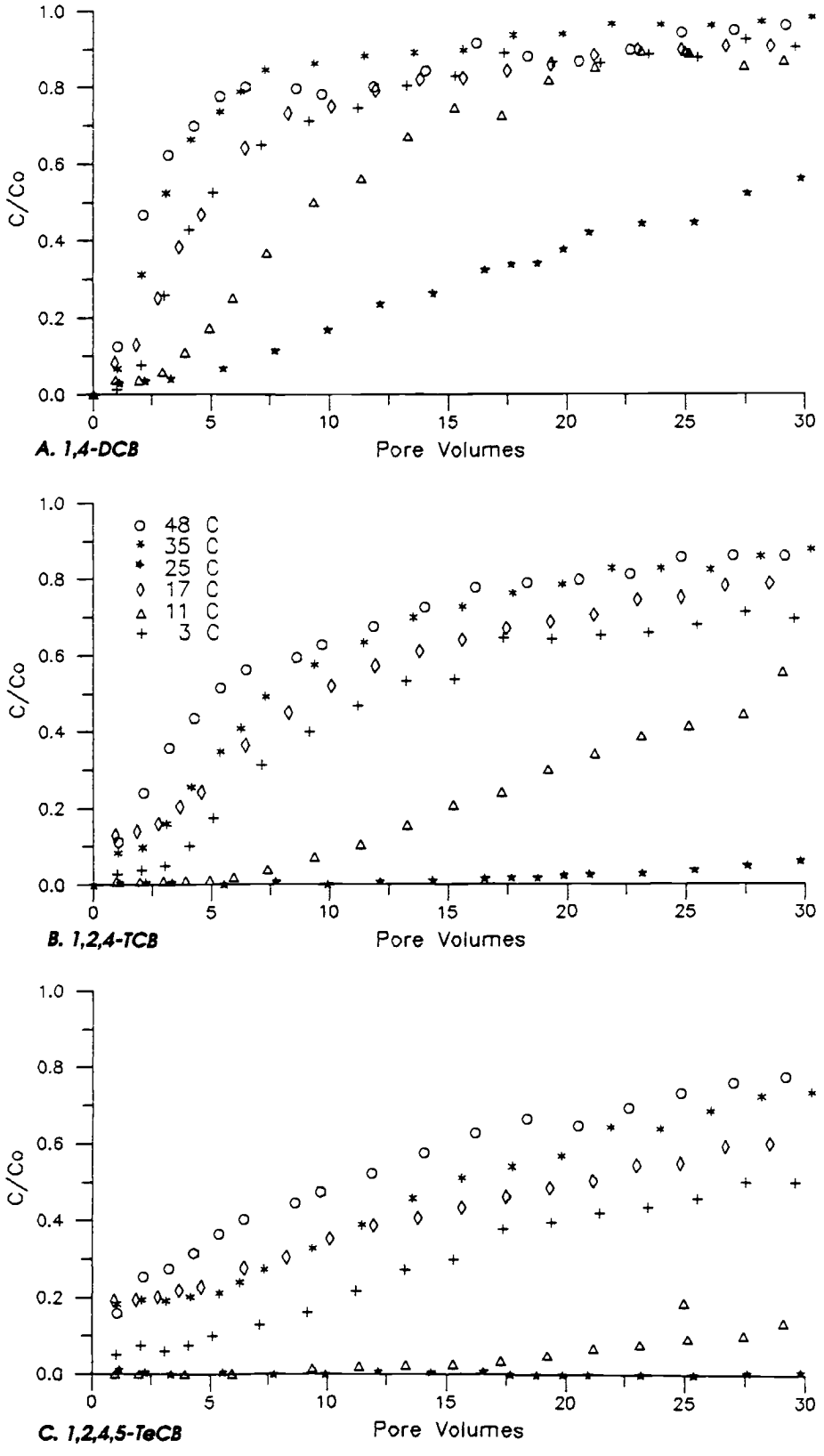

Figure 4.18 Effect of temperature on sorption

enthalpy of the overall sorption process. The intercept is different in each case, corresponding to increased entropy for the sorption reaction.

The van't Hoff equation (20) was used to calculate the enthalpy of the sorption reaction, with results shown in Table 4.10. Enthalpy changes that occur during sorption result from both the sorbent/sorbate interaction and the increased hydrogen bonding upon solute molecule removal from solution (the solvent effect). The sorbate/sorbent interaction enthalpy is not expected to change over the series of compounds, but the solvent effect enthalpy decreases, resulting from increased hydrogen bonding upon larger molecule removal from solution.

The experimental data (Table 4.10) show enthalpies of -3.9 kcal mol^{-1} for DCB, -3.7 kcal mol^{-1} for TCB, and -4.9 kcal mol^{-1} for TeCB. This decrease in enthalpy over the series of compounds may be due to the solvent effect.

The van't Hoff equation (Figure 4.19) was used to calculate the thermodynamic K at 25°C, for the three compounds. This represents the partition coefficient between a pure organic phase and water. The Gibbs free energy was calculated using equation (11), where $\Delta G°$ for DCB was -4.3 kcal mol^{-1}, -4.9 kcal mol^{-1} for TCB, and -5.4 kcal mol^{-1} for TeCB. These small sorption energies are consistent with a van der Waals interaction.

The entropy of the overall sorption process was calculated from $\Delta G°$ and $\Delta H°$ values (Table 4.10), and is slightly positive for the three compounds (0.4 to 1.2 kcal mol^{-1}). There are two entropy effects in the sorption process (Section 2.1.1). These are the decreased entropy in moving a solute molecule from liquid to a sorbed state, and the increased entropy from the solvent effect (decreased water molecule structure due to the solute molecule removal from solution). Experimental values do show that the solvent effect entropy is greater. The solvent effect entropy is considered a major driving force for the sorption of hydrophobic compounds from aqueous solution [*Frank and Evans, 1945*].

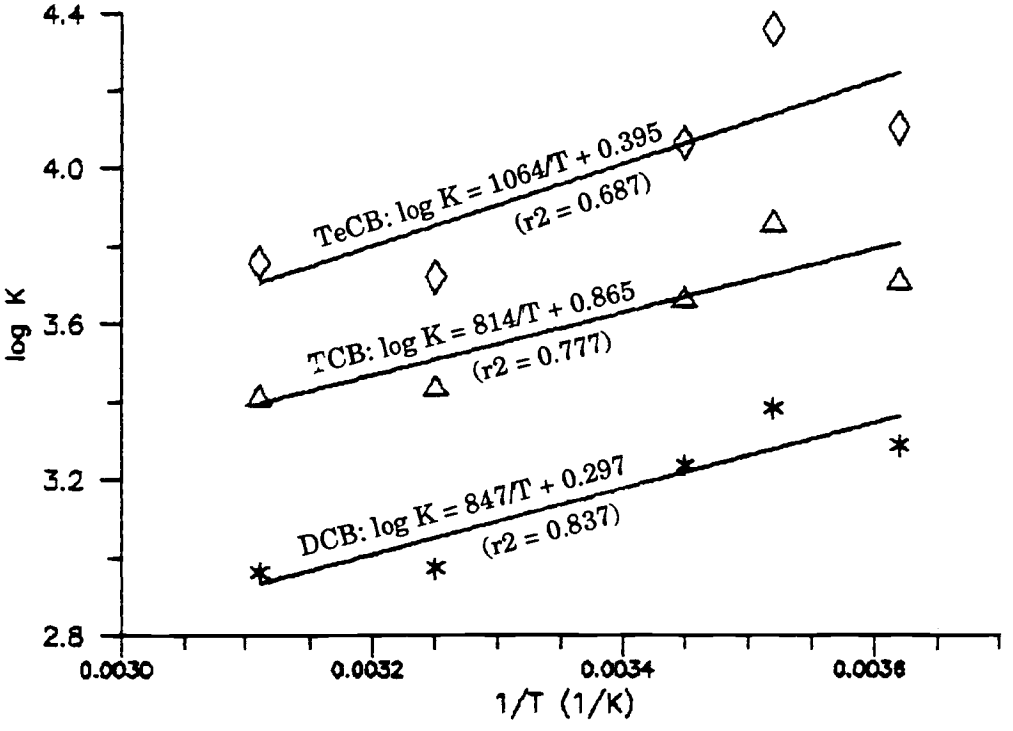

Figure 4.19 Sorption at different temperature

Table 4.10 Thermodynamic results

K versus T (van't Hoff Equation)			
Compound	ΔH° (kcal mol^{-1})	$T\Delta S^\circ$ (kcal mol^{-1})	ΔG° (kcal mol^{-1})
DCB	-3.88 ± 0.12	+0.40 ± 0.12	-4.28 ± 0.12
TCB	-3.73 ± 0.15	+1.17 ± 0.15	-4.90 ± 0.14
TeCB	-4.87 ± 0.24	+0.54 ± 0.24	-5.41 ± 0.23

$$\log K = [-\Delta H / 2.3R]1/T + \Delta S / 2.3R$$

$$\Delta H = -2.3R\,(Slope)$$

$$\Delta G = -RT \ln K \text{ at } 25°C$$

$$T\Delta S = \Delta H - \Delta G$$

Sorption rate versus T (Arrhenius Equation)		
	k_f *versus T*	k_b *versus T*
Compound	E_a (kcal mol^{-1})	E_a (kcal mol^{-1})
DCB	+4.95	+1.55
TCB	+2.06	-1.02
TeCB	+0.74	+0.01

$$E_a = -2.3R\,(Slope)$$

4.5.2.3.2 Chemical Sorption Rate

The change in the sorption and desorption rates of the three solutes over the 3 to 48°C temperature range are shown in Figure 4.20A and B. The rates (k_f and k_b) shown are first-order model fits to breakthrough curves (see Table 4.9).

If the slow sorption is caused by a slow first-order chemical reaction, then slow chemical reaction theory can be used to estimate thermodynamic parameters from the rate versus temperature data. Two theories that can explain slow chemical reactions are the collision theory and the transition state theory. The collision theory describes the reaction proceeding at a rate controlled by the frequency of collisions of molecules at a specific orientation [*Fressenden et al., 1982*], where the frequency of collisions are smaller for more specific orientations. Reaction kinetics are described with the Arrhenius equation:

$$k_b = A \exp\left[\frac{-E_a}{RT}\right] \tag{77}$$

where k_b is the reaction rate, E_a is the activation energy, and A is the collision frequency (and steric) factor. The transition state theory is a more energetic approach, where the slow reaction results from the energy barrier in creating an activated complex and the slow decay of the complex. A comparison between these two approaches can lead to the calculation of the activated complex enthalpy and entropy.

The plot of k_b versus $1/T$ (Figure 4.20B) shows little trend with increasing temperature, as the k_b for DCB decreases, the k_b for TCB increases, and the k_b for TeCB does not change. The forward rate coefficient (k_f) was calculated from desorption rate and K_p (equation 9), and it shows a regular trend of decreasing rate with increasing temperature (Figure 4.20A). Scatter in the rate data is understandable since model fits to data are only fair to good (ssq = 0.2 to 2.0). Even with these well characterized particles, it may not be possible to completely separate several rate-limiting steps. Since the diffusion time into porous particles is about one minute, a faster chemical reaction rate

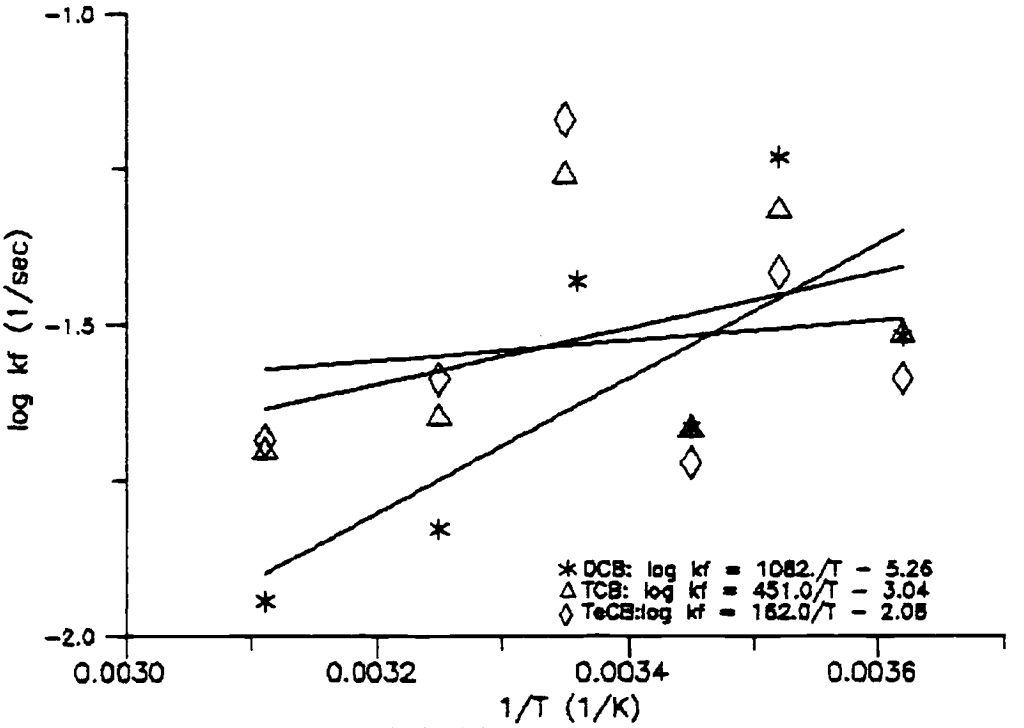

A. First-order sorption rate coefficient (k_f)

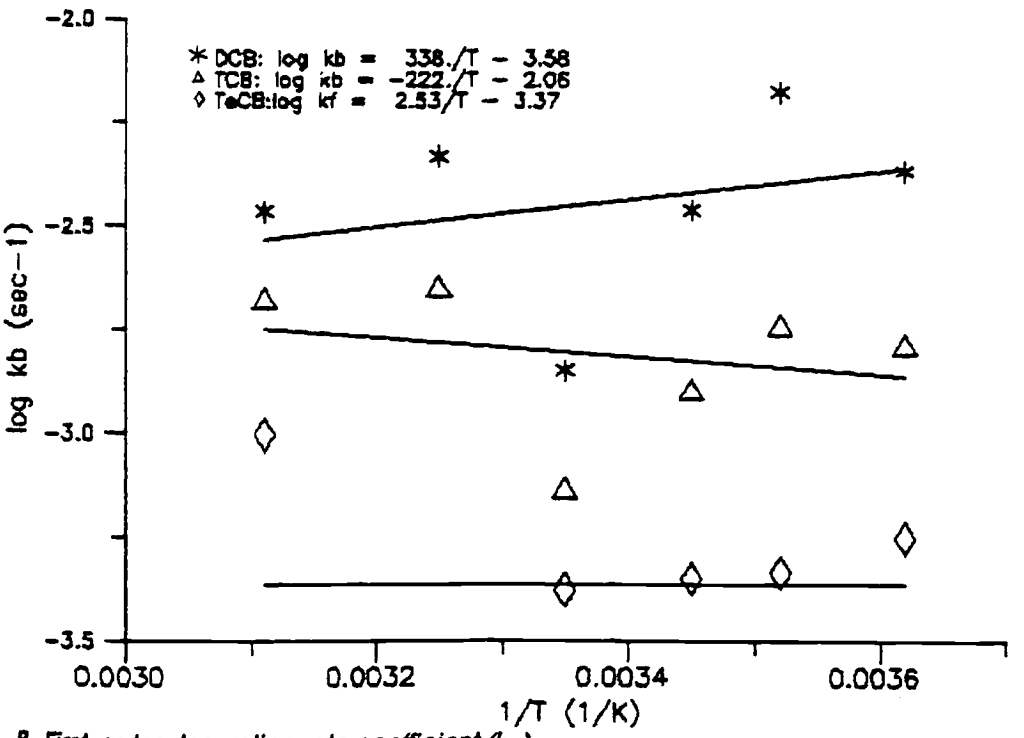

B. First-order desorption rate coefficient (k_b)

Figure 4.20 Arrhenius plots of reaction rates

will not be observed, as it will be masked by the slower diffusion rate. The rate-limiting step also may not be entirely caused by slow chemical reaction.

Sorption and desorption rate data were fit to the Arrhenius equation (77) to calculate the activation energy (E_a in Table 4.10). The E_a values calculated with k_b range from +0.8 to +5.0 kcal mol^{-1}, and with k_f range from -1.0 to +1.6 kcal mol^{-1}. These values are near the reported values for collisions by diffusion in aqueous solution (+3 to 5 kcal mol^{-1}) [*Stumm and Morgan, 1981*], but most of the data in this research indicate that a slow binding and release step is rate limiting.

4.5.2.3.3 Diffusion Rate

The sorption rates obtained from model fits of breakthrough curves at different temperatures (Table 4.9) can be compared to the expected rate if diffusion were the rate-limiting sorption step. A case where diffusion through immobile fluid is assumed to cause all of the slow sorption is examined with use of equation (40). In this case, the diffusion coefficient through spherical particles is calculated by assuming that D_{mobile} (for a solute) is equal to a factor times D_{KCl}, where this factor is 1.5 for DCB, 1.9 for TCB, and 3.7 for TeCB. The total dispersion observed (D_{total}) is that obtained from the equilibrium model fit to data (Table 4.9), so it includes hydrodynamic dispersion and spreading due to the slow process. The diffusion in spherical particles (D_a) necessary to cause the observed slow sorption is calculated (Table 4.11) for all of the experiments at different temperatures.

Linear regression of diffusion coefficients over the temperature range shows a decrease of 66 percent for DCB, 17 percent decrease for TCB, and a 13 percent increase for TeCB. The correlation was very poor, with r^2 = 0.392, 0.016, and 0.005 for the three compounds. A graph of these data (Figure 4.21) show considerable scatter, with no observable trend. If the sorption rate was controlled by the diffusion rate, then it should increase 16.3 percent from 3 to 48°C, according to the Wilke-Chang equation (39). As the calculated D_a values do not indicate this trend, the sorption rate is not caused by

Table 4.11 Calculated diffusion coefficient on surface E

Solute	Spherical Diffusion Coefficient (D_A) x 10^9*					
	3°C	11°C	17°C	25°C	35°C	48°C
DCB	13.5	24.2	7.63	11.9	9.76	5.46
	$D_A = 2.52 \times 10^{-10} T + 8.67 \times 10^{-8}$ ($r^2 = 0.392$)					
TCB	5.68	6.69	4.74	13.8	5.41	3.92
	$D_A = 2.82 \times 10^{-11} T + 1.51 \times 10^{-8}$ ($r^2 = 0.016$)					
TeCB	4.31	4.29	3.43	12.3	4.85	4.04
	$D_A = 1.47 \times 10^{-11} T + 1.18 \times 10^{-1}$ ($r^2 = 0.005$)					

*equation (90)

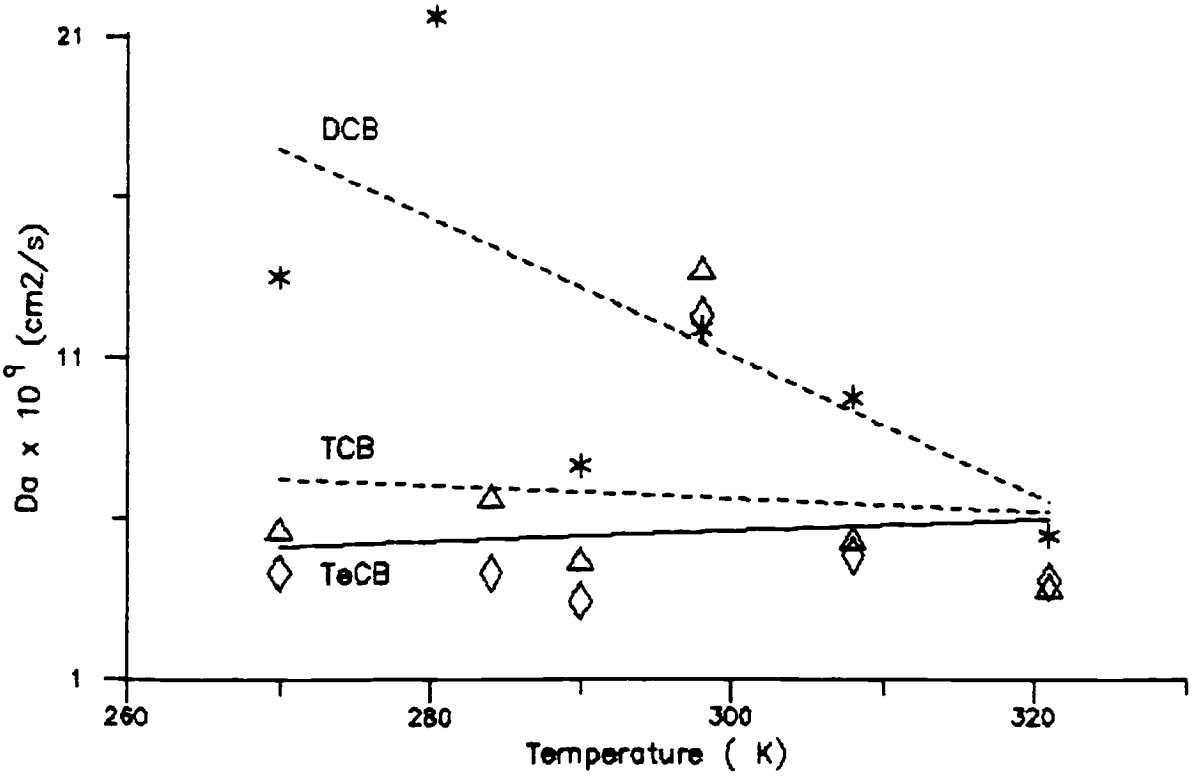

Figure 4.21 Temperature effect on particle diffusion

diffusion through immobile fluid.

The diffusion rate through the bound organic layer is quantified by α_i (ρ_b k_b) as defined in Section 2.2.4.2. First-order model fits to breakthrough curves at different temperatures can be compared to the expected change in the diffusion rate over the 45°C range (a 16.3 percent increase). The change in k_b with temperature (Table 4.9) is illustrated in Figure 4.20B. Linear regression produced the following results for the compounds: for DCB, k_b = -3.0 x 10^{-5} T + 1.3 x 10^{-2} (r^2 = 0.097), for TCB, k_b = 1.1 x 10^{-5} T - 1.6 x 10^{-3} (r^2 = 0.12), and for TeCB, k_b = 1.4 x 10^{-5} T - 3.4 x 10^{-3} (r^2 = 0.43). Calculating the change in k_b (or α_i) over the temperature range with these equations produces a 32 percent decrease for DCB, a 40 percent increase for TCB, and a 200 percent increase for TeCB. Since there is poor correlation with the expected 16 percent increase from the Wilke-Chang equation, diffusion through the bound organic layer is an unlikely rate-limiting step.

4.5.3 Phenyl Polymer Modified 20 μm Silica with 10 nm Pores

Five column experiments were performed with a phenyl-polymer modified 20-μm silica (Appendix C-15) that has a 10 nm average intraparticle pore size (surface F). The model results are presented in Table 4.12, and two breakthrough curves are shown in Figure 4.22A and B. The K_p averaged 47.9 ± 33.4 $cm^3 g^{-1}$ with values ranging from 17 to 109, although there was no correlation with concentration. The K_{oc} averaged 4320, which was about the same as the phenyl-modified 100-μm silica (surface E). Sorption was reversible (K_{ps}/K_{pd} = 0.92 ± 0.34) for the five experiments.

The concentrations of DCB used in experiments varied from 400 ppb to 19 ppm, so an isotherm was developed (Figure 4.22C) and compared to the isotherm obtained from batch experiments. At lower concentrations, breakthrough curves show more tailing (Figure 4.22A, 676 ppb) than for experiments at higher concentration (Figure 4.22B, 19 ppm). Using the average K_p for each experiment (C_o), an isotherm was obtained (Figure 4.22C), where S = 70.3 $C^{0.925}$ (r^2 = 0.864), similar to the isotherm developed from

Table 4.12 DCB sorption onto phenyl polymer modified silicas

				Equilibrium Model						First Order Model				Two Region Model				
Exp.	Solute	Dia.	D_{KCl}	K_{pS}[1]	K_{pD}[2]	rev.	K_p	D	D/D_{KCl}	ssq	K_p	N_D	k_b	ssq	K_p	N_D	α_e	f	ssq
		(μm)	(cm^2/s)	(cm^3/g)			(cm^3/g)		(cm^2s)		(cm^3/g)		(s^{-1})		(cm^3/g)		(s^{-1})		
U-1 SP	PQ-U	2	0.0185	16.49	4.759	3.465	16.69	0.0109	0.75	0.6657	43.18	1.552	0.0000620	3.0546	14.50	0.7022	0.000659	0.007	2.590
U-2 SQ	PQ-U	Solid	0.0536	3.451	2.773	1.245	8.664	7.65	142	0.1037	7.380	0.229	0.0000776	0.9551	1.930	0.1828	0.000248	0.045	0.0650
ave.				6.87 ± 6.47		2.36							0.000070						
F-1 QV	PQ-I	20	0.00518	25.06	25.71	0.975	35.401	0.591	114	0.0876	24.62	1.967	0.000560	0.1717	24.23	2.108	0.00244	0.015	0.1635
F-2 QW	PQ-I	Porous	0.0117	17.31	42.58	0.407	20.329	0.429	36.7	0.3150	14.40	2.266	0.000984	0.0523	29.94	0.7990	0.000826	0.260	0.8692
F-3 SJ	PQ-I	(11 nm	0.00475	104.0	109.4	0.951	124.91	0.0177	3.73	0.2831	110.2	6.236	0.000380	0.3980	117.11	2.0830	0.00232	0.382	0.3229
F-5 SK	PQ-I	Pore)	0.00887	49.67	55.76	0.891	46.504	0.0860	9.70	0.2322	38.71	4.130	0.00210	0.3228	43.89	0.6993	0.00228	0.528	0.2599
F-4 SL	PQ-I		0.0129	28.56	20.98	1.361	22.229	0.0670	5.15	0.1825	19.83	3.944	0.00388	0.2347	21.13	1.2080	0.00389	0.446	0.1868
ave.				47.9 ± 33.4		0.917			36.5				0.00067				0.0043		
G-1 QX	PQ-J	20	0.000855	32.09	28.69	1.119	31.425	0.0679	79.4	0.1153	27.94	4.730	0.00106	0.2380	33.79	0.7880	0.000651	0.577	0.1700
G-2 QY	PQ-J	(27 nm	0.00339	20.31	16.78	1.210	19.875	0.114	33.6	0.0677	15.63	2.718	0.00132	0.5404	15.71	2.569	0.00257	0.129	0.5392
G-3 QZ	PQ-J	Pore)	0.00165	17.48	22.46	0.778	16.887	0.120	72.7	0.1694	15.13	3.820	0.00182	0.2732	18.01	0.7440	0.000707	0.527	0.0833
ave.				23.0 ± 6.19					40.1				0.0016				0.0029		
E-5 QP	PQ-E	100	0.858	8.015	9.949	0.806	11.810	0.517	60.6	0.1348	8.98	2.195	0.00417	0.1377	8.983	2.593	0.00750	0.024	0.1160
E-1 QQ	PQ-E	(27 nm	0.00629	18.23	28.80	0.633	18.777	0.140	222	0.2124	14.57	2.701	0.000439	0.5534	19.08	0.578	0.000232	0.451	0.3220
E-2 RN	PQ-E	Pore)	0.000889	59.45	53.24	1.117	54.00	0.0251	282	0.0592	45.97	3.608	0.000542	0.2864	53.65	1.119	0.00131	0.408	0.1030
E-3 SR	PQ-E		0.00501	72.38	56.85	1.273	84.82	0.0448	8.94	0.2512	63.86	3.259	0.000385	0.5854	77.81	1.143	0.00146	0.352	0.3319
E-4 TD	PQ-E		0.00114	98.41	92.39	1.065	109.1	0.0635	55.8	0.2720	82.42	2.840	0.000312	0.4635	85.48	2.121	0.00326	0.142	0.4655
E-9 SS	PQ-E		0.0139	105.5	115.6	0.913	88.13	0.594	42.7	0.6544	62.64	2.045	0.00142	0.7633	71.20	1.124	0.00826	0.189	0.6582
ave.				60.6					32.0				0.00038				0.0034		
H-2 RA	PQ-L	425	0.0560	16.71	17.56	0.952	15.26	0.107	1.91	0.1941	10.89	6.204	0.00281	0.4450	16.66	0.1902	0.000190	0.606	0.2538
H-3 RO	PQ-L	(11 nm	0.00520	26.81	24.99	1.073	25.95	0.222	4.27	0.0661	22.55	3.006	0.000754	0.2438	25.39	0.9334	0.00107	0.435	0.0767
H-1 RP	PQ-L	Pore)	0.00421	23.63	23.80	0.993	22.47	0.237	56.3	0.0997	19.61	2.963	0.000835	0.3138	22.35	0.8780	0.000979	0.424	0.0885
ave.				22.2 ± 4.13					33.6				0.0011				0.0015		

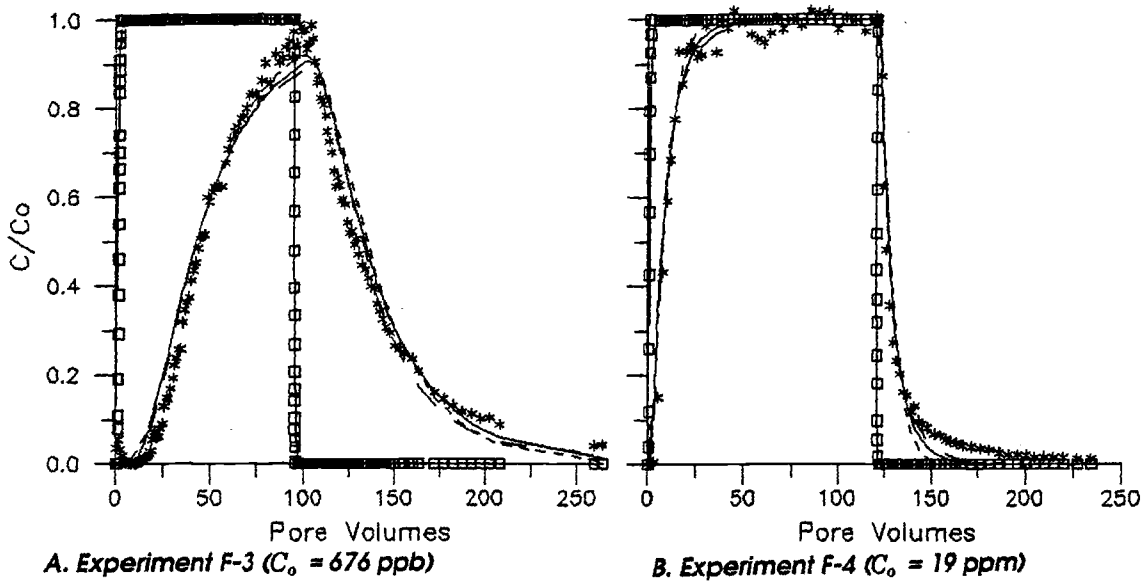

A. Experiment F-3 (C_o = 676 ppb)

B. Experiment F-4 (C_o = 19 ppm)

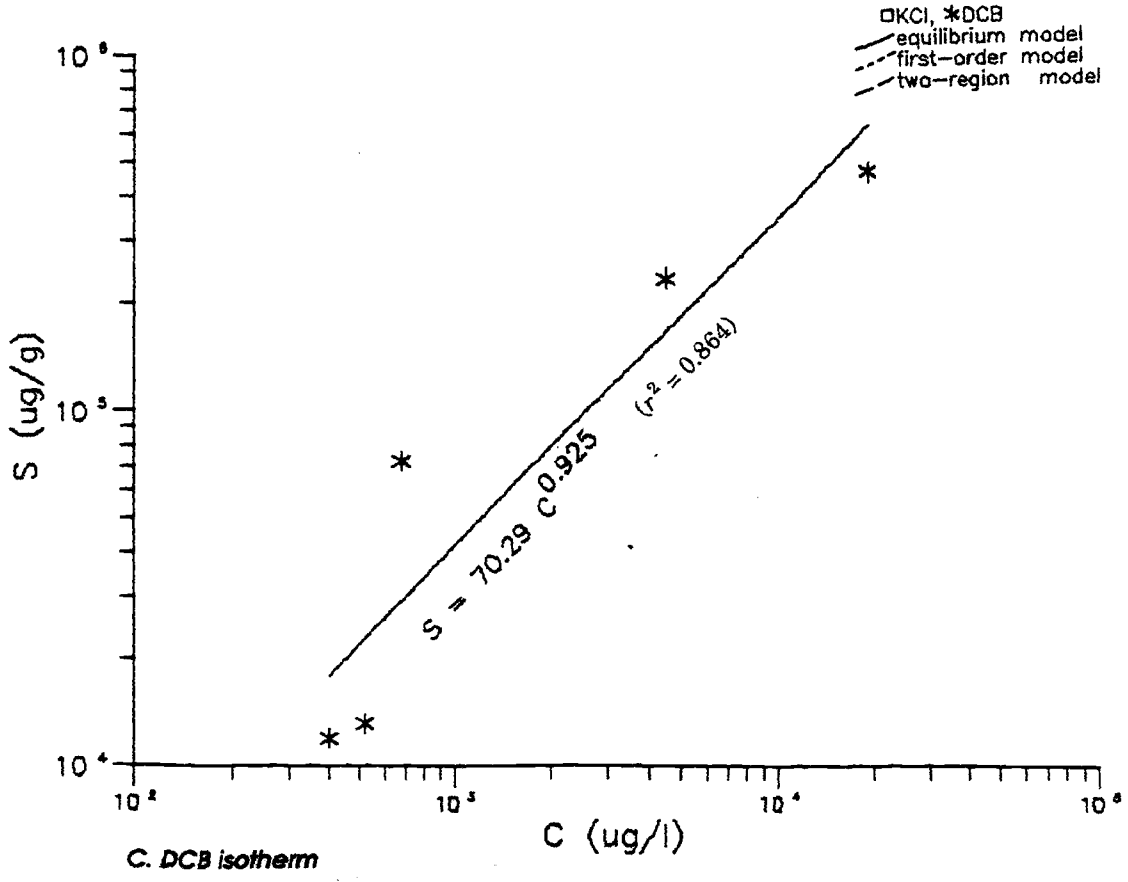

C. DCB isotherm

Figure 4.22 DCB sorption onto phenyl polymer surface F (20 μm diameter with 11 nm pores)

batch experiments (exponent = 0.91).

The equilibrium model D_{DCB}/D_{KCl} (Table 4.12) averaged 36.5 ± 45.0, indicating a variable amount of nonequilibrium sorption. The first-order model, however, indicates fairly consistent slow sorption values between experiments, with ω varying from 2 to 7 and k_b averaging 6.7 x 10^{-4} s^{-1}. The two-region model also had a consistent rate coefficient (α_e) of 4.3 x 10^{-3} s^{-1}, even with f varying from 0.02 to 0.53. The $\alpha_e/K_p\rho_b$ from the two-region model is 2.5 x 10^{-4} s^{-1}.

One desorption was performed after 62 days (experiment F-2), and it had a much larger desorption K_p (43) than sorption (17), which could indicate some irreversible sorption. However, K_p values were within the range of those obtained from other experiments, and no irreversible sorption was observed with batch experiments over a 2 week period.

4.5.4 Phenyl Polymer Modified 20 μm Silica with 27.5 nm Pores

Three column experiments of DCB sorption were performed on a phenyl-polymer modified 20-μm silica that had a 27.5 nm average pore diameter (surface G). Breakthrough curves are shown in Appendix C-16, and modeling results in Table 4.12. The K_p averaged 23.0 ± 6.2 $cm^3 g^{-1}$, and the K_{oc} averaged 2270, showing less partitioning than observed on the other 20-μm surface (surface F) with the same f_{oc}. Two breakthrough curves are shown in Figure 4.23A and B. Desorption was performed after 54 days in one experiment (Figure 4.23B), and it showed a slightly larger desorption K_p (22.5) compared to the sorption K_p (17.5). An experiment in which immediate desorption was performed (Figure 4.23A) showed slightly greater sorption K_p than the desorption K_p.

The equilibrium model D_{DCB}/D_{KCl} averaged 40.1 ± 36.5, indicating a fair degree of nonequilibrium sorption. The first-order model fits to the three experiments showed a consistent amount of nonequilibrium with ω ranging from 2.7 to 4.8, and k_b averaging 1.6 x 10^{-3} s^{-1}. This rate is 140 percent larger than that obtained from the other 20-μm

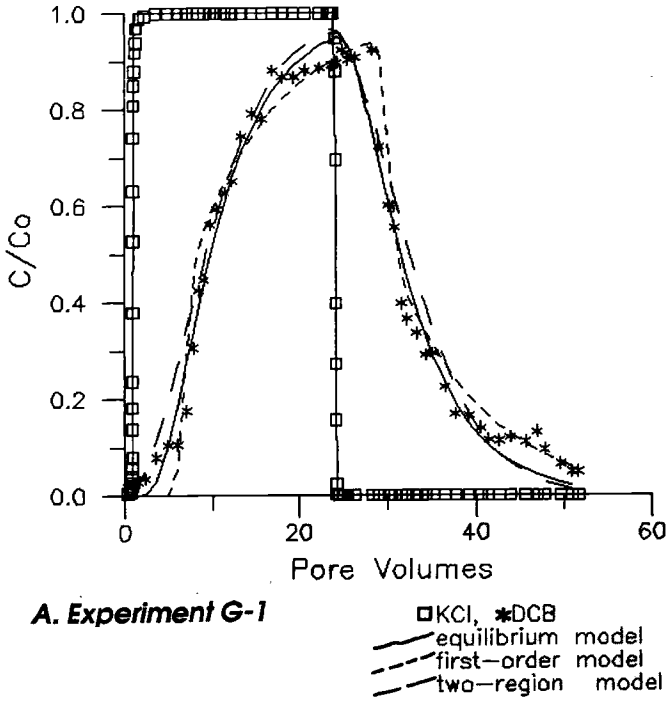

A. Experiment G-1

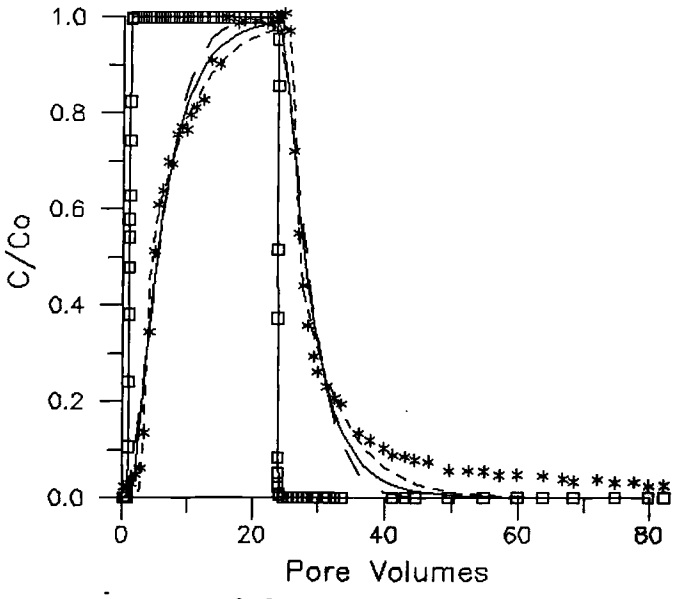

B. Experiment G-3

Figure 4.23 DCB sorption onto phenyl polymer surface G (20 μm diameter with 27 nm pores)

phenyl-polymer surface with smaller pores (surface F).

The two-region model fits to breakthrough curves had an average α_e of 2.9 x 10^{-3} s^{-1}, which is slower than the other 20-μm silica that had smaller pores (surface F). The sorption rate is partially controlled by diffusion through immobile pore fluid, since the smaller particles with more tortuous flow paths exhibited slower rates.

4.5.5 Phenyl Polymer Modified 425 μm Silica with 11 nm Pores

Three column experiments were performed with sorption of DCB onto a phenyl-polymer modified 425-μm silica, which has an average pore diameter of 11 nm (surface H). This silica differs from surface F only by particle size, the pore diameter is identical for both surfaces. Breakthrough curves of experiments are in Appendix C-17, and the modeling results are shown in Table 4.12.

Sorption onto the 425-μm surface had an average K_p of 22.2 ± 4.1 $cm^3 g^{-1}$ and a K_{oc} of 2100, somewhat smaller than other phenyl polymer modified surfaces. The sorption was reversible (K_{ps}/K_{pd} = 1.01), and there was a large amount of nonequilibrium sorption exhibited based on the equilibrium model D_{DCB}/D_{KCl} ratio (33.6 ± 28.4) and the tailing, which is shown in Figure 4.24A and B.

The first-order model shows a consistent amount of nonequilibrium sorption with ω values ranging from 3 to 6 and a k_b averaging 1.1 x 10^{-3} s^{-1}. This sorption rate was 74 percent faster than the 20-μm particle with same pore size (surface F). The two-region model fit to the data had an average α_e of 1.5 x 10^{-3} s^{-1}, which is 180 percent slower than the 20-μm silica with the same pore size. There appears to be some indication that the sorption rate is slower for the larger particle, indicating diffusion through immobile fluid is causing some of the slow sorption.

4.5.6 Phenyl Polymer Modified 2 μm solid Silica

A phenyl polymer silane was bound to a 1.9-μm nonporous silica (surface U), resulting in an f_{oc} of 0.0044, or about a third that determined on the porous silicas. The calculated monolayer surface area coverage (Table 3.1) was about 100 percent on the

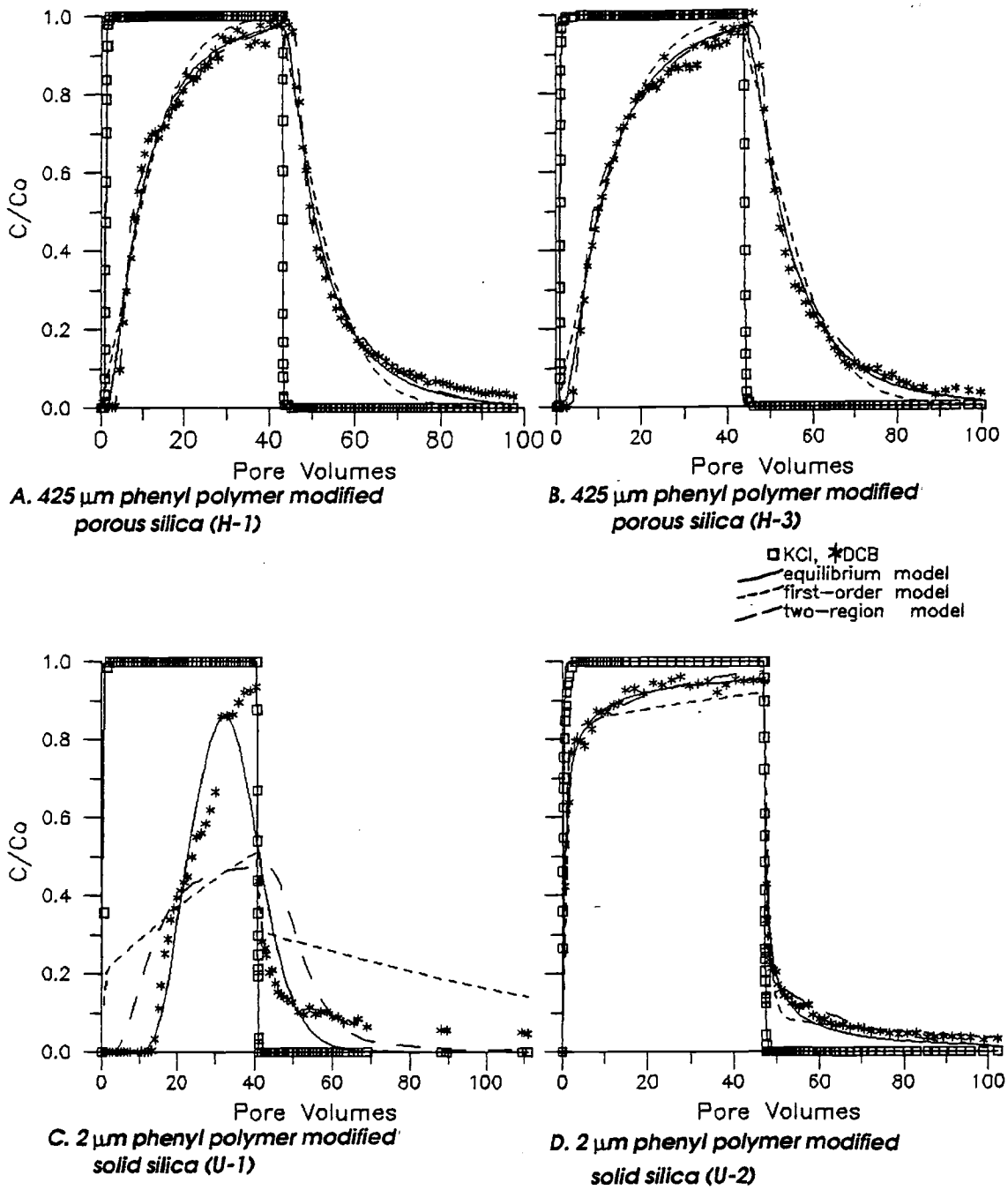

Figure 4.24 Particle structure effect on DCB sorption

solid surface, compared to 2 to 15 percent on the porous surfaces. Two column experiments of DCB sorption were performed on the 2-μm nonporous silica (Figure 4.24C and D), with the modeling results shown in Table 4.12.

The partition coefficient averaged 6.9 ± 6.5 $cm^3 g^{-1}$, and the average K_{oc} was 1560, smaller than other phenyl-polymer modified silicas. Since the polymer is more densely packed on the surface, sorption sites may be less accessible. This could lead to slower chemical sorption into the polymer. The sorption K_p was over twice that for desorption (K_{ps}/K_{pd} = 2.4 ± 1.6), possibly indicating some irreversible sorption.

The equilibrium model dispersion for DCB was 142 times larger than the dispersion observed for KCl for experiment U-2 (Figure 4.24D). The first-order model fit to the two experiments produced ω values of 0.2 and 1.5, and an average k_b of 7.0 x 10^{-5} s^{-1}. The model fit was good for experiment U-2 (ssq = 0.35), but poor for experiment U-1 (ssq = 3.1).

The two-region model fits to the experiments were considerably better than first-order model fits, where α_e averaged 4 x 10^{-4} s^{-1}, and f averaged 0.014. The small value of f (fraction mobile sites) indicates that slow sorption can be modeled with mainly slow sorption sites, which is mathematically close to the first-order model where all of the sites exhibit slow sorption. The $\alpha_e/\rho_b K_p$ was 6.6 x 10^{-5} s^{-1}, equal to that obtained in the first-order model fit to data.

4.6 C_{18} and Phenyl Polymer Modified 100 μm Silica

A 100-μm porous silica was modified by binding both a C_{18}-polymer and a phenyl-polymer (about equal mixture) to the surface (X). In this case, sorption onto the bound organic phase occurs by parallel reactions, fast (equilibrium) sorption onto the C_{18} fraction, and slow sorption onto the phenyl-polymer fraction. Since the polymerization of phenyl groups produces strong and slow sorption, the sorption rate on the phenyl-polymer fraction of this surface should increase. Sorption on this surface is heterogeneous, which is observed to produce more peak spreading [*Antle et al., 1985*].

Two column experiments were performed with this heterogeneous surface (Figure 4.25A and B), with modeling results shown in Table 4.13. The average K_p was 30.0 ± 1.8 $cm^3 g^{-1}$, which was reversible within 2 percent in both cases. The equilibrium model DCB dispersion was 11 to 26 times greater than the KCl dispersion, indicating some nonequilibrium, but not as great as on the pure phenyl-polymer modified surfaces. Visually (Figure 4.25A and B), breakthrough curve tailing appears greater than tailing observed on the C_{18} silica, but less than that seen on the phenyl-polymer silica.

This parallel sorption can be modeled with a first-order model (single rate) where ω was 6 to 8, and the k_b was 1-3 x 10^{-3} s^{-1}, or about three-fold faster than the phenyl-polymer bound to 100-μm silica (surface E). The rate on the heterogeneous surface is 2-6 fold slower than the rate observed for C_{18} polymer bound to 100-μm porous silica (surface C).

A two-region model can be interpreted in terms of a slow reaction in parallel with a fast reaction. Fitting the two region model to experiment X-2 produced a slow reaction rate of 8.0 x 10^{-4} s^{-1}, which is still twice as large as the phenyl-polymer surface (k_b = 3.8 x 10^{-4} s^{-1}), although the standard error in the calculated rate is about 30 percent.

4.7 Alcoholic Modified Surface

A silane with six carbons in an aliphatic chain, an ether group (C-O-C), and two alcoholic groups was bound to a 100-μm silica (surface R). The surface is mainly nonpolar, but has some dipole moment due to the functional groups. Because of the polar functional groups, sorption of hydrophobic compounds is expected to be smaller than on a pure nonpolar silane. Three column experiments were performed with the sorption of DCB (Appendix C-19), where the K_p averaged 0.99 ± 0.02 $cm^3 g^{-1}$. Model results are shown in Table 4.13, and the results of two experiments are illustrated in Figure 4.25C and D. The K_p is smaller than all other organic surfaces as well as unbound surfaces, and the calculated K_{oc} (114) is also about an order of magnitude smaller than for organic modified surfaces.

Table 4.13 DCB sorption onto functional group modified silica

			Equilibrium Model							First Order Model				Two Region Model				
Exp.	Sorbent	D_{KCl}	K_{pS}[1]	K_{pD}[2]	rev.	K_p	D	D/D_{KCl}	ssq	K_p	N_D	k_b	ssq	K_p	N_D	α_e	f	ssq
		(cm^2/s)	(cm^3/g)			(cm^3/g)		(cm^2/s)		(cm^3/g)		(s^{-1})		(cm^3/g)		(s^{-1})		
X-1 RR	PQ-P C_{18}+Øpoly	0.00932	31.72	31.65	1.002	28.92	0.107	11.5	0.0164	26.98	7.324	0.00228	0.0477	27.73	2.258	0.00323	0.470	0.0200
X-2 RS	PQ-P C_{18}+Øpoly	0.00437	28.86	28.45	1.014	25.98	0.116	26.5	0.0247	23.97	5.896	0.00206	0.0709	25.01	1.839	0.00263	0.484	0.0485
ave.			30.02 ± 1.76					19.0										
R-1 RE	PQ-G DIOLpoly	0.00693	6.630	3.848	1.723	4.083	0.0121	1.75	0.0894	---	---	---	---	---	---	---	---	---
R-2 RH	PQ-G DIOLpoly	0.0256	3.063	2.833	1.081	2.568	0.00401	15.7	0.0688	2.308	451.8	0.358	0.0811	2.32	2846.0	0.817	1.019	0.0799
R-3 RI	PQ-G DIOLpoly	0.00656	1.752	1.836	0.954	1.744	0.00649	0.99	0.0239	1.538	10296	18.0	0.0297	2.02	0.0527	0.0000223	1.407	0.0229
ave.			3.33 ± 1.80		1.25			6.13				1.1						
T-1 ST	PQ-K AMINpoly (pH = 7.0)	0.0490	4.325	2.889	1.466	5.249	0.0300	0.97	0.6083	4.992	6.933	0.00603	0.6188	5.21	1.409	0.000971	0.782	0.6031
T-2 SU	PQ-K AMINpoly (pH = 3.9)	0.00316	3.713	5.420	0.685	2.801	0.00711	2.25	0.1628	2.562	1000000.	1060.	0.1509	2.67	610121	262.0	0.225	0.1432
T-3 SV	PQ-K AMINpoly (pH = 2.3)	0.00457	2.037	4.177	0.488	2.819	0.0118	2.58	0.1820	2.516	350.9	0.376	0.1863	2.52	351.0	0.150	1.303	0.1848
T-4 SW	PQ-K AMINpoly (pH = 1.0)	0.00467	4.009	3.711	1.080	2.768	0.0184	3.94	0.1784	2.322	61.45	0.0701	0.1994	3.41	0.1418	0.0000596	0.995	0.0731

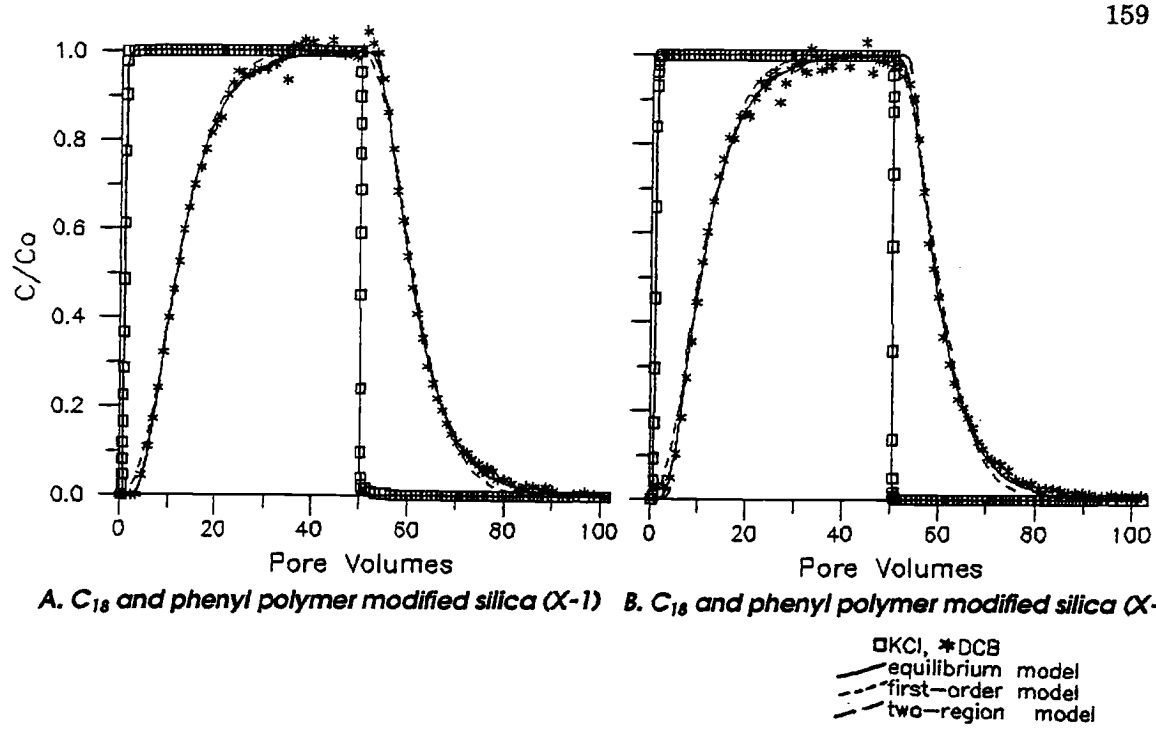

A. C_{18} and phenyl polymer modified silica (X-1) *B. C_{18} and phenyl polymer modified silica (X-2)*

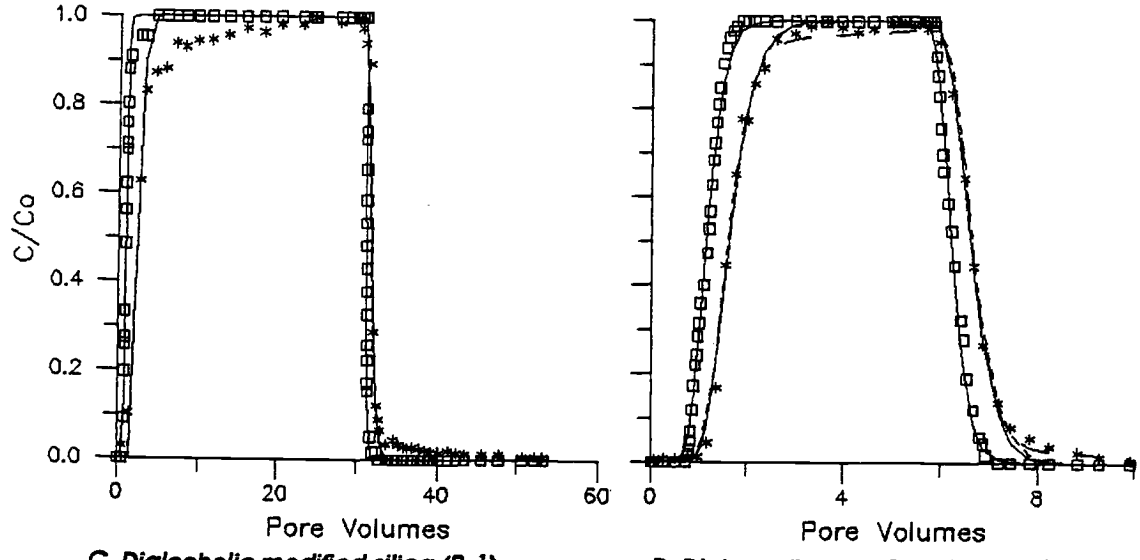

C. Dialcoholic modified silica (R-1) *D. Dialcoholic modified silica (R-3)*

Figure 4.25 DCB sorption onto heterogeneous surfaces

Sorption onto the alcoholic modified surface was fast (Figure 4.25C and D), indicated by the lack of tailing in breakthrough curves and and by the equilibrium model D_{DCB}/D_{KCl} ratio (0.964). The first-order model ω values were large (26 to 10,000), and k_b averaged 1.1 s^{-1}. The two-region model fits to two experiments had a difference in α_e of five orders of magnitude, indicating difficulty in fitting data to a unique set of parameters. Multiple experiment fitting model (MFITIM), discussed in Section 5.3.3, is used to improve this fit.

4.8 Amine Modified Silica

A silane with a two carbon chain and terminating amine group was bound to a 100-μm silica surface (surface T). The fraction of bound carbon by weight (f_{oc}) was 0.8 percent, and the fraction of bound nitrogen by weight was 0.3 percent. Amine surfaces are strong Lewis bases and will ionize at low pH. This will decrease sorption of a hydrophobic solute, such as a chlorinated benzene, at low pH [*Horvath et al., 1978*].

Four column experiments of DCB sorption were performed on this amine surface at different pH values (7.00, 3.88, 2.28, and 1.03), shown in Figure 4.26A through D. Model results are presented in Table 4.13. The K_p did not show a significant change over the pH range (K_p was 3.56, 4.57, 3.11, and 3.86 respectively), indicating the amine group pK_a was not between 1 and 7. The pK_a of aliphatic amines should be in the range of 7 to 10 [*Fressenden et al., 1982*], with a net positive charge below this value. The low K_p values are about the same as sorption onto unbonded silica. At low pH values, the silica is more neutrally charged (pH_{iep} = 2.0), which may lead to greater sorption onto the silica surface.

Tailing visually increases as the pH decreases, which is also indicated by the increasing equilibrium model dispersion ratio (D_{DCB}/D_{KCl} = 0.97, 2.25, 2.58, and 3.94).

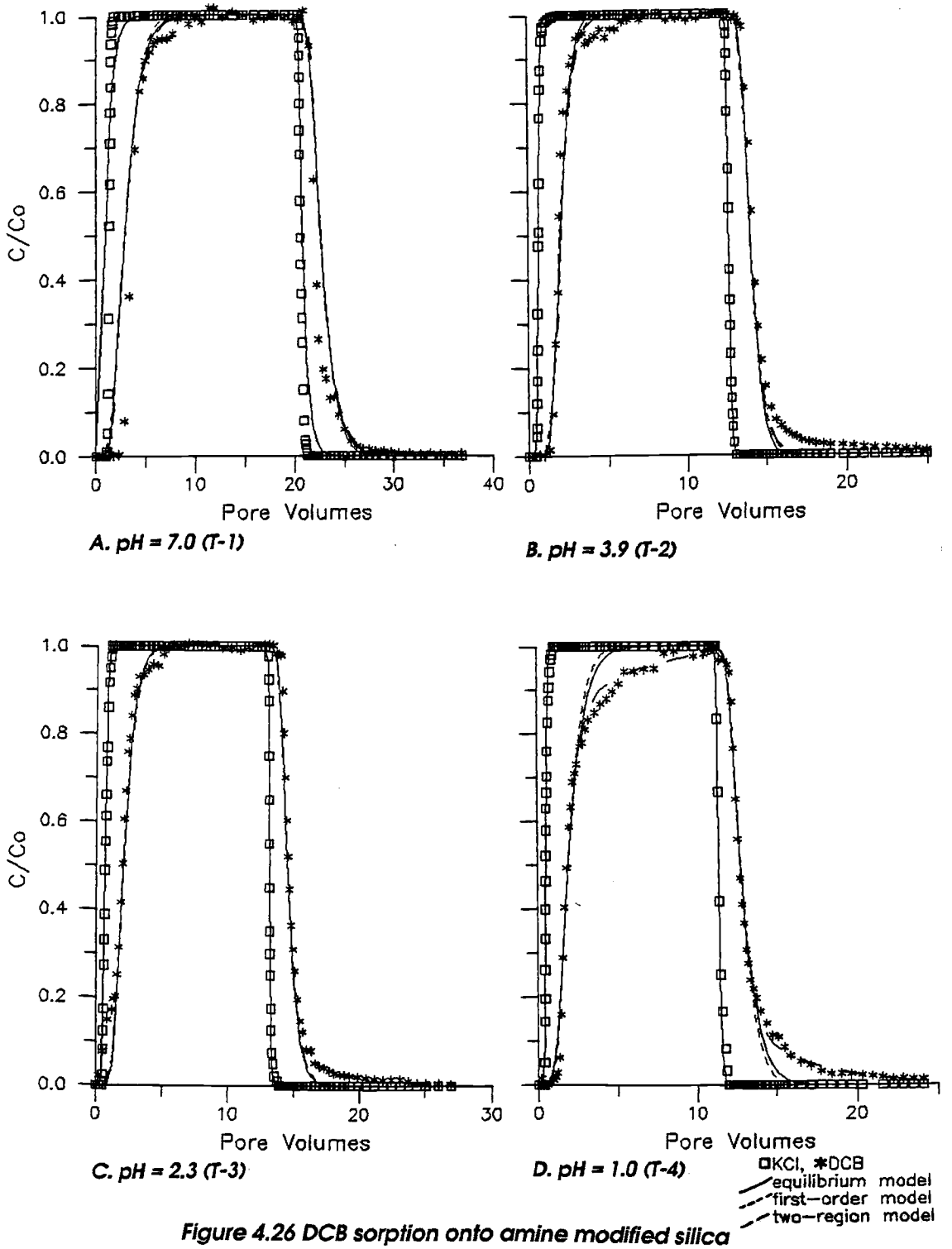

Figure 4.26 DCB sorption onto amine modified silica

The equilibrium model, however, did not fit all the tailing in the data for the lower pH values. The first-order model fits to data indicated that ω decreased at lower pH, indicating increasing nonequilibrium sorption. The two-region model fit to experiment T-4 (Figure 4.26D) fit the tailing, and does indicate a small α_e value.

CHAPTER 5
DISCUSSION

5.1 Sorption on Mineral Surfaces

5.1.1 Sorption Energy

The energy that causes the hydrophobic solutes used in this research to sorb to organic surfaces is primarily due to the solvent effect and less to the interaction with the surface. Sorption of hydrophobic solutes to mineral surfaces may have a smaller interaction energy. The solvent effect results from the energy changes caused by solute molecule removal from aqueous solution. Van der Waals interactions between hydrophobic solutes and the mineral surface are small, on the order of 0.01 - 1.0 kcal mol^{-1} [*Blevins, 1982*], whereas the solvent effect energy is on the order of 0.1 to 5 kcal mol^{-1} (Table 2.2). The partitioning due to the solvent effect is directly proportional to the solute-molecule hydrophobic surface area, which is proportional to the solute molecular weight for the chlorinated-benzene series studied. For example, *Yalkowsky* [*1979*] presented a relationship between hydrophobic surface area and solubility for halogenated benzenes (equation 13). As the solubility is related to K_{ow}, and since the sorption is mainly an entropy effect, then a relationship between K_{ow} and K_p should also hold for partitioning to mineral surfaces as well as to an organic phase. Considering only chlorinated benzenes, one finds:

$$\log K_p = 0.441 \log K_{ow} - 1.09 \quad (r^2 = 0.946, n = 7) \tag{78}$$

which is shown in Figure 5.1B. This is similar to the relationship found by *Karickhoff* [*1984*], shown as equation (4) of Chapter 1. Therefore, a high correlation between K_p and molecular weight is also consistent with the hypothesis that the solvent effect is the main driving force of the sorption process.

Since the surface area of the chlorinated benzenes is linearly related to molecular weight (Table 3.4), then there should be a correlation between solute molecular weight and K_p. Considering all chlorinated compounds (Table 5.1), there is a fair correlation

Table 5.1 Sorption of hydrophobic organic solutes onto mineral surfaces [a]

Solute		Sorbent[b]		K_p	K_p	k_b	t	exp.
	C_0 (ppb)	type	name	($cm^3\ g^{-1}$)	($cm^3/100\ m^2$)	(s^{-1})	(hr)	type[c]
DCA	217.	silica	J	3.16	49.6	---	<1	b1
DCP	185.	silica	J	0.46	7.24	---	<0.5	b1
TCA	212.	silica	J	0.78	12.3	---	<1	b1
TCE	210.	silica	J	0.60	9.45	---	<2	b1
TCE	187.	silica	AC	3.17	8.16	---	<1	b1
TCE	176.	silica	K	13.4	4.28	---	<2	b1
TCE	176.	alumina	AD	3.59	3.94	---	<20	b1
PCE	192.	silica	J	2.65	41.7	---	<2	b1
NT[d]	1000	silica	I	4.78	2.36	---	<0.2	b1
NT	1000	silica	W	9.86	2.45	---	<0.2	b1
NT	1000	silica	AV	1.62	1.92	---	<0.5	b1
NT	1000	silica	AR	2830	572.	---	<2	b1
NT	1000	silica	P	5.67	2.29	---	<0.5	b1
1,4-DCB	6000	silica	AE	3.86	238	---	<10	b1
1,4-DCB	810.	silica	AE	2.74	169	---	<5	b1
1,4-DCB	198-674	silica	I	4.05	2.00	0.024	---	c4
1,4-DCB	390	silica	V	2.17	0.497	0.013	---	c1
1,4-DCB	1380	alumina	Y	0.346	0.110	270	---	c1
1,4-DCB	574-1300	alumina	Z	0.339	0.278	0.055	---	c2
1,2,4-TCB	148-468	silica	V	7.90	1.81	0.15	---	c2
1,2,4-TCB	223	alumina	Y	1.00	0.318	---	---	c1
1,2,4-TCB	200	alumina	Z	0.95	0.718	---	---	c1
1,2,4,5-TeCB	187-235	silica	V	12.3	2.82	.049	---	c2
1,2,4,5-TeCB	216	alumina	Y	7.34	2.33	---	---	c1
1,2,4,5-TeCB	176	alumina	Z	4.37	3.58	---	---	c1
PCB	118	silica	P	25.8	10.4	---	---	b1

[a] Data compiled from Tables 4.1, 4.2, and 4.4.

[b] Sorbent properties are found in Table 3.1.

[c] b = batch, c = column, n = number of experiments.

[d] NT = *p*-nitrotoluene

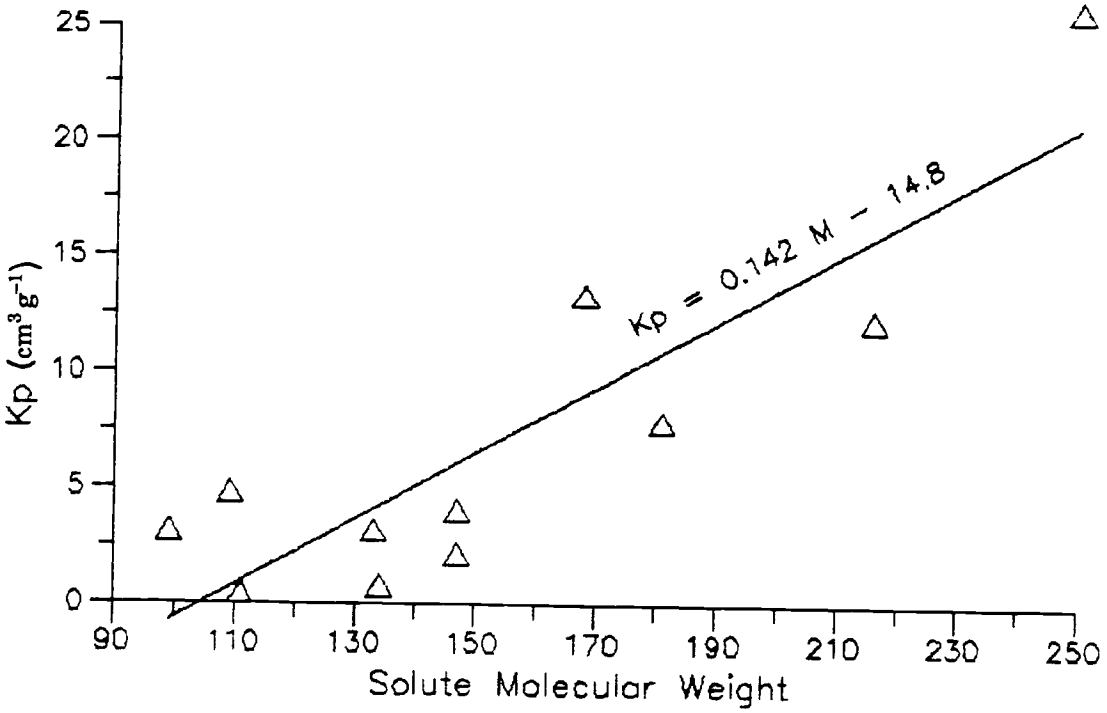

A. Effect of solute molecular weight on K_p (from Table 5.1) for sorption of chlorinated solutes onto porous silica only

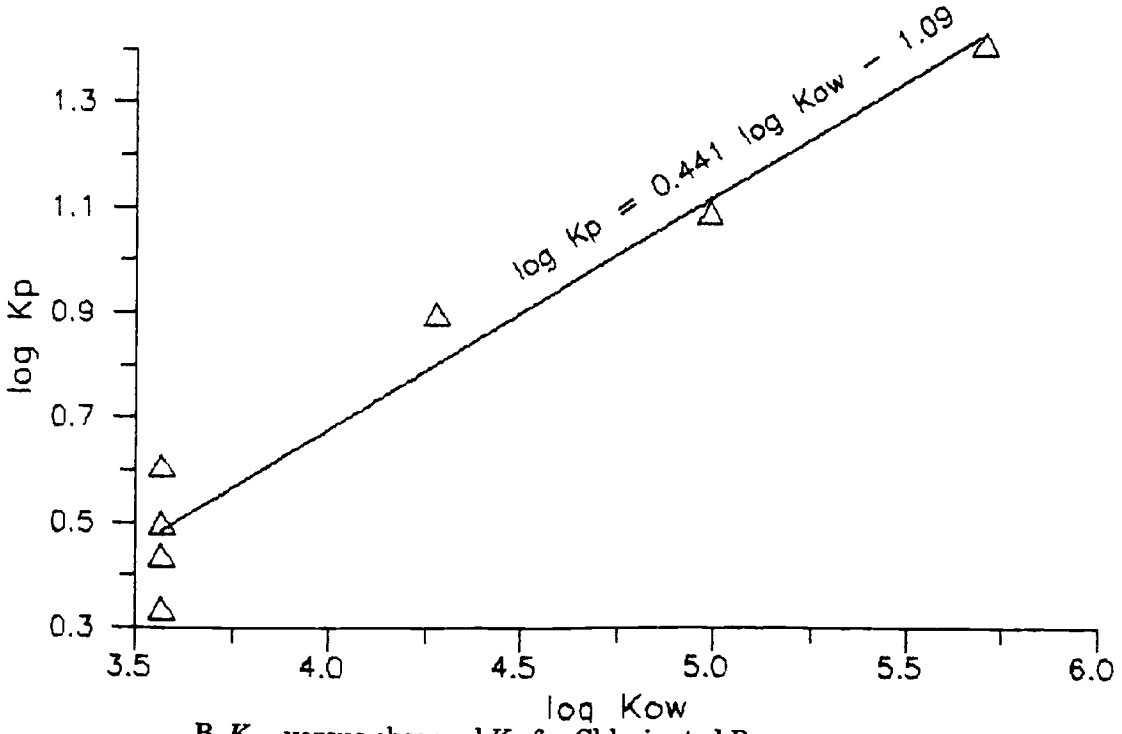

B. K_{ow} versus observed K_p for Chlorinated Benzenes

Figure 5.1 Sorption onto silica - the solvent effect

between solute molecular weight and K_p for porous silica surfaces (Figure 5.1A):

$$K_p = 0.142M - 14.8 \quad (r^2 = 0.771,\ n = 11) \tag{79}$$

where M is the solute molecular weight. These relationships imply that a reasonable estimate of chlorinated benzene sorption onto silica can be obtained with only knowledge of solute properties.

Because the surface areas of sorbents vary, K_p is expressed per unit surface area rather than percent mass for the different surfaces in Table 5.1. K_p ($cm^3/100\ m^2$) is plotted against solute molecular weight in Figure 5.2 (chlorinated benzenes only). A more regular increase in K_p is observed in Figure 5.2 than in Figure 5.1A, where the difference in the sorbent surface area was not taken into account. As molecular weight increases, there is an increase in sorption onto the silica and alumina, as described by the equations on Figure 5.2. Sorption onto silica is up to an order of magnitude greater than onto alumina, consistent with the findings of others.

Schwarzenbach and Westall [1981] show that sorption onto porous silica is observed to average 50 percent greater than onto porous alumina, and sorption onto kaolinite is an order of magnitude greater than onto silica. Kaolinite has a pH_{iep} of 4.6 [*Stumm and Morgan, 1981*], so at neutral pH, it may have less surface charge than silica or alumina. As more neutral surfaces have weaker bonding with water, there is less energy to displace water molecules, and consequently sorption is energetically more favorable. In addition, the weak attractions of hydrophobic molecules to uncharged surfaces are stronger than with charged surfaces. The difference in sorption between silica, alumina, and kaolinite indicates the surface interaction also plays a role in the overall sorption energy.

The effect of solute/surface interactions is seen in a correlation between K_p and sorbent surface area. The K_p for DCB decreased 46 percent with a two-fold increase in silica surface area (surfaces I versus V of Table 5.1), but did not change with a three-fold increase in alumina surface area (surfaces Y versus Z of Table 5.1). The K_p for TCB

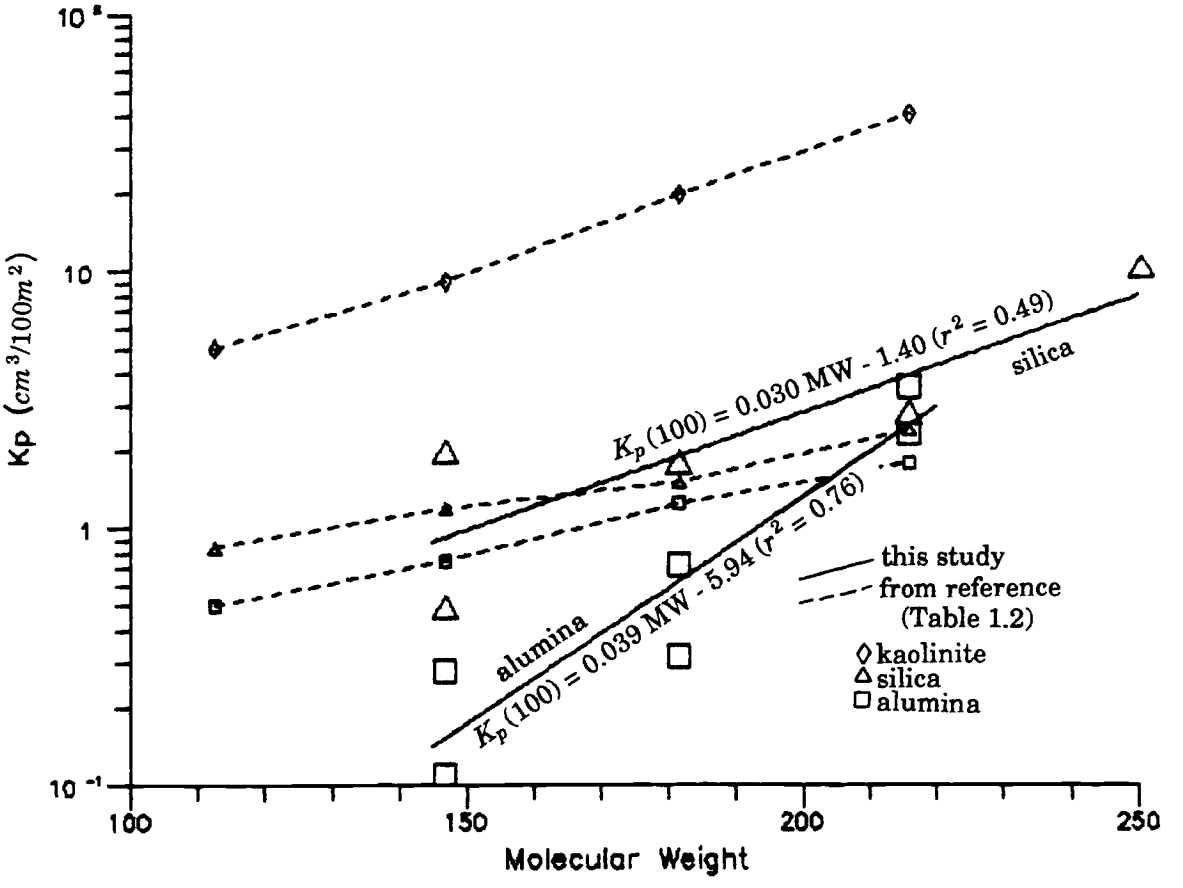

Figure 5.2 Chlorinated benzene sorption onto mineral surfaces

increased 5 percent with a three-fold increase in alumina surface area, and the K_p for TeCB increased 70 percent with a three-fold increase in alumina surface area (surfaces Y versus Z). The K_p for nitrotoluene did not change for a two-fold increase in silica surface area (surfaces P and I of Table 5.1). This lack of correlation between K_p and surface area indicates that the solute-surface forces are less important than the solvent effect. Other researchers have noted a weak correlation between surface area and K_p (equation 5) [*McCarthy et al., 1981*].

5.1.2 Sorption Rate

Sorption on unbonded surfaces is relatively fast; the first-order desorption rate coefficient (k_b) from column experiments (Table 4.4) for DCB release from silica averaged 0.024 s^{-1} for the 100-μm surface and 0.013 s^{-1} for the 425-μm surface. The corresponding first-order k_f's (calculated with k_b and K_p) for DCB are 0.041 s^{-1} for the 100-μm surface, and 0.012 s^{-1} for the 425-μm surface. The k_b's for TCB and TeCB were 0.15 s^{-1} and 0.049 s^{-1}, respectively. The respective k_f's were 0.50 s^{-1} and 0.25 s^{-1}. These correspond to reaction half-lives (equation 12 in Chapter 2) of 2 to 60 seconds.

If the surface reaction is fast, then the sorption and desorption rates should reflect the diffusion time into the porous particles. The time required to reach 50 percent equilibration in 100-μm porous particles is 0.6 seconds (Table 2.6), and is 15 seconds for 500-μm particles. The observed time scale for DCB is longer than predicted, but about equal to the predicted value for TCB and TeCB. The slow desorption rate for DCB could reflect either a slow chemical sorption step (unlikely for mineral surfaces), or smaller tortuosities than are used in calculating diffusion equilibration times (Table 2.6). The diffusion time through immobile pore fluid (Table 2.7) is expected to be smaller for DCB, but the data are inconclusive due to the considerable scatter.

Tortuosity can be calculated using equation (40) of Chapter 2, and observed dispersion for the solute and conservative tracer. With the simplification that R_{mobile} equals

$R_{immobile}$, equation (40) reduces to:

$$D_{total} = \phi D_{mobile} + \frac{(1-\phi) r^2 v^2}{15 \tau D_o} \tag{80}$$

where D_{total} is the total spreading observed in the system (estimated with the equilibrium model), D_{mobile} is the expected hydrodynamic dispersion for the DCB solute molecule ($1.5D_{KCl}$), ϕ is θ_e/θ, r is the particle radius, and τ is tortuosity. The second term on the right-hand side of equation (80) is for intraparticle diffusion.

Tortuosity is calculated to be 0.02 for the 100-μm particles (experiment I-1), and 0.16 for the 425-μm particles (experiment I-2). These are an order of magnitude smaller than aggregate-particle tortuosities of 0.4 to 0.9 that are observed by others [*Rose, 1977*]. Smaller tortuosities are observed when the pore dimensions are on the same order of magnitude of dimension as the solute molecules. However, 99 percent of the pores are greater than 20 nm in size and the smallest pores of the porous silicas used are 6 nm (Figure 3.2), versus the chlorinated benzene maximum dimension of 1.1 nm (Table 3.4).

5.2 Sorption on Organic-Modified Surfaces

The average first-order desorption rates for organic-modified silicas vary over four orders of magnitude from 0.1 s^{-1} for C_8 modified silica to 10^{-5} s^{-1} for phenyl-polymer-modified silica (Table 5.2). The most likely causes of slow sorption are illustrated in Figure 1.1. Intraparticle diffusion can be quantified by the two-region model rate coefficient (α_e), diffusion through a bound organic layer by the first-order model rate coefficient (α_i, or $\rho_b \; k_b$), and the binding step by the first-order model desorption rate (k_b). The two-region model $\alpha_e/\rho_b K_p$ is dimensionally equivalent to k_b (equation 54).

Table 5.2 Sorption rates on organic modified surfaces

Solute	Sorbent [1] type	dia.(μm)	N	K_p ($cm^3 g^{-1}$)	K_{oc} ($cm^3 g^{-1}$)	D_{solute}/D_{KCl}	k_f (s^{-1})	k_b (s^{-1})	half-life (min)	α_e (s^{-1})
CB	Ø-poly (E)	100	2	7.95	580	29.8	0.0067	0.0020	5.8	0.002
DCB	C_1-poly (A)	100	4	326	22800	4.80	0.097	0.00071	28	0.003
	C_1-poly (O)	2	1	92.5	6510	3.21	0.0089	0.00023	50	0.007
	C_1-poly (AI)	2	1	53.1	23700	9.04	0.019	0.00085	14	0.004
	C_8-poly (B)	100	7	25.9	3800	1.51	0.92	0.085	0.14	0.002
	C_{18}-poly (C)	100	3	23.0	2200	3.97	0.063	0.0065	1.8	0.008
DCB	Ø-mono (D)	100	4	4.1	2560	1.30	0.021	0.012	0.011	0.0001
	Ø-mono (Q)	100	2	5.2	693	1.30	2.6	1.2	0.012	0.50
DCB	Ø-poly (U)	2	2	6.87	1560	142	0.00020	0.000070	64	0.00045
	Ø-poly (F)	20	5	47.9	4320	36.5	0.013	0.00067	17	0.0043
	Ø-poly (G)	20	3	23.0	2270	40.1	0.015	0.0016	7.2	0.0029
	Ø-poly (E)	100	5	60.6	4420	32.0	0.0096	0.00038	30	0.0034
	Ø-poly (H)	425	3	22.2	2100	33.6	0.010	0.0011	11	0.0015
DCB	Ø + C_{18} (X)	100	2	30.0	6820	18.5	0.018	0.0022	5.3	0.0029
	Alcohol (R)	100	3	3.33	114	0.964	0.28	0.20	0.058	0.41
	Amine (T)	100	4	3.58	442	0.970	0.16	0.11	0.11	0.050
TCB	Ø-poly (E)	100	5	135.3	9880	54.1	0.040	0.00070	16	0.012
TeCB	Ø-poly (E)	100	3	396.9	28970	63.5	0.083	0.00050	23	0.017
PCB	Ø-poly (E)	100	2	968	70660	11.0	0.12	0.00030	38	0.042

[1] Sorbent properties found in Table 3.1.

data compiled from Tables 4.5, 4.6, 4.7, 4.12, and 4.13.

5.2.1. Diffusion through Immobile Pore Fluid

Slow rearrangement of molecules in space can be due to long diffusional paths, constricted diffusional channels in a solid matrix, or diffusion through a dense or highly viscous material. Diffusion through immobile fluid for organic-modified porous silicas should be the same as for unmodified silica of the same size.

Porous silica modified with an organic silane may have more constricted internal pore space, as the silane may polymerize across some small pore channels. Therefore, diffusion through modified porous particles may be different from that of unbonded silica. Diffusion through aqueous internal fluid in organic-modified silica is examined by considering both the effect of particle size and pore size.

The desorption rate on the C_1 polymer bound to 100-μm porous silica (k_b = 7 x 10^{-4} s^{-1}) was similar to that on C_1-modified 2-μm solid silica (k_b = 5 x 10^{-4} s^{-1}). This suggests that the slow sorption is not caused by diffusion through immobile pore fluid, but is a function of the nature of the bound C_1 organic.

The effect of particle size can also be seen by comparing the 425-μm (surface H; Figure 4.24A and B) and 20-μm phenyl-modified porous silica (surface F; Figure 4.22A and B). The average k_b's for the larger particle were 40 percent faster than for the smaller particle. For the two-region model fits, α_e was 1.8 times smaller for the larger versus smaller particle, however.

Phenyl modified surfaces E (100 μm; Figure 4.13A and B) and G (20 μm; Figure 4.23A and B) also differed only by particle size (same pore diameter). In this case, both the first-order and two-region model rate coefficients were smaller for the larger particle. Therefore, there is some effect of particle size on the sorption rate due to intraparticle diffusion that cannot be discounted. However, most of the observed slow sorption is apparently due to the nature of the bound organic layer; since phenyl-polymer bound surfaces had rates four orders of magnitude slower that C_8 bound to the same particle (100 μm).

Two of the 20-μm particles modified with a phenyl polymer differ only in the average pore size (11 versus 27.5 nm). Desorption tailing was greater for the smaller (surface G; Figure 4.23A and B) compared to the larger pore-size particle (surface F; Figure 4.22A and B). Both the first-order and two-region model rate coefficients were about 60 percent greater for the larger pore-size particles. This suggests that tortuosity (by changing the pore size) has some effect on the sorption rate. However, similar to a change in particle size, most of the slow sorption is still caused by the nature of the bonded phase, since there is a four-order-of-magnitude difference in sorption rate for different organic-bound porous silicas.

The phenyl polymer bound to a solid silica surface (surface U) had a desorption rate (2×10^{-4} s^{-1}) slower than the 100-μm (4×10^{-4} s^{-1}) or 425-μm phenyl polymer bound surface (7×10^{-4} s^{-1}), further indicating slow sorption is predominantly caused by the nature of the bound organic layer and not by diffusion through immobile pore fluid.

Interpretation of the DCB sorption data in terms of the equilibrium model gave large values of total dispersion, which can be interpreted as due to slow intraaggregate mass transfer. Tortuosity was is calculated using equation (80) for the various organic-modified sorbents, as shown in Table 5.3. Surfaces that exhibited the fastest sorption (C_8, C_{18}, and Diol) had the largest tortuosities (0.16, 0.013, and 0.02); these are still somewhat smaller that the 0.66 average reported by others [*Rose, 1977*]. In chromatography, the combined intraparticle effects of tortuous and constricted flow paths reduce the molecular diffusion coefficient to a value of 0.4 to 0.9 times that of the bulk-phase value. A similar reduction is expected for diffusion within reasonable open particles [*Giddings, 1965*].

The phenyl-polymer-modified 100- and 20-μm particles had significantly smaller calculated tortuosities (4 to 10 times) than aliphatic chain modified particles. It is unlikely that the phenyl polymer could clog more pore space than aliphatic polymers, since its molecular dimensions are smaller than most aliphatic silanes. In addition, since the calculated values of tortuosity are three orders of magnitude smaller than

Table 5.3 Calculated tortuosity

Particle Size	Modifier	Calculated Tortuosity*	N
100 µm, 27 nm pore	C_1	0.0041	2
	C_8	0.16	3
	C_{18}	0.013	3
	Ø-mono	0.024	6
20 µm, 10 nm pore	Ø-poly	0.00051	5
20 µm, 27 nm pore	Ø-poly	0.00047	3
100 µm, 27 nm pore	Ø-poly	0.00033	4
425 µm, 11 nm pore	Ø-poly	0.062	3
100 µm, 27 nm pore	C_{18}+Ø-poly	0.0010	2
	Dialcoholic	0.020	3
	Amine	0.0028	4

*Calculated tortuosity (equation 90) assumes all observed slow sorption is caused by diffusion through immobile pore space.

those reported by others, it is unlikely that diffusion through the porous particles is causing the observed slow sorption.

The phenyl-polymer-modified 425-μm particle had a tortuosity of 0.06. This value is more reasonable compared to values obtained on smaller particles, due to the larger particle radius used in equation (80). The diffusion time into a particle of this size (Table 2.5) is on the order of 36 seconds, compared to 2 seconds for 100-μm or smaller particles.

In summary, diffusion through immobile pore water did not cause most of the observed slow sorption rate for 425-μm and smaller particles used in this research. It did, however, have some effect on the sorption rate, as some of the larger or more tortuous particles had smaller rate coefficients, and thus had longer times to reach sorption equilibrium.

5.2.2 Diffusion through the Bound Organic

Sorption of 1,4-DCB onto several phenyl-polymer modified silicas is slower than onto the C_{18} or unbonded silica, suggesting that the nature of the surface phase is important. The phenyl-monomer silica did not produce any slow kinetic effects, suggesting that the polymerization is important. The C_{18}-polymer silica has as high an organic content as the phenyl polymer, but did not show any kinetic effects. This further implies that pore clogging (expected for both the C_{18} polymer and phenyl polymer) by itself is not causing slow sorption, but the rate is controlled by the nature of the bound organic phase.

Diffusion through the bound organic layer is characterized by α_i (equivalent to $\rho_b k_b$) obtained from a first-order model fit of the data. Aliphatic chain-modified silicas (C_1, C_8, and C_{18}) differ only in the thickness of the organic layer; the same organic sorption sites are present, and they are all bound to 100-μm porous particles. The thickness of the bound organic layer varies from 0.5 nm for C_1, 1.6 nm for C_8, and to 2.5 nm for C_{18}. Thickness should affect the diffusion path length, so longer chain-modified

surfaces should exhibit slower sorption.

This, in fact, is not the case (Table 5.2); the C_1-modified surface exhibits the slowest rate (6×10^{-4} s^{-1}), at least an order of magnitude slower then that for C_8 or C_{18}-modified silica. The C_1 surface also exhibits stronger retention (10-fold), so the sorption mechanism is apparently not the same as the other aliphatic chain-modified silica. Aliphatic chains with less than four methyl groups are rigidly bound to surfaces [*El-Hassan et al., 1986*]. The rigidity leads to more limited access by solute molecules [*Beaufils et al., 1985*], which may cause slow sorption.

Both the C_8- and C_{18}-modified silicas exhibit similar retention (K_p or K_{oc}), but there is a difference in the sorption rate. The C_{18} surface (Table 5.2) has an average desorption rate about 10-fold slower than the C_8, suggesting an increase due to diffusion path length; however, an unambiguous interpretation is not possible as variation in data is considerable. *Beaufils* [*1985*] suggest that bond rotation and motion of long aliphatic chains in aqueous solution should lead to faster equilibration times for C_{18} versus shorter aliphatic chains bound on surfaces, which is contrary to the observed slower sorption onto the C_{18} surface.

The chlorinated benzenes used in this research are disk-like molecules with a thickness of 0.35 nm, and diameter of 0.8 to 1.1 nm (Table 3.4). The thickness of the bound aliphatic surfaces therefore represents less than three molecular layers to diffuse through, so describing the rate-limiting step as diffusion through the bound organic layer to the surface is not appropriate. When the scale of observation is large compared to individual surface forces, forces can be averaged into a monocontinuum of resistance with a diffusion model. This is not the case here where diffusion distance is only several molecular layers. At this scale, the slow approach to equilibrium is more correctly described as a binding-step limitation.

The thickness of the bound phenyl-polymer is 1.8 nm, and also represents less than two molecular layers in thickness, suggesting that diffusion through the bound

organic layer is not an appropriate model for the observed slow sorption. Binding a phenyl monomer versus phenyl polymer should have the effect of changing only the density of phenyl groups on the surface, as illustrated in Figure 5.3. The polymerization produces phenyl groups tightly packed on the surface, whereas the monomer bound to a surface has variable distance between phenyl groups.

If sorption is the attraction between pi electrons in the chlorinated benzene and the surface benzene ring, then this binding energy should be the same for the two surfaces. The only difference between the two surfaces should be the diffusion through the organic layer. The phenyl polymer covers about 50 percent more surface area and the fraction carbon on the surface is twice as great compared to the monomer (Figure 5.3). The K_{oc} is four times greater for the polymer than the monomer, indicating a stronger binding energy. What can be concluded from the results summarized on Figure 5.3 is that the close phenyl spacing provides for increased sorption energy and slow sorption, as suggested previously by *Jinno [1985]*.

To further distinguish slow diffusion from binding, a surface was prepared with both a C_{18} polymer and a phenyl polymer. If the sorption rate is controlled by diffusion through the bound organic layer, then the rate may decrease since the organic layer is thicker compared to a pure phenyl modified surface. If the sorption rate is controlled by the binding step, then sorption should proceed with a fast reaction (C_{18} portion) in parallel with a slow reaction (phenyl portion), and the two region model can be used to estimate the overall sorption rate (Section 2.2.5.2). The sorption rate on this surface (Table 5.2) is about 4.7 times faster than on the phenyl-polymer surface, which does not confirm either hypothesis. The rate is consistent with the hypothesis that closely-spaced phenyl groups are the cause of the slow sorption, since probably fewer phenyl groups are closely spaced on this surface.

Diffusion of molecules through organic material in subsurface media will be retarded relative to that in water due to the non-liquid nature of organic phases. Diffusion behavior in natural organic phases is expected to bear some resemblance to

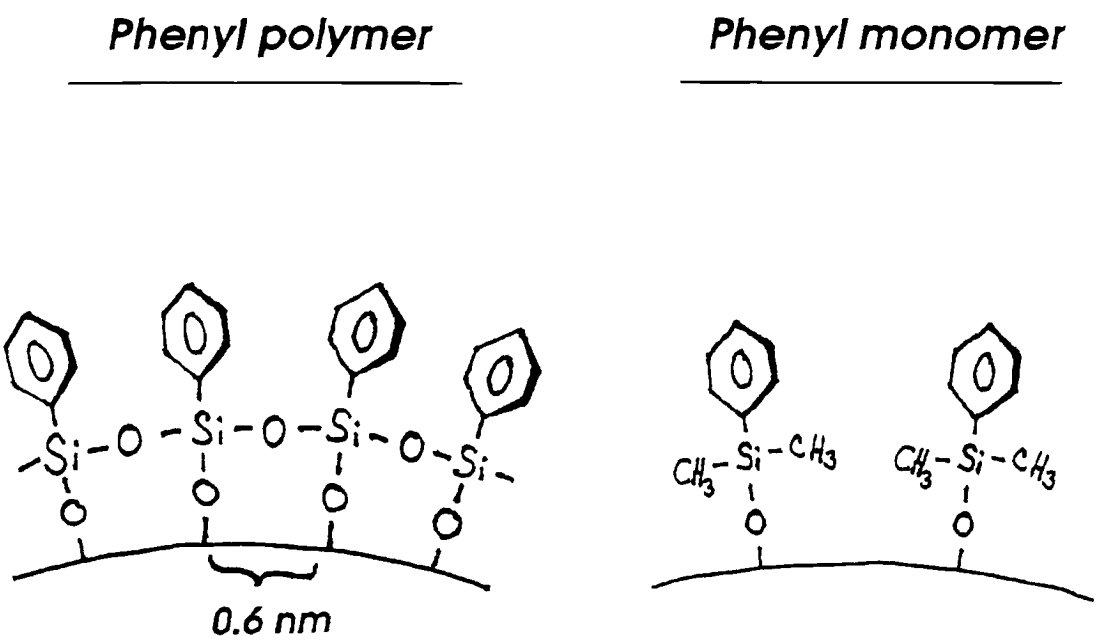

5.1%	surface area coverage	3.3%
0.0137	f_{oc}	0.0075
1700	K_{oc}	400
0.00006	k_b	0.02

Figure 5.3 Effect of polymerization of the bound organic on the sorption of DCB
(data from Tables 4.6 and 4.7)

diffusion through membranes and in polymers. The lag time (t_l) for passage of a diffusing molecule through a homogeneous membrane is [*Barrer, 1939*]:

$$t_1 = \frac{h_m^2}{6\,D_m} \tag{81}$$

where h_m and D_m are the membrane thickness and diffusivity, respectively.

The relative diffusion coefficients for 1,4-DCB in the bound-organic phase are assumed to be 200-1000 times slower then diffusion in water [*Barrer, 1939*] (Table 3.4), giving an estimated D_m of 0.8-4.0 x 10^{-9} $cm^2\,s^{-1}$. The lag time is assumed to be equal to the reaction half-life, which is calculated from the first-order model k_b (Table 5.4) with equation (12). The lag time varied from 0.05 minutes for dialcoholic-modified surface to 30 minutes for the phenyl-modified surface. The organic layer thicknesses calculated from (71) then varied from 10^3 to 10^5 nm, or 3 to 5 orders of magnitude larger than the actual thickness. This further indicates that diffusion through the bound organic layer could not cause most of the observed slow sorption.

The Wilke-Chang equation (39) includes the effect of increasing molar volume (proportional to molecular weight) and temperature on the molecular diffusion coefficient. The change in the sorption rate over the series of chlorinated benzenes studied (Table 4.9) can be compared to the expected decrease of 25 percent from the Wilke-Chang equation. A plot of the bound organic rate coefficient (α_i) versus molecular weight of the chlorinated benzene (Figure 5.4) shows a decrease averaging 92 percent from chlorobenzene to pentachlorobenzene. This poor correlation suggests that diffusion through the bound organic layer is not the rate-limiting step in the sorption process. Although α_i is not dimensionally equivalent to diffusion coefficient, they are directly proportional; i.e., they differ by a length scale.

The change in the sorption rate of chlorinated benzenes at different temperatures can be compared to the expected increase in diffusion rate through the bound organic layer. The Wilke-Chang equation predicts a 16 percent increase in diffusion rate over a

Table 5.4 Calculated bound organic layer thickness

Sorbent Modifier[1]	Thickness (nm)	Reaction half-life (min)	Calculated Thickness[2] (nm)
C_1	0.5	18.3	$2.3 - 5.1 \times 10^4$
C_8	1.6	0.178	$2.3 - 5.1 \times 10^3$
C_{18}	2.5	1.78	$0.7 - 1.6 \times 10^4$
Phenyl	1.8	30.4	$3.0 - 6.6 \times 10^4$
C_{18}+Phenyl	2.5	5.25	$1.2 - 2.8 \times 10^4$
Dialcoholic	1.5	0.058	$1.3 - 2.9 \times 10^3$
Amine	0.8	0.105	$1.7 - 3.9 \times 10^3$

[1]On 100 μm porous silica

[2]Calculated with equation (31)

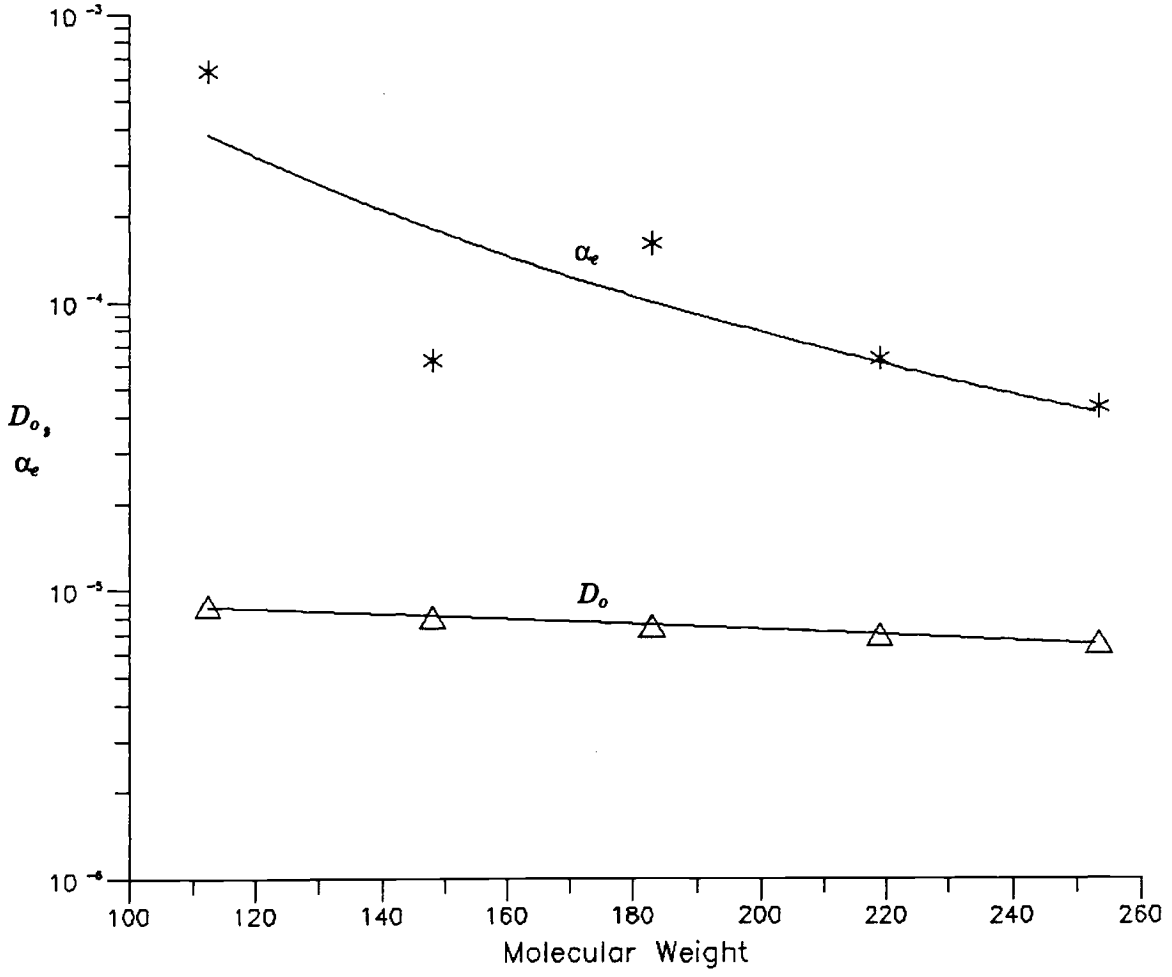

Figure 5.4 Diffusion rate through the bound organic

45°C temperature increase, which applies to any compound. The change in α_i is shown in Figure 4.20B, and shows an average increase of 31 percent for DCB, a decrease of 33 percent for TCB, and a 5 percent increase for TeCB. This also suggests that diffusion through the bound organic layer is not the rate-limiting step.

5.2.3 Chemical Binding and Release Step

Desorption rates for organic-modified surfaces from column experiments (Table 5.2) ranged from 2 x 10^{-4} to 1.0 s^{-1}, where C_1 and phenyl-modified surfaces exhibited the slowest rates (2 x 10^{-4} to 10^{-3} s^{-1}). Rates on phenyl-modified surfaces are consistent with batch experiments. The slow approach to equilibrium appears to be related to the nature of the surface phase, as equilibration times were 5 to 100 times greater than those with aliphatic surfaces. Diffusion through immobile pore fluid makes only a small contribution to the observed slow sorption.

Sorption or desorption that exhibits a chemical-kinetic limitation is expected in cases of strong chemical binding rather than in cases of non-specific sorption or hydrophobic partitioning. Slow chemical changes typically arise due to the presence of an activation barriers. Strong binding is expected to result in slow breakup of a complex. Sorption may still be fast, exhibiting diffusion control. The C_1-modified surface does, in fact, exhibit significantly stronger sorption (about 10-fold) compared to other hydrophobic organic-modified surfaces. The sorption rates on the C_1-modified solid silica were the same as on a C_1-modified porous-silica, indicating that the nature of the bound C_1 polymer is causing the slow sorption. The phenyl-modified surfaces have about the same K_{oc} values (Table 5.2) as C_8 or C_{18}-modified surfaces.

Slow chemical sorption can also be caused by steric hindrance reaching the binding site. Adjacent surface groups on the phenyl-polymer surface are approximately 0.6 nm apart (Figure 5.5), and solute molecules bind to this surface with an optimum distance of 0.3 nm [*Miller et al., 1985*]. This sorption site therefore requires a specific orientation of the planar solute molecule, which could cause the slow approach to equilibrium. The

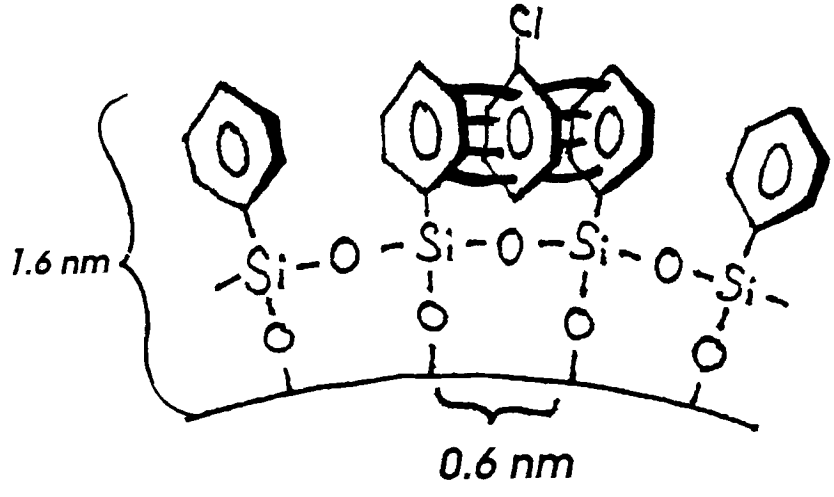

Multiple pi-pi electron interactions

Optimum binding distance – 0.3 nm

Figure 5.5 Proposed binding site on the phenyl polymer surface

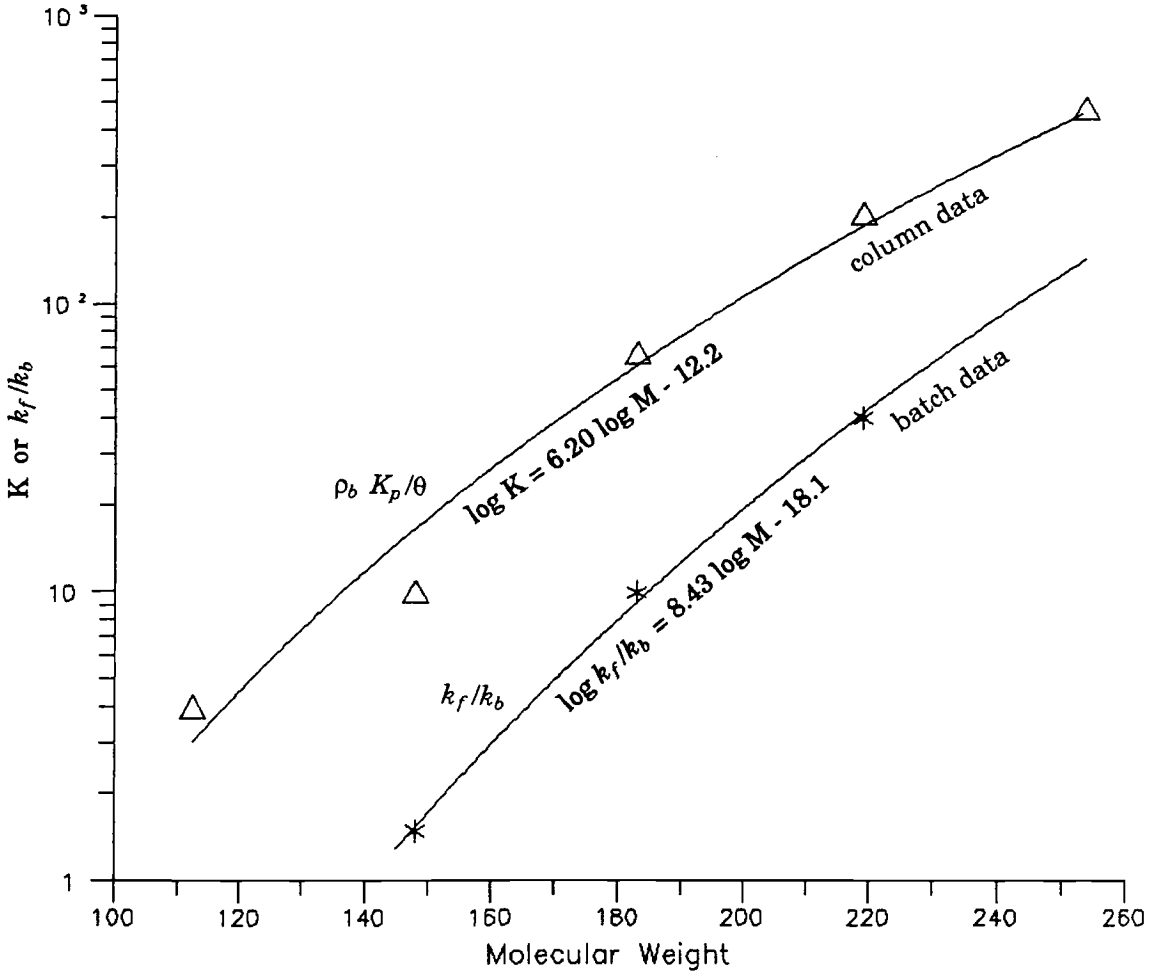

Figure 5.6 Binding step - rate data

increased binding energy of the phenyl-polymer compared to the phenyl-monomer surface probably results from pi-pi electron interaction on both sides of the sorbing aromatic compound [*Jinno et al., 1985*].

Calculation of an equilibrium constant (K) from batch data as the ratio of forward to reverse reaction rates (equation 9) shows a 27-fold increase going from DCB to TeCB (Figure 5.6) versus a 20-fold increase for the same series from column data. Similar slopes of K and k_f/k_b indicate that the data are consistent with a chemical rate-limiting sorption step. The difference in actual values of $K_p \rho_b/\theta$ and k_f/k_b results from use of different phenyl surfaces (different f_{oc}) in batch and column experiments. The difference between these two curves is reduced by accounting for this 30 percent difference in bound carbon mass.

Published rates of sorption onto organic-modified surfaces were not found, but some literature exists for sorption onto natural soils. *Schwarzenbach and Westall* [*1981*] reported that sorption was noticeably slow in column experiments at velocities greater than 0.01 cm s^{-1} (residence time of 48 minutes), but did not determine actual rates. Using a first-order-model ratio of residence time to reaction half-life (equation 12), a k_b calculated from their data should be less than 10^{-3} s^{-1} in order to have noticeable kinetic effects.

Wu and Gschwend [*1986*] interpreted the kinetics of sorption in terms of the diffusion rate through aggregate particles. Even though diffusion was rate limiting, reaction half lives (and k_b values) can be obtained from their graphs (in Table 1.1), for comparison to k_b values obtained in this study. The value for DCB was 10^{-2} s^{-1}, compared to 10^{-4} to 1.0 s^{-1} determined for various surfaces in this study. Their sorption data corresponds most closely to that observed on the C_{18} polymer-modified silica (surface C) with a rate of 7 x 10^{-3} s^{-1}. *Oliver* [*1985*] reports a sorption rate of 8 x 10^{-7} s^{-1} of DCB onto natural soil, about 2.5 orders of magnitude slower than even the phenyl-modified surfaces.

The desorption rate coefficient of TCB on natural soil [*Wu and Gschwend, 1986*] was calculated to be 6 x 10^{-3} s^{-1}, or an order of magnitude faster than that observed on the phenyl-modified surface in this study. The TeCB desorption rate coefficient on natural soil was 2 x 10^{-3} s^{-1} [*Wu and Gschwend, 1986*], compared to 5 x 10^{-4} s^{-1} estimated on the phenyl surface in this study. Finally, sorption of PCB on natural soil (k_b = 6 x 10^{-4} s^{-1}) [*Wu and Gschwend, 1986*] is also faster than observed on a phenyl-modified surface (k_b = 3 x 10^{-4} s^{-1}).

Desorption rates of chlorinated benzenes on natural soils are generally observed to be faster than on a phenyl surface, whereas DCB sorption onto a C_{18} surface occurs at approximately the same rate as on soil. The rates reported by *Wu and Gschwend [1986]* may be faster than in natural systems as they reported that the gas-stripping apparatus used to measure rates had the effect of breaking the aggregate particles apart, which would affect the diffusion-controlled sorption rate.

5.2.4 Sorption Energy

Partition coefficients for chlorinated benzene sorption on organic-modified surfaces are summarized in Table 5.5. The K_p values for sorption on aliphatic-bonded silica vary from 325 $cm^3 g^{-1}$ for C_1 surfaces to 24 $cm^3 g^{-1}$ for C_8 and C_{18} surfaces; the greater sorption for C_1 surfaces is also reflected in the K_{oc} values. The K_{oc} values for phenyl-polymer surfaces range from 1500 to 4400 $cm^3 g^{-1}$, somewhat higher than for the phenyl-monomer surfaces (K_{oc} was 693 to 2560).

The surface bonded with both the phenyl polymer and the C_{18} polymer had a K_{oc} (6800) higher than either individual organic modified surface. Surfaces modified with alcoholic or amine groups showed 10-fold less sorption due to the more polar nature of the surface, as compared to aliphatic- or phenyl-modified surfaces.

Sorption of DCB on natural soils (Table 1.1) shows considerable variability (K_{oc} = 609 ± 451), but the K_{oc} averaged less than observed on the organic-modified surfaces in

Table 5.5 Sorption energies on organic modified surfaces[a]

Solute		Sorbent			K_p	Reverse	K_{oc}	ΔG^1(surface)	ΔG^2(100% organic)
	C_o (ppb)	modifier[b]	Dia. (μm)	N[c]	(cm^3/g)	K_w/K_{wf}		(Kcal/mol)	(Kcal/mol)
CB	2600-3200	Ø poly (E)	100	2	7.95 ± 5.68	3.60	580	-0.70	-4.05
DCB	76-500	C_1 poly (A)	100	4	326. ± 137.	0.68	22800	-2.89	-5.86
	1160	C_1 poly (O)	2, solid	1	92.48	0.93	6510	-2.93	-5.12
	99	C_1 poly (AI)	2,solid	1	53.12	0.76	23700	-2.56	-5.89
	106-1210	C_8 poly (B)	100	7	25.9 ± 5.39	0.87	3800	-1.39	-4.95
	266-353	C_{18} poly (C)	100	3	23.0 ± 1.61	0.97	2180	-1.32	-4.64
DCB	172-1200	Ø mono (D)	100	4	4.1 ± 1.1	0.84	2560	-0.30	-4.79
	320-480	Ø mono (Q)	100	2	5.2 ± 1.6	0.84	693	-0.44	-4.01
DCB	901-997	Ø poly (U)	2,solid	2	6.87 ± 6.47	2.36	1560	-1.32	-4.63
	400-19,000	Ø poly (F)	20	5	47.9 ± 33.4	0.92	4320	-1.76	-5.24
	42-502	Ø poly (G)	20	3	23.0 ± 6.19	1.04	2270	-1.32	-4.85
	370-1160	Ø poly (E)	100	5	60.6 ± 41.9	0.96	4420	-1.90	-5.25
	380-518	Ø poly (H)	425	3	22.2 ± 4.15	1.01	2100	-1.30	-4.81
DCB	344-365	Ø+C_{18} (X)	100	2	30.0 ± 1.76	1.02	6820	-1.48	-5.42
	163-946	Dialcohoic (R)	100	3	0.994 ± .017	1.25	114	+0.54	-2.60
	525-658	Amine (T)	100	4	3.58 (pH = 7)	0.93	442	-0.22	-3.40
TCB	30-500	Ø poly (E)	100	5	135. ± 64.9	1.26	9880	-2.37	-5.73
TeCB	138-701	Ø poly (E)	100	3	397. ± 204.	1.08	28970	-3.01	-6.36
PCB	277-308	Ø poly (E)	100	2	968 ± 222	0.96	70700	-3.54	-6.89

[a]data compiled from Tables 4.5, 4.6, 4.7, 4.12, and 4.13.

[b]Sorbent properties found in Table 3.1.

[c]Number of experiments.

[d]$\Delta G = -RT \ln (\rho_b K_p/\theta)$

[e]$\Delta G^\circ = -RT \ln (K_p f_c M_{om}/f_{oc} V_{om})$

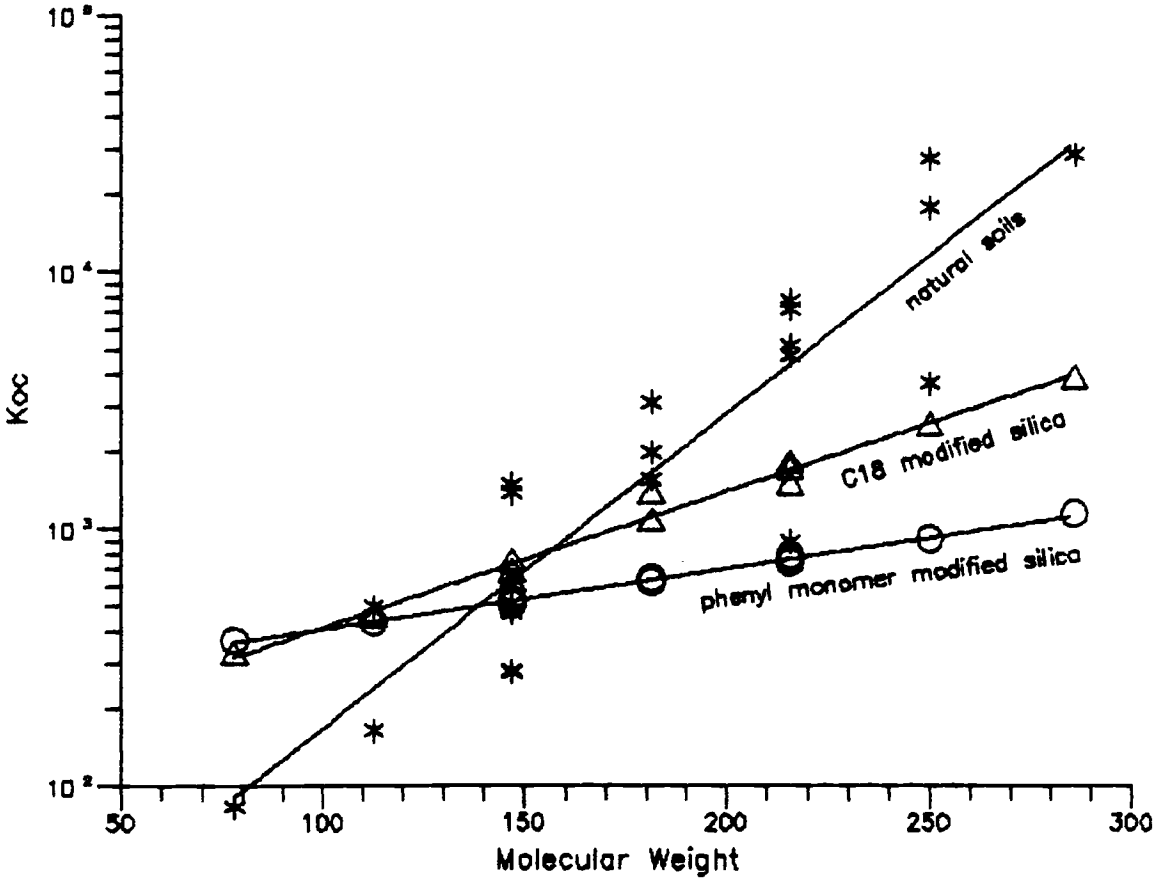

data from reference (Table 1.1)

Figure 5.7 Chlorinated benzene sorption to natural and organic modified surfaces

this study. The K_{oc} values for chlorinated-benzene sorption on natural soils are shown as a function of molecular weight (Figure 5.7). The trend is log-linear, as sorption of PCB and HCB are considerably higher than other compounds in the series. A log-linear trend is expected, since over the series of chlorinated benzenes there is an even, incremental increase in molecule surface area (Table 3.4), which is log-linearly related to K_{oc} (equations 3, 13 and 14).

Also plotted in Figure 5.7 are the K_{oc}'s obtained from literature for sorption onto C_{18} and phenyl-monomer modified surfaces (Table 2.3) for a water-acitonitrile mixture. To facilitate comparison, the K_{oc} values were normalized to the K_{oc} for DCB in natural soil. Values reflect a linear but smaller increase in the sorption energy over the series, compared to natural soils. As the solvent effect is a major portion of the overall sorption energy, and the surface tension in the mixed system is smaller than pure water, a lower slope is expected.

For comparison, K_{oc} values obtained in this study (Table 5.5) are shown in Figure 5.8 together with values from literature (from Figure 5.7). The K_{oc} values for DCB show a decrease in sorption energy C_1, phenyl + C_{18}, phenyl polymer, aliphatic chains, phenyl monomer, amine, and alcoholic. Sorption of DCB onto natural soils is almost an order of magnitude less than most model surfaces, with K_{oc} values similar to the phenyl-monomer and amine surfaces. The retention of aromatic compounds on phenyl surfaces was observed to be 20 percent greater than retention on a C_{18} surface [*Thus et al, 1985*], whereas a difference of 34 percent was observed in this study.

The aliphatic and phenyl surfaces probably exhibit increased sorption compared to soil since they are pure hydrophobic matter with no polar functional groups. Chlorinated benzenes sorb predominantly to hydrophobic organic matter, and do not sorb as much in the presence of polar functional groups.

Retention on alcoholic- and amine-modified surfaces was about half that on hydrophobic modified silica, reflecting the presence of polar functional groups. The dialcoholic

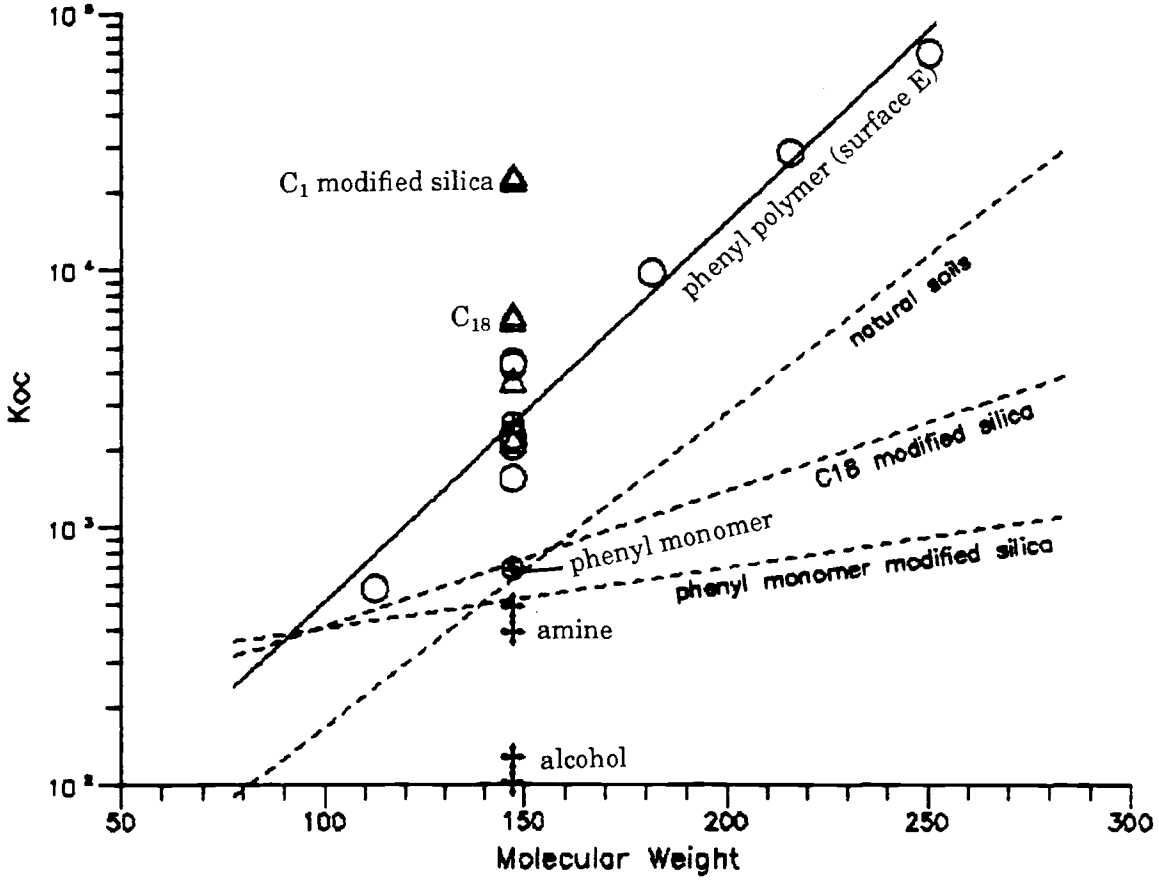

Figure 5.8 Sorption onto organic modified surfaces

functional group is less polar than the unbonded silica [*Macherey-Nagel, 1987*], but more polar than most silanes and has the ability to hydrogen bond with water. It is expected to have a smaller K_{oc} than aliphatic modified silica [Larsson et al., 1982]. Amine surfaces are strong Lewis bases and ionize at low pH. These silanes are used as weak anion exchangers at low pH for carbohydrate separation. Sorption of hydrophobic compounds is less than on aliphatic chains, since the surface is more polar.

The increase in K_{oc} over the series of chlorinated benzenes on the phenyl polymer surface is similar to that observed with natural soils. Both the K_{oc} values of the phenyl polymer and natural soil indicate a log-linear trend with molecular weight. A log-linear increase in sorption energy with molecular weight is expected as K_{oc} is log-linearly related to the increase in solute molecule surface area (equations 3, 13, and 14). The departure from this trend may reflect an interaction with the mineral surface for the higher-molecular-weight compounds. *Karickhoff [1984]* suggested that sorption onto mineral surfaces for polycyclic compounds (with large K_{oc} values) causes increased retention that is not accounted for by considering only sorption to the bound organic matter.

Energies calculated from the molecular connectivity indices (column 2 in Table 2.1) for sorption onto a 100 percent organic phase, show the following relationship:

$$\Delta G^\circ = -0.045\,M + 0.802 \quad r^2 = 1.000 \tag{82}$$

The observed trend for sorption on the phenyl polymer surface (from Table 5.5) can be compared by normalizing K_p's to a 100 percent organic surface (equation 10):

$$\Delta G^\circ = -0.020\,M - 1.96 \quad r^2 = 0.942 \tag{83}$$

The data show less of an increase in sorption energy with molecular weight than is calculated from the model. Experimental data (Table 5.5) show larger ΔG° values for DCB, TCB, and TeCB, but essentially the same values for PCB. This increased sorption energy for DCB, TCB, and TeCB may be due to the dominating importance of pi-pi electron interactions for these compounds. The decreased sorption for PCB may reflect

increased steric hindrance, reducing access to some of the binding sites.

Entropy changes that occur as a result of sorption include decreased structure of water molecules upon solute molecule removal from aqueous solution (solvent effect), and the increased structure as the solute molecule is moved from a liquid to a sorbed state. If the solvent effect entropy change is greater, then there is a net positive entropy change for sorption. Enthalpic changes include the sorbent/sorbate versus the solute/solvent interaction, and increased hydrogen bonding of water upon solute-molecule removal from solution. Both the solvent effect enthalpy and the solute/surface interaction enthalpy are negative.

The entropy and enthalpy were estimated from sorption at different temperatures (Table 4.10), and can be compared to the limited data available in literature. Partitioning between octanol and water (Table 2.3) show values of -4 to -7 kcal mol^{-1} for DCB, TCB, and TeCB. Enthalpies calculated on the phenyl-modified surface in this study (Table 4.10, van't Hoff data) are negative, but less than observed on partitioning to octanol. This difference can be accounted for using equations (3) and (11), to calculate ΔG° for K_{oc} rather than K_{ow}: -4.8, -5.6, and -5.8 kcal mol^{-1} (for DCB, TCB, and TeCB respectively). These values are similar to that observed on the phenyl surface (-4.3 kcal mol^{-1} for DCB, -4.9 kcal mol^{-1} for TCB, and -5.4 kcal mol^{-1} for TeCB).

The entropy for water to octanol partitioning (Table 2.3; reported as $T\Delta S$) is positive and on the order of 1 to 2 kcal mol^{-1}. The observed trend was similar, with values of 0.4 for DCB, 1.2 for TCB, and 0.5 for TeCB. The positive $T\Delta S$ suggests that the solvent effect dominates the entropy change. Partitioning from water to fish fat (Table 2.3) [*Opperhulzen et al., 1988*] is an entropy driven reaction, with enthalpy values being positive. This system is not comparable to that observed with partitioning to octanol, or to organic modified surfaces in this research. Octanol/water partitioning, however, is used as an analogy to sorption between aqueous solution and natural soil organic matter.

5.2.5 Binding Mechanism

In liquid chromatography of small polar molecules, kinetic resistances are typically less important than diffusional resistances for porous packing with a diameter larger than 5 to 10 μm; for larger molecules that bind at multiple sites on the surface, kinetic resistances should dominate [*Horvath and Melander, 1983*]. Results are generally for mobile phases less polar than water, however. For example, increased band spreading due to slow kinetics for more-strongly retained species was observed for a series of organic acids on a C_{18}-modified surface [*Horvath and Lin, 1978*]. Activation energies for binding were on the order of 3 kcal mol^{-1}, near that expected for a diffusion limitation. For dissociation, activation energies were on the order of 7 to 9 kcal mol^{-1} [*Horvath and Lin, 1978*], in the range of typical weak chemical interactions.

Sorption-rate data at different temperatures were used to calculate the activation energy (Table 4.10) with the Arrhenius equation. Data were considerably more scattered than partition data, and the resulting activation energy values from both k_f and k_b data did not indicate a trend with increasing molecular weight. The activation energies calculated from k_b ranged from +0.8 to +5.0 kcal mol^{-1}, which are in the range of reported values (+3 to 5 kcal mol^{-1}) for collision by diffusion in aqueous solution [*Stumm and Morgan, 1981*].

In the case of an aromatic compound partitioning to a phenyl-polymer surface, pi electron interactions between the carbon atoms of benzene rings are stronger than van der Waals attractions between other hydrophobic surfaces [*Hanai and Hubert, 1984; Jinno et al, 1985*]. The electron cloud associated with the phenyl ring has the ability to undergo further induced delocalization; it is a weak hydrogen bond acceptor (10 times weaker than normal hydrogen bonds) [*Blevins, 1982*]. This pi electron interaction is relatively constant for aromatics even with different hydrophobic or polar functional groups. In the chlorinated benzene series, 1,2,3,4-TeCB has a slightly greater dipole moment, and has less ability to delocalize pi electrons [*Haken et al., 1983*].

As phenyl groups are bound to the silica surface without an aliphatic chain, they do not move [*El-Hassan et al., 1986*]; as functional groups bound on a long aliphatic chain exhibit motion. This lack of movement for the bound phenyl groups decreases the mass transfer of solute molecules to sorption sites. Additional decrease in mass transfer is caused by the presence of closely spaced phenyl groups. Adjacent bound phenyl groups (when bound as a polymer) are separated by an average distance of 0.6 nm, and aromatic groups bind with an average distance of 0.3 nm [*Miller et al., 1985*]. There may be some increased time to reach a binding site due to this specific orientation, since the strongest binding sites are not at the water-organic interface, but in the interior of the bound organic layer.

In a study where one, two, or three phenyl groups were attached to a single silica atom [*Jinno et al, 1985*], increased sorption as well as slower sorption was observed with increasing density of phenyl groups. This was interpreted as multiple pi electron interactions on both sides of the sorbing aromatic solute [*Okamoto et al., 1985*]. Sorption energies of different substituted aromatics were less than 20 percent different [*Hanai and Hubert, 1985*], and this was interpreted as meaning the binding mechanism was through the pi electrons in the benzene ring. Slower sorption is observed with polyaromatics or aromatics with large attached functional groups, which was interpreted as steric hindrance in reaching the preferred binding site [*Toyohide et al., 1982*].

Strong binding interactions in some cases can include irreversible sorption, as concluded with sorption of chlorinated phenols [*Isaacson and Frink, 1983*]. Since this also produces tailing, it can be misinterpreted as tailing due to kinetic limitations. With all the surfaces in this study, sorption reversibility (K_{ps}/K_{pd} in Table 5.5) averaged 0.96 ± 0.15 (n = 92), indicating little nonreversible sorption. Mass balance for all experiments also indicated no irreversible sorption. Sorbent/sorbate combinations that exhibited the greatest deviation from reversibility were the poorer quality experiments (due to difficulty analyzing solute concentration or grain rearrangement in the column). Additionally, six experiments that were sorbed for 60 days before desorption also showed no

irreversible sorption.

5.3 Application to Natural Systems

5.3.1 Sorption Mechanisms and Rates

Chlorinated benzenes partition more strongly to natural than to artifical mineral surfaces. This may be due to natural surfaces containing other oxides or traces of natural organic matter. Sorption onto mineral surfaces needs to be accounted for even in cases where organic matter is present. Sorption to organic-modified model surfaces (Figure 5.8) is greater than onto natural soil. This is probably due to natural organic matter having a smaller percent hydrophobic mass than a model hydrophobic surface. Figure 5.8 also shows that heterogeneous surfaces can be made that simulate the sorption found in natural systems.

The slow desorption rates observed for phenyl-polymer surfaces are probably due to steric limitation in reaching the binding site of closely spaced benzene rings [*Jinno et al, 1985*]. As natural organic matter averages 4 to 6 benzene rings per molecular weight of 500 [*Thurman, 1985*], closely spaced benzene rings are possible. Other researchers have suggested that slow sorption is caused by the rate of penetration into natural organic matter [*Isaacson and Frink, 1983*], and by the chemical sorption and desorption rate [*Leeheer et al., 1971*]. Both cases illustrate that kinetic limitations in natural soils can be caused by the nature of the bound organic phase.

Rates that are important in natural systems depend on the residence time of the flow system. As described in *Bahr and Rubin* [*1987*], laboratory reaction rates can be scaled up and compared to field residence times by use of the Damkohler number (equation 38), which is the ratio of residence time to reaction time. Rates observed in the experiments reported here are generally faster than would be important in ground water situations, but would be important near pumping wells or small field sites. By the same token, kinetic reactions important on a field scale ($<10^{-6}$ s^{-1}) would be difficult to

observe in the laboratory.

For example, Figure 5.9 illustrates that even for the high velocities sometimes associated with aquifer cleanup, $k_b > 10^{-4}$ s^{-1} is little different from equilibrium behavior, and K_p determines the extent of flushing needed. As K_p decreases, k_b becomes increasingly more important. The residence times in these small-field-scale systems are on the order of hundreds of hours or greater; and the reaction half lives (Table 5.2) for the sorbent/sorbates determined in this study ranged from 1 to 60 minutes. The corresponding ratio of residence to reaction time (Damkohler number) is then 100 or greater, indicating essentially equilibrium behavior.

Slower desorption rates reported by other researchers would have some effect in field situations. Desorption rates on the order of 10^{-6} to 10^{-7} s^{-1} were observed for desorption of three polychlorinated biphenyls from river sediments [*Coates and Elzerman, 1986*]. Values were three-fold lower for sediments containing montmorillonite versus kaolinite. First-order rate coefficients of 0.03 to 1.0 x 10–5 s^{-1} were reported for sorption of PCB and HCB onto various soils [*Karickhoff and Morris, 1985*], using a series-reaction model to interpret data. Values reported earlier for pyrene (10^{-5} s^{-1}), phenanthrene (5 x 10^{-5} s^{-1}), and naphthalene (3 x 10^{-4} s^{-1}) were also faster [*Karickhoff, 1980*].

The rate of 5 x 10^{-7} s^{-1} corresponds to a reaction half-life of 400 hours. In this case, kinetics should be considered for modeling field systems where the aquifer residence times are up to 800 days ($N_D < 50$). Significant departure from equilibrium behavior (where $N_D < 10$) are be observed in flow systems where residence times would be less than 150 days.

The change from a laboratory to field scale offers additional complexities. Columns used in this research were fully saturated, so volatilization of the solute was ignored. A model of equilibrium partitioning between solid, liquid, and gas-phases [*Baehr, 1987*] indicates that for highly volatile compounds, gas phase transport will increase the mobility in a partially saturated system compared to a fully saturated system, since

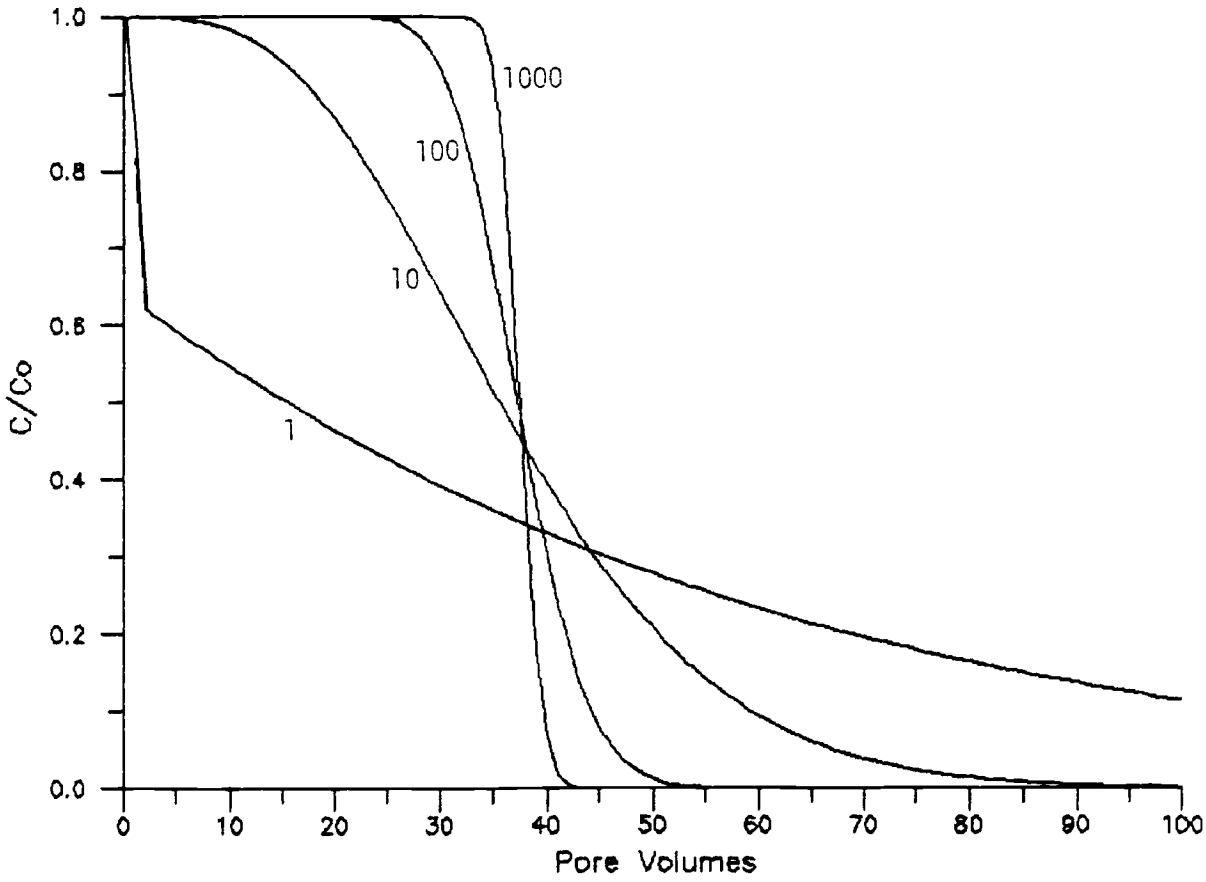

Figure 5.9 Effect of the desorption rate on field desorption

first-order model with a length = 20 m, v = 0.03 cm/s,
D = 0.01 cm^2/s, $\theta = 0.4$, $\rho_b = 1.5$, curves for various values of N_D;
note that k_b (s^{-1}) equals N_D times 1.7×10^{-6}.

diffusion in the gas phase can be greater than advective movement in the aqueous phase. Mass loss from biodegradation was also ignored in this study, even though it is observed in the laboratory and field with several chlorinated benzenes [*MacKay et al., 1987*].

Reactions occurring in the laboratory may not yield the same results as in the field where some catalysts such as other ions or micro-environmental conditions are missing or sporadic [*Graham-Bryce, 1981*]. A study of pesticide sorption in the laboratory and at a field site [*Elabd et al., 1986*] showed no correlation between field K_p and field f_{oc}, indicating other interactions were significant. In addition, the variation of parameters in the field that were constant in the laboratory led to difficulty in applying results to the field scale. Others have also observed that the mean K_p from several field sites [*Schultin et al., 1987; MacKay et al., 1986*] had little correlation to laboratory K_p's.

In simulation of laboratory results at the field scale, the effect of variation of f_{oc} (or K_p) was calculated by modifying the one-dimensional numerical solution (MOB2) to include a stochastically varying K_p. The specifics of the numerical scheme used are found in Section 2.2.7. A random variation in the sorbent mass (f_{oc}) with covariance structure is assumed, where K_p is equivalent to K_{oc} times f_{oc} (equation 2). Three cases were considered: $f_{oc} = 0.01 \pm 0.0001$, $f_{oc} = 0.01 \pm 0.001$, and $f_{oc} = 0.01 \pm 0.01$. This would simulate soil organic matter gradually changing in a profile, with correlation at a small distance, but no correlation at a large distance.

Soil organic matter is correlated with clay content, so in layered soil where layers had a different clay content, a vertical correlation scale would be equal to half of a formation thickness. The integral scale for this simulation (distance over which data are correlated) [*Andersson and Shapiro, 1983*] is 2.5 nodes, with 100 total nodes in the soil profile.

Values of f_{oc} (and corresponding K_p) for the three cases are shown in Table 5.6, where the first case shows K_p varying from 21 to 31, the second case K_p varies from 14

Table 5.6 Simulated K_p values for Stochastic Cases

Case 1 $f_{oc} = 0.01 \pm 0.0001$		Case 2 $f_{oc} = 0.01 \pm 0.001$		Case 3 $f_{oc} = 0.01 \pm 0.01$	
$K_{p,i}$	$f_{oc,i}$	$K_{p,i}$	$f_{oc,i}$	$K_{p,i}$	$f_{oc,i}$
26.797	0.01072	38.681	0.01227	42.966	0.01719
30.672	0.01227	42.938	0.01718	81.724	0.03269
30.760	0.01230	43.216	0.01729	82.603	0.03304
31.440	0.01258	45.366	0.01815	89.403	0.03576
28.684	0.01144	36.398	0.01456	61.043	0.02442
26.282	0.01051	29.053	0.01162	37.815	0.01513
25.425	0.01017	26.343	0.01054	29.246	0.01170
25.631	0.01025	26.997	0.01080	31.314	0.01253
26.267	0.01051	29.008	0.01160	37.673	0.01507
25.338	0.01014	26.070	0.01043	28.383	0.01135
25.330	0.01013	26.844	0.01042	28.303	0.01132
26.182	0.01047	28.737	0.01149	36.817	0.01473
24.461	0.00978	23.294	0.00932	19.687	0.00784
26.641	0.01066	30.188	0.01208	41.406	0.01656
28.519	0.01141	36.128	0.01445	60.189	0.02408
30.851	0.01234	43.501	0.01740	83.506	0.03340
29.101	0.01164	37.970	0.01519	66.015	0.02641
25.923	0.01837	27.918	0.01117	34.229	0.01369
25.195	0.01008	25.615	0.01025	26.946	0.01078
21.725	0.00869	14.645	0.00586	-7.746	-0.00310
21.231	0.00849	13.081	0.00523	-12.692	-0.00508
21.264	0.00851	13.185	0.00527	-12.363	-0.00495
21.524	0.00861	14.007	0.00560	-9.764	-0.00391
23.383	0.00935	19.885	0.00795	8.825	0.00353
26.548	0.01062	29.895	0.01196	40.478	0.01619
27.215	0.01089	32.004	0.01280	47.149	0.01886
27.059	0.01082	31.511	0.01260	45.590	0.01824
27.475	0.01099	32.828	0.01313	49.755	0.01990

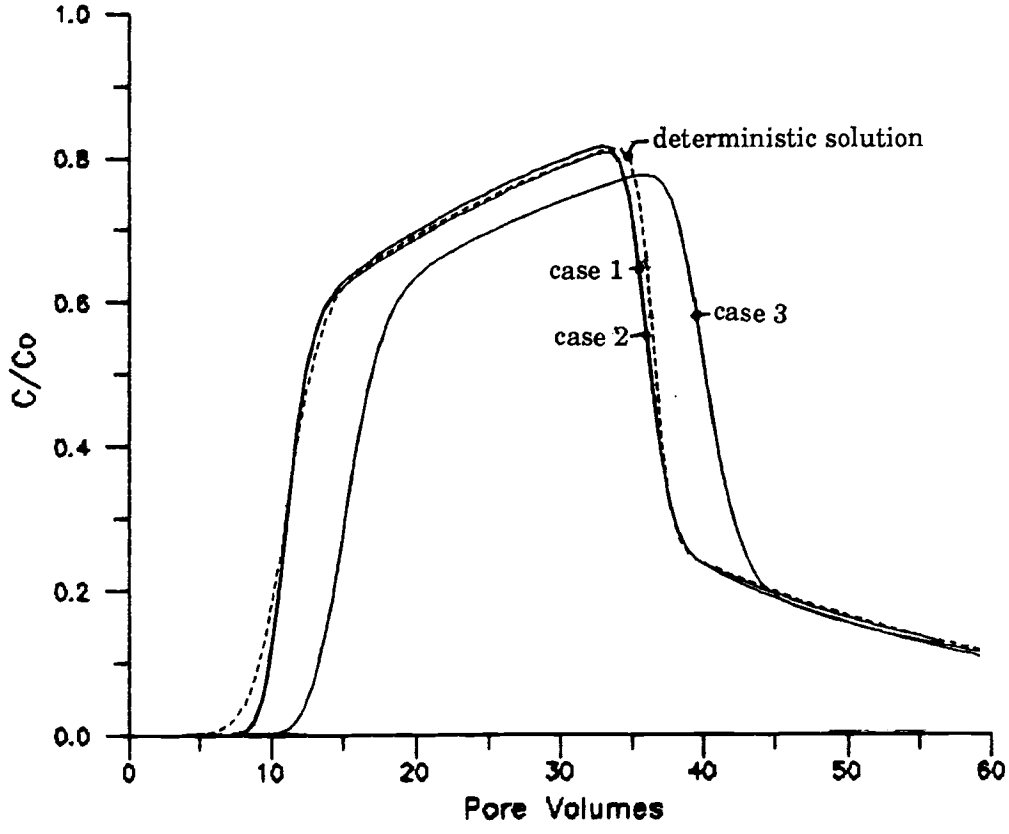

Figure 5.10 Effect of random variation of f_{oc} on the breakthrough curve

to 45, and in the third case K_p varies between 0 and 90. A single model run with each case produced breakthrough curves (shown in Figure 5.10) where little difference is observed in the curve shape compared to the deterministic solution. Usually, many realizations (runs) of the stochastic model are performed to produce an average breakthrough curve, which is then compared to the deterministic model, but this was not necessary for this example.

Results are intuitively appealing, since in one-dimensional flow a change in K_p (or retardation factor) is analogous to series resistors; all flow must go through every node, so the value of the individual nodes are not important, only the average K_p. The fact that no additional spreading is observed with randomly varying K_p in one dimension is an artifact of the case considered. In an actual field situation, variation of f_{oc} would increase the observed spreading, as different parts of the flow system would have a different solute velocity (defined with respect to retardation factor in equation 29). A two dimensional simulation of randomly varying K_p [*Daugarty et al., 1987*] showed that additional spreading results; this could be misinterpreted as kinetic effects. A case of stochastic variation of K_p near pumping wells [*Valocchi, 1986*] demonstrated that non-equilibrium sorption exhibits a strong spatial dependence.

Randomly varying the velocity [*Parker and van Genuchten, 1984*] results in increased dispersion even in a one-dimensional case (with no change in K_p). Varying several parameters in 2 or 3 dimensional simulations [*Sposito and Barry, 1987*] showed that the average value of the parameter was not equal to the stochastic parameter average. Dispersion is a function of scale [*Andersson et al., 1983*], since at different scales, different processes are being averaged into dispersion.

This demonstrates that spreading observed in a field situation could be caused by a slow sorption step, or by spatial variation in velocity or aquifer properties (dispersion or f_{oc}). Clearly, scaling up of parameters obtained at the laboratory scale to the field scale should be done through intermediate scale studies for accurate application of the mechanisms and rates obtained at a small scale.

5.3.2 Methods to Determine Sorption Mechanism

A series of experiments was performed in this study to separate possible rate limiting steps (Figure 1.1). Using model surfaces, considerable control of the geometry and size of the mineral surface and bound organic layer is possible. This type of control is not possible with natural systems, but some of the methods developed can still be applied to natural soils to determine the sorption mechanism.

Diffusion through immobile pore fluid can be examined in natural systems by separating particles of different size and then determining if the larger particle exhibits slower sorption (as done in this study). Results can be quantified by calculating apparent tortuosity (equation 40) using the equilibrium model dispersion coefficients. Experiments run at different temperature can also be used to determine if the change in intraparticle diffusion (same equation) over a temperature range is consistent with expected change in diffusion (Stokes-Einstein equation 39). Removal of the bound organic material and comparison of sorption rates on bound and unbound particles can also quantify the effect of the diffusion rate in the immobile pore fluid.

The diffusion rate through the bound organic layer can be quantified with a series of compounds, and compared to the expected change in diffusion rate from the Stokes-Einstein equation. Any quantification of the physical dimensions of the bound organic layer can be used to estimate the diffusion rate through the bound organic layer [*Barrer, 1939*]. The sorption of a series of compounds at different temperature can be used to determine if a chemical reaction can adequately describe the sorption kinetics. In addition, the sorption energy and activation energy can be estimated and compared to published values.

5.3.3 Optimum Methods to Determine Sorption Parameters

As many as five parameters can be estimated from a single breakthrough curve, and since some are related, this leads to the conclusion that there are more than one set of parameters that can fit the data in many cases. Spreading of a breakthrough curve is

a function of hydrodynamic dispersion and a slow rate process. Independent determination of dispersion (see Section 2.2.2) is necessary to properly separate it from the slow rate process. The partition coefficient can also be independently determined from the area in front of the breakthrough curve. An exeriment run at low velocity (exhibiting little kinetics) provides for the best determination of K_p.

The most accurate velocity to determine the rate parameter is when the ratio of the residence time is equal to the reaction time (equation 38). Figure 2.8 describes this point of maximum sensitivity of the rate parameter when the Damkohler number equals 1.44. At these high velocities, the spreading due to the slow rate process exhibits maximum effect, as shown in Figure 2.7. Performing experiments at these velocities and obtaining reliable (and enough) samples is difficult with the apparatus described in this research. Continuous detection of solute concentration, and injection of a solute pulse without interrupting the flow through the column, and use of smaller columns would make this feasible. This is essentially a liquid chromatograph system. Additionally, injecting a small injection pulse would decrease column degradation.

A hypothetical example of determining the reaction rate from small pulse injections is illustrated in Figure 5.11 (analogous to Figure 2.7). Low velocity injections produce sharp peaks with a defined retardation factor. By simulating injections at larger velocities, more kinetic spreading is observed (and more dispersion). Eventually, at very fast velocities, the solute does not have time to react with the column material, and the breakthrough curve appears conservative (retardation factor = 1). There is an intermediate velocity where the residence time is equal to the reaction time, as observed by the flat breakthrough curve. The desorption rate coefficient (k_b) can be determined from velocity by:

$$k_b = \frac{1.44\, v\, \theta}{l\, \rho_b K_p} = \frac{1.44\, v}{[R_f - 1]\, l} \tag{84}$$

where l is the column length, and K_p is determined from a low velocity (or batch) experiment. Experimentally, all velocities are not obtainable, nor is continuous detection at

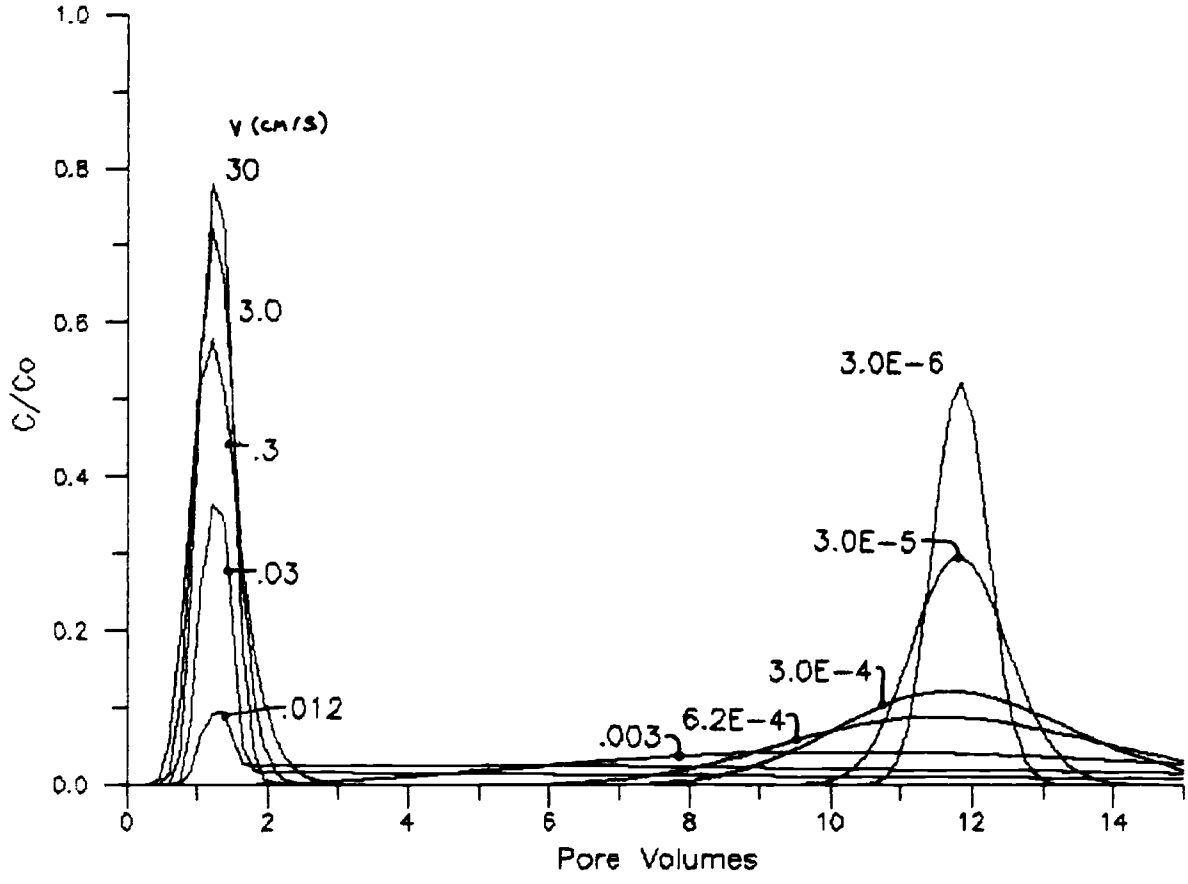

$K_p = 25\ cm^3 g^{-1}\ k_b = 2 \times 10^{-4}\ s^{-1}$

Figure 5.11 Effect of velocity on small injection pulse breakthrough curves

the concentrations of interest. Column experiments were performed at different velocities for some sorbent/sorbate combinations in this research. Sorption rates (and other parameters) were determined for each experiment, where error between the best experiments is 2 to 3 fold (similar accuracy stated by other researchers), and at worst, 5 orders of magnitude. The largest error were those sorbent/sorbate combinations exhibiting fast sorption, where there is considerable error in determining a k_b value from a breakthrough curve that exhibits essentially no kinetics.

Theoretically, a single sorbent/sorbate combination has a single sorption rate and partition coefficient. Simple averaging of several experiments (when deviations are several orders of magnitude) may not produce the best set of parameters that accurately represent the experimental data. This is because the rate parameter sensitivity is nonlinear (Figure 2.8); there is greater error in fitting the rate parameter for experiments run at low velocities.

The analytical solution of the nonequilibrium solute transport model (CFITIM) was modified to be able to determine parameters from several experiments simultaneously that minimize the total error in fitting all experiments. The program, MFITIM, is listed in Appendix D, with an example input file (Appendix E) and output file (Appendix F). A total of three parameters are optimized with the two-region model (K_p, α_e, and f), and two parameters with the first-order model (K_p and k_b). Eight cases were run with the sorbent/sorbate combinations listed in Table 5.7; cases were chosen as examples where a large variation in a parameter existed between experiments. The program, MFITIM, can obtain better results than a simple average of individual experiments by adjusting parameters and arriving at a lower total error. This is illustrated in Table 5.7 where a better fit is obtained in each case. Five cases of the two-region model are shown, with representative 2 or 3 experiments from each sorbent/sorbate combination.

Obtaining a better fit (lower total error) in most cases is not equal to the average value of individual experiments. Since error is nonlinear for the rate parameter (Figure 2.8), large N_D's can be adjusted to a greater extent without affecting error, compared to

Table 5.7 Multiple experiment parameter estimation results

Sorbent	Solute	N	Single-Experiment Method parameter	Σssq/N	Multiple-Experiment Method parameter	Σssq/N	Δssq
C_1 poly, 100 μm (A)	DCB	2	K_p = 450, 330 α_e = 940, 0.0078 f = 0.59, 0.30	2.369	K_p = 347 α_e = 1.2 f = 0.32	2.331	+1.6%
Ø poly, 20 μm (G)	DCB	2	K_p = 16, 34 α_e = 0.0056, 0.0014 f = 0.13, 0.58	2.163	K_p = 25 α_e = 0.0013 f = 0.33	2.067	+4.4%
Ø poly, 100 μm (E)	DCB	2	K_p = 19, 85 α_e = 0.00075, 0.0070 f = 0.45, 0.14	>10	K_p = 83 α_e = 0.0055 f = 0.11	7.258	>+30%
Ø poly, 425 μm (H)	DCB	3	K_p = 22, 17, 25 α_e = 0.0020, 0.00039, 0.0022 f = 0.42, 0.60, 0.43	1.921	K_p = 18 α_e = 0.0089 f = 0.47	0.790	+59%
Ø poly, 100 μm (E)	TeCB	2	K_p = 108, 542 α_e = 0.021, 0.0052 f = 0.028, 0.29	9.333	K_p = 340 α_e = 0.017 f = 0.016	4.429	+52%

experiments with small N_D's. This is illustrated with the first case (surface A), where the average α_e of two experiments is 460 with a six order of magnitude difference in the values. The multiple experiment fit average α_e is 1.2, where the experiment with the large N_D is adjusted to a greater extent. The average K_p and f values from MFITIM are also different from the arithmetic average of the individual experiments.

This program is most useful when there is a wide variation in velocity between experiments. This is best illustrated with the last case (TeCB) where there is a two fold difference in velocity. Theoretically, a unique rate parameter can be best determined from several experiments (same sorbent and sorbate) run at different velocities. Considering experiments as vertical lines a fixed distance apart in Figure 2.8, fitting a single rate parameter to multiple experiments is then equivalent to moving these vertical lines (keeping the fixed distances) along the x-axis to a point of lowest error. This multiple experiment method should yield more accurate chemical parameters from breakthrough curves than is possible from modeling single breakthrough curves, which can be used for more accurate determination of the sorption mechanism.

CHAPTER 6
CONCLUSIONS

Sorption kinetics were examined with the use of model sorbents in order to quantify the rate of diffusion through immobile pore fluid, the rate of diffusion through the bound organic layer, and the chemical binding and release rate. Slow sorption and desorption, as evidenced by tailing in breakthrough curves, were observed with phenyl and C_1 polymer modified surfaces, but not with several other organic modified surfaces, nor with unbound silica and alumina.

The observed slow sorption and desorption appear to be caused by the chemical binding and release step, as evidenced by similar sorption rates onto porous and solid particles modified with a phenyl or C_1 polymer. Sorption and desorption of solutes on both the C_1- and phenyl-polymer surfaces were modeled accurately with a first-order reversible reaction and a single rate parameter (k_b). The rate data from column experiments at different temperature, and through a series of compounds, indicate that a diffusion process was not causing the observed slow sorption. The data was consistent with the binding and release rate causing the observed slow sorption. The rates observed for chlorinated benzene sorption onto the phenyl-polymer surface were slower than rates observed by others in natural soil [*Wu and Gschwend, 1986*], but rates on other organic-modified surfaces were up to 3-fold faster than in soil.

The binding energy for sorption of chlorinated benzenes onto the phenyl-polymer surface is stronger than on either the phenyl-monomer surface or aliphatic chain organic-modified surfaces. This is probably caused by the stronger interactions between pi electrons in the benzene ring of the solute molecule and surface phenyl molecules [*Jinno et al., 1985*]. Sorption onto the phenyl-polymer surface versus the phenyl-monomer surface is stronger and slower. The difference in rate is apparently due to a steric hindrance in reaching the strongest binding sites between the closely spaced phenyl groups on the polymer surface. Here, multiple pi-pi electron interactions are possible [*Hanai et al., 1985*]. In addition, since the phenyl groups are bound close to the surface [*El-Hassan, 1986*], they do not move; this decreases the the mass transfer rate of

solute molecules to binding sites. Long aliphatic chains bound to the surface exhibit motion that increases the mass transfer rate to surface sites.

Sorption energies for the series of chlorinated benzenes are small, ranging from -4.0 kcal mol^{-1} for chlorobenzene to -6.9 kcal mol^{-1} for pentachlorobenzene, and are consistent with the van der Waals interactions expected. Sorption energies are slightly stronger than estimated values from physico-chemical data for most of the chlorinated benzenes sorbing onto phenyl-polymer surface. This may reflect the increased binding energy of the pi-pi electron interactions compared to simple van der Waals interactions. Sorption energies were considerably weaker for amine and alcohol modified surfaces, as expected, since hydrophobic solutes sorb less in the presence of polar functional groups. Sorption energies observed with natural soils are smaller than those observed on the hydrophobic surfaces in this research, but greater than those observed on surfaces modified with amine or alcoholic groups. Apparently, both sorption energies and rates observed in natural soils can be simulated with model sorbents.

The sorption of chlorinated benzenes onto the phenyl-polymer surface is caused mainly by the negative enthalpy (-4 to -5 kcal mol^{-1}), and to a lesser extent by the positive entropy of the sorption reaction ($T\Delta S$ was 0.4 to 1.2 kcal mol^{-1}). The positive entropy change indicates that the disordering of water molecules upon solute removal from solution (entropy portion of the solvent effect) is greater than the negative entropy of moving the solute molecule from liquid to sorbed state. The negative enthalpy is composed of both the solute/surface interaction energy and the increased hydrogen bonding due to the solvent effect. The decrease in enthalpy from DCB to TeCB may be caused by the solvent effect, as the surface interaction energy should not change over the series of compounds. The entropic and enthalpic changes appear to indicate that the solvent effect is the major component of the overall sorption reaction. The calculated solvent effect and interaction energies are approximately equal, showing that removal of hydrophobic solutes from solution is as much a driving force as is the interaction energy with the surface.

The diffusion rate through the bound organic layer is apparently relatively fast due to the small thickness of the organic layer. This conclusion is also consistent with the rate data for the series of chlorinated benzenes and sorption at different temperatures. In addition, the calculated diffusion rate through a bound organic layer of this thickness [*Barrer, 1939*] is considerably faster than that observed.

The slow approach to equilibrium is partially caused by diffusion through immobile pore fluid since a difference in the sorption rate is observed with particles of a different size or different tortuosity, although the effect is small. Diffusion through immobile pore fluid has only a minor effect on the overall sorption rate, since most of the slow sorption is still observed when the C_1- or phenyl-polymer is bound to solid particles. The expected diffusion rates for 500 μm particles or smaller are less than one minute, and pore clogging expected by binding organic compounds to the surface did not seem to affect this diffusion rate, since some organic-bound particles had the same sorption rate as unbonded particles.

Kinetic limitations cause a considerable increase in the time needed to desorb solutes from surfaces. The relative transport versus chemical (sorption) time scales suggest that chlorinated benzene sorption would be kinetically limited only in some field situations involving residence times of 100 hours or less such as near pumping wells, in soils, or in small scale aquifer cleanup operations. Desorption rates observed by other researchers would have an effect on intermediate scale flow systems (residence times to 800 days). Kinetics are postulated to cause some of the difference between observed ion transport and equilibrium model predictions even in large aquifers [*Jennings, 1987*]. Desorption of solutes from soil can be made faster by increasing temperature, addition of a cosolvent to water, and addition of a organic colloid phase.

Further investigation of the interactions in natural systems can be made with model surfaces for polar and ionic interactions, and with a wider variety of solutes. Application of some of the methods used in this research to natural soils can be made to determine the rate limiting sorption step. Accurate kinetic parameters are needed to

determine the sorption mechanism, which can be done with a single experiment run at optimum velocity, or multiple experiments run at different velocities. Development of better methods for integrating modeling and experimentation are needed in order to produce more accurate rate data.

A. KCl Column Modeling Data

																EQUILIB MODEL			
NAME	DATE	misc.	Q (cm3/s)	ave vel v (cm/s)	pore vol (cm3)	pv injec	column area (cm2)	col le (cm)	col volume (cm3)	total poro- sity	actual poro- sity	built density (g/cm3)	SORBENT surf name	bound organic	KCl init conc (Molar)	KCl final conc (Molar)	KCl Rf	KCl Peclet	KCl D (cm2/s)	SSQ (error)
A1	10-13-86	pH=7.02	0.0284	0.04182	9.506	6.00	0.785	14.00	10.99	0.865	0.887	0.330	PQ-M	none	7.90E-03	3.20E-03	1.026	77.22	7.58E-03	0.1117
A2	10-13-86	pH=9.83	0.0284	0.04182	9.506	6.00	0.785	14.00	10.99	0.865	0.787	0.330	PQ-M	none	7.90E-03	4.00E-03	0.910	155.9	3.76E-03	0.0470
A3	10-14-86	pH=3.85	0.0284	0.04182	9.506	6.00	0.785	14.00	10.99	0.865	0.836	0.330	PQ-M	none	2.00E-03	6.30E-03	0.966	171.9	3.41E-03	0.0081
A4	10-14-86	pH=2.04	0.0284	0.04182	9.506	6.00	0.785	14.00	10.99	0.865	0.816	0.330	PQ-M	none	1.60E-02	2.50E-02	0.943	191.8	3.05E-03	0.0083
A5	10-14-86	pH=6.98	0.0284	0.04182	9.506	6.00	0.785	14.00	10.99	0.865	0.429	0.330	PQ-M	none	1.30E-05	5.00E-05	0.496	142.1	4.12E-03	0.0226
A6	2-21-87	vary	0.0283	0.05223	2.709	10.00	0.636	5.00	3.18	0.852	0.545	0.361	PQ-E	none	1.00E-05	1.50E-05	0.639	102.9	2.54E-03	0.0225
A7	2-21-87	ionic	0.0167	0.03082	2.709	10.00	0.636	5.00	3.18	0.852	0.839	0.361	PQ-E	none	1.00E-04	1.50E-04	0.985	58.94	2.61E-03	0.0585
A8	2-21-87	strength	0.0167	0.03082	2.709	10.00	0.636	5.00	3.18	0.852	0.947	0.361	PQ-E	none	1.00E-02	1.50E-02	1.111	58.13	2.65E-03	0.0528
A9	2-21-87	range	0.0183	0.03377	2.709	10.00	0.636	5.00	3.18	0.852	0.894	0.361	PQ-E	none	1.00E-01	1.50E-01	1.049	56.05	3.01E-03	0.0316
A11	2-21-87	vary	0.0183	0.03326	2.751	7.50	0.636	5.00	3.18	0.865	0.632	0.330	PQ-M	none	1.00E-05	1.50E-05	0.731	81.16	2.05E-03	0.0698
A12	2-21-87	ionic	0.0183	0.03326	2.751	7.50	0.636	5.00	3.18	0.865	0.896	0.330	PQ-M	none	1.00E-04	1.50E-04	1.036	131.4	1.27E-03	0.0958
A36	3-23-87		0.0233	0.03431	9.506	3.60	0.785	14.00	10.99	0.865	0.644	0.330	PQ-M	none	1.00E-03	2.50E-03	0.744	104.5	4.60E-03	0.0090
A13	2-21-87	strength	0.0183	0.03326	2.751	7.50	0.636	5.00	3.18	0.865	0.932	0.330	PQ-M	none	1.50E-04	1.00E-02	1.077	131.0	1.27E-03	0.0041
A14	2-21-87	range	0.0183	0.03326	2.751	7.50	0.636	5.00	3.18	0.865	0.916	0.330	PQ-M	none	1.00E-02	1.50E-02	1.059	173.3	9.60E-04	0.0173
A15	2-21-87		0.0183	0.03326	2.751	7.50	0.636	5.00	3.18	0.865	0.948	0.330	PQ-M	none	1.50E-02	1.00E-01	1.096	131.0	1.27E-03	0.0050
A16	2-21-87		0.0183	0.03326	2.751	7.50	0.636	5.00	3.18	0.865	0.932	0.330	PQ-M	none	1.00E-01	1.50E-01	1.077	164.1	1.01E-03	0.0062
A18	3-2-87	vary	0.0183	0.03326	2.751	3.60	0.636	5.00	3.18	0.865	0.982	0.330	PQ-M	none	1.00E-05	1.00E-03	1.135	233.8	7.11E-04	0.0471
A19	3-2-87	ionic	0.0183	0.03326	2.751	3.60	0.636	5.00	3.18	0.865	0.811	0.330	PQ-M	none	1.00E-05	1.00E-04	0.937	97.06	1.71E-03	0.1880
A20	3-2-87	strength	0.0183	0.03326	2.751	3.60	0.636	5.00	3.18	0.865	0.928	0.330	PQ-M	none	1.00E-05	1.00E-02	1.073	213.1	7.80E-04	0.0179
A21	3-2-87	range	0.0183	0.03326	2.751	3.60	0.636	5.00	3.18	0.865	0.925	0.330	PQ-M	none	1.00E-05	1.00E-01	1.069	181.8	9.15E-04	0.0125
A22	3-14-87	vary	0.0183	0.02695	9.506	3.60	0.785	14.00	10.99	0.865	0.849	0.330	PQ-M	none	1.00E-02	2.00E-02	0.981	152.0	2.48E-03	0.0282
A23	3-14-87	velocity	0.0367	0.05405	9.506	3.60	0.785	14.00	10.99	0.865	0.798	0.330	PQ-M	none	1.00E-02	2.00E-02	0.923	147.1	5.14E-03	0.0233
A24	3-14-87		0.0733	0.10795	9.506	3.60	0.785	14.00	10.99	0.865	0.829	0.330	PQ-M	none	1.00E-02	2.00E-02	0.958	110.8	1.36E-02	0.0159
A25	3-14-87		0.1633	0.24049	9.506	3.60	0.785	14.00	10.99	0.865	0.841	0.330	PQ-M	none	1.00E-02	2.00E-02	0.972	77.53	4.34E-02	0.0353
A26	3-14-87		0.0083	0.01222	9.506	3.60	0.785	14.00	10.99	0.865	0.810	0.330	PQ-M	none	1.00E-02	2.00E-02	0.936	150.3	1.14E-03	0.0047
A35	3-23-87	vary vel	0.00333	0.00490	9.506	3.60	0.785	14.00	10.99	0.865	0.843	0.330	PQ-M	none	1.00E-02	2.00E-02	0.974	254.8	2.69E-04	0.0085
A27	3-14-87		0.00167	0.00246	9.506	3.60	0.785	14.00	10.99	0.865	0.817	0.330	PQ-M	none	1.00E-02	2.00E-02	0.944	380.4	9.05E-05	0.0019
A28	3-16-87	vary	0.025	0.03682	9.506	3.60	0.785	14.00	10.99	0.865	0.370	0.330	PQ-M	none	2.40E-05	1.00E-05	0.428	296.0	1.74E-03	0.0122
A29	3-16-87	initial	0.025	0.03682	9.506	3.60	0.785	14.00	10.99	0.865	0.435	0.330	PQ-M	none	6.40E-05	1.00E-05	0.503	123.3	4.18E-03	0.0119
A30	3-16-87	ionic	0.025	0.03682	9.506	3.60	0.785	14.00	10.99	0.865	0.415	0.330	PQ-M	none	1.05E-04	1.00E-05	0.480	159.7	3.23E-03	0.0042
A31	3-16-87	strength	0.025	0.03682	9.506	3.60	0.785	14.00	10.99	0.865	0.446	0.330	PQ-M	none	3.76E-04	1.00E-05	0.516	177.8	2.90E-03	0.0012
A32	3-16-87		0.025	0.03682	9.506	3.60	0.785	14.00	10.99	0.865	0.495	0.330	PQ-M	none	1.05E-03	1.00E-05	0.572	213.7	2.41E-03	0.0051
A33	3-16-87		0.025	0.03682	9.506	3.60	0.785	14.00	10.99	0.865	0.745	0.330	PQ-M	none	1.00E-02	1.00E-05	0.861	242.8	2.12E-03	0.0197
A34	3-16-87		0.025	0.03682	9.506	3.60	0.785	14.00	10.99	0.865	0.869	0.330	PQ-M	none	1.00E-01	1.00E-05	1.005	152.4	3.38E-03	0.0080
A10	2-21-87		0.0183	0.03377	2.709	10.00	0.636	5.00	3.18	0.852	0.735	0.361	PQ-E	none	1.50E-01	1.00E-05	0.863	40.94	4.12E-03	0.0158
A17	2-21-87		0.0183	0.03326	2.751	7.50	0.636	5.00	3.18	0.865	0.940	0.330	PQ-M	none	1.50E-01	1.00E-05	1.087	185.1	8.99E-04	0.0047
A37	3-23-87	init.	0.025	0.03682	9.506	3.60	0.785	14.00	10.99	0.865	0.579	0.330	PQ-M	none	2.50E-03	1.00E-05	0.669	284.1	1.81E-03	0.0100
A38	3-23-87	conc.	0.025	0.03682	9.506	3.60	0.785	14.00	10.99	0.865	0.649	0.330	PQ-M	none	5.00E-03	1.00E-05	0.750	457.5	1.13E-03	0.0420
A39	3-23-87		0.025	0.03682	9.506	3.60	0.785	14.00	10.99	0.865	0.824	0.330	PQ-M	none	3.50E-02	1.00E-05	0.953	206.9	2.49E-03	0.0150
A40	3-23-87		0.025	0.03682	9.506	3.60	0.785	14.00	10.99	0.865	0.941	0.330	PQ-M	none	1.00E+00	1.00E-05	1.088	149.4	3.45E-03	0.0070

B.1 Solute and KCl Column Modeling Data

EXPERIMENT NAME	LAB NAME	DATE	misc.	COLUMN DATA Q (cm3/s)	ave vel v (cm/s)	pore vol (cm3)	pv inject	column area (cm2)	col lg (cm)	col volume (cm3)	total porosity	bulk density (g/cm3)	surf name	bound organic	KCl initial conc (-log molar)	KCl final conc	EQUILIB MODEL KCl Rf	KCl Peclet	KCl D (cm2/s)	SSQ (error)	SOLUTE name	conc ppb	planimeter sorb (solute) Kp (cm3/g)	desorb Kp (cm3/g)	mass balance PV/PVinj	reverse Kps/Kpd	EQUILIBRIUM MODEL solute Rf	solute Kp (cm3/g)	solute Peclet	solute D (cm2/s)	SSQ (error)
I-6	Y	5-31-86		0.01700	0.0309	7.702	1.62	0.636	14.0	8.904	0.865	0.330	PQ-N	none	5.0	2.6	0.994	130.1	3.33E-03	0.1087	DCB	371.4			1.133		0.998	-0.005	16.55	2.61E-02	0.7230
I-7	Z	6-03-86		0.01700	0.0309	7.702	3.80	0.636	14.0	8.904	0.865	0.330	PQ-N	none	5.0	1.1	1.029	62.85	6.88E-03	0.0252	DCB	296.5	5.731	4.304	1.025	1.332	2.280	1.355	50.54	8.56E-03	0.2700
I-8	ZZ	6-05-86		0.00330	0.00486	9.506	3.60	0.785	14.0	10.99	0.865	0.330	PQ-N	none	5.0	2.8	0.228	9.150	7.44E-03	0.2868	DCB	673.6	5.235	2.479	1.195	2.112	1.633	1.559	56.41	1.21E-03	0.1885
I-9	ZB	6-11-86		0.00330	0.00486	9.500	3.25	0.785	14.0	10.99	0.865	0.330	PQ-N	none	5.0	2.7	0.952	64.34	1.06E-03	0.3300	DCB	386.1	3.346	2.300	0.968	1.455	2.355	3.552	24.78	2.75E-03	0.2422
I-1	ZC	6-17-86		0.00630	0.00928	9.506	2.50	0.785	14.0	10.99	0.865	0.330	PQ-N	none	5.0	2.7	1.009	140.4	9.25E-04	0.2058	DCB	198.4	4.220	4.782	1.138	0.882	2.540	4.037	52.46	2.48E-03	0.1375
I-1	ZC	6-17-86	remodel	0.00630	0.00928	9.506	2.50	0.785	14.0	10.99	0.865	0.330	PQ-N	none	5.0	2.7	1.009	140.4	9.25E-04	0.2058	DCB	198.4	4.220	4.782	1.138	0.882	2.540	4.037	52.46	2.48E-03	0.1375
I-1	ZC	6-17-86	remodel	0.00630	0.00928	9.506	2.50	0.785	14.0	10.99	0.865	0.330	PQ-N	none	5.0	2.7	1.009	140.4	9.25E-04	0.2058	DCB	198.4	4.220	4.782	1.138	0.882	2.540	4.037	52.46	2.48E-03	0.1375
I-2	SF	7-10-87		0.02204	0.0422	13.070	23.70	0.636	25.0	15.90	0.822	0.437	PQ-V	none	2.0	1.7	0.968	207.4	5.08E-03	0.0691	DCB	1627.	3.013	3.001	0.988	1.004	3.762	5.193	66.88	1.58E-02	0.1415
I-2	SF	7-10-87	remodel	0.02204	0.0422	13.070	23.70	0.636	25.0	15.90	0.822	0.437	PQ-V	none	2.0	1.7	0.968	207.4	5.08E-03	0.0691	DCB	1627.	3.013	3.001	0.988	1.004	3.762	5.193	66.88	1.58E-02	0.1415
I-2	SF	7-10-87	remodel	0.02204	0.0422	13.070	23.70	0.636	25.0	15.90	0.822	0.437	PQ-V	none	2.0	1.7	0.968	207.4	5.08E-03	0.0691	DCB	1627.	3.013	3.001	0.988	1.004	3.762	5.193	66.88	1.58E-02	0.1415
I-3	SG	7-13-87	alumina	0.01886	0.0376	12.529	20.05	0.636	25.0	15.90	0.788	0.721	AL-A	none	2.0	1.7	1.128	118.5	7.94E-03	1.1790	DCB	1375.	0.565	0.234	0.959	2.415	1.829	0.906	9.447	9.96E-02	0.5044
I-4	SH	7-15-87	alumina	0.01971	0.0387	12.736	22.19	0.636	25.0	15.90	0.801	0.678	AL-B	none	2.0	1.7	1.121	361.9	2.67E-03	0.0783	DCB	1305.	0.355	0.336	0.974	1.057	1.349	0.412	159.8	6.05E-03	0.0292
I-4	SH	7-15-87	remodel	0.01971	0.0387	12.736	22.19	0.636	25.0	15.90	0.801	0.678	AL-B	none	2.0	1.7	1.121	361.9	2.67E-03	0.0783	DCB	1305.	0.355	0.336	0.974	1.057	1.349	0.412	159.8	6.05E-03	0.0292
I-5	SI	7-17-87	alumina	0.00480	0.0094	12.736	4.30	0.636	25.0	15.90	0.801	0.678	AL-B	none	2.0	1.7	1.077	197.8	1.19E-03	0.4893	DCB	574.4	0.252	0.412	1.004	0.612	1.289	0.341	184.6	1.28E-03	0.3824
I-2	SF	7-10-87		0.02204	0.0422	13.070	23.68	0.636	25.0	15.90	0.822	0.437	PQ-V	none	2.0	1.7	0.968	207.4	5.08E-03	0.0691	TCB	467.9	4.772	5.080	0.992	0.939	5.543	8.542	45.59	2.31E-02	0.1566
I-2	SF	7-10-87	remodel	0.02204	0.0422	13.070	23.68	0.636	25.0	15.90	0.822	0.437	PQ-V	none	2.0	1.7	0.968	207.4	5.08E-03	0.0691	TCB	467.9	4.772	5.080	0.992	0.939	5.543	8.542	45.59	2.31E-02	0.1566
I-10	SD	7-08-87		0.03555	0.0680	13.070	41.19	0.636	25.0	15.90	0.822	0.437	PQ-V	none	2.0	1.7	0.979	180.6	9.41E-03	0.0178	TCB	147.8	10.47	11.31	1.012	0.926	6.138	9.660	53.01	3.21E-02	0.1329
I-3	SG	7-13-87	alumina	0.01886	0.0376	12.529	20.05	0.636	25.0	15.90	0.788	0.721	AL-A	none	2.0	1.7	1.128	118.5	7.94E-03	1.1790	TCB	223.3	2.018	2.000	0.988	1.009	2.742	1.904	23.64	3.98E-02	0.1090
I-4	SH	7-15-87	alumina	0.01971	0.0387	12.736	22.19	0.636	25.0	15.90	0.801	0.678	AL-B	none	2.0	1.7	1.121	361.9	2.67E-03	0.0783	TCB	200.2	1.166	1.246	0.971	0.936	2.066	1.259	31.85	3.04E-02	0.0365
EXP		DATE	MISC	Q(CM3/S)	velocity	PV	PV INJ	area	lo	C vol	Θ	Pb	SURF	BOUND	KCL	KCL	Rf	P	D (KCl)	ssq	NAME	conc	Ksorb	K des	MASS	revers	Rf	Kp	P	D	ssq
I-2	SF	7-10-87		0.02204	0.0422	13.070	23.68	0.636	25.0	15.90	0.822	0.437	PQ-V	none	2.0	1.7	0.968	207.4	5.08E-03	0.0691	TeCB	235.1	8.493	9.001	1.008	0.944	8.957	14.96	39.403	2.67E-02	0.1031
I-2	SF	7-10-87	remodel	0.02204	0.0422	13.070	23.68	0.636	25.0	15.90	0.822	0.437	PQ-V	none	2.0	1.7	0.968	207.4	5.08E-03	0.0691	TeCB	235.1	8.493	9.001	1.008	0.944	8.957	14.96	39.403	2.67E-02	0.1031
I-10	SD	7-08-87		0.03555	0.0680	13.070	41.19	0.636	25.0	15.90	0.822	0.437	PQ-V	none	2.0	1.7	0.979	180.6	9.41E-03	0.0178	TeCB	187.8	15.76	16.01	1.031	0.984	8.858	14.77	44.535	3.82E-02	0.0962
I-3	SG	7-13-87	alumina	0.01886	0.0376	12.529	20.05	0.636	25.0	15.90	0.788	0.721	AL-A	none	2.0	1.7	1.128	118.5	7.94E-03	1.1790	TeCB	216.8	7.354	7.320	0.994	1.005	7.331	6.919	20.759	4.53E-02	0.1257
I-4	SH	7-15-87	alumina	0.01971	0.0387	12.736	22.19	0.636	25.0	15.90	0.801	0.678	AL-B	none	2.0	1.7	1.121	361.9	2.67E-03	0.0783	TeCB	175.6	4.232	4.512	0.985	0.938	4.797	4.486	13.601	7.11E-02	0.1087
A-3	QA	6-19-86		0.09500	0.1410	9.429	130.0	0.785	14.0	10.99	0.858	0.349	PQ-A	Cl poly	5.0	2.7	0.938	105.2	1.88E-02	>10	DCB	98.4	152.8	329.1	1.433	0.464	68.31	165.5	33.64	5.87E-02	0.3637
A-4	QB	6-23-86	sorb	0.12600	0.1871	9.429	166.0	0.785	14.0	10.99	0.858	0.349	PQ-A	Cl poly	5.0	2.7	0.958	108.1	2.42E-02	6.4400	DCB	79.1	126.8		1.416	0.417	72.45	175.7	2.160	1.21E+00	0.8062
A-4	QG	7-19-86	desorb	0.04410	0.0655	9.429	d(26days)	0.785	14.0	10.99	0.858	0.349	PQ-A	Cl poly	2.7	5.0	0.958	108.1	8.48E-03	6.4400	DCB	79.1		304.3	1.416	0.417	72.45	175.7	2.160	4.24E-01	0.8062
A-1	RF	4-28-87	d=34 hrs	0.02550	0.0467	2.728	224.8	0.636	5.00	3.18	0.858	0.349	PQ-A	Cl poly	2.0	1.7	1.047	20.72	1.13E-02	0.0077	DCB	216.1	498.7	414.7	1.057	1.203	196.0	479.4	4.286	5.45E-02	0.8062
A-1	RF	4-28-87	remodel	0.02550	0.0467	2.728	224.8	0.636	5.00	3.18	0.858	0.349	PQ-A	Cl poly	2.0	1.7	1.047	20.72	1.13E-02	0.0077	DCB	216.1	498.7	414.7	1.057	1.203	196.0	479.4	4.286	5.45E-02	0.8062
A-1	RF	4-28-87	remodel	0.02550	0.0467	2.728	224.8	0.636	5.00	3.18	0.858	0.349	PQ-A	Cl poly	2.0	1.7	1.047	20.72	1.13E-02	0.0077	DCB	216.1	498.7	414.7	1.057	1.203	196.0	479.4	4.286	5.45E-02	0.8062
A-2	RJ	5-28-87		0.02830	0.0519	2.728	295.5	0.636	5.00	3.18	0.858	0.349	PQ-A	Cl poly	2.0	1.7	1.287	8.928	2.90E-02	0.0562	DCB	76.2	300.6	477.6	1.212	0.629	145.6	355.5	5.581	4.65E-02	0.5230
A-2	RJ	5-28-87	remodel	0.02830	0.0519	2.728	295.5	0.636	5.00	3.18	0.858	0.349	PQ-A	Cl poly	2.0	1.7	1.287	8.928	2.90E-02	0.0562	DCB	76.2	300.6	477.6	1.212	0.629	145.6	355.5	5.581	4.65E-02	0.5230
O-2	RV	6-23-87		0.04450	0.0920	5.126	268.1	0.785	10.6	8.321	0.616	0.940	PQ-Q	ClpolyS	2.0	1.7	[illegible]	2.827	3.45E-01	0.0466	DCB	1160.	89.01	95.96	0.930	0.928	163.4	106.4	19.085	5.11E-02	1.0610
O-1	SA	7-01-87		0.02063	0.0415	2.513	240.3	0.785	5.05	3.964	0.634	0.898	PQ-R	ClpolyS	2.0	1.7	4.872	1.275	1.64E-01	4.1250	DCB	99.4	45.99	60.26	1.05	0.763	111.2	77.82	5.544	3.78E-02	0.3224
O-1	SA	7-01-87	remodel	0.02063	0.0415	2.513	240.3	0.785	5.05	3.964	0.634	0.898	PQ-R	ClpolyS	2.0	1.7	4.872	1.275	1.64E-01	4.1250	DCB	99.4	45.99	60.26	1.05	0.763	111.2	77.82	5.544	3.78E-02	0.3224
O-1	SA	7-01-87	remodel	0.02063	0.0415	2.513	240.3	0.785	5.05	3.964	0.634	0.898	PQ-R	ClpolyS	2.0	1.7	4.872	1.275	1.64E-01	4.1250	DCB	99.4	45.99	60.26	1.05	0.763	111.2	77.82	5.544	3.78E-02	0.3224
EXP		DATE	MISC	Q(CM3/S)	velocity	PV	PV INJ	area	lo	C vol	Θ	Pb	SURF	BOUND	KCL	KCL	Rf	P	D (KCl)	ssq	NAME	conc	Ksorb	K des	MASS	revers	Rf	Kp	P	D	ssq
B-2	QC	6-24-86		0.06000	0.0897	9.363	26.93	0.785	14.0	10.99	0.852	0.363	PQ-B	CB poly	5.0	2.7	0.865	73.49	1.71E-02	> 10	DCB	105.7	23.91	28.28	1.067	0.845	11.14	23.80	38.82	3.24E-02	0.1083
B-2	QC	6-24-86	pv≤1.178	0.06000	0.0897	9.363	26.93	0.785	14.0	10.99	0.852	0.363	PQ-B	CB poly	5.0	2.7	1.019	73.50	1.71E-02	7.3520	DCB	105.7	23.91	28.28	1.067	0.845	13.14	28.42	40.58	3.09E-02	0.8000
B-3	QD	6-25-86	sorb	0.01900	0.0284	9.363	21.22	0.785	14.0	10.99	0.852	0.363	PQ-B	CB poly	5.0	2.7	0.810	46.62	8.53E-03	0.2112	DCB	107.5	18.86		1.083	0.685	11.17	23.87	26.52	1.50E-02	0.0861
B-3	QD	6-25-86	pv≤1.441	0.01900	0.0284	9.363	21.22	0.785	14.0	10.99	0.852	0.363	PQ-B	CB poly	5.0	2.7	1.166	53.10	7.49E-03	0.0153	DCB	107.5	18.86		1.083	0.685	15.87	34.90	35.75	1.11E-02	0.0221
B-3	QE	7-15-86	desorb	0.01570	0.0235	9.363	d(20days)	0.785	14.0	10.99	0.852	0.363	PQ-B	CB poly	2.7	5.0	0.810	46.62	7.05E-03	0.2112	DCB	107.5		27.53	1.083	0.685	11.17	23.87	26.52	1.24E-02	0.0861
B-3	QE	7-15-86	pv≤1.131	0.01570	0.0235	9.363	d(20days)	0.785	14.0	10.99	0.852	0.363	PQ-B	CB poly	2.7	5.0	1.00F	0.0215	1.53E+01	0.4010	DCB	107.5		27.53	1.083	0.685	17.27	38.19	35.88	9.16E-03	0.0226
B-5	QF	7-17-86		0.00600	0.0090	9.363	16.49	0.785	14.0	10.99	0.852	0.363	PQ-B	CB poly	5.0	3.0	1.078	172.3	7.29E-04	0.0228	DCB	538.1	27.18	28.71	1.018	0.947	13.64	29.67	26.51	4.74E-03	0.1481
B-4	QH	7-31-86		0.01300	0.0194	9.363	32.20	0.785	14.0	10.99	0.852	0.363	PQ-B	CB poly	5.0	3.0	1.009	44.83	6.07E-03	1.5250	DCB	386.4	28.58	27.73	1.011	1.031	13.53	29.41	25.94	1.05E-02	0.1739
B-4	QH	7-31-86	pv≤1.100	0.01300	0.0194	9.363	32.20	0.785	14.0	10.99	0.852	0.363	PQ-B	CB poly	5.0	3.0	1.110	44.48	6.12E-03	0.0097	DCB	386.4	28.58	27.73	1.011	1.031	14.88	32.58	25.94	1.05E-02	0.1740
B-1	RK	6-02-87		0.02030	0.0375	7.586	28.05	0.636	14.0	8.904	0.852	0.363	PQ-B	CB poly	2.0	1.7	0.939	37.43	1.40E-02	0.0228	DCB	737.1	26.45	27.08	0.988	0.977	13.09	28.37	28.00	1.87E-02	0.0801
B-1	RK	6-02-87	remodel	0.02030	0.0375	7.586	28.05	0.636	14.0	8.904	0.852	0.363	PQ-B	CB poly	2.0	1.7	0.939	37.43	1.40E-02	0.0228	DCB	737.1	26.45	27.08	0.988	0.977	13.09	28.37	28.00	1.87E-02	0.0801
B-1	RK	6-02-87	remodel	0.02030	0.0375	7.586	28.05	0.636	14.0	8.904	0.852	0.363	PQ-B	CB poly	2.0	1.7	0.939	37.43	1.40E-02	0.0228	DCB	737.1	26.45	27.08	0.988	0.977	13.09	28.37	28.00	1.87E-02	0.0801
B-6	SO	7-30-87	LooseCol	0.02102	0.0388	7.586	34.91	0.636	14.0	8.904	0.852	0.363	PQ-B	CB poly	2.0	1.7	1.000	18.33	2.96E-02	0.3924	DCB	1113.	15.31	16.03	0.995	0.955	7.677	15.67	27.15	2.00E-02	0.0170
B-7	TC	9-22-87	DiffusCo	0.02480	0.0458	7.586	33.70	0.636	14.0	8.904	0.852	0.363	PQ-B	CB poly	2.0	1.7	1.071	19.04	3.37E-02	0.8072	DCB	1207.	26.73	39.57	0.986	0.676	12.54	27.09	13.91	4.61E-02	0.1496
B-7	TC	9-22-87	remodel	0.02480	0.0458	7.586	33.70	0.636	14.0	8.904	0.852	0.363	PQ-B	CB poly	2.0	1.7	1.071	19.04	3.37E-02	0.8072	DCB	1207.	26.73	39.57	0.986	0.676	12.54	27.09	13.91	4.61E-02	0.1496

EXPERIMENT NAME	LAB NAME	DATE	misc.	FIRST ORDER MODEL (or ORGANIC) solute Rf fixed=F	solute Kp (cm3/g)	solute Peclet fixed=	F*Dkcl	solute D (cm2/s)	solute omega (DAI)	solute kb F(s-1)	solute alpha i (g/cm3s)	SSQ (error)	E2 (nonequil spread)	E3 (tailing) (skew)	MOBILE IMMOBILE MODEL solute Rf fixed=F	solute Kp (cm3/g)	solute P fixed=F	*Dkcl	solute D (cm2/s)	solute omega fixed=F	solute alpha e (g/cm3s)	solute beta fixed=F	solute mobile porosity F	solute f (frac)	SSQ
I-6	Y	5-31-86																							
I-7	Z	6-03-86																							
I-8	ZZ	6-05-86																							
I-9	ZB	6-11-86																							
I-1	ZC	6-17-86		2.468	3.848	93.61	F:1.50	1.39E-03	63.90	2.88E-02	9.52E-03	0.1625	5.18E-01	7.06E-01	2.603	4.20	166.3	F:1.50	7.81E-04	0.7011	1.86E-04	0.8537	0.40 F	1.098	0.1153
I-1	ZC	6-17-86	remodel	2.717 F	4.501	140.4	F:1.00	9.25E-04	14.79	5.71E-03	1.88E-03	0.4034	3.79E+00	1.34E+01	2.717 F	4.50	140.4	F:1.00	9.25E-04	0.3605	9.56E-05	0.8540	0.40 F	1.082	0.1214
I-1	ZC	6-17-86	remodel	2.462	3.832	52.01	F:3.00	2.50E-03	503.7	2.28E-01	7.53E-02	0.1568	3.64E-02	3.73E-02	2.639	4.30	93.60	F:1.50	1.39E-03	0.1644	4.36E-05	0.9076	0.40 F	1.179	0.1115
I-2	SF	7-10-87		3.628	4.941	66.91	F:3.00	1.58E-02	1E+06	6.42E+02	2.81E+02	0.1258	3.51E-05	3.51E-05											
I-2	SF	7-10-87	remodel	3.724	5.122	138.3	F:1.50	7.62E-03	68.09	4.22E-02	1.84E-02	0.1397	1.09E+00	1.80E+00											
I-2	SF	7-10-87	remodel	2.600 F	3.008	207.4	F:1.00	5.08E-03	6.057	6.38E-03	2.79E-03	2.3576	1.30E+01	1.28E+02	2.600 F	3.01	207.4	F:1.00	5.08E-03	14.895	1.00E-02	0.0050 F	0.40 F	-0.296	2.8240
I-3	SG	7-13-87	alumina	1.562	0.614	71.86	F:1.50	1.31E-02	100000 F	2.68E+02	1.93E+02	0.6114	9.30E-05	9.30E-05	1.366 F	0.400	71.86	F:1.50	1.31E-02	55992	3.37E+01	0.8899 F	0.40 F	1.934	0.7020
I-4	SH	7-15-87	alumina																						
I-4	SH	7-15-87	remodel	1.292 F	0.345	362.0	F:1.00	2.67E-03	10.44	5.53E-02	3.75E-02	0.1102	1.77E+00	6.77E+00	1.292 F	0.345	362.0	F:1.00	2.67E-03	160.5	9.93E-02	0.0200 F	0.40 F	-1.622	0.0999
I-5	SI	7-17-87	alumina																						
I-2	SF	7-10-87		5.491	8.444	215.5		4.89E-03	39.72	1.49E-02	6.52E-03	0.1525	3.63E+00	1.10E+01											
I-2	SF	7-10-87	remodel	5.469	8.402	109.2	F:1.90	9.65E-03	53.43	2.02E-02	8.81E-03	0.1527	1.36E+00	2.41E+00											
I-10	SD	7-08-87		6.030	9.457	60.20	F:3.00	2.82E-02	285.1	1.54E-01	6.74E-02	0.1327	1.47E-01	1.59E-01	6.030	9.46	60.20	F:3.00	2.82E-02	409.1	4.45E-01	0.0001	0.40 F	-0.097	0.1326
I-3	SG	7-13-87	alumina																						
I-4	SH	7-15-87	alumina																						
EXP		DATE	MISC	RF 1st	Kp	P		D 1st	omega	kb	alpha i	ssq	E2	E3	RF 2nd	Kp	P	*Dkcl	D 2nd	omega	alpha e	B	Θe	f	ssq
I-2	SF	7-10-87		8.905	14.86	1000		1.05E-03	32.47	6.93E-03	3.03E-03	0.1158	2.43E+01	3.38E+02											
I-2	SF	7-10-87	remodel	8.767	14.60	56.05	F:3.70	1.88E-02	119.6	2.60E-02	1.14E-02	0.1094	3.68E-01	4.40E-01											
I-10	SD	7-08-87		8.686	14.45	45.00		3.78E-02	138.8	4.91E-02	2.15E-02	0.0966	2.54E-01	2.88E-01	8.669	14.42	45.00	F:4.00	3.78E-02	4195.2	4.56E+00	0.5736	0.40 F	0.585	0.0936
I-3	SG	7-13-87	alumina																						
I-4	SH	7-15-87	alumina																						
A-3	QA	6-19-86																							
A-4	QB	6-23-86	sorb	95.53	232.4	352.0	F:3.00	7.44E-03	6.720	9.50E-04	3.32E-04	0.4644	5.13E+01	1.37E+03											
A-4	QG	7-19-86	desorb	95.53	232.4	352.0	F:3.00	2.60E-03	6.720	3.32E-04	1.16E-04	0.4644	5.13E+01	1.37E+03											
A-1	RF	4-28-87	d=34 hrs	160.1	391.1	6.910	F:3.00	3.38E-02	6.720	3.95E-04	1.38E-04	0.1359	1.02E+00	1.53E+00	175.9	430.01	6.910	F:3.00	3.38E-02	2.714	1.01E-02	0.6420	0.40 F	0.643	0.0676
A-1	RF	4-28-87	remodel	166.8 F	407.6	13.81	F:1.50	1.69E-02	8.275	4.66E-04	1.63E-04	0.1715	1.65E+00	3.01E+00	185.3	453.09	13.81	F:1.50	1.69E-02	0.968	3.62E-03	0.5922	0.40 F	0.593	0.0705
A-1	RF	4-28-87	remodel	186.8 F	456.8	20.72	F:1.00	1.13E-02	6.413	3.23E-04	1.13E-04	0.3147	3.20E+00	8.32E+00	186.8 F	456.78	20.72	F:1.00	1.13E-02	1.277	4.77E-03	0.5231	0.40 F	0.523	0.0806
A-2	RJ	5-28-87		128.5	313.5	2.976	F:3.00	8.71E-02	185.9	1.51E-02	5.28E-03	1.7070	1.58E-02	1.59E-02	130.3	317.88	2.976	F:3.00	8.71E-02	874.0 F	3.63E+00	0.0201	0.40 F	0.017	1.6800
A-2	RJ	5-28-87	remodel	137.6	335.7	5.952	F:1.50	4.36E-02	208.2	1.58E-02	5.52E-03	1.0459	2.82E-02	2.86E-02	136.7	333.78	5.952	F:1.50	4.36E-02	106000	4.40E+02	0.3049	0.40 F	0.304	0.9893
O-2	RV	6-23-87		86.78	56.21	0.942	F:3.00	1.04E+00	2.289	2.32E-04	2.18E-04	2.6990	4.02E-01	4.83E-01	90.52	58.66	0.942	F:3.00	1.04E+00	2.157	7.49E-03	0.0528	0.40 F	0.046	2.6870
O-1	SA	7-01-87		99.99	69.90	16.37	F:3.00	1.28E-02	9.875	8.19E-04	7.35E-04	0.3849	1.62E+00	2.35E+00	106.6	74.63	16.37	F:3.00	1.28E-02	0.807	2.65E-03	0.6695	0.40 F	0.670	0.2993
O-1	SA	7-01-87	remodel	102.7	71.82	33.44	F:1.50	6.26E-03	7.780	6.28E-04	5.64E-04	0.3948	4.21E+00	1.31E+01	110.5	77.35	33.44	F:1.50	6.26E-03	1.057	3.47E-03	0.5922	0.40 F	0.592	0.2961
O-1	SA	7-01-87	remodel	76.25 F	53.14	47.39	F:1.00	4.42E-03	10.46	1.14E-03	1.02E-03	1.8594	4.41E+00	1.42E+01	76.25 F	53.14	47.39	F:1.00	4.42E-03	10.056	3.30E-02	3E-05	0.40 F	-0.008	1.8576
EXP		DATE	MISC	RF 1st	Kp	P	*Dkcl	D 1st	omega	kb	alpha i	ssq	E2	E3	RF 2nd	Kp	P	*Dkcl	D 2nd	omega	alpha e	B	Θe	f	ssq
B-2	QC	6-24-86		13.92	30.32	71.78	F:1.50	1.75E-02	207.1	1.03E-01	3.73E-02	0.8971	2.99E-01	3.45E-01	13.90	30.28	71.78	F:1.50	1.75E-02	238.4	6.11E-01	2E-06	0.40 F	-0.036	0.8946
B-2	QC	6-24-86	pv≤1.178																						
B-3	QD	6-25-86	sorb	11.59	24.86	35.40	F:1.50	1.12E-02	87.54	1.68E-02	6.09E-03	0.3770	3.38E-01	3.97E-01	11.65	25.00	35.40	F:1.50	1.12E-02	2.427	1.97E-03	0.8413	0.40 F	0.876	0.3766
B-3	QD	6-25-86	pv≤1.441	11.53	24.72	18.01	F:3.00	2.21E-02	784.5	1.51E-01	5.49E-02	0.4330	1.91E-02	1.93E-02											
B-3	QE	7-15-86	desorb																						
B-3	QE	7-15-86	pv≤1.131	11.53	24.72	18.01	F:3.00	1.82E-02	784.5	1.25E-01	4.53E-02	0.4330	1.91E-02	1.93E-02											
B-5	QF	7-17-86																							
B-4	QH	7-31-86																							
B-4	QH	7-31-86	pv≤1.100	13.59	29.55	29.65	F:1.50	9.18E-03	30.44	3.36E-03	1.22E-03	0.3103	8.36E-01	1.20E+00	38.33	87.62	29.65	F:1.50	9.18E-03	0.0925	5.14E-05	0.3469	0.40 F	0.344	0.2175
B-1	RK	6-02-87		12.75	27.57	301.5		1.74E-03	25.16	5.73E-03	2.08E-03	0.0728	1.02E+01	6.42E+01	12.36	26.66	22.06		2.38E-02	14188	1.52E+01	0.7414	0.40 F	0.765	0.0801
B-1	RK	6-02-87	remodel	12.43 F	26.83	24.95	F:1.50	2.10E-02	526.1	1.23E-01	4.47E-02	0.0872	4.01E-02	4.09E-02	12.40 F	26.76	24.95	F1.50	2.10E-02	6724.1	7.20E+00	0.3344 F	0.40 F	0.323	0.0720
B-1	RK	6-02-87	remodel	12.40 F	26.76	37.43	F:1.00	1.40E-02	67.14	1.58E-02	5.72E-03	0.0809	4.71E-01	5.87E-01	12.40 F	26.76	37.43	F1.00	1.40E-02	78.092	8.36E-02	0.0050 F	0.40 F	-0.036	0.0806
B-6	SO	7-30-87	LooseCol	7.398	15.02	27.15	F:3.00	2.00E-02	710.2	3.08E-01	1.12E-01	0.0176	2.86E-02	2.90E-02	7.394	15.01	25.61		2.12E-02	238.5	2.64E-01	0.9623	0.40 F	1.039	0.0173
B-7	TC	9-22-87	DiffusCo	10.85	23.11	6.347	F:3.00	1.01E-01	471267	1.56E+02	5.68E+01	0.2158	1.11E-05	1.11E-05	10.88	23.19	6.347	F:3.00	1.01E-01	68509	7.23E+01	0.3623	0.32 F	1.021	0.2890
B-7	TC	9-22-87	remodel	15.12 F	33.14	133.5	F:1.00	4.30E-03	8.878	2.06E-03	7.46E-04	1.1425	1.31E+01	1.31E+01	15.12 F	33.14	133.5	F:1.00	4.80E-03	0.2194	2.32E-04	0.7676	0.32 F	0.795	0.7788

B.2 Solute and KCl Column Modeling Data

NAME		DATE	misc.	COLUMN DATA Q (cm3/s)	ave vel v (cm/s)	pore vol (cm3)	pv inject	column area (cm2)	col le (cm)	col volume (cm3)	total poro-sity	bulk density (g/cm3)	surf name	bound organic	EQUILIB MODEL KCl initial conc (-log	KCl final conc Molar)	KCl Rf	KCl Peclet	KCl D (cm2/s)	SSQ (error)	SOLUTE name	conc ppb	planimeter sorb (solute) Kp (cm3/g)	desorb Kp (cm3/g)	mass balance PV/PVinj	reverse Kps/Kpd	EQUILIBRIUM MODEL solute Rf	solute Kp (cm3/g)	solute Peclet	solute D (cm2/s)	SSQ (error)
C-2	BJ	8-05-86		0.04100	0.0754	7.613	33.50	0.636	14.0	8.904	0.855	0.356	PO-C	C18poly	5.0	3.0	1.078	83.07	1.27E-02	0.0353	DCB	353.1	23.08	24.61	0.981	0.938	11.08	24.21	12.30	8.58E-02	0.0168
C-2	BJ	8-05-86	remodel	0.04100	0.0754	7.613	33.50	0.636	14.0	8.904	0.855	0.356	PO-C	C18poly	5.0	3.0	1.078	83.07	1.27E-02	0.0353	DCB	353.1	23.08	24.61	0.981	0.938	11.08	24.21	12.30	8.58E-02	0.0168
C-1	CK	8-07-86	sorb	0.00380	0.00699	7.613	17.60	0.636	14.0	8.904	0.855	0.356	PO-C	C18poly	5.0	3.0	1.036	103.9	9.42E-04	0.0199	DCB	266.4	25.89		0.977	1.125	11.57	25.39	34.91	2.80E-03	0.0968
C-1	CK	8-08-86	desorb	0.00430	0.00791	7.613	d(15hrs)	0.636	14.0	8.904	0.855	0.356	PO-C	C18poly	3.0	5.0	1.036	103.9	1.07E-03	0.0199	DCB	266.4		23.01	0.977	1.125	11.57	25.39	34.91	3.17E-03	0.0968
C-1	CK	8-08-86	pv21.039	0.00380	0.00699	7.613	17.60	0.636	14.0	8.904	0.855	0.356	PO-C	C18poly	5.0	3.0	1.076	103.3	9.47E-04	0.0282	DCB	266.4	25.89		0.977	1.125	12.02	26.47	34.74	2.82E-03	0.1057
C-1	CK	8-08-86	remodel	0.00380	0.00699	7.613	17.60	0.636	14.0	8.904	0.855	0.356	PO-C	C18poly	5.0	3.0	1.076	103.3	9.47E-04	0.0282	DCB	266.4	25.89		0.977	1.125	12.02	26.47	34.74	2.82E-03	0.1057
C-1	CK	8-08-86	remodel	0.00380	0.00699	7.613	17.60	0.636	14.0	8.904	0.855	0.356	PO-C	C18poly	5.0	3.0	1.076	103.3	9.47E-04	0.0282	DCB	266.4	25.89		0.977	1.125	12.02	26.47	34.74	2.82E-03	0.1057
C-3	BL	8-10-86	sorb	0.01270	0.0234	7.613	19.90	0.636	14.0	8.904	0.855	0.356	PO-C	C18poly	5.0	3.0	1.308	22.28	1.47E-02	0.2688	DCB	282.2	18.28		1.010	0.855	9.799	21.13	10.29	3.21E-02	0.3205
C-3	BL	8-10-86	pv21.071	0.01270	0.0234	7.613	19.90	0.636	14.0	8.904	0.855	0.356	PO-C	C18poly	5.0	3.0	1.000	3.011	1.09E-01	0.7221	DCB	282.2	18.28		1.010	0.855	10.05	21.74	24.52	1.33E-02	0.0509
C-3	BT	10-13-86	desorb	0.02220	0.0408	7.613	d(62days)	0.636	14.0	8.904	0.855	0.356	PO-C	C18poly	3.0	5.0	1.308	22.28	2.57E-02	0.2688	DCB	282.2		21.39	1.010	0.855	9.799	21.13	10.20	5.60E-02	0.3205
C-3	BT	10-13-86	pv21.071	0.02220	0.0408	7.613	d(62days)	0.636	14.0	8.904	0.855	0.356	PO-C	C18poly	3.0	5.0	0.860	24.52	2.33E-02	0.0051	DCB	282.2		21.39	1.010	0.855	11.71	25.72	6.567	8.70E-02	0.0446
EXP		DATE	MISC	Q(CM3/S)	velocity	PV	PV INJ	area	le	C vol	θ	Pb	SURF	BOUND	KCL	KCL	Rf	P	D (KCl)	ssq	NAME	conc	Ksorb	K des	MASS	revers	Rf	Kp	P	D	ssq
D-3	GN	8-13-86	sorb	0.00190	0.00283	9.407	4.38	0.785	14.0	10.99	0.856	0.352	PO-B	PHEmono	5.0	2.0	0.994	195.9	2.02E-04	0.0517	DCB	172.1	6.106		1.003	1.097	3.446	5.948	70.11	5.65E-04	0.1866
D-3	GN	8-14-86	desorb	0.00250	0.00372	9.407	d(17hrs)	0.785	14.0	10.99	0.856	0.352	PO-B	PHEmono	2.0	5.0	0.994	195.9	2.66E-04	0.0517	DCB	172.1		5.564	1.003	1.097	3.466	5.997	70.11	7.43E-04	0.1866
D-4	[illegible]	8-19-86	sorb	0.00790	0.01176	9.407	10.50	0.785	14.0	10.99	0.856	0.352	PO-B	PHEmono	5.0	2.0	1.010	70.91	2.32E-03	0.0097	DCB	478.8	4.472				2.637	3.981	25.31	6.45E-03	0.1790
D-4	DU	10-22-86	desorb	0.07870	0.1171	9.407	d(44days)	0.785	14.0	10.99	0.856	0.352	PO-B	PHEmono	2.0	5.0	—				DCB	478.8									
D-1	RL	6-04-87		0.00616	0.0092	7.123	6.151	0.785	10.6	8.321	0.856	0.352	PO-B	PHEmono	2.0	1.7	1.033	136.1	7.14E-04	0.0114	DCB	599.1	3.334	2.828	1.029	1.179	2.428	3.473	33.098	2.94E-03	0.0924
D-1	RL	6-04-87	remodel	0.00616	0.0092	7.123	6.151	0.785	10.6	8.321	0.856	0.352	PO-B	PHEmono	2.0	1.7	1.033	136.1	7.14E-04	0.0114	DCB	599.1	3.334	2.828	1.029	1.179	2.428	3.473	33.098	2.94E-03	0.0924
D-2	RN	6-08-87		0.00652	0.0097	7.123	5.660	0.785	10.6	8.321	0.856	0.352	PO-B	PHEmono	2.0	1.7	1.075	136.8	7.52E-04	0.0313	DCB	506.2	2.186	4.621	1.016	0.473	2.191	2.896	32.28	3.19E-03	0.0809
D-2	RN	6-08-87	remodel	0.00652	0.0097	7.123	5.660	0.785	10.6	8.321	0.856	0.352	PO-B	PHEmono	2.0	1.7	1.075	136.8	7.52E-04	0.0313	DCB	506.2	2.186	4.621	1.016	0.473	2.191	2.896	32.28	3.19E-03	0.0809
O-2	SN	7-28-87		0.00465	0.0069	3.397	17.960	0.785	5.05	3.964	0.857	0.351	PO-T	PHEmono	2.0	1.7	1.381	103.1	3.39E-04	0.1090	DCB	889.9	3.773	5.479	1.032	0.689	2.628	3.975	78.021	4.47E-04	0.1380
O-2	SN	7-28-87	remodel	0.00465	0.0069	3.397	17.960	0.785	5.05	3.964	0.857	0.351	PO-T	PHEmono	2.0	1.7	1.381	103.1	3.39E-04	0.1090	DCB	889.9	3.773	5.479	1.032	0.689	2.628	3.975	78.021	4.47E-04	0.1380
O-1	SN	7-29-87		0.00301	0.0045	3.397	6.532	0.785	5.05	3.964	0.857	0.351	PO-T	PHEmono	2.0	1.7	1.381	111.5	2.03E-04	0.0106	DCB	1198.	2.792	3.551	0.991	0.786	2.582	3.863	93.854	2.41E-04	0.0485
O-1	SN	7-29-87	remodel	0.00301	0.0045	3.397	6.532	0.785	5.05	3.964	0.857	0.351	PO-T	PHEmono	2.0	1.7	1.381	111.5	2.03E-04	0.0106	DCB	1198.	2.792	3.551	0.991	0.786	2.582	3.863	93.854	2.41E-04	0.0485
O-1	SN	7-29-87	remodel	0.00301	0.0045	3.397	6.532	0.785	5.05	3.964	0.857	0.351	PO-T	PHEmono	2.0	1.7	1.381	111.5	2.03E-04	0.0106	DCB	1198.	2.792	3.551	0.991	0.786	2.582	3.863	93.854	2.41E-04	0.0485
E-17	RT	6-20-87		0.01070	0.0197	2.709	22.000	0.636	5.00	3.18	0.852	0.361	PO-E	PHEpoly	2.0	1.7	1.031	92.85	1.06E-03	0.0055	CB	2640.	4.873	13.96	1.046	0.349	4.079	7.267	1.774	5.57E-02	0.2561
E-17	RT	6-20-87	remodel	0.01070	0.0197	2.709	22.000	0.636	5.00	3.18	0.852	0.361	PO-E	PHEpoly	2.0	1.7	1.031	92.85	1.06E-03	0.0055	CB	2640.	4.873	13.96	1.046	0.349	4.079	7.267	1.774	5.57E-02	0.2561
E-18	RW	6-24-87		0.00843	0.0156	2.709	52.930	0.636	5.00	3.18	0.852	0.361	PO-E	PHEpoly	2.0	1.7	0.954	97.25	8.00E-04	0.0466	CB	3174.	11.32	1.652	0.962	6.852	3.942	6.943	12.82	6.07E-03	0.5301
EXP		DATE	MISC	Q(CM3/S)	velocity	PV	PV INJ	area	le	C vol	θ	Pb	SURF	BOUND	KCL	KCL	Rf	P	D (KCl)	ssq	NAME	conc	Ksorb	K des	MASS	revers	Rf	Kp	P	D	ssq
E-5	GP	8-23-86	sorb	0.12600	0.1884	9.363	30.70	0.785	14.0	10.99	0.852	0.361	PO-E	PHEpoly	5.0	2.0	0.792	2.074	1.27E+00	0.3290	DCB	564.3	8.015		1.027	0.806	5.350	10.266	2.596	1.02E+00	0.1289
E-5	GP	8-23-86	desorb	0.00940	0.0141	9.363	d(30 min)	0.785	14.0	10.99	0.852	0.361	PO-E	PHEpoly	2.0	5.0	0.792	2.074	9.49E-02	0.3290	DCB	564.3		9.949	1.027	0.806	5.350	10.266	2.596	7.58E-02	0.1289
E-5	GP	8-23-86	pv21.105	0.06770	0.1012	9.363	30.70	0.785	14.0	10.99	0.852	0.361	PO-E	PHEpoly	5.0	2.0	0.874	1.651	8.58E-01	0.3411	DCB	564.3	8.015	9.949	1.027	0.806	6.004	11.810	2.741	5.17E-01	0.1348
E-1	DQ	9-12-86	sorb	0.00940	0.0141	9.363	28.80	0.785	14.0	10.99	0.852	0.361	PO-E	PHEpoly	5.0	2.0	0.998	31.29	6.29E-03	0.0528	DCB	368.9	18.23		1.052	0.633	8.956	18.777	1.409	1.40E-01	0.2124
E-1	DR	9-24-86	desorb	0.01900	0.0284	9.363	d(12days)	0.785	14.0	10.99	0.852	0.361	PO-E	PHEpoly	2.0	5.0	[illegible]	31.29	1.27E-02	0.0528	DCB	368.9		28.78	1.052	0.633	8.956	18.777	1.409	2.82E-01	0.2124
E-1	DQQR	9-12-86	remodel	0.00940	0.0141	9.363	28.80	0.785	14.0	10.99	0.852	0.361	PO-E	PHEpoly	5.0	2.0	0.998	31.29	6.29E-03	0.0528	DCB	368.9	18.23		1.052	0.633	8.956	18.777	1.409	1.40E-01	0.2124
E-1	DQQR	9-12-86	remodel	0.00940	0.0141	9.363	28.80	0.785	14.0	10.99	0.852	0.361	PO-E	PHEpoly	5.0	2.0	0.998	31.29	6.29E-03	0.0528	DCB	368.9	18.23		1.052	0.633	8.956	18.777	1.409	1.40E-01	0.2124
E-2	RM	6-09-87		0.00793	0.0146	2.709	38.46	0.636	5.00	3.18	0.852	0.361	PO-E	PHEpoly	2.0	1.7	0.943	82.27	8.89E-04	0.0127	DCB	569.6	59.45	53.24	1.031	1.117	23.88	53.999	2.916	2.51E-02	0.0592
E-2	RM	6-09-87	remodel	0.00793	0.0146	2.709	38.46	0.636	5.00	3.18	0.852	0.361	PO-E	PHEpoly	2.0	1.7	0.943	82.27	8.89E-04	0.0127	DCB	569.6	59.45	53.24	1.031	1.117	23.88	54.00	2.916	2.51E-02	0.0592
E-3	SR	8-07-87		0.00867	0.0160	2.709	47.65	0.636	5.00	3.18	0.852	0.361	PO-E	PHEpoly	5.0	4.5	0.408	15.97	5.01E-03	0.3216	DCB	1157.	72.38	56.85	0.967	1.273	36.94	84.82	1.787	4.48E-02	0.2512
E-3	SR	8-07-87	remodel	0.00867	0.0160	2.709	47.65	0.636	5.00	3.18	0.852	0.361	PO-E	PHEpoly	5.0	4.5	0.408	15.97	5.01E-03	0.3216	DCB	1157.	72.38	56.85	0.967	1.273	36.94	84.82	1.787	4.48E-02	0.2512
E-3	SR	8-07-87	remodel	0.00867	0.0160	2.709	47.65	0.636	5.00	3.18	0.852	0.361	PO-E	PHEpoly	5.0	4.5	0.408	15.97	5.01E-03	0.3216	DCB	1157.	72.38	56.85	0.967	1.273	36.94	84.82	1.787	4.48E-02	0.2512
E-4	TD	10-08-87	d=16 hrs	0.01041	0.0192	2.709	106.01	0.636	5.00	3.18	0.852	0.361	PO-E	PHEpoly	3.0	2.7	0.880	84.61	1.14E-03	0.2444	DCB	395.2	98.41	92.39	0.991	1.065	47.24	109.1	1.512	6.35E-02	0.2720
E-4	TD	10-08-87	remodel	0.01041	0.0192	2.709	106.01	0.636	5.00	3.18	0.852	0.361	PO-E	PHEpoly	3.0	2.7	0.880	84.61	1.14E-03	0.2444	DCB	395.2	98.41	92.39	0.991	1.065	47.24	109.1	1.512	6.35E-02	0.2720
E-4	TD	10-08-87	remodel	0.01041	0.0192	2.709	106.01	0.636	5.00	3.18	0.852	0.361	PO-E	PHEpoly	3.0	2.7	0.880	84.61	1.14E-03	0.2444	DCB	395.2	98.41	92.39	0.991	1.065	47.24	109.1	1.512	6.35E-02	0.2720
EXP		DATE	MISC	Q(CM3/S)	velocity	PV	PV INJ	area	le	C vol	θ	Pb	SURF	BOUND	KCL	KCL	Rf	P	D (KCl)	ssq	NAME	conc	Ksorb	K des	MASS	revers	Rf	Kp	P	D	ssq
E-6	SY	8-18-87	3 C	0.04601	0.0849	2.709	247.13	0.636	5.00	3.18	0.852	0.361	PO-E	PHEpoly	2.0	1.7	0.976	9.963	4.26E-02	0.2037	DCB	1928.	26.43	28.15	0.971	0.939	10.72	22.94	0.9178	4.63E-01	0.0691
E-6	SY	8-18-87	remodel	0.04601	0.0849	2.709	247.13	0.636	5.00	3.18	0.852	0.361	PO-E	PHEpoly	2.0	1.7	0.976	9.963	4.26E-02	0.2037	DCB	1928.	26.43	28.15	0.971	0.939	10.72	22.94	0.9178	4.63E-01	0.0691
E-6	SY	8-18-87	remodel	0.04601	0.0849	2.709	247.13	0.636	5.00	3.18	0.852	0.361	PO-E	PHEpoly	2.0	1.7	0.976	9.963	4.26E-02	0.2037	DCB	1928.	26.43	28.15	0.971	0.939	10.72	22.94	0.9178	4.63E-01	0.0691
E-7	SI	8-17-87	11 C	0.04448	0.0821	2.709	236.93	0.636	5.00	3.18	0.852	0.361	PO-E	PHEpoly	2.0	1.7	1.105	12.47	3.29E-02	0.0897	DCB	1971.	31.86	38.70	0.962	0.823	12.87	28.01	1.674	2.45E-01	0.1404
E-7	SI	8-17-87	remodel	0.04448	0.0821	2.709	236.93	0.636	5.00	3.18	0.852	0.361	PO-E	PHEpoly	2.0	1.7	1.105	12.47	3.29E-02	0.0897	DCB	1971.	31.86	38.70	0.962	0.823	12.87	28.01	1.674	2.45E-01	0.1404
E-7	SI	8-17-87	remodel	0.04448	0.0821	2.709	236.93	0.636	5.00	3.18	0.852	0.361	PO-E	PHEpoly	2.0	1.7	1.105	12.47	3.29E-02	0.0897	DCB	1971.	31.86	38.70	0.962	0.823	12.87	28.01	1.674	2.45E-01	0.1404
E-8	SZ	8-19-87	17 C	0.04152	0.0766	2.709	216.11	0.636	5.00	3.18	0.852	0.361	PO-E	PHEpoly	2.0	1.7	1.102	0.8171	4.69E-01	0.2919	DCB	1898.	46.00	35.49	0.990	1.296	11.09	23.81	0.5938	6.45E-01	0.0829
E-8	SZ	8-19-87	remodel	0.04152	0.0766	2.709	216.11	0.636	5.00	3.18	0.852	0.361	PO-E	PHEpoly	2.0	1.7	1.102	0.8171	4.69E-01	0.2919	DCB	1898.	46.00	35.49	0.990	1.296	11.09	23.81	0.5938	6.45E-01	0.0829
E-8	SZ	8-19-87	remodel	0.04152	0.0766	2.709	216.11	0.636	5.00	3.18	0.852	0.361	PO-E	PHEpoly	2.0	1.7	1.102	0.8171	4.69E-01	0.2919	DCB	1898.	46.00	35.49	0.990	1.296	11.09	23.81	0.5938	6.45E-01	0.0829
E-9	SS	8-04-87	25 C	0.04976	0.0918	2.709	847.03	0.636	5.00	3.18	0.852	0.361	PO-E	PHEpoly	2.0	1.7	1.106	33.12	1.39E-02	0.0321	DCB	548.6	105.5	115.6	0.984	0.913	38.34	88.13	0.7732	5.94E-01	0.6544
E-9	SS	8-04-87	remodel	0.04976	0.0918	2.709	847.03	0.636	5.00	3.18	0.852	0.361	PO-E	PHEpoly	2.0	1.7	1.106	33.12	1.39E-02	0.0321	DCB	548.6	105.5	115.6	0.984	0.913	38.34	88.13	0.7732	5.94E-01	0.6544
E-9	SS	8-04-87	remodel	0.04976	0.0918	2.709	847.03	0.636	5.00	3.18	0.852	0.361	PO-E	PHEpoly	2.0	1.7	1.106	33.12	1.39E-02	0.0321	DCB	548.6	105.5	115.6	0.984	0.913	38.34	88.13	0.7732	5.94E-01	0.6544
E-10	TA	8-20-87	35 C	0.04706	0.0868	2.709	244.64	0.636	5.00	3.18	0.852	0.361	PO-E	PHEpoly	2.0	1.7	0.667	44.14	9.84E-03	0.0100	DCB	1252.	12.74	14.73	0.997	0.865	5.826	11.39	0.6712	6.47E-01	0.1103
E-10	TA	8-20-87	remodel	0.04706	0.0868	2.709	244.64	0.636	5.00	3.18	0.852	0.361	PO-E	PHEpoly	2.0	1.7	0.667	44.14	9.84E-03	0.0100	DCB	1252.	12.74	14.73	0.997	0.865	5.826	11.39	0.6712	6.47E-01	0.1103
E-10	TA	8-20-87	remodel	0.04706	0.0868	2.709	244.64	0.636	5.00	3.18	0.852	0.361	PO-E	PHEpoly	2.0	1.7	0.667	44.14	9.84E-03	0.0100	DCB	1252.	12.74	14.73	0.997	0.865	5.826	11.39	0.6712	6.47E-01	0.1103
E-11	TB	8-21-87	48 C	0.04877	0.0900	2.709	260.81	0.636	5.00	3.18	0.852	0.361	PO-E	PHEpoly	2.0	1.7	0.918	7.604	5.92E-02	0.0442	DCB	1013.	32.64	39.06	1.048	0.835	7.764	15.96	0.3585	1.26E+00	0.0882
E-11	TB	8-21-87	remodel	0.04877	0.0900	2.709	260.81	0.636	5.00	3.18	0.852	0.361	PO-E	PHEpoly	2.0	1.7	0.918	7.604	5.92E-02	0.0442	DCB	1013.	32.64	39.08	1.048	0.835	7.764	15.96	0.3585	1.26E+00	0.0882
E-11	TB	8-21-87	remodel	0.04877	0.0900	2.709	260.81	0.636	5.00	3.18	0.852	0.361	PO-E	PHEpoly	2.0	1.7	0.918	7.604	5.92E-02	0.0442	DCB	1013.	32.64	39.08	1.048	0.835	7.764	15.96	0.3585	1.26E+00	0.0882

NAME		DATE	misc.	FIRST ORDER MODEL (or ORGANIC) solute Rf fixed=F	solute Kp (cm3/g)	solute Peclet fixed=F	FXDkcl	solute D (cm2/s)	solute omega (DAI)	solute kb F(s-1)	solute alpha i (g/cm3s)	SSQ (error)	E2 (nonequil spread)	E3 (tailing) (skew)	solute Rf fixed=F	solute Kp (cm3/g)	solute P fixed=F	FXDkcl	solute D (cm2/s)	solute omega fixed=F	solute alpha e (g/cm3s)	solute beta fixed=F	solute mobile pore-F	solute f (frac)	SSQ
C-2	BJ	8-05-86		10.37	22.50	27.69	F:3.00	3.81E-02	17.64	1.01E-02	3.61E-03	0.0226	1.28E+00	2.15E+00	10.50	22.82	27.69	F:3.00	3.81E-02	2.714	3.85E-03	0.6420	0.40 F	0.660	0.0199
C-2	BJ	8-05-86	remodel	10.53	22.89	55.38	F:1.50	1.91E-02	13.00	7.35E-03	2.62E-03	0.0239	3.49E+00	9.91E+00	10.67	23.22	55.38	F:1.50	1.91E-02	3.748	8.07E-03	0.5130	0.40 F	0.518	0.1493
C-1	CK	8-07-86	sorb																						
C-1	CK	8-08-86	desorb																						
C-1	CK	8-08-86	pv21.039	10.53	22.89	34.60	F:3.00	2.83E-03	113.2	5.93E-03	2.11E-03	0.4430	2.50E-01	2.83E-01	29.64	68.78	34.60	F:3.00	2.83E-03	0.0896	1.79E-05	0.3550	0.40 F	0.351	0.2374
C-1	CK	8-08-86	remodel	11.38	24.93	68.87	F:1.50	1.42E-03	49.74	2.39E-03	8.52E-04	[illegible]	1.15E+00	1.85E+00	12.39 F	27.36	68.87	F:1.50	1.42E-03	6724.0	1.34E+00	0.3341	0.40 F	0.322	0.0719
C-1	CK	8-08-86	remodel	11.18 F	24.45	103.9	F:1.00	9.42E-04	26.39	1.29E-03	4.61E-04	0.6166	3.26E+00	8.87E+00	11.18 F	24.45	103.9	F:1.00	9.42E-04	0.8735	1.74E-04	0.8125	0.40 F	0.846	0.4151
C-3	BL	8-10-86	sorb																						
C-3	BL	8-10-86	pv21.071																						
C-3	BT	10-13-86	desorb																						
C-3	BT	10-13-86	pv21.071																						
EXP		DATE	MISC	Rf 1st	Kp	P	FXDkcl	D 1st	omega	kb	alpha i	ssq	E2	E3	Rf 2nd	Kp	P	FXDkcl	D 2nd	omega	alpha e	B	θe	f	ssq
D-3	GN	8-13-86	sorb																						
D-3	GN	8-14-86	desorb																						
D-4	[illegible]	8-19-86	sorb																						
D-4	DU	10-22-86	desorb																						
D-1	RL	6-04-87		2.317	3.203	26.75		3.63E-03	1E+06	6.57E+02	2.31E+02	0.0750	8.64E-06	8.64E-06	2.322	3.215	35.23		2.76E-03	544308	1.88E+02	0.3670	0.40 F	0.291	0.0786
D-1	RL	6-04-87	remodel	2.377	3.349	90.76	F:1.50	1.07E-03	18.32	1.15E-02	4.05E-03	0.1047	1.66E+00	3.63E+00	2.539	3.743	90.76	F:1.50	1.07E-03	0.3109	1.08E-04	0.8595	0.40 F	1.114	0.0379
D-2	RN	6-08-87		2.121	2.726	45.60	F:3.00	2.26E-03	37.46	3.06E-02	1.08E-02	0.0866	3.40E-01	4.29E-01	2.272	3.093	45.60	F:3.00	2.26E-03	0.1320	4.83E-05	0.8960	0.40 F	1.233	0.0505
D-2	RN	6-08-87	remodel	2.169	2.843	91.20	F:1.50	1.13E-03	16.10	1.26E-02	4.44E-03	0.0884	1.65E+00	3.69E+00	2.294	3.147	91.20	F:1.50	1.13E-03	0.3562	1.30E-04	0.8617	0.40 F	1.166	0.0526
O-2	SN	7-28-87		2.607	3.924	26.01	F:3.00	1.34E-03	1100 F	9.37E-01	3.29E-01	0.2825	8.98E-03	9.04E-03	2.648	4.024	26.01	F:3.00	1.34E-03	778349	4.26E+02	0.2300	0.40 F	0.086	0.2341
O-2	SN	7-28-87	remodel	2.599	3.904	68.72	F:1.50	5.08E-04	14355	1.23E+01	4.31E+00	0.1176	1.81E-03	1.81E-03	2.597	3.899	68.72	F:1.50	5.08E-04	0.0193	1.06E-05	0.9999	0.40 F	1.334	0.1378
O-1	SN	7-29-87		2.518	3.706	37.18	F:3.00	6.08E-04	1E+06	5.84E+02	2.05E+02	0.0994	1.35E-05	1.35E-05	2.522	3.716	37.18	F:3.00	6.08E-04	100000	3.54E+01	0.2472	0.40 F	0.103	0.1244
O-1	SN	7-29-87	remodel	2.541	3.762	74.36	F:1.50	3.04E-04	2229	1.28E+00	4.50E-01	0.0536	1.23E-02	1.24E-02	2.554	3.794	74.36	F:1.50	3.04E-04	5273.4	1.87E+00	0.3998	0.40 F	0.357	0.0489
O-1	SN	7-29-87	remodel	2.300 F	3.174	111.5	F:1.00	2.03E-04	26.72	1.82E-02	6.39E-03	0.5078	1.33E+00	2.62E+00	2.300 F	3.174	111.5	F:1.00	2.03E-04	68.177 F	2.42E-02	0.0050 F	0.40 F	-0.350	0.4929
E-17	RT	6-20-87		4.227	7.616	30.95	F:3.00	3.19E-03	1.982	2.43E-03	8.76E-04	0.4440	9.10E+00	5.76E+01	4.268	7.713	30.95	F:3.00	3.19E-03	1.666	2.63E-03	0.2820	0.40 F	0.225	0.4390
E-17	RT	6-20-87	remodel	4.990 F	9.417	92.85	F:1.00	1.06E-03	1.765	1.75E-03	6.31E-04	0.4892	3.36E+01	6.77E+02	4.990 F	9.417	92.85	F:1.00	1.06E-03	0.980	1.55E-03	0.3743	0.40 F	0.350	0.4588
E-18	RW	6-24-87		2.648	3.889	32.42	F:3.00	2.40E-03	1.065	2.01E-03	7.26E-04	1.0590	1.18E+01	1.06E+02	2.878	4.432	32.42	F:3.00	2.40E-03	0.671	8.35E-04	0.4250	0.40 F	0.401	1.0200
EXP		DATE	MISC	Rf 1st	Kp	P	FXDkcl	D 1st	omega	kb	alpha i	ssq	E2	E3	Rf 2nd	Kp	P	FXDkcl	D 2nd	omega	alpha e	B	θe	f	ssq
E-5	GP	8-23-86	sorb																						
E-5	GP	8-23-86	desorb																						
E-5	GP	8-23-86	pv21.105	4.806 F	8.98	98.22	F:1.00	1.44E-02	2.195	4.17E-03	1.51E-03	0.1377	2.81E+01	4.78E+02	4.806 F	8.983	98.22	F:1.00	1.44E-02	2.593	7.50E-03	0.1170	0.40 F	0.024	0.1160
E-1	DQ	9-12-86	sorb	6.838	13.78	10.43	F:3.00	1.89E-02	2.973	5.11E-04	1.85E-04	0.4960	2.56E+00	6.13E+00	8.396	17.46	10.43	F:3.00	1.89E-02	0.526	2.11E-04	0.4980	0.40 F	0.502	0.2660
E-1	DR	9-24-86	desorb	6.838	13.78	10.43	F:3.00	3.81E-02	2.973	1.03E-03	3.73E-04	0.4960	2.56E+00	6.13E+00	8.396	17.46	10.43	F:3.00	3.81E-02	0.526	4.27E-04	0.4980	0.40 F	0.502	0.2660
E-1	DQQR	9-12-86	remodel	10.96 F	23.51	31.29	F:1.00	6.29E-03	1.722	1.74E-04	6.27E-05	1.2605	1.50E+01	1.33E+02	10.96 F	23.51	31.29	F:1.00	6.29E-03	0.392	1.57E-04	0.5535	0.40 F	0.562	0.4199
E-1	DQQR	9-12-86	remodel	7.174	14.57	20.86	F:1.50	9.43E-03	2.701	4.39E-04	1.59E-04	0.5534	5.72E+00	2.35E+01	9.083	19.08	20.86	F:1.50	9.43E-03	0.578	2.32E-04	0.4532	0.40 F	0.451	0.3220
E-2	RM	6-09-87		20.13	45.15	27.42	F:3.00	2.67E-03	3.804	5.82E-04	2.10E-04	0.2840	6.51E+00	2.83E+01	23.86	54.00	27.42	F:3.00	2.67E-03	0.919	1.08E-03	0.4530	0.40 F	0.452	0.0759
E-2	RM	6-09-87	remodel	20.48	45.97	54.85	F:1.50	1.33E-03	3.608	5.42E-04	1.96E-04	0.2864	1.38E+01	1.11E+02	23.73	53.65	54.85	F:1.50	1.33E-03	1.119	1.31E-03	0.4110	0.40 F	0.408	0.1030
E-3	SR	8-07-87		24.81	56.19	5.323	F:3.00	1.50E-02	5.259	7.07E-04	2.55E-04	0.5080	9.32E-01	1.38E+00	33.58	76.88	5.323	F:3.00	1.50E-02	0.411	5.26E-04	0.5534	0.40 F	0.556	0.2123
E-3	SR	8-07-87	remodel	28.06	63.86	44.49	F:1.50	1.80E-03	3.259	3.85E-04	1.39E-04	0.5854	1.27E+01	9.48E+01	33.97	77.81	44.49	F:1.50	1.80E-03	1.143	1.46E-03	0.3552	0.40 F	0.352	0.3319
E-3	SR	8-07-87	remodel	28.38 F	64.62	87.69	F:1.00	9.12E-04	3.176	3.71E-04	1.34E-04	0.5862	2.57E+01	3.62E+02	28.38 F	64.62	87.69	F:1.00	9.12E-04	1.613	2.06E-03	0.3103	0.40 F	0.304	0.4716
E-4	TD	10-08-87	d=16 hrs	35.54	81.52	28.20	F:3.00	3.41E-03	2.900	3.23E-04	1.16E-04	0.4624	9.18E+00	5.20E+01	39.32	90.44	28.20	F:3.00	3.41E-03	1.435	2.21E-03	0.2761	0.40 F	0.271	0.4445
E-4	TD	10-08-87	remodel	35.92	82.42	41.35	F:1.50	2.32E-03	2.840	3.12E-04	1.13E-04	0.4635	1.38E+01	1.10E+02	37.22	85.48	41.35	F:1.50	2.32E-03	2.121	3.26E-03	0.1511	0.40 F	0.142	0.4655
E-4	TD	10-08-87	remodel	41.42 F	95.40	77.81	F:1.00	1.23E-03	2.563	2.44E-04	8.80E-05	0.5768	2.89E+01	4.52E+02	41.42 F	95.40	77.81	F:1.00	1.23E-03	1.508	2.32E-03	0.2394	0.40 F	0.234	0.4721
EXP		DATE	MISC	Rf 1st	Kp	P	FXDkcl	D 1st	omega	kb	alpha i	ssq	E2	E3	Rf 2nd	Kp	P	FXDkcl	D 2nd	omega	alpha e	B	θe	f	ssq
E-6	SY	8-18-87	3 C	6.460	12.89	3.320	F:3.00	1.28E-01	2.738	8.52E-03	3.07E-03	0.2271	8.66E-01	1.28E+00	9.258	19.49	3.320	F:3.00	1.28E-01	0.183	1.24E-03	0.4622	0.40 F	0.461	0.0266
E-6	SY	8-18-87	remodel	8.134	16.84	26.36	F:1.50	1.61E-02	[illegible]	4.31E-03	1.55E-03	0.2518	1.12E+01	7.87E+01	9.961	21.15	26.36	F:1.50	1.61E-02	0.532	3.62E-03	0.3490	0.40 F	0.336	0.0756
E-6	SY	8-18-87	remodel	12.56 F	27.28	9.960	F:1.00	4.26E-02	1.243	1.83E-03	6.59E-04	0.6680	6.79E+00	3.09E+01	12.56 F	27.28	9.960	F:1.00	4.26E-02	0.273	1.85E-03	0.3238	0.40 F	0.311	0.0726
E-7	SI	8-17-87	11 C	9.090	19.09	4.157	F:3.00	9.87E-02	5.224	1.06E-02	3.83E-03	0.1997	6.30E-01	8.42E-01	10.99	23.57	4.157	F:3.00	9.87E-02	0.246	1.62E-03	0.6057	0.40 F	0.619	0.1388
E-7	SI	8-17-87	remodel	9.921	21.05	8.313	F:1.50	4.94E-02	3.622	6.67E-03	2.41E-03	0.2179	1.86E+00	3.68E+00	11.20	24.07	8.313	F:1.50	4.94E-02	0.636	4.18E-03	0.4830	0.40 F	0.484	0.1580
E-7	SI	8-17-87	remodel	15.95 F	35.28	12.47	F:1.00	3.29E-02	1.939	2.13E-03	7.69E-04	0.7656	5.65E+00	2.22E+01	15.95 F	35.28	12.47	F:1.00	3.29E-02	0.353	2.32E-03	0.3920	0.40 F	0.387	0.2671
E-8	SZ	8-19-87	17 C	5.812	11.36	3.320	F:3.00	1.15E-01	1.764	5.62E-03	2.03E-03	0.1973	1.29E+00	2.22E+00	10.20	21.70	3.320	F:3.00	1.15E-01	0.175	1.07E-03	0.3604	0.40 F	0.349	0.0871
E-8	SZ	8-19-87	remodel	7.337	14.96	27.19	F:1.50	1.41E-02	1.429	3.46E-03	1.25E-03	0.2085	1.42E+01	1.73E+02	7.344	14.97	27.19	F:1.50	1.41E-02	1.420	3.70E-03	0.1385	0.40 F	0.086	0.2085
E-8	SZ	8-19-87	remodel	18.26 F	40.74	31.39	F:1.00	1.22E-02	0.668	5.93E-04	2.14E-04	0.9712	4.20E+01	9.50E+02	18.26 F	40.74	31.39	F:1.00	1.22E-02	0.299	3.83E-03	0.1910	0.40 F	0.175	0.3934
E-9	SS	8-04-87	25 C	26.41	59.96	11.04	F:3.00	4.16E-02	2.147	1.55E-03	5.60E-04	0.7614	4.76E+00	1.63E+01	30.30	69.16	11.04	F:3.00	4.16E-02	1.026	7.54E-03	0.2290	0.40 F	0.221	0.6452
E-9	SS	8-04-87	remodel	27.54	62.64	22.08	F:1.50	2.08E-02	2.045	1.42E-03	5.11E-04	0.7633	1.00E+01	6.13E+01	31.17	71.20	33.12	F:1.50	1.39E-02	1.124	8.26E-03	0.1977	0.40 F	0.189	0.6582
E-9	SS	8-04-87	remodel	47.84 F	110.5	33.12	F:1.00	1.39E-02	1.438	5.64E-04	2.04E-04	1.2930	2.21E+01	2.68E+02	47.84 F	110.5	33.12	F:1.00	1.39E-02	0.832	6.11E-03	0.1590	0.40 F	0.152	0.9281
E-10	TA	8-20-87	35 C	4.288	7.760	14.71	F:3.00	2.95E-02	0.922	4.87E-03	1.76E-03	0.1883	9.38E+00	6.08E+01	5.388	10.36	14.71	F:3.00	2.95E-02	0.407	2.83E-03	0.3549	0.40 F	0.329	0.1641
E-10	TA	8-20-87	remodel	4.444	8.128	29.43	F:1.50	1.48E-02	0.926	4.67E-03	1.69E-03	0.1894	1.91E+01	2.30E+02	4.638	8.586	29.43	F:1.50	1.48E-02	0.793	5.51E-03	0.2447	0.40 F	0.183	0.1810
E-10	TA	8-20-87	remodel	6.820 F	13.74	44.13	F:1.00	9.84E-03	0.637	1.90E-03	6.86E-04	0.3633	5.05E+01	1.44E+03	6.820 F	13.74	44.13	F:1.00	9.84E-03	0.412	2.88E-03	0.2740	0.40 F	0.240	0.2492
E-11	TB	8-21-87	48 C	3.855	6.738	2.540	F:3.00	1.77E-01	0.543	3.42E-03	1.23E-03	0.1798	2.57E+00	6.51E+00	5.682	11.05	2.540	F:3.00	1.77E-01	0.172	1.24E-03	0.3250	0.40 F	0.294	0.0761
E-11	TB	8-21-87	remodel	4.361	7.932	5.069	F:1.50	8.88E-02	0.639	3.42E-03	1.24E-03	0.1836	4.71E+00	1.76E+01	5.961	11.71	5.069	F:1.50	8.88E-02	0.272	1.96E-03	0.2965	0.40 F	0.262	0.1011
E-11	TB	8-21-87	remodel	16.19 F	35.85	7.600	F:1.00	5.92E-02	0.265	3.14E-04	1.13E-04	0.5798	2.52E+01	3.54E+02	16.19 F	35.85	7.600	F:1.00	5.92E-02	0.148	1.06E-03	0.1326	0.40 F	0.110	0.2175

B.3 Solute and KCl Column Modeling Data

COLUMN DATA — EQUILIB MODEL — SOLUTE — planimeter — EQUILIBRIUM MODEL — FIRST ORDER MODEL (or ORGANIC) — MOBILE IMMOBILE MODEL

NAME	DATE	misc.	θ (cm3/s)	ave vel v (cm/s)	pore vol (cm3)	pv inject	column area (cm2)	col le (cm)	col volume (cm3)	total pore-sity	bulk density (g/cm3)	surf name	bound organic	KCl initial conc (-logMolar)	KCl final conc	KCl Rf	KCl Peclet	KCl D (cm2/s)	SSQ (error)	name	conc ppb	sorb (solute) Kp (cm3/g)	desorb Kp (cm3/g)	mass balance PV/PVinj	reverse Kps/Kpd	solute Rf	solute Kp (cm3/g)	solute Peclet	solute D (cm2/s)	SSQ (error)
E-12 RI	6-26-87		0.02863	0.0528	2.709	140.78	0.636	5.00	3.18	0.852	0.361	PQ-E	PHEpoly	2.0	1.7	0.964	43.27	6.11E-03	0.0202	TCB	500.4	81.42	85.17	1.006	0.956	35.97	82.54	1.747	1.51E-01	0.0855
E-12 RI	6-26-87	remodel	0.02863	0.0528	2.709	140.78	0.636	5.00	3.18	0.852	0.361	PQ-E	PHEpoly	2.0	1.7	0.964	43.27	6.11E-03	0.0202	TCB	500.4	81.42	85.17	1.006	0.956	35.97	82.54	1.747	1.51E-01	0.0855
E-13 RI	6-30-87		0.02905	0.0536	2.709	156.37	0.636	5.00	3.18	0.852	0.361	PQ-E	PHEpoly	2.0	1.7	0.918	20.90	1.28E-02	0.6638	TCB	197.1	84.61	90.41	0.954	0.936	39.20	90.16	1.261	2.13E-01	0.1256
E-13 RI	6-30-87	remodel	0.02905	0.0536	2.709	156.37	0.636	5.00	3.18	0.852	0.361	PQ-E	PHEpoly	2.0	1.7	0.918	20.90	1.28E-02	0.6638	TCB	197.1	84.61	90.41	0.954	0.936	39.20	90.16	1.261	2.13E-01	0.1256
E-14 SB	7-02-87		0.07169	0.1323	2.709	244.50	0.636	5.00	3.18	0.852	0.361	PQ-E	PHEpoly	2.0	1.7	1.034	55.28	1.20E-02	0.3101	TCB	30.6	138.7	88.19	0.992	1.573	39.01	89.71	0.3287	2.01E+00	0.4840
E-14 SB	7-02-87	remodel	0.07169	0.1323	2.709	244.50	0.636	5.00	3.18	0.852	0.361	PQ-E	PHEpoly	2.0	1.7	1.034	55.28	1.20E-02	0.3101	TCB	30.6	138.7	88.19	0.992	1.573	39.01	89.71	0.3287	2.01E+00	0.4840
E-15 SC	7-07-87		0.04131	0.0762	2.709	207.74	0.636	5.00	3.18	0.852	0.361	PQ-E	PHEpoly	2.0	1.7	0.941	65.01	5.86E-03	0.0059	TCB	430.1	203.8	116.1	0.960	1.755	103.8	242.5	0.7120	5.35E-01	0.4098
E-15 SC	7-07-87	remodel	0.04131	0.0762	2.709	207.74	0.636	5.00	3.18	0.852	0.361	PQ-E	PHEpoly	2.0	1.7	0.941	65.01	5.86E-03	0.0059	TCB	430.1	203.8	116.1	0.960	1.755	103.8	242.5	0.7120	5.35E-01	0.4098
E-15 SC	7-07-87	remodel	0.04131	0.0762	2.709	207.74	0.636	5.00	3.18	0.852	0.361	PQ-E	PHEpoly	2.0	1.7	0.941	65.01	5.86E-03	0.0059	TCB	430.1	203.8	116.1	0.960	1.755	103.8	242.5	0.7120	5.35E-01	0.4098
E-6 SY	8-18-87	3 C	0.04601	0.0849	2.709	247.13	0.636	5.00	3.18	0.852	0.361	PQ-E	PHEpoly	2.0	1.7	0.976	9.963	4.26E-02	0.2037	TCB	465.1	108.2	52.53	1.008	2.060	42.07	96.93	0.3863	1.10E+00	0.0499
E-6 SY	8-18-87	remodel	0.04601	0.0849	2.709	247.13	0.636	5.00	3.18	0.852	0.361	PQ-E	PHEpoly	2.0	1.7	0.976	9.963	4.26E-02	0.2037	TCB	465.1	108.2	52.53	1.008	2.060	42.07	96.93	0.3863	1.10E+00	0.0499
E-6 SY	8-18-87	remodel	0.04601	0.0849	2.709	247.13	0.636	5.00	3.18	0.852	0.361	PQ-E	PHEpoly	2.0	1.7	0.976	9.963	4.26E-02	0.2037	TCB	465.1	108.2	52.53	1.008	2.060	42.07	96.93	0.3863	1.10E+00	0.0499
E-7 SX	8-17-87	11 C	0.04448	0.0821	2.709	236.93	0.636	5.00	3.18	0.852	0.361	PQ-E	PHEpoly	2.0	1.7	1.105	12.47	3.29E-02	0.0897	TCB	481.0	131.6	101.9	0.968	1.291	70.75	164.6	0.4703	8.73E-01	0.4363
E-7 SX	8-17-87	remodel	0.04448	0.0821	2.709	236.93	0.636	5.00	3.18	0.852	0.361	PQ-E	PHEpoly	2.0	1.7	1.105	12.47	3.29E-02	0.0897	TCB	481.0	131.6	101.9	0.968	1.291	70.75	164.6	0.4703	8.73E-01	0.4363
E-7 SX	8-17-87	remodel	0.04448	0.0821	2.709	236.93	0.636	5.00	3.18	0.852	0.361	PQ-E	PHEpoly	2.0	1.7	1.105	12.47	3.29E-02	0.0897	TCB	481.0	131.6	101.9	0.968	1.291	70.75	164.6	0.4703	8.73E-01	0.4363
E-8 SZ	8-19-87	17 C	0.04152	0.0766	2.709	216.11	0.636	5.00	3.18	0.852	0.361	PQ-E	PHEpoly	2.0	1.7	1.102	0.8171	4.69E-01	0.2919	TCB	183.0	73.18	67.17	1.047	1.089	34.50	79.07	0.3672	1.04E+00	0.1226
E-8 SZ	8-19-87	remodel	0.04152	0.0766	2.709	216.11	0.636	5.00	3.18	0.852	0.361	PQ-E	PHEpoly	2.0	1.7	1.102	0.8171	4.69E-01	0.2919	TCB	183.0	73.18	67.17	1.047	1.089	34.50	79.07	0.3672	1.04E+00	0.1226
E-8 SZ	8-19-87	remodel	0.04152	0.0766	2.709	216.11	0.636	5.00	3.18	0.852	0.361	PQ-E	PHEpoly	2.0	1.7	1.102	0.8171	4.69E-01	0.2919	TCB	183.0	73.18	67.17	1.047	1.089	34.50	79.07	0.3672	1.04E+00	0.1226
E-9 SS	8-04-87	25 C	0.04976	0.0918	2.709	847.03	0.636	5.00	3.18	0.852	0.361	PQ-E	PHEpoly	2.0	1.7	1.106	33.12	1.39E-02	0.0321	TCB	85.2	262.1	202.6	0.998	1.294	114.6	268.1	0.8811	5.21E-01	1.7400
E-9 SS	8-04-87	remodel	0.04976	0.0918	2.709	847.03	0.636	5.00	3.18	0.852	0.361	PQ-E	PHEpoly	2.0	1.7	1.106	33.12	1.39E-02	0.0321	TCB	85.2	262.1	202.6	0.998	1.294	114.6	268.1	0.8811	5.21E-01	1.7400
E-9 SS	8-04-87	remodel	0.04976	0.0918	2.709	847.03	0.636	5.00	3.18	0.852	0.361	PQ-E	PHEpoly	2.0	1.7	1.106	33.12	1.39E-02	0.0321	TCB	85.2	262.1	202.6	0.998	1.294	114.6	268.1	0.8811	5.21E-01	1.7400
E-10 TA	8-20-87	35 C	0.04706	0.0868	2.709	244.64	0.636	5.00	3.18	0.852	0.361	PQ-E	PHEpoly	2.0	1.7	.667	44.14	9.84E-03	0.0100	TCB	209.1	44.16	52.46	1.051	0.842	20.22	45.36	0.3712	1.17E+00	0.2134
E-10 TA	8-20-87	remodel	0.04706	0.0868	2.709	244.64	0.636	5.00	3.18	0.852	0.361	PQ-E	PHEpoly	2.0	1.7	0.667	44.14	9.84E-03	0.0100	TCB	209.1	44.16	52.46	1.051	0.842	20.22	45.36	0.3712	1.17E+00	0.2134
E-10 TA	8-20-87	remodel	0.04706	0.0868	2.709	244.64	0.636	5.00	3.18	0.852	0.361	PQ-E	PHEpoly	2.0	1.7	0.667	44.14	9.84E-03	0.0100	TCB	209.1	44.16	52.46	1.051	0.842	20.22	45.36	0.3712	1.17E+00	0.2134
E-11 TB	8-21-87	48 C	0.04877	0.0900	2.709	260.81	0.636	5.00	3.18	0.852	0.361	PQ-E	PHEpoly	2.0	1.7	0.918	7.604	5.92E-02	0.0442	TCB	160.5	47.34	61.97	1.009	0.764	23.81	53.82	0.2523	1.78E+00	0.0448
E-11 TB	8-21-87	remodel	0.04877	0.0900	2.709	260.81	0.636	5.00	3.18	0.852	0.361	PQ-E	PHEpoly	2.0	1.7	0.918	7.604	5.92E-02	0.0442	TCB	160.5	47.34	61.97	1.009	0.764	23.81	53.82	0.2523	1.78E+00	0.0448
E-11 TB	8-21-87	remodel	0.04877	0.0900	2.709	260.81	0.636	5.00	3.18	0.852	0.361	PQ-E	PHEpoly	2.0	1.7	0.918	7.604	5.92E-02	0.0442	TCB	160.5	47.34	61.97	1.009	0.764	23.81	53.82	0.2523	1.78E+00	0.0448

NAME	DATE	misc.	solute Rf fixed=F	solute Kp (cm3/g)	solute Peclet fixed=F	FIXkcl	solute D (cm2/s)	solute omega (DAI)	solute kb F(s-1)	solute alpha i (g/cm3s)	SSQ (error)	E2 (nonequil spread)	E3 (tailing) (stev)	solute Rf fixed=F	solute Kp (cm3/g)	solute P fixed=F	FIXkcl	solute D (cm2/s)	solute omega fixed=F	solute alpha e (g/cm3s)	solute beta fixed=F	solute mobile pore= F	solute f (frac)	SSQ
E-12 RI	6-26-87		27.39	62.28	15.53	F:3.00	1.70E-02	2.613	1.05E-03	3.78E-04	0.3380	5.52E+00	2.10E+01	33.75	77.30	15.53	F:3.00	1.70E-02	0.609	2.58E-03	0.3950	0.40 F	0.393	0.2110
E-12 RI	6-26-87	remodel	28.53	64.97	22.77	F:1.50	1.16E-02	2.394	9.19E-04	3.32E-04	0.4114	8.86E+00	4.88E+01											
E-13 RI	6-30-87		27.30	62.06	6.967	F:3.00	3.85E-02	3.260	1.33E-03	4.80E-04	0.3506	1.98E+00	3.99E+00	35.81	82.16	6.967	F:3.00	3.85E-02	0.470	2.02E-03	0.3733	0.40 F	0.371	0.1076
E-13 RI	6-30-87	remodel	29.78	67.92	23.92	F:1.50	1.12E-02	2.691	1.00E-03	3.62E-04	0.3724	8.30E+00	4.34E+01											
E-14 SB	7-02-87		37.97	87.26	18.43	F:3.00	3.59E-02	0.794	5.68E-04	2.05E-04	0.3579	2.20E+01	2.67E+02	39.65	91.23	18.43	F:3.00	3.59E-02	0.685	7.25E-03	0.0389	0.40 F	0.028	0.3354
E-14 SB	7-02-87	remodel	37.95	87.21	18.19	F:1.50	3.64E-02	0.793	5.68E-04	2.05E-04	0.3578	2.17E+01	2.61E+02											
E-15 SC	7-07-87		58.18	135.0	21.67	F:3.00	1.76E-02	2.303	6.14E-04	2.22E-04	0.9324	9.09E+00	5.08E+01	58.02	134.58	21.67	F:3.00	1.76E-02	2.335	1.42E-02	0.0122	0.40 F	0.004	0.9301
E-15 SC	7-07-87	remodel	59.11	137.1	34.22	F:1.50	1.11E-02	2.255	5.92E-04	2.14E-04	0.9937	1.47E+01	1.23E+02											
E-15 SC	7-07-87	remodel	68.77 F	159.9	65.01	F:1.00	5.86E-03	1.983	4.46E-04	1.61E-04	1.0060	3.18E+01	5.42E+02	68.77 F	159.94	65.01	F:1.00	5.86E-03	0.646	3.94E-03	0.3953	0.40 F	0.394	0.6302
E-6 SY	8-18-87	3 C	14.92	32.85	2.210	F:4.50	1.92E-01	2.832	3.46E-03	1.25E-03	0.4167	6.79E-01	9.19E-01	26.97	61.28	2.210	F:4.50	1.92E-01	0.239	1.62E-03	0.3329	0.40 F	0.328	0.0571
E-6 SY	8-18-87	remodel	20.16	45.22	20.81	F:1.90	2.04E-02	1.849	1.64E-03	5.92E-04	0.4928	1.02E+01	6.32E+01											
E-6 SY	8-18-87	remodel	35.05 F	80.36	9.960	F:1.00	4.26E-02	1.166	5.82E-04	2.10E-04	1.1410	3.06E+00	4.10E+01	35.05 F	80.36	9.960	F:1.00	4.26E-02	0.457	3.10E-03	0.2110	0.40 F	0.203	0.1727
E-7 SX	8-17-87	11 C	24.51	55.49	2.770	F:4.50	1.48E-01	4.257	2.97E-03	1.07E-03	0.7588	5.99E-01	7.82E-01	89.09	207.91	2.770	F:4.50	1.48E-01	0.166	1.09E-03	0.2369	0.40 F	0.234	0.3019
E-7 SX	8-17-87	remodel	28.06	63.86	6.563	F:1.90	6.25E-02	3.011	1.83E-03	6.59E-04	0.8200	2.03E+00	4.12E+00											
E-7 SX	8-17-87	remodel	50.47 F	116.8	12.47	F:1.00	3.29E-02	1.665	5.53E-04	1.99E-04	1.5780	7.20E+00	3.33E+01	50.47 F	116.75	12.47	F:1.00	3.29E-02	0.485	3.18E-03	0.2995	0.40 F	0.296	0.6532
E-8 SZ	8-19-87	17 C	14.23	31.22	2.770	F:4.50	1.38E-01	1.660	1.92E-03	6.94E-04	0.2449	1.44E+00	2.52E+00	18.30	42.01	2.770	F:4.50	1.38E-01	0.453	2.77E-03	0.2956	0.40 F	0.286	0.2044
E-8 SZ	8-19-87	remodel	18.22	40.64	21.47	F:1.90	1.78E-02	1.442	1.28E-03	4.63E-04	0.2798	1.33E+01	1.04E+02											
E-8 SZ	8-19-87	remodel	30.73 F	70.17	31.39	F:1.00	1.22E-02	1.034	5.33E-04	1.92E-04	0.7162	2.84E+01	4.39E+02	30.73 F	70.17	31.39	F:1.00	1.22E-02	0.651	3.99E-03	0.1460	0.40 F	0.135	0.5180
E-9 SS	8-04-87	25 C	72.21	168.1	7.360	F:4.50	6.24E-02	3.502	9.03E-04	3.26E-04	1.6058	2.04E+00	6.15E+00	72.57	168.91	7.360	F:4.50	6.24E-02	3.165	2.33E-02	0.0500 F	0.40 F	0.044	1.5990
E-9 SS	8-04-87	remodel	76.97	179.3	17.43	F:1.90	2.63E-02	3.071	7.42E-04	2.68E-04	1.6076	5.53E+00	2.09E+01											
E-9 SS	8-04-87	remodel	99.45 F	232.4	33.12	F:1.00	1.39E-02	2.514	4.69E-04	1.69E-04	1.8760	1.29E+01	9.67E+01	99.45 F	232.35	33.12	F:1.00	1.39E-02	1.857	1.36E-02	0.1100	0.40 F	0.106	1.8010
E-10 TA	8-20-87	35 C	10.49	22.39	9.100	F:4.50	4.77E-02	1.364	2.50E-03	9.02E-04	0.3492	5.46E+00	2.12E+01	11.81	25.52	9.100	F:4.50	4.77E-02	0.796	5.53E-03	0.2291	0.40 F	0.207	0.3254
E-10 TA	8-20-87	remodel	11.17	24.00	23.23	F:1.90	1.87E-02	1.329	2.27E-03	8.19E-04	0.3504	1.45E+01	1.25E+02											
E-10 TA	8-20-87	remodel	21.47 F	48.31	44.13	F:1.00	9.84E-03	0.846	7.18E-04	2.59E-04	0.8484	4.74E+01	1.20E+03	21.47 F	48.31	44.13	F:1.00	9.84E-03	0.560	3.89E-03	0.1517	0.40 F	0.136	0.6589
E-11 TB	8-21-87	48 C	7.629	15.65	1.690	F:4.50	2.66E-01	1.195	3.24E-03	1.17E-03	0.2175	1.07E+00	1.68E+00	12.05	26.08	1.690	F:4.50	2.66E-01	0.210	1.51E-03	0.3050	0.40 F	0.290	0.0902
E-11 TB	8-21-87	remodel	10.58	22.61	4.002	F:1.90	1.12E-01	1.126	2.12E-03	7.64E-04	0.2355	2.91E+00	7.39E+00											
E-11 TB	8-21-87	remodel	24.16 F	54.66	7.600	F:1.00	5.92E-02	0.626	4.86E-04	1.76E-04	0.8056	1.12E+01	7.49E+01	24.16 F	54.66	7.600	F:1.00	5.92E-02	0.310	2.23E-03	0.1567	0.40 F	0.143	0.3073

EXP	DATE	MISC	θ(CM3/S)	velocity	PV	PV INJ	area	le	C vol	θ	Pb	SURF	BOUND	KCL	KCL	Rf	P	D (KCl)	ssq	NAME	conc	Ksorb	K des	MASS	revers	RF	Kp	P	D	ssq
E-14 SB	7-02-87		0.07169	0.1323	2.709	244.50	0.636	5.00	3.18	0.852	0.361	PQ-E	PHEpoly	2.0	1.7	1.034	55.28	1.20E-02	0.3101	TeCB	700.8	135.3	144.3	0.969	0.938	67.96	158.0	0.8724	7.58E-01	0.2444
E-14 SB	7-02-87	remodel	0.07169	0.1323	2.709	244.50	0.636	5.00	3.18	0.852	0.361	PQ-E	PHEpoly	2.0	1.7	1.034	55.28	1.20E-02	0.3101	TeCB	700.8	135.3	144.3	0.969	0.938	67.96	158.0	0.8724	7.58E-01	0.2444
E-15 SC	7-07-87		0.04131	0.0762	2.709	207.74	0.636	5.00	3.18	0.852	0.361	PQ-E	PHEpoly	2.0	1.7	0.941	65.01	5.86E-03	0.0059	TeCB	571.4	438.0	536.9	0.954	0.816	265.7	624.6	0.8748	4.36E-01	0.2531
E-15 SC	7-07-87	remodel	0.04131	0.0762	2.709	207.74	0.636	5.00	3.18	0.852	0.361	PQ-E	PHEpoly	2.0	1.7	0.941	65.01	5.86E-03	0.0059	TeCB	571.4	438.0	536.9	0.954	0.816	265.7	624.6	0.8748	4.36E-01	0.2531
E-15 SC	7-07-87	remodel	0.04131	0.0762	2.709	207.74	0.636	5.00	3.18	0.852	0.361	PQ-E	PHEpoly	2.0	1.7	0.941	65.01	5.86E-03	0.0059	TeCB	571.4	438.0	536.9	0.954	0.816	265.7	624.6	0.8748	4.36E-01	0.2531
E-6 SY	8-18-87	3 C	0.04601	0.0849	2.709	247.13	0.636	5.00	3.18	0.852	0.361	PQ-E	PHEpoly	2.0	1.7	0.976	9.963	4.26E-02	0.2037	TeCB	247.3	288.4	201.7	1.018	1.430	126.7	296.7	0.2835	1.50E+00	0.0624
E-6 SY	8-18-87	remodel	0.04601	0.0849	2.709	247.13	0.636	5.00	3.18	0.852	0.361	PQ-E	PHEpoly	2.0	1.7	0.976	9.963	4.26E-02	0.2037	TeCB	247.3	288.4	201.7	1.018	1.430	126.7	296.7	0.2835	1.50E+00	0.0624
E-6 SY	8-18-87	remodel	0.04601	0.0849	2.709	247.13	0.636	5.00	3.18	0.852	0.361	PQ-E	PHEpoly	2.0	1.7	0.976	9.963	4.26E-02	0.2037	TeCB	247.3	288.4	201.7	1.018	1.430	126.7	296.7	0.2835	1.50E+00	0.0624
E-7 SX	8-17-87	11 C	0.04448	0.0821	2.709	236.93	0.636	5.00	3.18	0.852	0.361	PQ-E	PHEpoly	2.0	1.7	1.105	12.47	3.29E-02	0.0897	TeCB	251.0	308.1	221.1	0.982	1.393	297.0	698.5	0.2952	1.39E+00	0.3846
E-7 SX	8-17-87	remodel	0.04448	0.0821	2.709	236.93	0.636	5.00	3.18	0.852	0.361	PQ-E	PHEpoly	2.0	1.7	1.105	12.47	3.29E-02	0.0897	TeCB	251.0	308.1	221.1	0.982	1.393	297.0	698.5	0.2952	1.39E+00	0.3846
E-7 SX	8-17-87	remodel	0.04448	0.0821	2.709	236.93	0.636	5.00	3.18	0.852	0.361	PQ-E	PHEpoly	2.0	1.7	1.105	12.47	3.29E-02	0.0897	TeCB	251.0	308.1	221.1	0.982	1.393	297.0	698.5	0.2952	1.39E+00	0.3846
E-8 SZ	8-19-87	17 C	0.04152	0.0766	2.709	216.11	0.636	5.00	3.18	0.852	0.361	PQ-E	PHEpoly	2.0	1.7	1.102	0.8171	4.69E-01	0.2919	TeCB	216.6	260.5	153.6	1.042	1.696	107.6	251.7	0.2647	1.45E+00	0.4845
E-8 SZ	8-19-87	remodel	0.04152	0.0766	2.709	216.11	0.636	5.00	3.18	0.852	0.361	PQ-E	PHEpoly	2.0	1.7	1.102	0.8171	4.69E-01	0.2919	TeCB	216.6	260.5	153.6	1.042	1.696	107.6	251.7	0.2647	1.45E+00	0.4845
E-8 SZ	8-19-87	remodel	0.04152	0.0766	2.709	216.11	0.636	5.00	3.18	0.852	0.361	PQ-E	PHEpoly	2.0	1.7	1.102	0.8171	4.69E-01	0.2919	TeCB	216.6	260.5	153.6	1.042	1.696	107.6	251.7	0.2647	1.45E+00	0.4845
E-9 SS	8-04-87	25 C	0.04976	0.0918	2.709	847.03	0.636	5.00	3.18	0.852	0.361	PQ-E	PHEpoly	2.0	1.7	1.106	33.12	1.39E-02	0.0321	TeCB	138.1	563.6	563.6	1.029	1.000	340.5	801.2	0.7589	6.05E-01	1.5710
E-9 SS	8-04-87	remodel	0.04976	0.0918	2.709	847.03	0.636	5.00	3.18	0.852	0.361	PQ-E	PHEpoly	2.0	1.7	1.106	33.12	1.39E-02	0.0321	TeCB	138.1	563.6	563.6	1.029	1.000	340.5	801.2	0.7589	6.05E-01	1.5710
E-9 SS	8-04-87	remodel	0.04976	0.0918	2.709	847.03	0.636	5.00	3.18	0.852	0.361	PQ-E	PHEpoly	2.0	1.7	1.106	33.12	1.39E-02	0.0321	TeCB	138.1	563.6	563.6	1.029	1.000	340.5	801.2	0.7589	6.05E-01	1.5710
E-10 TA	8-20-87	35 C	0.04706	0.0868	2.709	244.64	0.636	5.00	3.18	0.852	0.361	PQ-E	PHEpoly	2.0	1.7	0.667	44.14	9.84E-03	0.0100	TeCB	77.14	75.34	115.3	1.050	0.653	43.83	101.1	0.3294	1.32E+00	0.2982
E-10 TA	8-20-87	remodel	0.04706	0.0868	2.709	244.64	0.636	5.00	3.18	0.852	0.361	PQ-E	PHEpoly	2.0	1.7	0.667	44.14	9.84E-03	0.0100	TeCB	77.14	75.34	115.3	1.050	0.653	43.83	101.1	0.3294	1.32E+00	0.2982
E-10 TA	8-20-87	remodel	0.04706	0.0868	2.709	244.64	0.636	5.00	3.18	0.852	0.361	PQ-E	PHEpoly	2.0	1.7	0.667	44.14	9.84E-03	0.0100	TeCB	77.14	75.34	115.3	1.050	0.653	43.83	101.1	0.3294	1.32E+00	0.2982
E-11 TB	8-21-87	48 C	0.04877	0.0900	2.709	260.81	0.636	5.00	3.18	0.852	0.361	PQ-E	PHEpoly	2.0	1.7	0.918	7.604	5.92E-02	0.0442	TeCB	65.27	76.02	103.1	1.047	0.737	47.82	110.5	0.2476	1.82E+00	0.3183
E-11 TB	8-21-87	remodel	0.04877	0.0900	2.709	260.81	0.636	5.00	3.18	0.852	0.361	PQ-E	PHEpoly	2.0	1.7	0.918	7.604	5.92E-02	0.0442	TeCB	65.27	76.02	103.1	1.047	0.737	47.82	110.5	0.2476	1.82E+00	0.3183
E-11 TB	8-21-87	remodel	0.04877	0.0900	2.709	260.81	0.636	5.00	3.18	0.852	0.361	PQ-E	PHEpoly	2.0	1.7	0.918	7.604	5.92E-02	0.0442	TeCB	65.27	76.02	103.1	1.047	0.737	47.82	110.5	0.2476	1.82E+00	0.3183

EXP	DATE	MISC	RF 1st	Kp	P	FIXkcl	D 1st	omega	kb	alpha i	ssq	E2	E3	RF 2nd	Kp	P	FIXkcl	D 2nd	omega	alpha e	B	θe	f	ssq
E-14 SB	7-02-87		46.40	107.2	18.42	F:3.00	3.59E-02	2.110	1.23E-03	4.44E-04	0.2987	8.36E+00	4.37E+01	46.74	107.95	18.42	F:3.00	3.59E-02	1.946	2.06E-02	0.0373	0.40 F	0.028	0.2920
E-14 SB	7-02-87	remodel	44.37	102.4	9.341	F:3.70	7.08E-02	2.222	1.36E-03	4.89E-04	0.2956	4.02E+00	1.22E+01											
E-15 SC	7-07-87		148.4	347.9	21.67	F:3.00	1.76E-02	2.823	2.92E-04	1.05E-04	0.7738	7.57E+00	3.63E+01	230.6	541.76	21.67	F:3.00	1.76E-02	0.857	5.23E-03	0.2907	0.40 F	0.290	0.3141
E-15 SC	7-07-87	remodel	147.0	344.6	17.57	F:3.70	2.17E-02	2.877	3.00E-04	1.08E-04	0.7706	6.02E+00	2.42E+01											
E-15 SC	7-07-87	remodel	207.5 F	487.4	65.01	F:1.00	5.86E-03	2.392	1.77E-04	6.38E-05	1.1410	2.69E+01	3.90E+02	207.5 F	487.36	65.01	F:1.00	5.86E-03	1.071	6.53E-03	0.2674	0.40 F	0.266	0.4065
E-6 SY	8-18-87	3 C	35.95	82.50	1.920	F:5.30	2.21E-01	1.906	9.26E-04	3.34E-04	0.4754	9.52E-01	1.41E+00	58.22	135.05	1.920	F:5.30	2.21E-01	0.349	2.37E-03	0.3140	0.40 F	0.311	0.1012
E-6 SY	8-18-87	remodel	48.00	110.9	10.69	F:3.70	3.97E-02	1.550	5.60E-04	2.02E-04	0.5669	6.61E+00	2.87E+01											
E-6 SY	8-18-87	remodel	104.8 F	245.0	9.960	F:1.00	4.26E-02	1.255	2.05E-04	7.41E-05	1.6920	7.79E+00	3.82E+01	104.8 F	245.0	9.960	F:1.00	4.26E-02	0.552	3.75E-03	0.1650	0.40 F	0.162	0.4077
E-7 SX	8-17-87	11 C	79.40	185.0	2.340	F:5.30	1.75E-01	2.651	5.55E-04	2.00E-04	0.9997	8.61E-01	1.23E+00	142.5	333.86	2.340	F:5.30	1.75E-01	0.406	2.66E-03	0.3129	0.40 F	0.312	0.3946
E-7 SX	8-17-87	remodel	85.24	198.8	3.370	F:3.70	1.22E-01	2.370	4.62E-04	1.67E-04	1.0640	1.39E+00	2.36E+00											
E-7 SX	8-17-87	remodel	119.9 F	280.6	12.47	F:1.00	3.29E-02	1.953	2.70E-04	9.73E-05	1.2560	6.28E+00	2.61E+01	119.9 F	280.62	12.47	F:1.00	3.29E-02	0.893	5.86E-03	0.2086	0.40 F	0.206	0.7031
E-8 SZ	8-19-87	17 C	34.28	78.54	2.340	F:5.30	1.64E-01	1.343	6.18E-04	2.23E-04	0.3025	1.64E+00	3.01E+00	34.29	78.58	2.340	F:5.30	1.64E-01	1.340	8.21E-03	0.0300	0.40 F	0.017	0.3025
E-8 SZ	8-19-87	remodel	43.92	101.3	11.02	F:3.70	3.48E-02	1.254	4.48E-04	1.62E-04	0.3383	8.39E+00	4.40E+01											
E-8 SZ	8-19-87	remodel	88.73 F	207.1	31.39	F:1.00	1.22E-02	1.124	1.96E-04	7.09E-05	1.1235	2.73E+01	4.02E+02	88.73 F	207.05	31.39	F:1.00	1.22E-02	0.807	4.95E-03	0.0948	0.40 F	0.091	0.9470
E-9 SS	8-04-87	25 C	159.7	374.5	6.309	F:5.30	7.28E-02	4.018	4.65E-04	1.68E-04	1.6530	1.55E+00	2.76E+00	160.8	377.05	6.309	F:5.30	7.28E-02	3.566	2.62E-02	0.0500 F	0.40 F	0.047	1.6560
E-9 SS	8-04-87	remodel	164.2	385.2	8.951	F:3.70	5.13E-02	3.731	4.20E-04	1.52E-04	1.6542	2.37E+00	5.19E+00											
E-9 SS	8-04-87	remodel	239.8 F	563.6	33.12	F:1.00	1.39E-02	2.320	1.78E-04	6.44E-05	2.0840	1.42E+01	1.15E+02	239.8 F	563.59	33.12	F:1.00	1.39E-02	0.310	2.28E-03	0.5250 F	0.40 F	0.525	2.1190
E-10 TA	8-20-87	35 C	19.71	44.15	8.490	F:5.30	5.11E-02	1.534	1.42E-03	5.14E-04	0.3274	4.99E+00	1.78E+01	19.68	44.10	8.490	F:5.30	5.11E-02	1.545	1.07E-02	0.0485	0.40 F	0.026	0.3273
E-10 TA	8-20-87	remodel	20.31	45.57	11.93	F:3.70	3.64E-02	1.509	1.36E-03	4.90E-04	0.3310	7.15E+00	3.34E+01											
E-10 TA	8-20-87	remodel	41.39 F	95.32	44.13	F:1.00	9.84E-03	0.953	4.10E-04	1.48E-04	1.1025	4.41E+01	1.03E+03	41.39 F	95.32	44.13	F:1.00	9.84E-03	0.601	4.18E-03	0.1350	0.40 F	0.127	0.9767
E-11 TB	8-21-87	48 C	15.25	33.63	1.460	F:5.30	3.08E-01	1.214	1.53E-03	5.54E-04	0.3008	1.05E+00	1.62E+00	18.86	42.14	1.460	F:5.30	3.08E-01	0.479	3.45E-03	0.2270	0.40 F	0.213	0.2976
E-11 TB	8-21-87	remodel	22.01	49.59	2.055	F:3.70	2.19E-01	1.157	9.91E-04	3.58E-04	0.3588	1.62E+00	2.96E+00											
E-11 TB	8-21-87	remodel	38.92 F	89.50	7.600	F:1.00	5.92E-02	0.868	4.12E-04	1.49E-04	0.7503	8.31E+00	4.33E+01	38.92 F	89.50	7.600	F:1.00	5.92E-02	0.545	3.93E-03	0.1194	0.40 F	0.110	0.5651

EXP	DATE	MISC	θ(CM3/S)	velocity	PV	PV INJ	area	le	C vol	θ	Pb	SURF	BOUND	KCL	KCL	Rf	P	D (KCl)	ssq	NAME	conc	Ksorb	K des	MASS	revers	RF	Kp	P	D	ssq
E-16 SE	7-09-87		0.05204	0.0960	2.709	276.63	0.636	5.00	3.18	0.852	0.361	PQ-E	PHEpoly	2.0	1.7	1.041	49.19	9.76E-03	0.1456	PCB	308.0	858.3	755.2	1.560	1.137	320.7	754.4	2.535	1.89E-01	0.4716
E-16 SE	7-09-87	remodel	0.05204	0.0960	2.709	276.63	0.636	5.00	3.18	0.852	0.361	PQ-E	PHEpoly	2.0	1.7	1.041	49.19	9.76E-03	0.1456	PCB	308.0	858.3	755.2	1.560	1.137	320.7	754.4	2.535	1.89E-01	0.4716
E-16 SE	7-09-87	remodel	0.05204	0.0960	2.709	276.63	0.636	5.00	3.18	0.852	0.361	PQ-E	PHEpoly	2.0	1.7	1.041	49.19	9.76E-03	0.1456	PCB	308.0	858.3	755.2	1.560	1.137	320.7	754.4	2.535	1.89E-01	0.4716
E-9 SS	8-04-87	25 C	0.04976	0.0918	2.709	847.03	0.636	5.00	3.18	0.852	0.361	PQ-E	PHEpoly	2.0	1.7	1.106	33.12	1.39E-02	0.0321	PCB	276.7	987.9	1269.1	1.043	0.778	542.7	1278.5	1.419	3.24E-01	1.1770
E-9 SS	8-04-87	remodel	0.04976	0.0918	2.709	847.03	0.636	5.00	3.18	0.852	0.361	PQ-E	PHEpoly	2.0	1.7	1.106	33.12	1.39E-02	0.0321	PCB	276.7	987.9	1269.1	1.043	0.778	542.7	1278.5	1.419	3.24E-01	1.1770
E-9 SS	8-04-87	remodel	0.04976	0.0918	2.709	847.03	0.636	5.00	3.18	0.852	0.361	PQ-E	PHEpoly	2.0	1.7	1.106	33.12	1.39E-02	0.0321	PCB	276.7	987.9	1269.1	1.043	0.778	542.7	1278.5	1.419	3.24E-01	1.1770

EXP	DATE	MISC	RF 1st	Kp	P	FIXkcl	D 1st	omega	kb	alpha i	ssq	E2	E3	RF 2nd	Kp	P	FIXkcl	D 2nd	omega	alpha e	B	θe	f	ssq
E-16 SE	7-09-87		250.0	587.6	16.40	F:3.00	2.93E-02	5.357	4.13E-04	1.49E-04	0.7674	3.04E+00	7.56E+00	329.3	774.80	16.40	F:3.00	2.93E-02	0.7693	5.91E-03	0.4734	0.40 F	0.473	0.3664
E-16 SE	7-09-87	remodel	240.9	566.2	8.784	F:3.70	5.47E-02	6.758	5.41E-04	1.95E-04	0.7276	1.29E+00	2.12E+00											
E-16 SE	7-09-87	remodel	228.8 F	537.6	49.19	F:1.00	9.76E-03	4.773	4.02E-04	1.45E-04	0.9060	1.02E+01	6.25E+01	228.8 F	537.63	49.19	F:1.00	9.76E-03	3.155	2.42E-02	0.1919	0.40 F	0.191	0.8838
E-9 SS	8-04-87	25 C	343.4	808.1	5.520	F:6.10	8.32E-02	4.577	2.46E-04	8.86E-05	1.3690	1.20E+00	1.92E+00	617.8	1455.7	5.520	F:6.10	8.32E-02	0.2591	1.90E-03	0.4408	0.40 F	0.441	1.1085
E-9 SS	8-04-87	remodel	345.7	813.5	5.914	F:3.70	7.76E-02	4.444	2.37E-04	8.55E-05	1.3752	1.32E+00	2.20E+00	368.7	867.8	5.914	F:3.70	7.76E-02	2.454	5.80E-02	0.1885	0.40 F	0.188	1.2891
E-9 SS	8-04-87	remodel	479.1 F	1128	33.12	F:1.00	1.39E-02	3.133	1.20E-04	4.34E-05	1.7636	1.05E+01	6.60E+01	479.1 F	1128.4	33.12	F:1.00	1.39E-02	1.837	1.35E-02	0.1645	0.40 F	0.164	1.4101

B.4 Solute and KCl Column Modeling Data

COLUMN DATA — EQUILIB MODEL (KCl) — SOLUTE planimeter — EQUILIBRIUM MODEL — FIRST ORDER MODEL (or ORGANIC) — MOBILE IMMOBILE MODEL

NAME		DATE	misc.	Q (cm3/s)	ave vel v (cm/s)	pore vol (cm3)	pv inject	column area (cm2)	col le (cm)	col volume (cm3)	total porosity	bulk density (g/cm3)	surf name	bound organic	KCl initial conc (-log molar)	KCl final conc	KCl Rf	KCl Peclet	KCl D (cm2/s)	SSQ (error)	name	conc ppb	sorb (solute) Kp (cm3/g)	desorb Kp (cm3/g)	mass balance PV/PVinj	reverse Kps/Kpd	solute Rf	solute Kp (cm3/g)	solute Peclet	solute D (cm2/s)	SSQ (error)	solute Rf fixed=F	solute Kp (cm3/g)	solute Peclet fixed=F	%Dkcl	solute D (cm2/s)	solute omega (DAI)	solute kb F(s-1)	solute alpha i (g/cm3s)	SSQ (error)	E2 (nonequil spread)	E3 (tailing) (skew)	solute Rf fixed=F	solute Kp (cm3/g)	solute P fixed=F	%Dkcl	solute D (cm2/s)	solute omega fixed=F	solute alpha e (g/cm3s)	solute beta fixed=F	solute mobile poro- F	solute f (frac)	SSQ
F-1	BV	10-27-86		0.02210	0.0406	7.622	24.00	0.636	14.0	8.904	0.856	0.354	PQ-I	PHEpoly	5.0	3.7	0.707	109.7	5.18E-03	0.1470	DCB	518.7	25.06	25.71	1.011	0.975	15.64	35.401	0.9617	5.91E-01	0.0876	6.641	13.64	1.025		5.54E-01	13.41	6.89E-03	2.44E-03	0.0762	5.51E-02	5.68E-02	6.566	13.46	0.9936		5.72E-01	13.98	1.62E-02	0.2379	0.40 F	0.197	0.0746
F-1	BV	10-27-86	remodel	0.02210	0.0406	7.622	24.00	0.636	14.0	8.904	0.856	0.354	PQ-I	PHEpoly	5.0	3.7	0.707	109.7	5.18E-03	0.1470	DCB	518.7	25.06	25.71	1.011	0.975	15.64	35.401	0.9617	5.91E-01	0.0876	11.27	24.83	276.0	F:3.00	2.06E-03	1.950	5.51E-04	1.95E-04	0.1750	1.18E+02	7.38E+03	12.32	27.37	276.0	F:3.00	2.06E-03	1.323	1.53E-03	0.2220	0.40 F	0.201	0.1490
F-1	BV	10-27-86	remodel	0.02210	0.0406	7.622	24.00	0.636	14.0	8.904	0.856	0.354	PQ-I	PHEpoly	5.0	3.7	0.707	109.7	5.18E-03	0.1470	DCB	518.7	25.06	25.71	1.011	0.975	15.64	35.401	0.9617	5.91E-01	0.0876	11.18	24.62	73.13	F:1.50	7.77E-03	1.967	5.60E-04	1.98E-04	0.1717	3.08E+01	5.30E+02	11.02	24.23	73.13	F:1.50	7.77E-03	2.108	2.44E-03	0.0564	0.40 F	0.015	0.1635
F-1	BV	10-27-86	remodel	0.02210	0.0406	7.622	24.00	0.636	14.0	8.904	0.856	0.354	PQ-I	PHEpoly	5.0	3.7	0.707	109.7	5.18E-03	0.1470	DCB	518.7	25.06	25.71	1.011	0.975	15.64	35.401	0.9617	5.91E-01	0.0876	11.50 F	25.39	51.58	F:1.00	1.10E-02	1.954	5.40E-04	1.91E-04	0.1737	2.20E+01	2.76E+02	11.50 F	25.39	51.58	F:1.00	1.10E-02	1.252	1.45E-03	0.2570	0.40 F	0.237	0.1346
F-2	BW	10-29-86	sorb	0.01970	0.0362	7.622	41.60	0.636	14.0	8.904	0.856	0.354	PQ-I	PHEpoly	5.0	3.7	0.662	43.25	1.17E-02	0.1388	DCB	399.2	17.31		1.156	0.407	9.407	20.329	1.181	4.29E-01	0.3150	7.494	15.70	5.064		1.00E-01	2.630 F	1.05E-03	3.71E-04	0.5352	1.45E+00	2.58E+00											
F-2	BW	10-29-86	sorb	0.01970	0.0362	7.622	41.60	0.636	14.0	8.904	0.856	0.354	PQ-I	PHEpoly	5.0	3.7	0.662	43.25	1.17E-02	0.1388	DCB	399.2	17.31		1.156	0.407	9.407	20.329	1.181	4.29E-01	0.3150	6.955	14.40	28.83	F:1.50	1.76E-02	2.266	9.84E-04	3.48E-04	0.0523	9.33E+00	5.67E+01											
F-2	BC	12-30-86	desorb	0.02100	0.0386	7.622	d(61days)	0.636	14.0	8.904	0.856	0.354	PQ-I	PHEpoly	3.7	5.0	0.662	43.25	1.25E-02	0.1388	DCB	399.2		42.58	1.156	0.407	9.407	20.329	1.181	4.57E-01	0.3150	7.494	15.70	5.064		1.07E-01	2.630 F	1.12E-03	3.95E-04	0.5352	1.45E+00	2.58E+00											
F-2	BWBC	10-29-86	remodel	0.01970	0.0362	7.622	41.60	0.636	14.0	8.904	0.856	0.354	PQ-I	PHEpoly	5.0	3.7	0.662	43.25	1.17E-02	0.1388	DCB	399.2	17.31		1.156	0.407	9.407	20.329	1.181	4.29E-01	0.3150	13.38 F	29.94	52.58	F:1.00	9.63E-03	1.510	3.15E-04	1.12E-04	1.1000	2.98E+01	4.93E+02	13.38 F	29.94	52.58	F:1.00	9.63E-03	0.7990	8.26E-04	0.2757	0.40 F	0.260	0.8692
F-3	SJ	7-20-87		0.00943	0.0140	3.393	93.59	0.785	5.05	3.964	0.856	0.354	PQ-I	PHEpoly	2.0	1.7	1.390	14.92	4.75E-03	2.0590	DCB	675.6	104.0	109.4	0.991	0.951	52.66	124.91	4.009	1.77E-02	0.2831	41.78	98.61	4.970	F:3.00	1.43E-02	35.14	2.39E-03	8.48E-04	0.3132	1.35E-01	1.44E-01	54.51	129.38	4.970	F:3.00	1.43E-02	0.0720	8.00E-05	0.7420	0.40 F	0.747	0.2479
F-3	SJ	7-20-87	remodel	0.00943	0.0140	3.393	93.59	0.785	5.05	3.964	0.856	0.354	PQ-I	PHEpoly	2.0	1.7	1.390	14.92	4.75E-03	2.0590	DCB	675.6	104.0	109.4	0.991	0.951	52.66	124.91	4.009	1.77E-02	0.2831	46.56	110.2	45.96	F:1.50	1.54E-03	6.236	3.80E-04	1.35E-04	0.3980	7.06E+00	3.22E+01	49.43	117.11	45.96	F:1.50	1.54E-03	2.0830	2.32E-03	0.3838	0.40 F	0.382	0.3229
F-3	SJ	7-20-87	remodel	0.00943	0.0140	3.393	93.59	0.785	5.05	3.964	0.856	0.354	PQ-I	PHEpoly	2.0	1.7	1.390	14.92	4.75E-03	2.0590	DCB	675.6	104.0	109.4	0.991	0.951	52.66	124.91	4.009	1.77E-02	0.2831	45.13 F	106.7	68.94	F:1.00	1.03E-03	6.220	3.92E-04	1.39E-04	0.4177	1.06E+01	6.74E+01	45.13 F	106.71	68.94	F:1.00	1.03E-03	3.3170	3.69E-03	0.2779	0.40 F	0.274	0.4043
F-5	SK	7-22-87		0.02763	0.0411	3.393	120.20	0.785	5.05	3.964	0.856	0.354	PQ-I	PHEpoly	2.0	1.7	1.242	23.40	8.87E-03	0.0709	DCB	4462.	49.67	55.76	1.002	0.891	20.23	46.504	2.415	8.60E-02	0.2322	16.15	36.63	7.800	F:3.00	2.66E-02	5.329	2.86E-03	1.01E-03	0.3096	1.29E+00	2.15E+00	19.43	44.56	7.800	F:3.00	2.66E-02	0.2920	9.51E-04	0.6300	0.40 F	0.639	0.2237
F-5	SK	7-22-87	remodel	0.02763	0.0411	3.393	120.20	0.785	5.05	3.964	0.856	0.354	PQ-I	PHEpoly	2.0	1.7	1.242	23.40	8.87E-03	0.0709	DCB	4462.	49.67	55.76	1.002	0.891	20.23	46.504	2.415	8.60E-02	0.2322	17.01	38.71	15.60	F:1.50	1.33E-02	4.130	2.10E-03	7.44E-04	0.3228	3.35E+00	9.12E+00	19.15	43.89	15.60	F:1.50	1.33E-02	0.6993	2.28E-03	0.5249	0.40 F	0.528	0.2599
F-5	SK	7-22-87	remodel	0.02763	0.0411	3.393	120.20	0.785	5.05	3.964	0.856	0.354	PQ-I	PHEpoly	2.0	1.7	1.242	23.40	8.87E-03	0.0709	DCB	4462.	49.67	55.76	1.002	0.891	20.23	46.504	2.415	8.60E-02	0.2322	23.40 F	54.16	23.40	F:1.00	8.87E-03	2.613	9.50E-04	3.36E-04	0.6828	8.21E+00	4.26E+01	22.80 F	52.71	23.40	F:1.00	8.87E-03	0.4967	1.62E-03	0.4914	0.40 F	0.493	0.3110
F-4	SL	7-24-87		0.02735	0.0407	3.393	119.24	0.785	5.05	3.964	0.856	0.354	PQ-I	PHEpoly	2.0	1.7	1.165	15.88	1.29E-02	0.7115	DCB	19035	28.56	20.98	1.050	1.361	10.19	22.229	3.066	6.70E-02	0.1825	8.458	18.03	7.800	F:3.00	2.64E-02	6.376	6.89E-03	2.44E-03	0.1755	9.51E-01	1.44E+00	9.403	20.32	7.800	F:3.00	2.64E-02	0.3242	1.05E-03	0.6834	0.40 F	0.709	0.1755
F-4	SL	7-24-87	remodel	0.02735	0.0407	3.393	119.24	0.785	5.05	3.964	0.856	0.354	PQ-I	PHEpoly	2.0	1.7	1.165	15.88	1.29E-02	0.7115	DCB	19035	28.56	20.98	1.050	1.361	10.19	22.229	3.066	6.70E-02	0.1825	9.202	19.83	33.26	F:1.50	6.18E-03	3.944	3.88E-03	1.37E-03	0.2347	6.70E+00	3.06E+01	9.740	21.13	33.26	F:1.50	6.18E-03	1.2080	3.89E-03	0.4486	0.40 F	0.446	0.1868
F-4	SL	7-24-87	remodel	0.02735	0.0407	3.393	119.24	0.785	5.05	3.964	0.856	0.354	PQ-I	PHEpoly	2.0	1.7	1.165	15.88	1.29E-02	0.7115	DCB	19035	28.56	20.98	1.050	1.361	10.19	22.229	3.066	6.70E-02	0.1825	11.24 F	24.76	49.90	F:1.00	4.12E-03	3.134	2.47E-03	8.73E-04	0.3682	1.32E+01	1.05E+02	11.24 F	24.76	49.90	F:1.00	4.12E-03	0.8271	2.67E-03	0.4599	0.40 F	0.459	0.2379
G-1	BX	10-31-86		0.02000	0.0289	9.682	22.60	0.785	14.0	10.99	0.881	0.291	PQ-J	PHEpoly	5.0	3.0	0.933	322.7	1.25E-03	8.6890	DCB	42.6	32.09	28.69	0.950	1.119	11.03	30.366	5.965	6.79E-02	0.1153																						
G-1	BX	10-31-86	pv%1.032	0.02000	0.0289	9.682	22.60	0.785	14.0	10.99	0.881	0.291	PQ-J	PHEpoly	5.0	3.0	0.971	473.7	8.55E-04	0.2179	DCB	42.6	32.09	28.69	0.950	1.119	11.38	31.425	5.964	6.79E-02	0.1153	10.23	27.94	157.9	F:3.00	2.56E-03	4.730	1.06E-03	3.08E-04	0.2380	2.72E+01	4.17E+02	12.16	33.79	157.9	F:3.00	2.56E-03	0.7880	6.51E-04	0.5670	0.40 F	0.577	0.1700
G-2	BY	11-05-86		0.02420	0.0350	9.682	24.10	0.785	14.0	10.99	0.881	0.291	PQ-J	PHEpoly	5.0	4.0	0.931	144.4	3.39E-03	0.1233	DCB	380.6	20.31	16.78	0.952	1.210	7.565	19.875	4.284	1.14E-01	0.0677	6.092	15.42	48.17	F:3.00	1.02E-02	2.795	1.37E-03	3.99E-04	0.5410	1.20E+01	9.22E+01	6.120	15.50	48.17	F:3.00	1.02E-02	2.636	2.64E-03	0.1860	0.40 F	0.134	0.5400
G-2	BY	11-05-86	remodel	0.02420	0.0350	9.682	24.10	0.785	14.0	10.99	0.881	0.291	PQ-J	PHEpoly	5.0	4.0	0.931	144.4	3.39E-03	0.1233	DCB	380.6	20.31	16.78	0.952	1.210	7.565	19.875	4.284	1.14E-01	0.0677	6.163	15.63	97.73	F:1.50	5.01E-03	2.718	1.32E-03	3.83E-04	0.5404	2.52E+01	3.77E+02	6.188	15.71	97.73	F:1.50	5.01E-03	2.569	2.57E-03	0.1819	0.40 F	0.129	0.5392
G-2	BY	11-05-86	remodel	0.02420	0.0350	9.682	24.10	0.785	14.0	10.99	0.881	0.291	PQ-J	PHEpoly	5.0	4.0	0.931	144.4	3.39E-03	0.1233	DCB	380.6	20.31	16.78	0.952	1.210	7.565	19.875	4.284	1.14E-01	0.0677	7.126 F	18.55	144.8	F:1.00	3.38E-03	2.238	9.13E-04	2.66E-04	0.6056	4.78E+01	1.29E+03	7.126 F	18.55	144.8	F:1.00	3.38E-03	1.259	1.26E-03	0.3592	0.40 F	0.344	0.5700
G-3	BZ	11-07-86	sorb	0.02300	0.0333	9.682	22.80	0.785	14.0	10.99	0.881	0.291	PQ-J	PHEpoly	3.0	2.9	1.012	282.1	1.65E-03	0.2658	DCB	502.3	17.48		1.051	0.778	6.578	16.887	3.872	1.20E-01	0.1694	5.993	15.12	94.01	F:3.00	4.95E-03	3.827	1.82E-03	5.30E-04	0.2726	1.71E+01	1.78E+02	6.960	18.04	94.01	F:3.00	4.95E-03	0.7360	6.99E-04	0.5180	0.40 F	0.529	0.0818
G-3	BZ	11-07-86	remodel	0.02300	0.0333	9.682	22.80	0.785	14.0	10.99	0.881	0.291	PQ-J	PHEpoly	3.0	2.9	1.012	282.1	1.65E-03	0.2658	DCB	502.3	17.48		1.051	0.778	6.578	16.887	3.872	1.20E-01	0.1694	5.997	15.13	98.00	F:1.50	4.75E-03	3.820	1.82E-03	5.28E-04	0.2732	1.78E+01	1.94E+02	6.950	18.01	98.00	F:1.50	4.75E-03	0.7440	7.07E-04	0.5167	0.40 F	0.527	0.0833
G-3	CD	1-01-87	desorb	0.02300	0.0333	9.682	d(54days)	0.785	14.0	10.99	0.881	0.291	PQ-J	PHEpoly	2.9	3.0	1.012	282.1	1.65E-03	0.2658	DCB	502.3		22.46	1.051	0.778	6.578	16.887	3.872	1.20E-01	0.1694	5.993	15.12	94.01	F:3.00	4.95E-03	3.827	1.82E-03	5.30E-04	0.2726	1.71E+01	1.78E+02	6.960	18.04	94.01	F:3.00	4.95E-03	0.7360	6.99E-04	0.5180	0.40 F	0.529	0.0818
EXP		DATE	MISC	Q(CM3/S)	velocity	PV	PV INJ	area	le	C vol	θ	Pb	SURF	BOUND	KCL	KCL	Rf	P	D (KCl)	ssq	NAME	conc	Ksorb	K des	MASS	revers	RF	Kp	P	D	ssq	RF 1st	Kp	P	F%Dkcl	D 1st	omega	kb	alpha i	ssq	E2	E3	RF 2nd	Kp	P	F%Dkcl	D 2nd	omega	alpha e	B	θe	f	ssq
H-2	RARB	11-14-86	d=3 days	0.02270	0.0349	9.111	28.00	0.785	14.0	10.99	0.829	0.418	PQ-L	PHEpoly	1.7	1.7	0.553	8.719	5.60E-02	0.0157	DCB	502.1	16.71	17.56	1.028	0.952	8.696	15.26	4.580	1.07E-01	0.1941	6.996	11.89	8.844		5.52E-02	3.460 F	1.44E-03	6.01E-04	0.4644	1.88E+00	3.80E+00											
H-2	RARB	11-14-87	remodel	0.02270	0.0349	9.111	28.00	0.785	14.0	10.99	0.829	0.418	PQ-L	PHEpoly	1.7	1.7	0.553	8.719	5.60E-02	0.0157	DCB	502.1	16.71	17.56	1.028	0.952	8.696	15.26	4.580	1.07E-01	0.1941	6.493	10.89	5.813	F:1.50	8.40E-02	6.204	2.81E-03	1.18E-03	0.4450	6.71E-01	9.17E-01	9.401	16.66	5.813	F:1.50	8.40E-02	0.1902	1.90E-04	0.5926	0.40 F	0.606	0.2538
H-2	RARB	11-14-87	remodel	0.02270	0.0349	9.111	28.00	0.785	14.0	10.99	0.829	0.418	PQ-L	PHEpoly	1.7	1.7	0.553	8.719	5.60E-02	0.0157	DCB	502.1	16.71	17.56	1.028	0.952	8.696	15.26	4.580	1.07E-01	0.1941	5.948	9.813	2.906	F:3.00	1.68E-01	141.2	7.11E-02	2.97E-02	0.3640	1.42E-02	1.44E-02	9.597	17.05	7.790		6.27E-02	0.7390	7.37E-04	0.5670	0.40 F	0.577	0.2490
H-3	RO	6-11-87		0.02600	0.0400	9.111	43.13	0.785	14.0	10.99	0.829	0.418	PQ-L	PHEpoly	2.0	1.7	1.113	107.6	5.20E-03	0.0097	DCB	518.4	26.81	24.99	1.011	1.073	14.08	25.95	2.522	2.22E-01	0.0661	12.20	22.21	35.87	F:3.00	1.56E-02	3.107	7.92E-04	3.31E-04	0.2441	9.73E+00	5.93E+01	13.74	25.27	35.87	F:3.00	1.56E-02	0.8190	9.35E-04	0.4650	0.40 F	0.464	0.0605
H-3	RO	6-11-87	remodel	0.02600	0.0400	9.111	43.13	0.785	14.0	10.99	0.829	0.418	PQ-L	PHEpoly	2.0	1.7	1.113	107.6	5.20E-03	0.0097	DCB	518.4	26.81	24.99	1.011	1.073	14.08	25.95	2.522	2.22E-01	0.0661	12.37	22.55	71.73	F:1.50	7.80E-03	3.006	7.54E-04	3.15E-04	0.2438	2.02E+01	2.33E+02	13.80	25.39	71.73	F:1.50	7.80E-03	0.9334	1.07E-03	0.4382	0.40 F	0.435	0.0767
H-1	RP	6-15-87		0.02540	0.0390	9.111	42.04	0.785	14.0	10.99	0.829	0.418	PQ-L	PHEpoly	2.0	1.7	1.117	129.9	4.21E-03	0.0034	DCB	384.2	23.63	23.80	0.996	0.993	12.33	22.47	2.302	2.37E-01	0.0997	10.77	19.37	43.31	F:3.00	1.26E-02	3.044	8.69E-04	3.63E-04	0.3143	1.17E+01	8.39E+01	12.28	22.38	43.31	F:3.00	1.26E-02	0.7610	8.49E-04	0.4540	0.40 F	0.451	0.0621
H-1	RP	6-15-87	remodel	0.02540	0.0390	9.111	42.04	0.785	14.0	10.99	0.829	0.418	PQ-L	PHEpoly	2.0	1.7	1.117	129.9	4.21E-03	0.0034	DCB	384.2	23.63	23.80	0.996	0.993	12.33	22.47	2.302	2.37E-01	0.0997	10.89	19.61	86.60	F:1.50	6.31E-03	2.963	8.35E-04	3.49E-04	0.3138	2.41E+01	3.30E+02	12.27	22.35	86.60	F:1.50	6.31E-03	0.8780	9.79E-04	0.4288	0.40 F	0.424	0.0885
H-1	RP	6-15-87	remodel	0.02540	0.0390	9.111	42.04	0.785	14.0	10.99	0.829	0.418	PQ-L	PHEpoly	2.0	1.7	1.117	129.9	4.21E-03	0.0034	DCB	384.2	23.63	23.80	0.996	0.993	12.33	22.47	2.302	2.37E-01	0.0997	12.96 F	23.72	129.9	F:1.00	4.21E-03	2.571	5.99E-04	2.51E-04	0.5031	4.30E+01	1.01E+03	12.96 F	23.72	129.9	F:1.00	4.21E-03	0.8493	9.47E-04	0.4147	0.40 F	0.409	0.1148
U-1	SP	7-31-87		0.01256	0.0249	5.350	40.58	0.785	10.6	8.321	0.643	0.875	PQ-U	PHEpolyS	2.0	1.7	0.321	14.23	1.85E-02	0.4210	DCB	997.2	16.49	4.759	0.636	3.465	23.71	16.69	24.089	1.09E-02	0.6657	23.71	16.69	4.742	F:3.00	5.56E-02	1.686	1.74E-04	1.52E-04	3.0450	2.58E+00	5.98E+00	1973	1449	4.742	F:3.00	5.56E-02	0.7022	6.35E-04	0.0075	0.40 F	0.007	2.5390
U-1	SP	7-31-87	remodel	0.01256	0.0249	5.350	40.58	0.785	10.6	8.321	0.643	0.875	PQ-U	PHEpolyS	2.0	1.7	0.321	14.23	1.85E-02	0.4210	DCB	997.2	16.49	4.759	0.636	3.465	23.71	16.69	24.089	1.09E-02	0.6657	59.74	43.18	81.03	F:1.50	3.26E-03	1.552	6.20E-05	5.43E-05	3.0546	5.05E+01	1.34E+03											
U-2	SQ	8-03-87		0.01818	0.0360	5.350	47.02	0.785	10.6	8.321	0.643	0.875	PQ-U	PHEpolyS	2.0	1.7	0.338	7.126	5.36E-02	0.4243	DCB	901.4	3.451	2.773	1.006	1.245	12.79	8.664	0.0499	7.65E+00	0.1037	8.165	5.266	2.375	F:3.00	1.61E-01	0.131	6.21E-05	5.43E-05	0.3511	1.40E+01	1.19E+02	3.629	1.93	2.375	F:3.00	1.61E-01	0.1828	2.48E-04	0.1391	0.40 F	-0.045	0.0635
U-2	SQ	8-03-87	remodel	0.01818	0.0360	5.350	47.02	0.785	10.6	8.321	0.643	0.875	PQ-U	PHEpolyS	2.0	1.7	0.338	7.126	5.36E-02	0.4243	DCB	901.4	3.451	2.773	1.006	1.245	12.79	8.664	0.0499	7.65E+00	0.1037	11.04	7.380	72.47	F:1.50	5.27E-03	0.229	7.76E-05	6.79E-05	0.9551	2.62E+02	3.62E+04											
U-2	SQ	8-03-87	remodel	0.01818	0.0360	5.350	47.02	0.785	10.6	8.321	0.643	0.875	PQ-U	PHEpolyS	2.0	1.7	0.338	7.126	5.36E-02	0.4243	DCB	901.4	3.451	2.773	1.006	1.245	12.79	8.664	0.0499	7.65E+00	0.1037	5.235 F	3.113	108.7	F:1.00	3.51E-03	0.225	1.60E-04	1.58E-04	1.0690	3.17E+02	5.69E+04	5.235 F	3.11	108.7	F:1.00	3.51E-03	0.2939	3.99E-04	0.1075	0.40 F	-0.014	0.1270
I-1	RR	6-17-87		0.02710	0.0500	7.586	49.16	0.636	14.0	8.904	0.852	0.363	PQ-P	C18+PHpo	2.0	1.7	0.961	75.16	9.32E-03	0.0976	DCB	344.3	31.72	31.65	1.042	1.002	13.33	28.92	6.556	1.07E-01	0.0164	12.28	26.45	25.05	F:3.00	2.80E-02	8.597	2.72E-03	9.89E-04	0.0456	2.46E+00	5.62E+00	12.60	27.20	25.05	F:3.00	2.80E-02	1.861	2.66E-03	0.5487	0.40 F	0.556	0.0192
I-1	RR	6-17-87	remodel	0.02710	0.0500	7.586	49.16	0.636	14.0	8.904	0.852	0.363	PQ-P	C18+PHpo	2.0	1.7	0.961	75.16	9.32E-03	0.0976	DCB	344.3	31.72	31.65	1.042	1.002	13.33	28.92	6.556	1.07E-01	0.0164	12.50	26.98	50.11	F:1.50	1.40E-02	7.324	2.28E-03	8.26E-04	0.0477	5.79E+00	2.33E+01	12.82	27.73	50.11	F:1.50	1.40E-02	2.258	1.23E-03	0.4703	0.40 F	0.470	0.0200
I-1	RR	6-17-87	remodel	0.02710	0.0500	7.586	49.16	0.636	14.0	8.904	0.852	0.363	PQ-P	C18+PHpo	2.0	1.7	0.961	75.16	9.32E-03	0.0976	DCB	344.3	31.72	31.65	1.042	1.002	13.33	28.92	6.556	1.07E-01	0.0164	14.49 F	31.65	75.16	F:1.00	9.32E-03	6.065	1.61E-03	5.83E-04	0.2974	1.07E+01	7.06E+01	14.49 F	31.65	75.16	F:1.00	9.32E-03	1.326	1.89E-03	0.5223	0.40 F	0.526	0.1444
I-2	RS	6-18-87		0.02710	0.0500	7.586	49.42	0.636	14.0	8.904	0.852	0.363	PQ-P	C18+PHpo	2.0	1.7	0.971	160.3	4.37E-03	0.0257	DCB	365.3	28.86	28.45	1.028	1.014	12.08	25.98	6.052	1.16E-01	0.0247	11.12	23.74	53.42	F:3.00	1.31E-02	6.239	2.20E-03	8.00E-04	0.0708	7.09E+00	3.35E+01	11.57	24.80	53.42	F:3.00	1.31E-02	1.633	2.33E-03	0.5188	0.40 F	0.523	0.0449
I-2	RS	6-18-87	remodel	0.02710	0.0500	7.586	49.42	0.636	14.0	8.904	0.852	0.363	PQ-P	C18+PHpo	2.0	1.7	0.971	160.3	4.37E-03	0.0257	DCB	365.3	28.86	28.45	1.028	1.014	12.08	25.98	6.052	1.16E-01	0.0247	11.22	23.57	106.9	F:1.50	6.55E-03	5.896	2.06E-03	7.49E-04	0.0709	1.50E+01	1.34E+02	11.66	25.01	106.9	F:1.50	6.55E-03	1.839	2.63E-03	0.4825	0.40 F	0.484	0.0485
EXP		DATE	MISC	Q(CM3/S)	velocity	PV	PV INJ	area	le	C vol	θ	Pb	SURF	BOUND	KCL	KCL	Rf	P	D (KCl)	ssq	NAME	conc	Ksorb	K des	MASS	revers	RF	Kp	P	D	ssq	RF 1st	Kp	P	F%Dkcl	D 1st	omega	kb	alpha i	ssq	E2	E3	RF 2nd	Kp	P	F%Dkcl	D 2nd	omega	alpha e	B	θe	f	ssq
A-1	[illegible]	3-12-87		0.02330	0.0425	7.675	29.76	0.636	14.0	8.904	0.862	0.338	PQ-G	DIOLpoly	2.0	1.7	0.976	85.85	6.93E-03	0.0450	DCB	942.4	6.630	3.848	0.938	1.723	2.601	4.083	49.23	1.21E-02	0.0894																						
A-2	RH	5-04-87		0.00680	0.0100	9.473	7.028	0.785	14.0	10.99	0.862	0.338	PQ-G	DIOLpoly	2.0	1.7	1.031	5.499	2.56E-02	0.0741	DCB	178.0	3.063	2.833	0.988	1.081	2.007	2.568	35.11	4.01E-03	0.0688	1.905	2.308	32.90		4.28E-03	451.8	3.58E-01	1.21E-01	0.0811	1.64E-02	1.67E-02	1.908	2.32	30.47		4.62E-03	2846.0	8.17E-01	0.7280	0.40 F	1.019	0.0799
A-3	RI	5-08-87		0.01000	0.0148	9.473	5.057	0.785	14.0	10.99	0.862	0.338	PQ-G	DIOLpoly	2.0	1.7	1.187	31.54	6.56E-03	0.0627	DCB	163.0	1.752	1.836	1.036	0.954	1.684	1.744	31.88	6.49E-03	0.0239	1.603	1.538	28.77		7.19E-03	10296	1.80E+01	6.09E+00	0.0297	3.95E-04	3.96E-04	1.794	2.02	37.63		5.50E-03	0.0527	2.23E-05	0.8813	0.40 F	1.407	0.0229
A-3	RI	5-08-87	remodel	0.01000	0.0148	9.473	5.057	0.785	14.0	10.99	0.862	0.338	PQ-G	DIOLpoly	2.0	1.7	1.187	31.54	6.56E-03	0.0627	DCB	163.0	1.752	1.836	1.036	0.954	1.684	1.744	31.88	6.49E-03	0.0239	1.703 F	1.793	31.54	F:1.00	6.56E-03	26.46	3.97E-02	1.34E-02	0.1046	2.03E-01	2.42E-01	1.703 F	1.79	31.54	F:1.00	6.56E-03	0.0376	1.59E-05	0.9290	0.40 F	1.590	0.0250
T-1	ST	8-10-87	pH=7.000	0.01321	0.0241	7.666	19.750	0.636	14.0	8.904	0.861	0.342	PQ-K	AMINpoly	2.0	1.7	1.113	6.886	4.90E-02	2.5950	DCB	658.0	4.235	2.889	1.041	1.466	3.082	5.249	11.257	3.00E-02	0.6083	2.980	4.992	53.44	F:3.00	6.32E-03	6.933	6.03E-03	2.06E-03	0.6188	1.40E+00	1.09E+01	3.067	5.21	53.44	F:3.00	6.32E-03	1.409	9.71E-04	0.6782	0.40 F	0.782	0.6031
T-2	SU	8-11-87	pH=3.880	0.00824	0.0150	7.666	12.000	0.636	14.0	8.904	0.861	0.342	PQ-K	AMINpoly	2.0	1.7	0.666	66.71	3.16E-03	0.0051	DCB	615.0	3.713	5.420	1.032	0.685	2.111	2.801	29.612	7.11E-03	0.1628	2.016	2.562	22.24	F:3.00	9.47E-03	1E+06	1.06E+03	3.61E+02	0.1509	5.65E-06	5.65E-06	2.060	2.67	22.24	F:3.00	9.47E-03	610121	2.62E+02	0.3414	0.40 F	0.225	0.1432
T-2	SU	8-11-87	remodel	0.00824	0.0150	7.666	12.000	0.636	14.0	8.904	0.861	0.342	PQ-K	AMINpoly	2.0	1.7	0.666	66.71	3.16E-03	0.0051	DCB	615.0	3.713	5.420	1.032	0.685	2.111	2.801	29.612	7.11E-03	0.1628	2.814 F	4.574	66.71	F:1.00	3.16E-03	2.627	1.56E-03	5.32E-04	1.4340	1.06E+01	8.39E+01	2.814 F	4.57	66.71	F:1.00	3.16E-03	0.0990	4.26E-05	0.7090	0.40 F	0.844	0.1963
T-3	SV	8-13-87	pH=2.284	0.00820	0.0150	7.666	12.445	0.636	14.0	8.904	0.861	0.342	PQ-K	AMINpoly	2.0	1.7	0.659	45.90	4.57E-03	0.0341	DCB	553.2	2.037	4.177	1.015	0.488	2.118	2.819	17.787	1.18E-02	0.1820	1.998	2.516	15.30	F:3.00	1.37E-02	350.9	3.76E-01	1.28E-01	0.1863	1.09E-02	1.10E-02	2.001	2.52	15.30	F:3.00	1.37E-02	351.0	1.50E-01	0.8841	0.40 F	1.303	0.1848
T-4	SW	8-14-87	pH=1.032	0.00805	0.0147	7.666	10.892	0.636	14.0	8.904	0.861	0.342	PQ-K	AMINpoly	2.0	1.7	0.548	44.03	4.67E-03	0.0556	DCB	525.4	4.009	3.711	1.020	1.080	2.098	2.768	11.213	1.84E-02	0.1784	1.921	2.322	14.68	F:3.00	1.40E-02	61.45	7.01E-02	2.39E-02	0.1994	5.49E-02	5.74E-02	2.351	3.41	14.68	F:3.00	1.40E-02	0.1418	5.96E-05	0.7694	0.40 F	0.935	0.0731

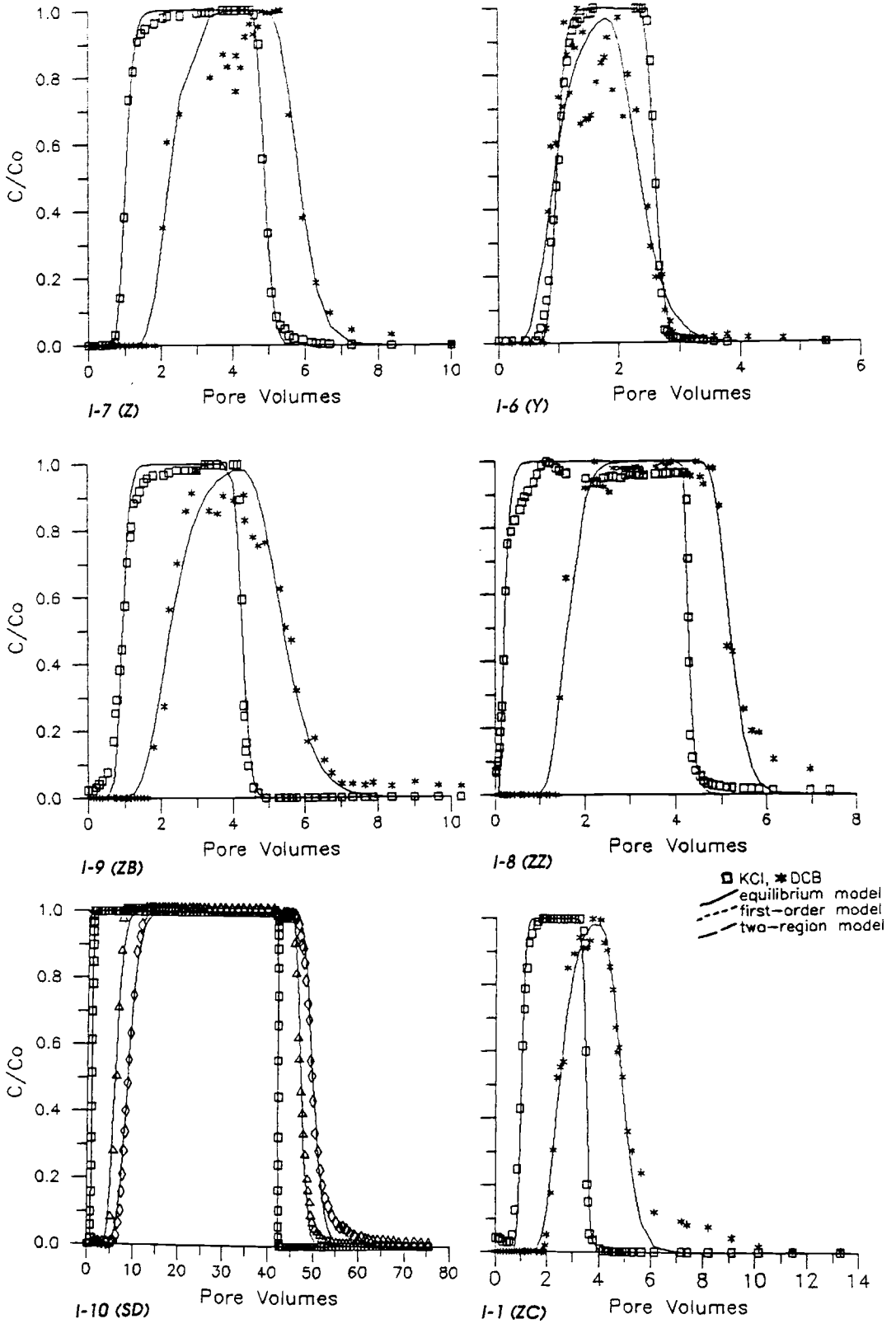

C.1 Unbonded Silica

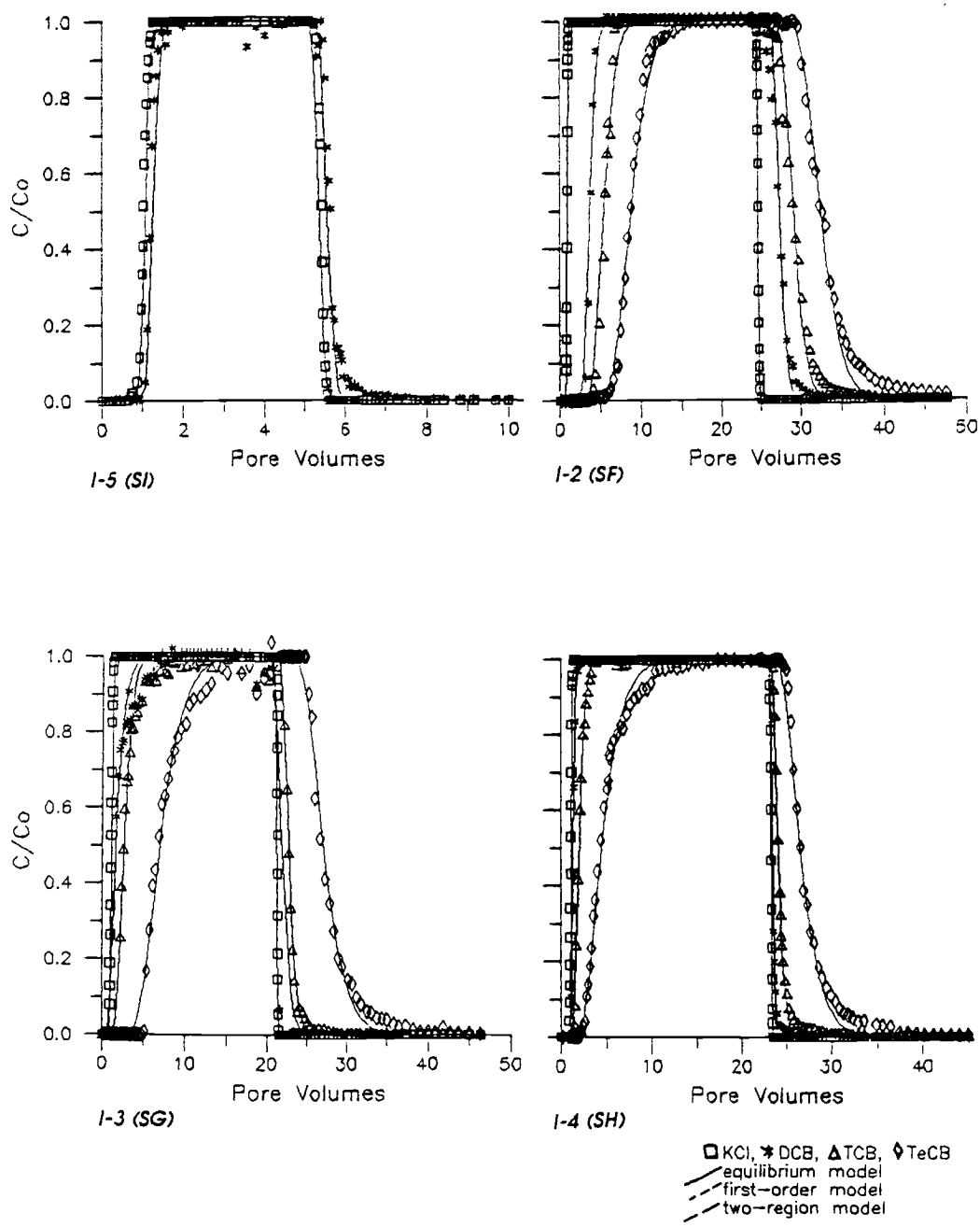

C.2 Unbonded Silica and Alumina

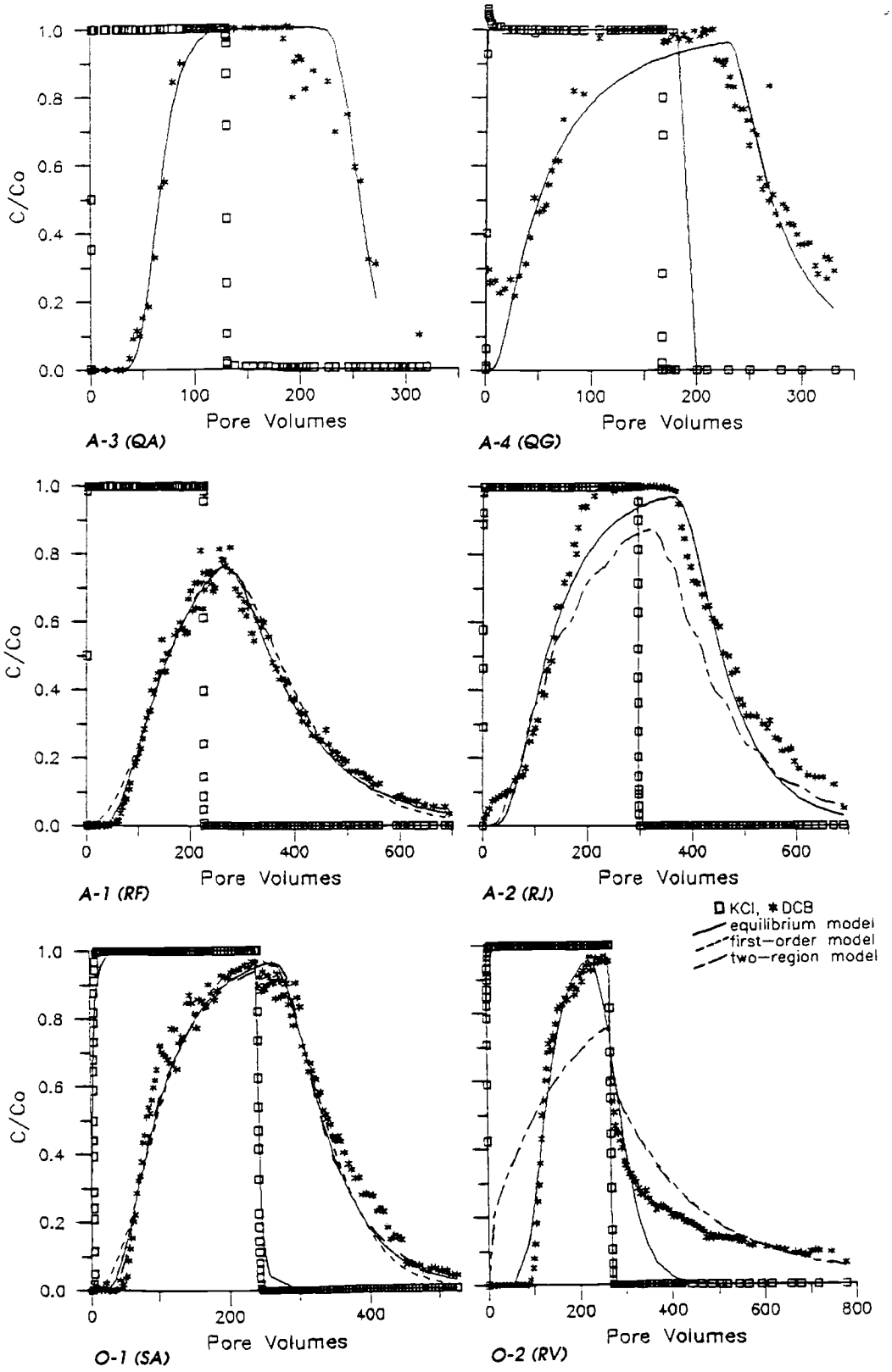

C.3 C_1 polymer modified Silica

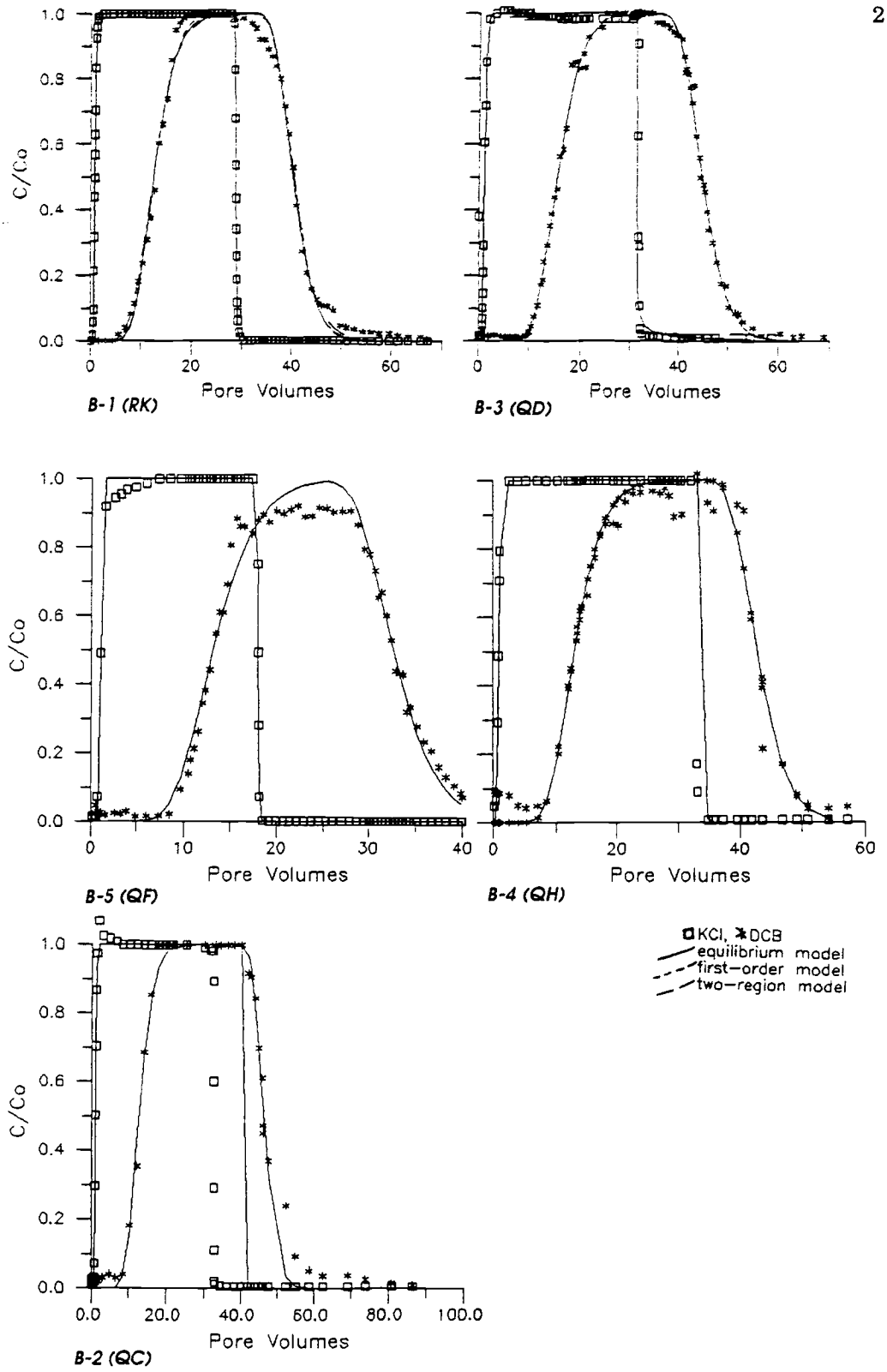

C.4 C_8 polymer modified Silica

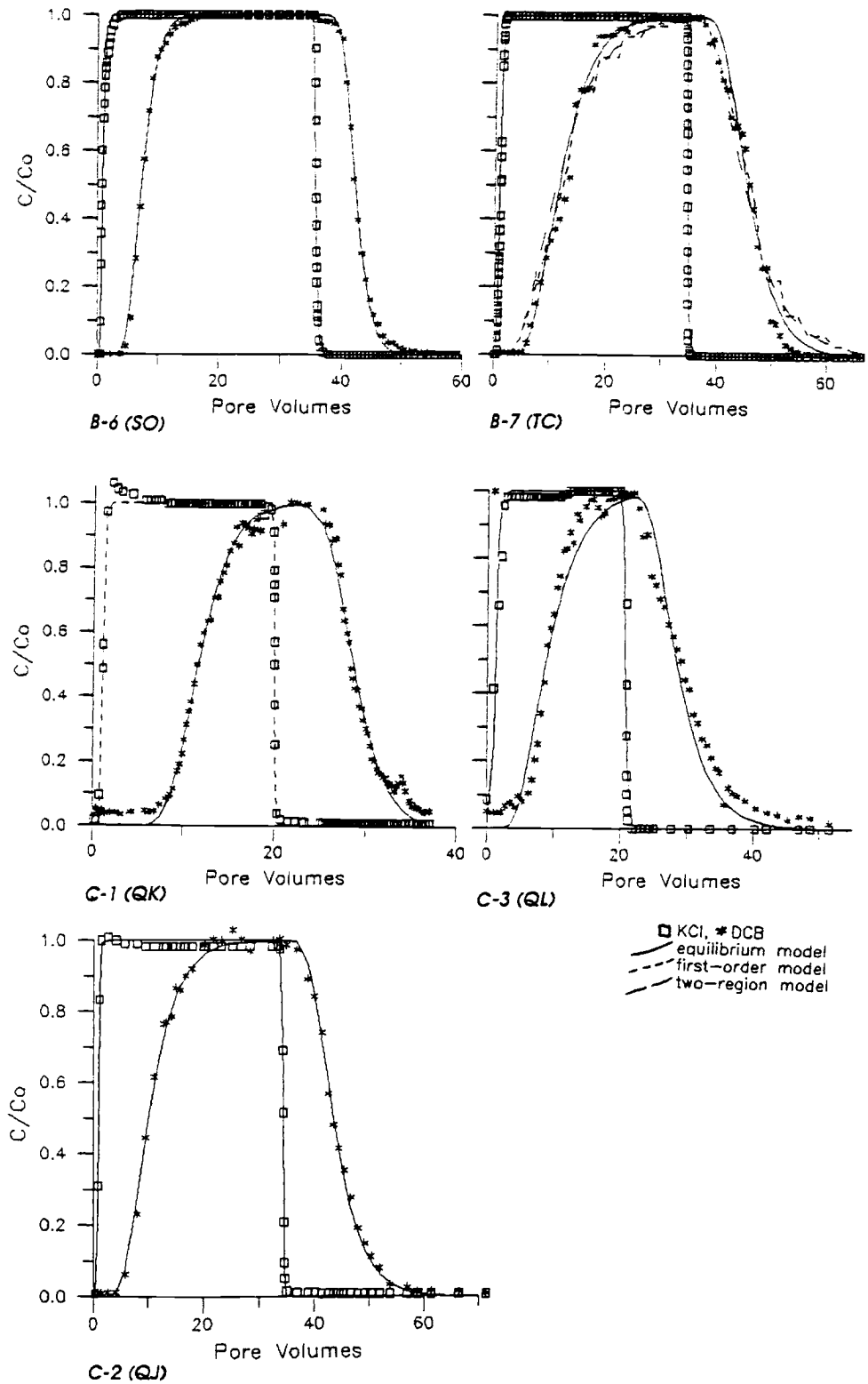

C.5 C_8 and C_{18} modified Silica

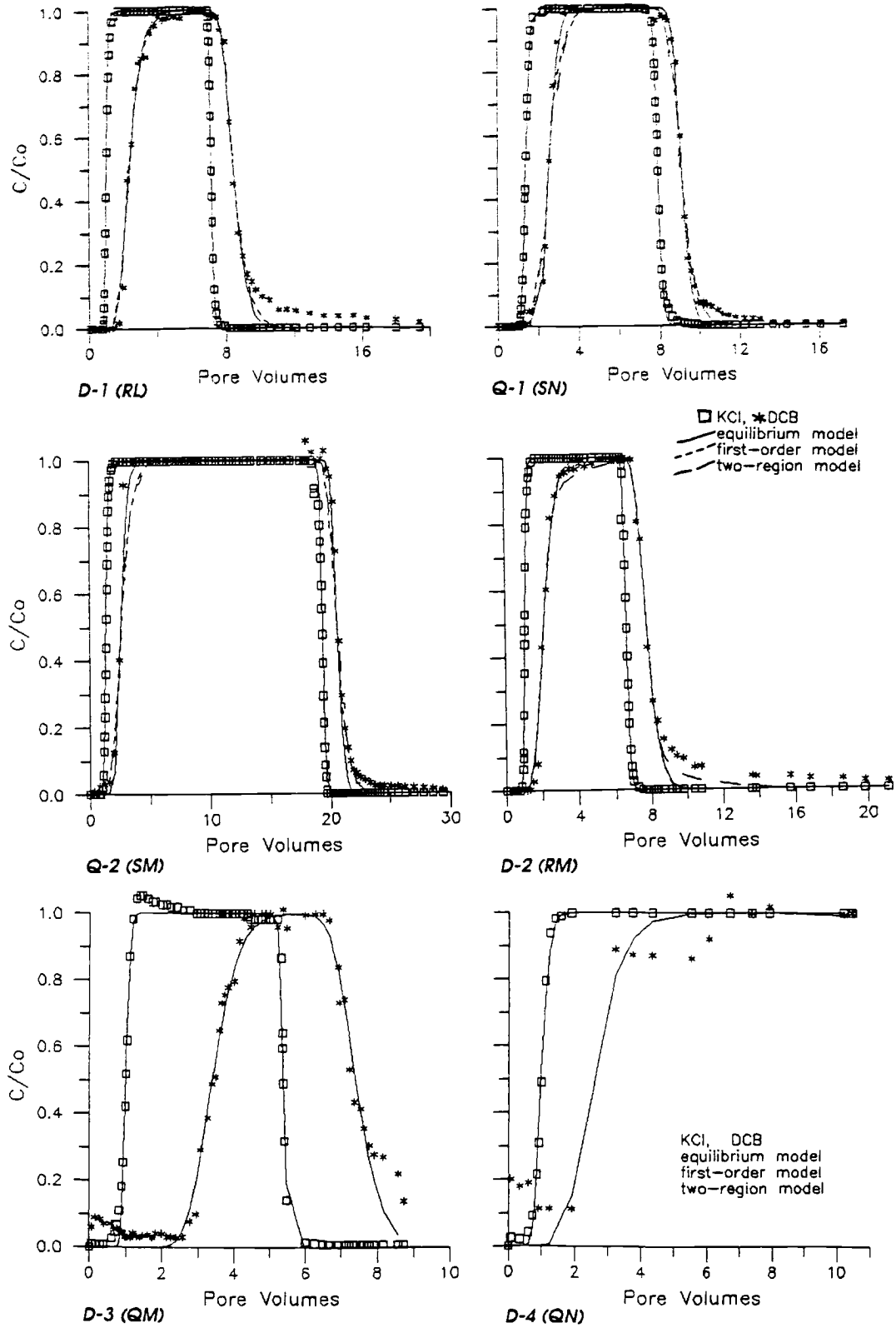

C.6 Phenyl monomer modified Silica

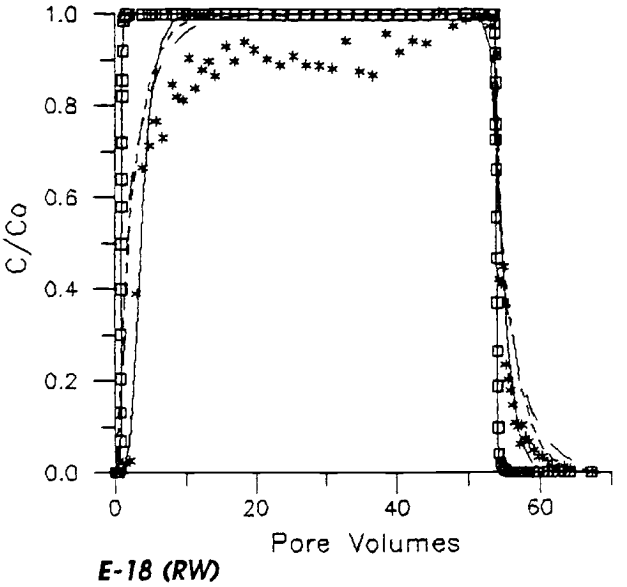

E-18 (RW)

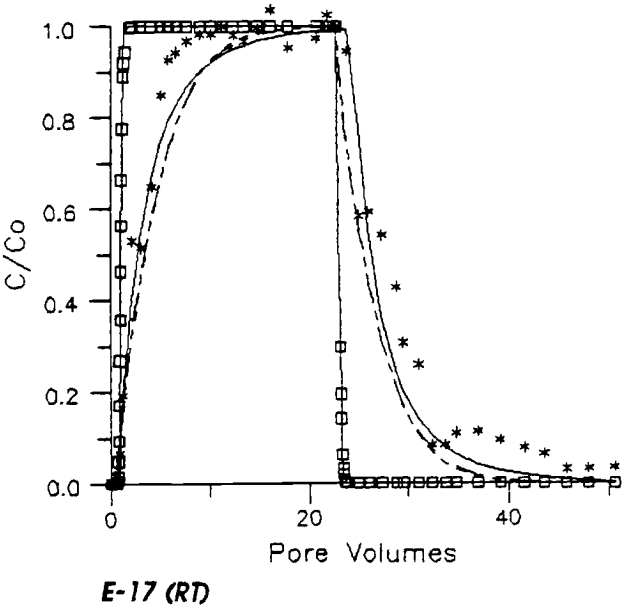

E-17 (RT)

C.7 Chlorobenzene on Surface E

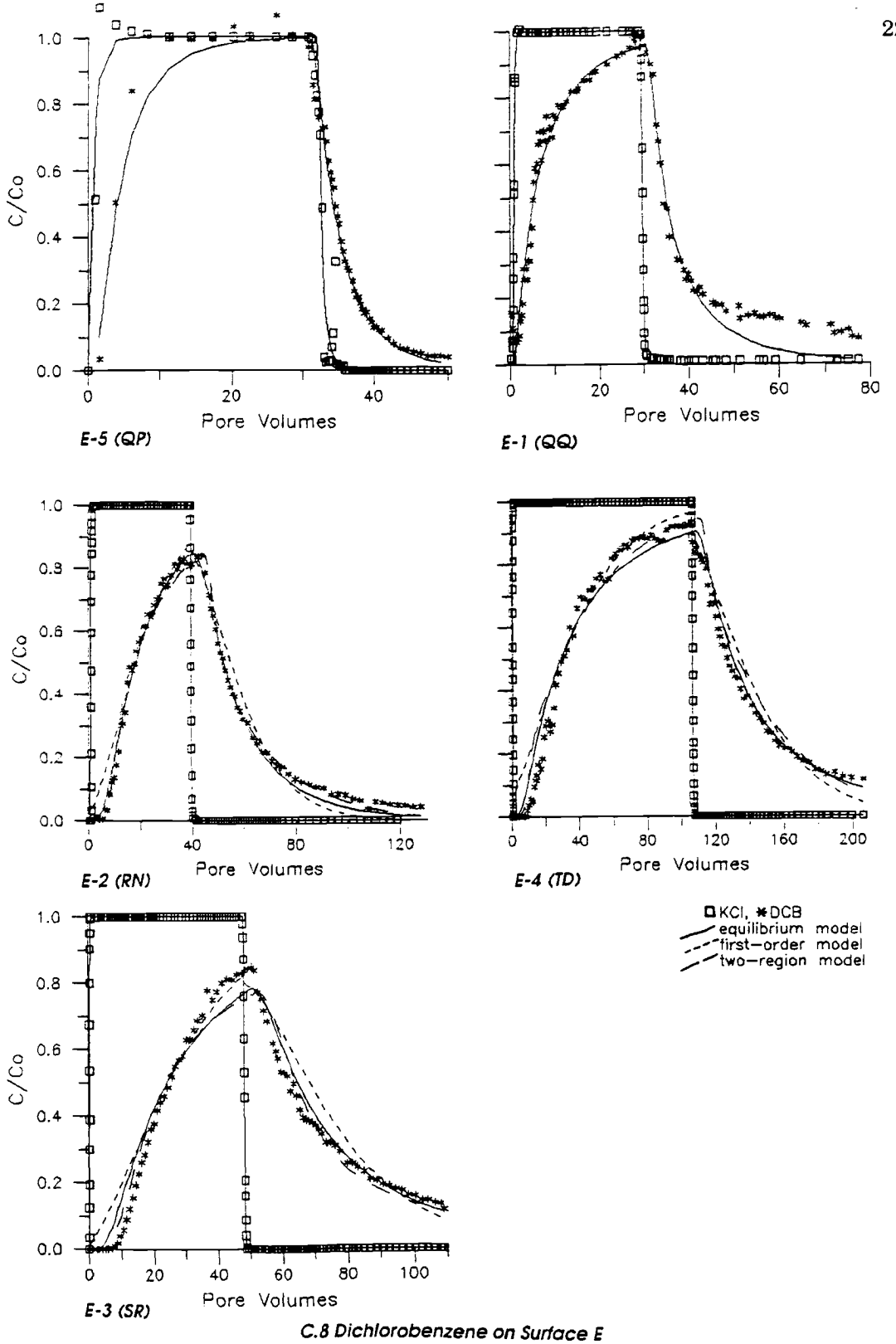

C.8 Dichlorobenzene on Surface E

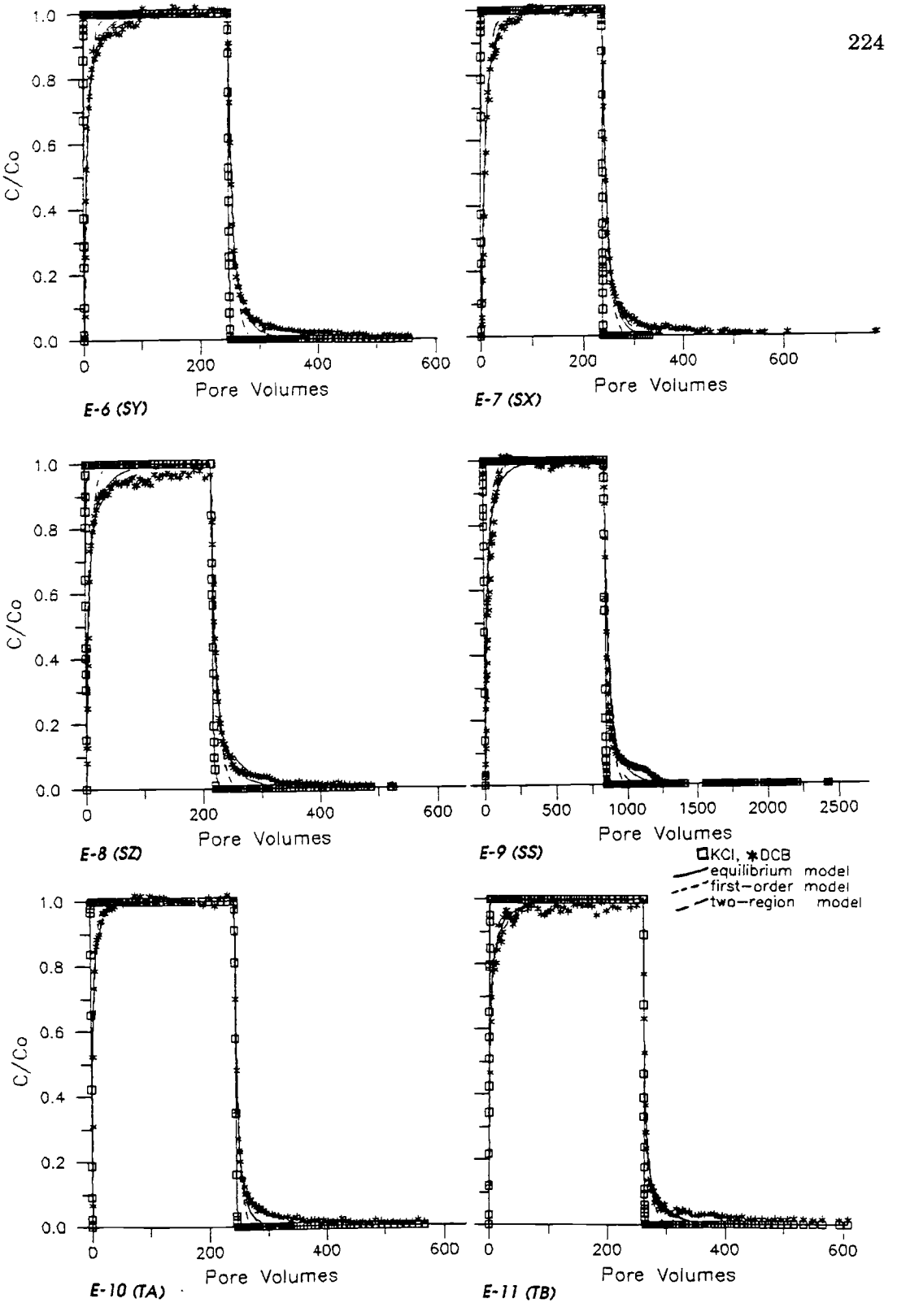

C.9 DCB at different temperature

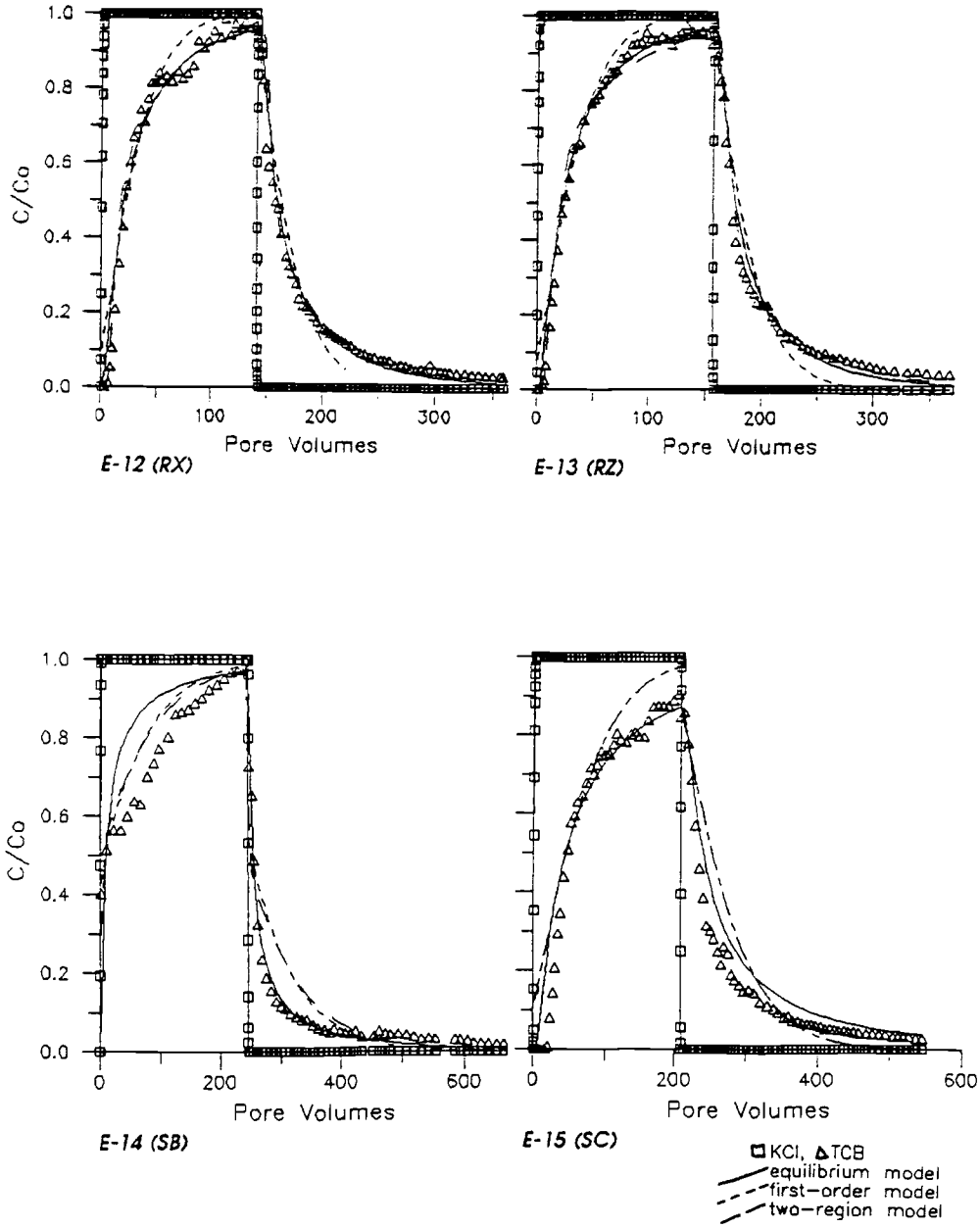

C.10 TCB on Surface E

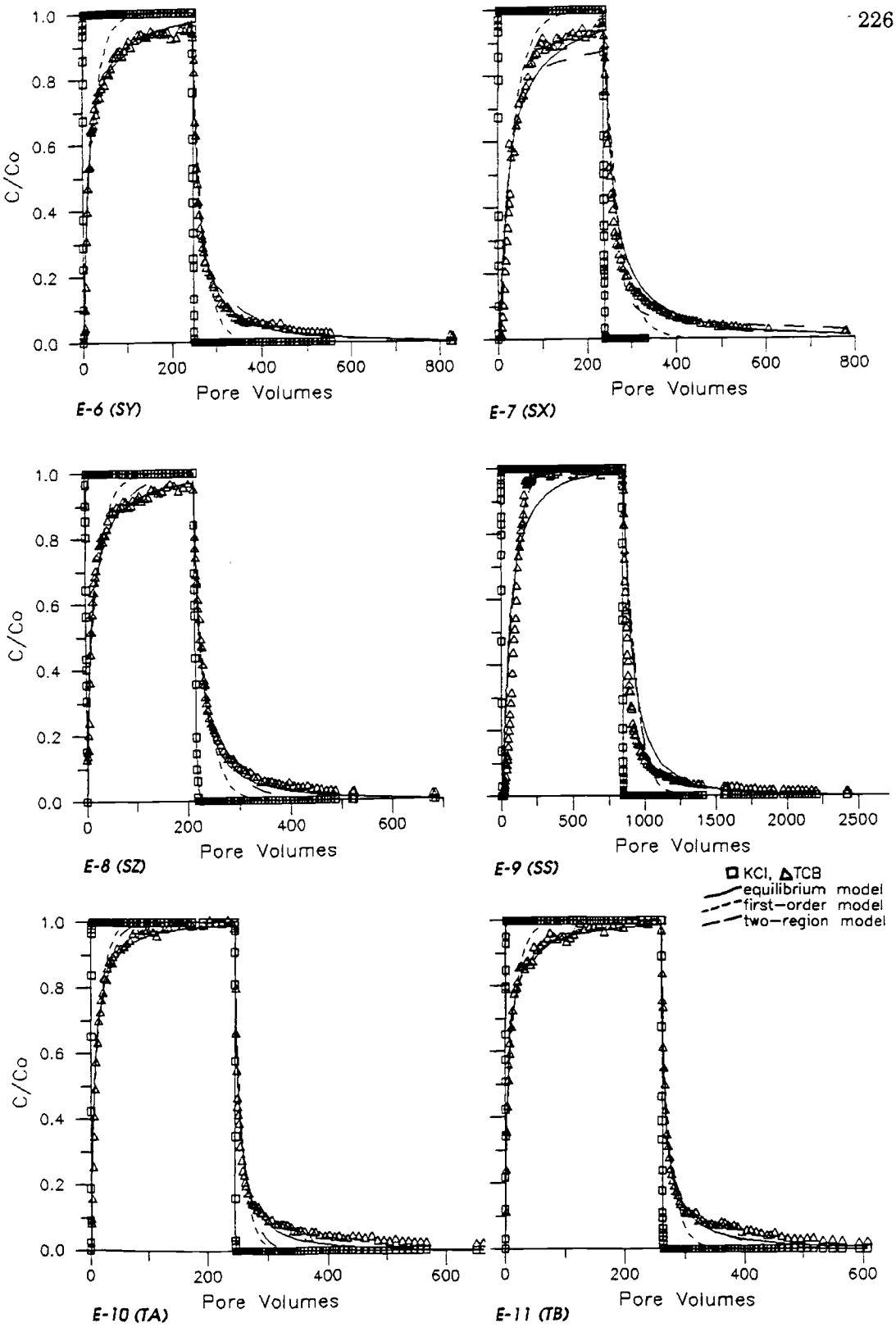

C.11 TCB at different temperature

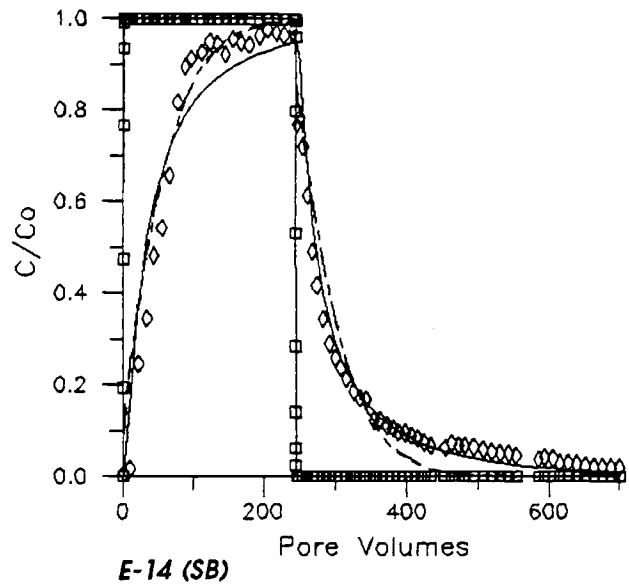

E-14 (SB)

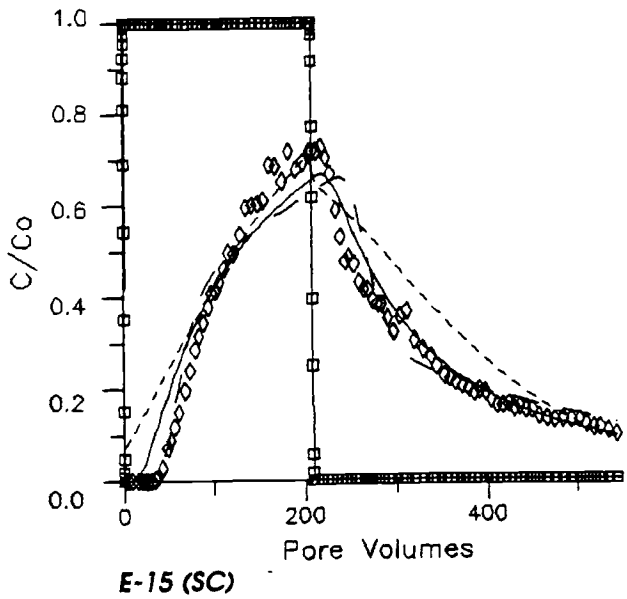

E-15 (SC)

C.12 TeCB on Surface E

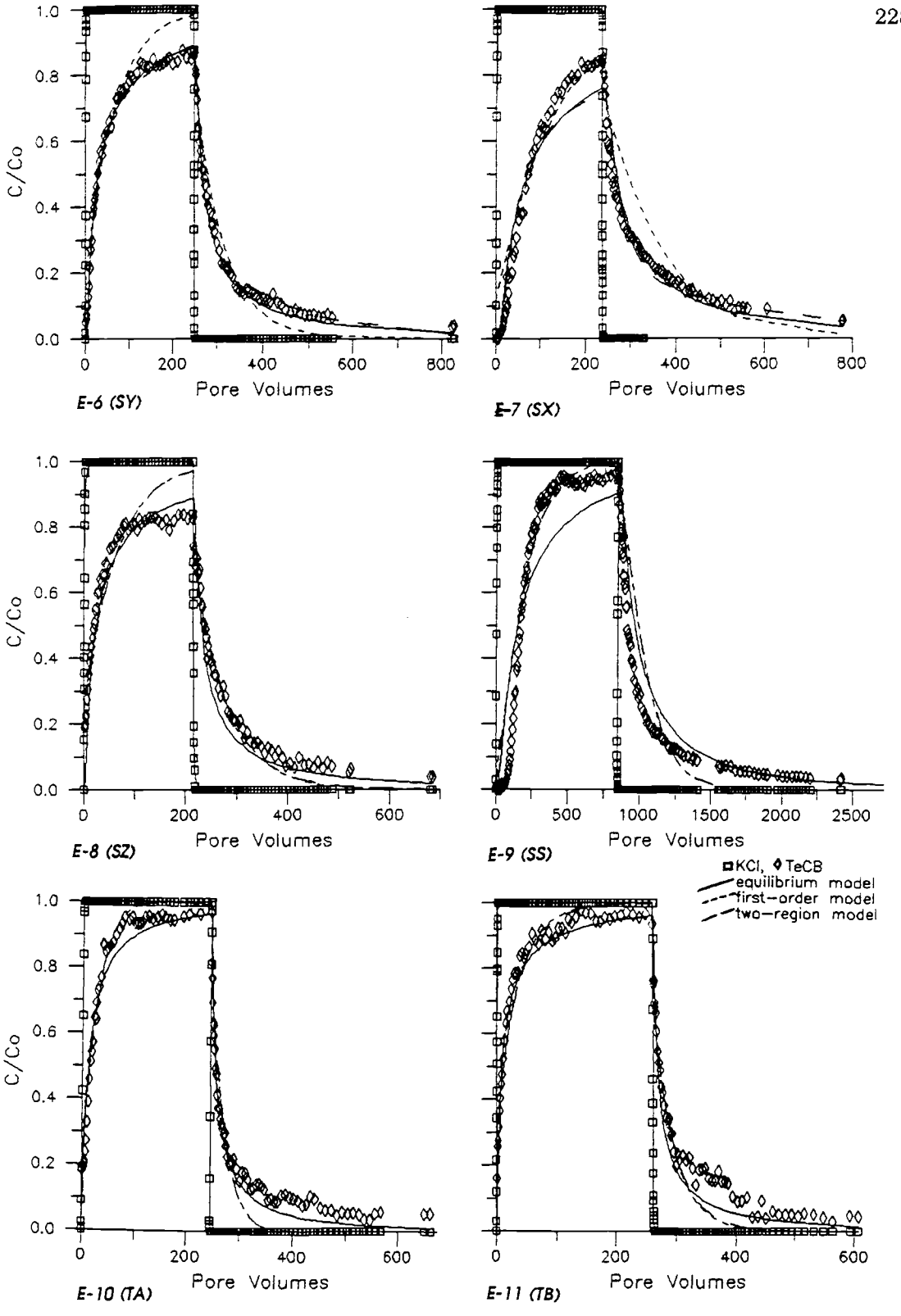

C.13 TeCB at different temperature

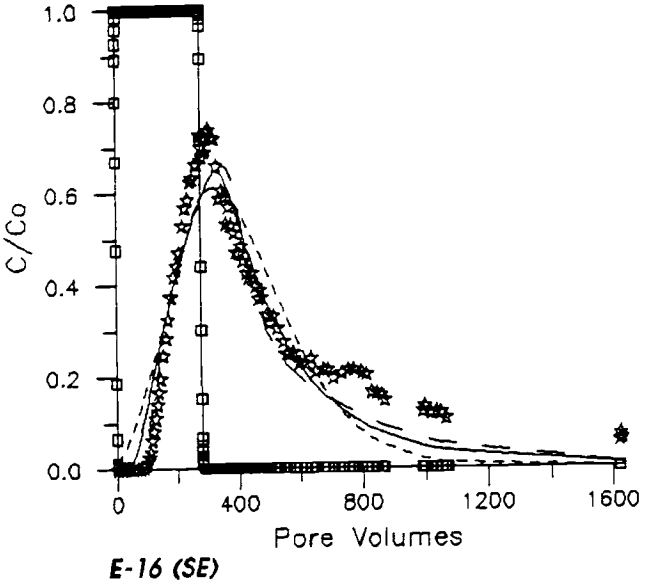

E-16 (SE)

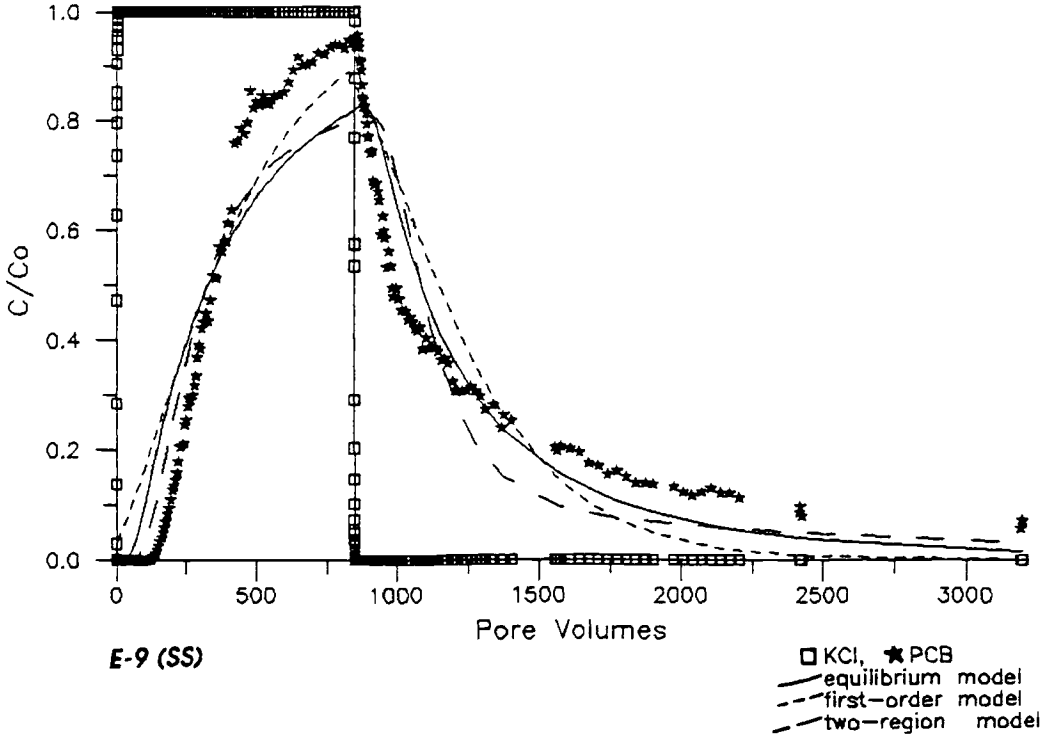

E-9 (SS)

C.14 PCB on Surface E

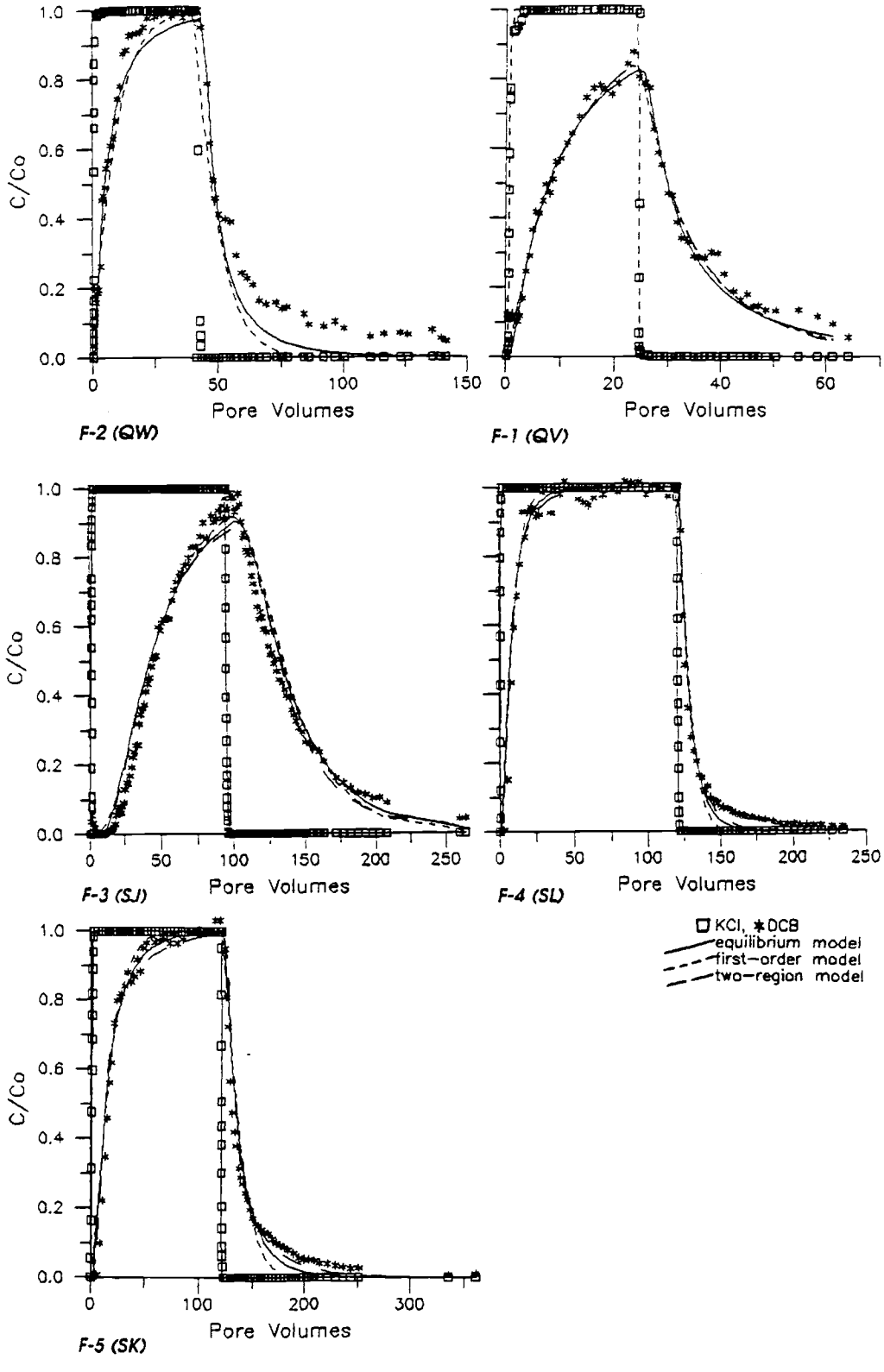

C.15 20 um phenyl polymer surface F

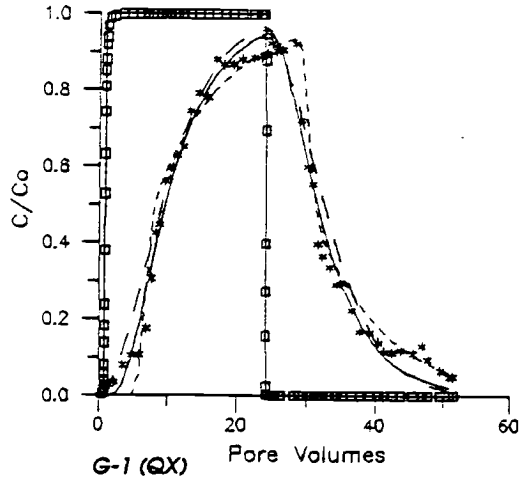

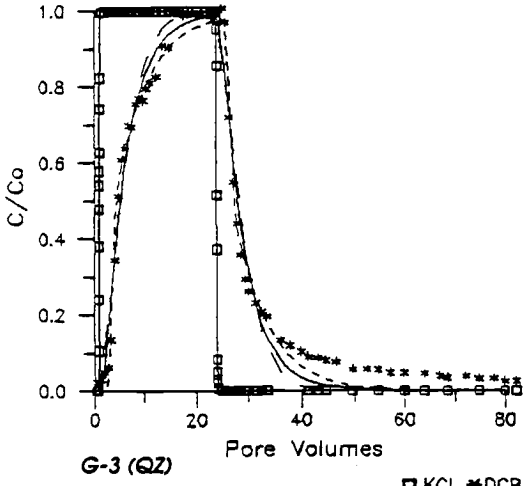

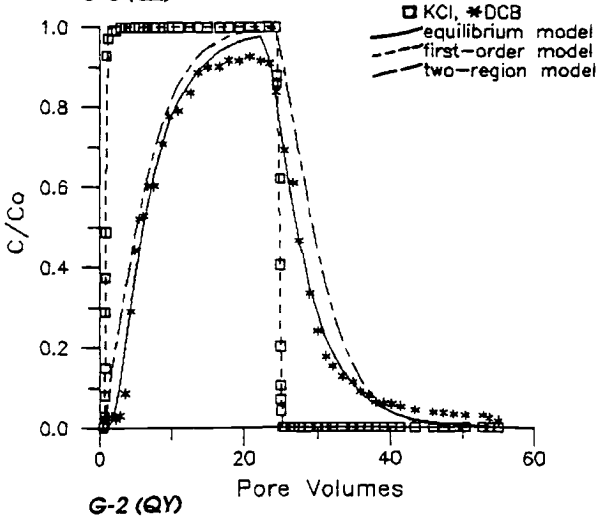

C.16 20 um phenyl polymer surface G

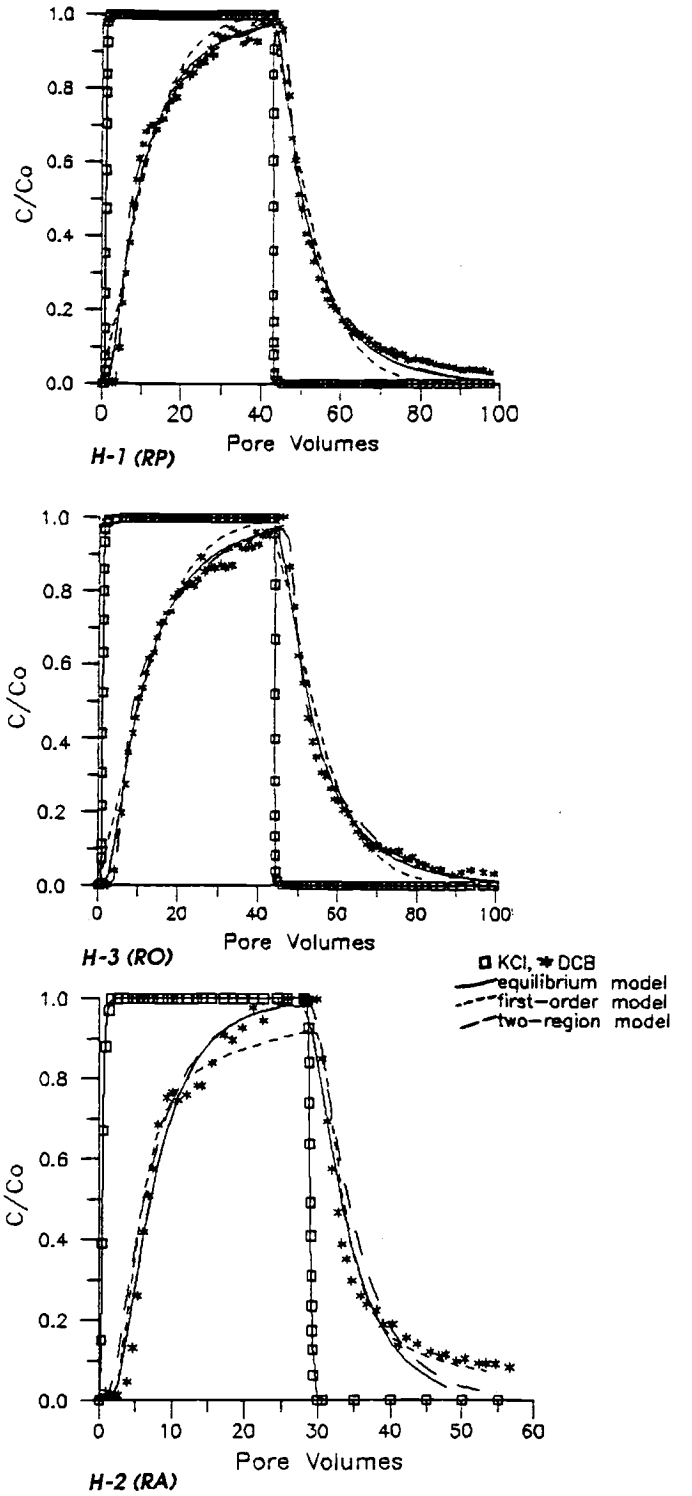

C.17 425 um phenyl polymer surface H

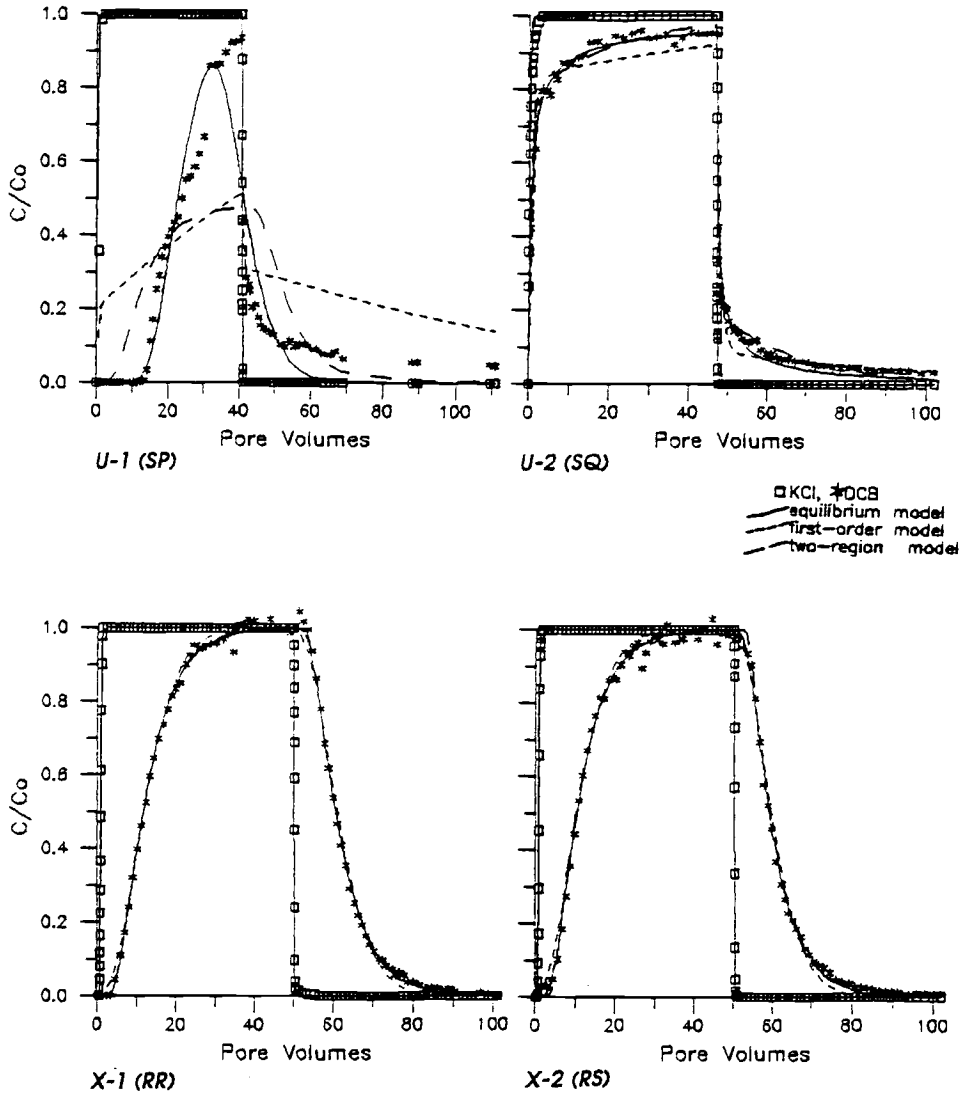

C.18 2 um phenyl surface and phenyl+C_{18} surface

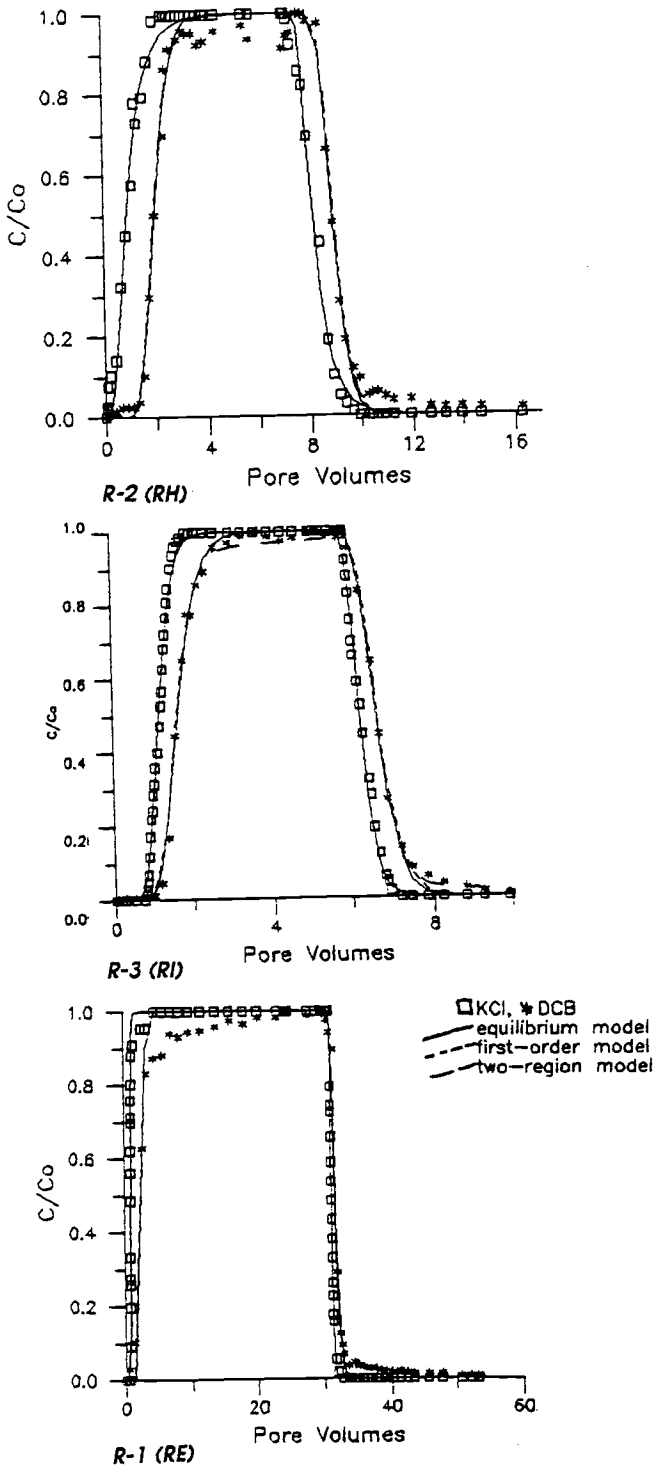

C.19 Dialcoholic surface

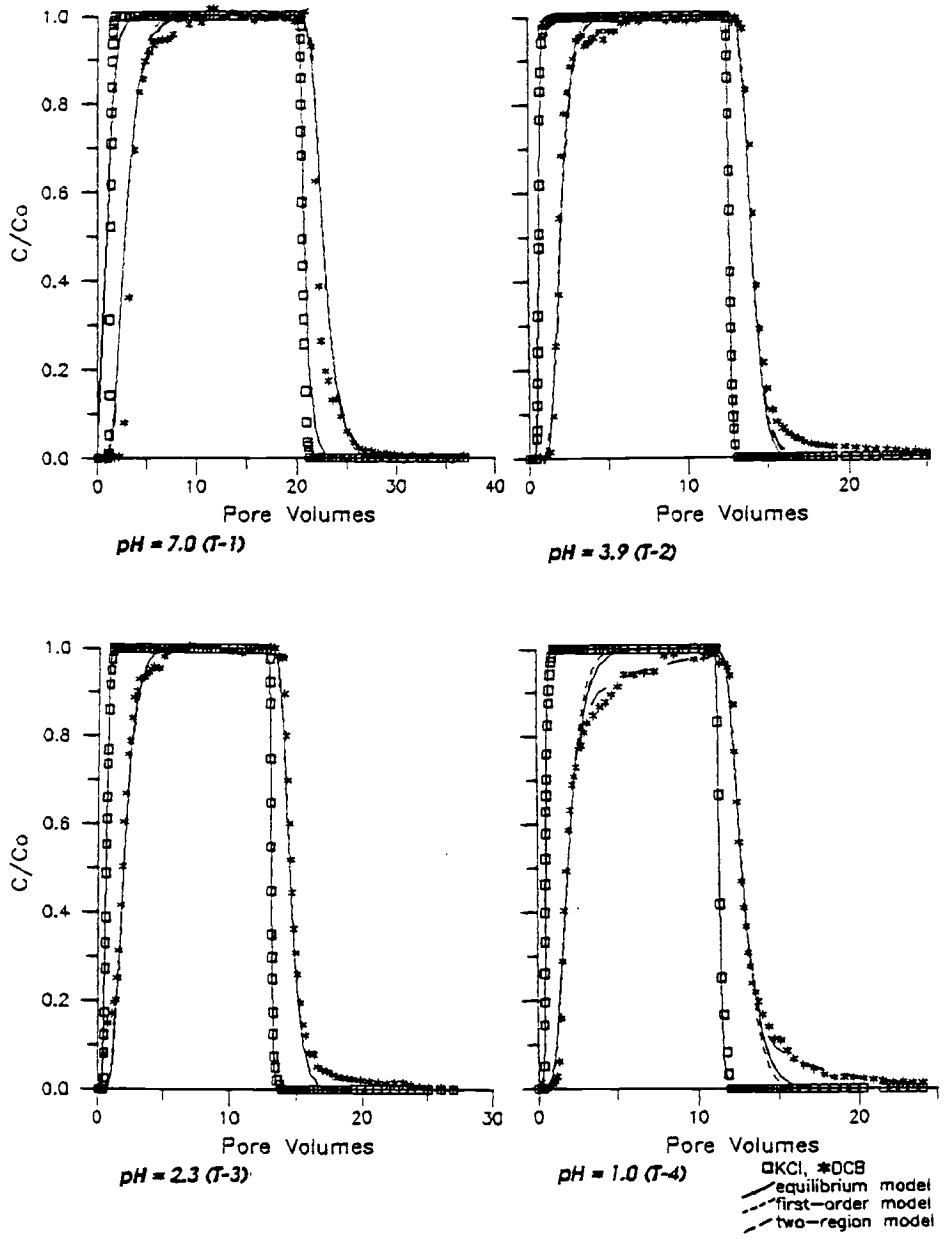

C.20 Amine Surface

```
C
C     ****************************************************************
C     *     MFITIM  -  MULTIPLE EXPERIMENT PARAMETER ESTIMATION      *
C     *           based on CFITIM by Rein van Genuchten (1981)       *
C     *     modified by Jim Szecsody and Karen Humes,  May, 1988     *
C     *  Non-linear Least Squares Analysis of Dimensional Parameters *
C     ****************************************************************
C
C     Note:  This version (1) assumes dispersion and pulse are fixed,
C     and only first order or two region model are used (R, B, Q variable)
C     and D, De, Pb, L same for all cases, velocity is different.
C
      IMPLICIT REAL*8(A-H,O-Z)
      DIMENSION Y(90,9),X(90,9),F(90,9),R(90,9),DELZ(90,5,9),B(10),E(5),
     1TH(10),NOB(9),QQ(5),CSS(9),XKP(9),XKB(9),FF(9),VEL(9),XAE(9),
     1P(5),PHI(5),Q(5,9),TB(10),A(5,5),D(5,5),INDEX(5),PEC(9),PUL(9)
      CHARACTER TITLE*60,BI(10)*3,FILEIN*20,FILEOUT*20,PLOTOUT*20
      DATA STOPCR/0.0005/
C
C     ----- OPEN I/O FILES -----
      WRITE(*,*)'INPUT FILENAME = ?'
      READ(*,19)FILEIN
   19 FORMAT(A20)
      OPEN(5,FILE=FILEIN,STATUS='OLD')
      WRITE(*,*)'OUTPUT FILENAME = ?'
      READ(*,21)FILEOUT
   21 FORMAT(A20)
      KP=6
      OPEN(6,FILE=FILEOUT,STATUS='NEW')
      WRITE(*,*)'PLOT FILENAME = ?'
      READ(*,21)PLOTOUT
      OPEN(7,FILE=PLOTOUT,STATUS='NEW')
C
C     ----- READ NUMBER OF CASES -----
      READ(5,1006) NC,KP
      IF(KP.NE.6) KP=1
      DO 120 NCASE=1,NC
      WRITE(KP,1000)
C
C     ----- READ INPUT PARAMETERS -----
      READ(5,1006) MODE,NDATA,NIT,NOB(NCASE)
      M=(MODE-1)/2
      IF(M.EQ.0) WRITE(KP,1021)
      IF(M.EQ.1) WRITE(KP,1022)
      IF(M.EQ.2) WRITE(KP,1023)
      N=MODE-2*M
      IF(N.EQ.1) WRITE(KP,1024)
      IF(N.EQ.2) WRITE(KP,1025)
      NU=3
      IF(MODE.GT.2) NU=5
      NU1=NU+1
      NU2=2*NU
      READ(5,1001) TITLE
      WRITE(KP,1002) TITLE
C
C     ----- READ COEFFICIENTS NAMES -----
      READ(5,1004) (BI(I),I=1,NU2)
C
C     ----- READ INITIAL ESTIMATES -----
      READ(5,1005) (B(I),I=NU1,NU2)
      IF(M.EQ.2) B(8)=1./B(7)
C
C     ----- READ INDICES -----
      READ(5,1006) (INDEX(I),I=1,NU)
      IF(M.EQ.2) INDEX(3)=0
      WRITE(KP,1007)
      DO 4  I=1,NU
      J=2*I-1
    4 WRITE(KP,1008) I,BI(J),BI(J+1),B(I+NU)
C     ----- READ COLUMN EXPERIMENT PARAMETERS -----
      READ(5,1005)VEL(NCASE),BULK,XLEN,TPORO,EPORO
      WRITE(KP,1026)VEL(NCASE),BULK,XLEN,TPORO,EPORO
      IF(NDATA.EQ.0) GO TO 10
C
C     ----- READ AND WRITE EXPERIMENTAL DATA -----
      DO 6 I=1,NOB(NCASE)
    6 READ(5,1005) X(I,NCASE),Y(I,NCASE)
   10 WRITE(KP,1009)
      DO 12 I=1,NOB(NCASE)
   12 WRITE(KP,1010) I,X(I,NCASE),Y(I,NCASE)
C
C     ----------
      NP=0
      DO 14 I=NU1,NU2
      TB(I)=B(I)
      IF(INDEX(I-NU).EQ.0) GO TO 14
      NP=NP+1
      K=2*NP-1
      J=2*(I-NU)-1
      BI(K)=BI(J)
      BI(K+1)=BI(J+1)
      B(NP)=B(I)
      TB(NP)=B(I)
      TH(NP)=B(NP)
   14 TH(I)=B(I)
C
C     ----------
      GA=0.02
      NIT=0
      NP2=2*NP
      CALL MODEL(TH,F(1,NCASE),NOB(NCASE),X(1,NCASE),INDEX,MODE)
      SSQ=0.
      DO 32 I=1,NOB(NCASE)
      R(I,NCASE)=Y(I,NCASE)-F(I,NCASE)
   32 SSQ=SSQ+R(I,NCASE)*R(I,NCASE)
      WRITE(KP,1011) (BI(J),BI(J+1),J=1,NP2,2)
      WRITE(KP,1012) NIT,SSQ,(B(I),I=1,NP)
C
C     ----- BEGIN OF ITERATION -----
   34 NIT=NIT+1
      GA=0.1*GA
      DO 38 J=1,NP
      TEMP=TH(J)
      TH(J)=1.01*TH(J)
      Q(J,NCASE)=0
      CALL MODEL(TH,DELZ(1,J,NCASE),NOB(NCASE),X(1,NCASE),INDEX,MODE)
      do 36 I=1,NOB(NCASE)
      DELZ(I,J,NCASE)=DELZ(I,J,NCASE)-F(I,NCASE)
   36 Q(J,NCASE)=Q(J,NCASE)+DELZ(I,J,NCASE)*R(I,NCASE)
      Q(J,NCASE)=100.*Q(J,NCASE)/TH(J)
C
C     ----- Q=XT*R (STEEPEST DESCENT) -----
   38 TH(J)=TEMP
      DO 44 I=1,NP
      DO 42 J=1,I
      SUM=0
```

```
      DO 40 K=1,NOB(NCASE)
   40 SUM=SUM+DELZ(K,I,NCASE)*DELZ(K,J,NCASE)
      D(I,J)=10000.*SUM/(TH(I)*TH(J))
   42 D(J,I)=D(I,J)
   44 E(I)=DSQRT(D(I,I))
   50 DO 52 I=1,NP
      DO 52 J=1,NP
   52 A(I,J)=D(I,J)/(E(I)*E(J))
C
C     ----- A IS THE SCALED MOMENT MATRIX -----
      DO 54 I=1,NP
      P(I)=Q(I,NCASE)/E(I)
      PHI(I)=P(I)
   54 A(I,I)=A(I,I)+GA
      CALL MATINV(A,NP,P)
C
C     ----- P/E IS THE CORRECTION VECTOR -----
      STEP=1.0
   56 DO 58 I=1,NP
   58 TB(I)=P(I)*STEP/E(I)+TH(I)
      DO 62 I=1,NP
      IF(TH(I)*TB(I))66,66,62
   62 CONTINUE
      SUMB=0
      CALL MODEL(TB,F(1,NCASE),NOB(NCASE),X(1,NCASE),INDEX,MODE)
      DO 64 I=1,NOB(NCASE)
      R(I,NCASE)=Y(I,NCASE)-F(I,NCASE)
   64 SUMB=SUMB+R(I,NCASE)*R(I,NCASE)
   66 SUM1=0.0
      SUM2=0.0
      SUM3=0.0
      DO 68 I=1,NP
      SUM1=SUM1+P(I)*PHI(I)
      SUM2=SUM2+P(I)*P(I)
   68 SUM3=SUM3+PHI(I)*PHI(I)
      ARG=SUM1/DSQRT(SUM2*SUM3)
      ARG1=0.
      IF(NP.GT.1) ARG1=DSQRT(1.-ARG*ARG)
      ANGLE=57.29578*DATAN2(ARG1,ARG)
C
C     ----------
      DO 72 I=1,NP
      IF(TH(I)*TB(I))74,74,72
   72 CONTINUE
      IF((SUMB-SSQ).LT.1.D-08)GO TO 80
   74 IF(ANGLE-30.0)76,76,78
   76 STEP=0.5*STEP
      GO TO 56
   78 GA=10.*GA
      GO TO 50
C
C     ----- PRINT COEFFICIENTS AFTER EACH ITERATION -----
   80 CONTINUE
      DO 82 I=1,NP
   82 TH(I)=TB(I)
      WRITE(KP,1012) NIT,SUMB,(TH(I),I=1,NP)
      DO 86 I=1,NP
      IF(DABS(P(I)*STEP/E(I))/(1.0D-20+DABS(TH(I)))-STOPCR) 86,86,94
   86 CONTINUE
      GO TO 96
   94 SSQ=SUMB
      IF(NIT.LE.MIT) GO TO 34
C
C     ----- END OF ITERATION LOOP -----
   96 CONTINUE
      CALL MATINV(D,NP,P)
C
C     ----- WRITE CORRELATION MATRIX -----
      DO 98 I=1,NP
   98 E(I)=DSQRT(DMAX1(D(I,I),1.D-20))
      WRITE(KP,1013) (I,I=1,NP)
      DO 102 I=1,NP
      DO 100 J=1,I
  100 A(J,I)=D(J,I)/(E(I)*E(J))
  102 WRITE(KP,1014) I,(A(J,I),J=1,I)
C
C     ----- READ FINAL PARAMETERS INTO ARRAYS -----
      XKP(NCASE)=(B(1)-1.0)*TPORO/BULK
      PEC(NCASE)=B(6)
      PUL(NCASE)=B(10)
      IF(MODE.GT.4)THEN
      XKB(NCASE)=B(3)*TPORO*VEL(NCASE)/(XKP(NCASE)*BULK*XLEN)
      ELSE
      XAE(NCASE)=B(3)*EPORO*VEL(NCASE)/XLEN
      FF(NCASE)=(B(2)*(TPRO+BULK*XKP(NCASE))-EPORO)/(BULK*XKP(NCASE))
      ENDIF
C
C     ----- CALCULATE 95% CONFIDENCE INTERVAL -----
      Z=1./FLOAT(NOB(NCASE)-NP)
      SDEV=DSQRT(Z*SUMB)
      TVAR=1.96+Z*(2.3779+Z*(2.7135+Z*(3.187936+2.466666*Z**2)))
      WRITE(KP,1015)
      DO 108 I=1,NP
      SECDEF=E(I)*SDEV
      TVALUE=TH(I)/SECDEF
      TSEC=TVAR*SECDEF
      TMCDE=TH(I)-TSEC
      TPCDE=TH(I)+TSEC
      J=2*I-1
  108 WRITE(KP,1016) I,BI(J),BI(J+1),TH(I),SECDEF,TVALUE,TMCDE,TPCDE
      WRITE(KP,1020)NCASE
  120 CONTINUE
C     ----- MULTIPLE EXPERIMENT PARAMETER ESTIMATION -----
      NU=5
      NU1=NU + 1
      NU2=2*NU
C
C     ----- AVERAGE VALUE OF DIMENSIONAL PARAMETERS -----
      AKP=0.0
      AKB=0.0
      AAE=0.0
      AF=0.0
      DO 122 NCASE = 1,NC
      AKP = AKP + XKP(NCASE)
      IF(MODE.GT.4)THEN
      AKB = AKB + XKB(NCASE)
      ELSE
      AAE = AAE + XAE(NCASE)
      AF = AF + FF(NCASE)
      ENDIF
  122 CONTINUE
C     ----- CALCULATE AVERAGE VALUE OF DIMENSIONLESS PARAMETERS -----
      AKP = AKP/NC
      ARETARD = AKP*BULK/TPORO + 1.0
      IF(MODE.GT.4)THEN
      AKB = AKB/NC
      AOMEGA = AKB*BULK*AKP*XLEN/(TPORO*VEL(1))
      ABETA = 1./ARETARD
      ELSE
      AAE = AAE/NC
      AOMEGA = AAE*XLEN/(TPORO*VEL(1))
      AF = AF/NC
```

```
      ABETA = (AF*BULK*AKP + EPORO)/(AKP*BULK + TPORO)
      ENDIF
C     ----- CALCULATE SUM(SSQ)/NC -----
      SSQ=0.0
      DO 127 NCASE = 1,NC
      NP=0
      B(6)=PEC(NCASE)
      B(7)=ARETARD
      B(8)=ABETA
      B(9)=AOMEGA*VEL(1)/VEL(NCASE)
      B(10)=PUL(NCASE)
      DO 125 I=NU1,NU2
      TB(I)=B(I)
      IF(INDEX(I-NU).EQ.0)GOTO 125
      NP=NP + 1
      K=2*NP-1
      J=2*(I-NU)-1
      BI(K)=BI(J)
      BI(K+1)=BI(J+1)
      B(NP)=B(I)
      TB(NP)=B(NP)
      TH(NP)=B(NP)
  125 TH(I)=B(I)
      GA=0.02
      NIT=0
      NP2=2*NP
      CALL MODEL(TH,F(1,NCASE),NOB(NCASE),X(1,NCASE),INDEX,MODE)
      DO 126 I=1,NOB(NCASE)
      R(I,NCASE)=Y(I,NCASE)-F(I,NCASE)
  126 SSQ=SSQ+R(I,NCASE)*R(I,NCASE)
  127 CONTINUE
      WRITE(KP,1027) (BI(J),BI(J+1),J=1,NP2,2)
      WRITE(KP,1012) NIT,SSQ,(B(I),I=1,NP)
C     ----- BEGIN ITERATION -----
  134 NIT=NIT+1
      GA=0.1*GA
      DO 138 J=1,NP
      QQ(J)=0.0
      DO 137 NCASE=1,NC
      TH(9)=TH(9)*VEL(1)/VEL(NCASE)
      TH(6)=PEC(NCASE)
      TH(10)=PUL(NCASE)
      TEMP=TH(J)
      TH(J)=1.01*TH(J)
      Q(J,NCASE)=0.
      CALL MODEL(TH,DELZ(1,J,NCASE),NOB(NCASE),X(1,NCASE),INDEX,MODE)
      DO 136 I=1,NOB(NCASE)
      DELZ(I,J,NCASE)=DELZ(I,J,NCASE)-F(I,NCASE)
  136 Q(J,NCASE)=Q(J,NCASE)+DELZ(I,J,NCASE)*R(I,NCASE)
      Q(J,NCASE)=100.*Q(J,NCASE)/TH(J)
      QQ(J)=QQ(J)+Q(J,NCASE)
C     ----- Q=XI*R (STEEPEST DESCENT) -----
  137 CONTINUE
  138 TH(J)=TEMP
      DO 144 I=1,NP
      DO 142 J=1,I
      SUM=0
      DO 141 NCASE = 1,NC
      DO 140 K=1,NOB(NCASE)
  140 SUM=SUM+DELZ(K,I,NCASE)*DELZ(K,J,NCASE)
  141 CONTINUE
      D(I,J)=10000.*SUM/(TH(I)*TH(J))
  142 D(J,I)=D(I,J)
  144 E(I)=DSQRT(D(I,I))
  150 DO 152 I=1,NP
      DO 152 J=1,NP
  152 A(I,J)=D(I,J)/(E(I)*E(J))
C     ----- A IS THE SCALED MOMENT MATRIX -----
      DO 154 I=1,NP
      P(I)=QQ(I)/E(I)
      PHI(I)=P(I)
  154 A(I,I)=A(I,I)+GA
      CALL MATINV(A,NP,P)
C     ----- P/E IS THE CORRECTION VECTOR -----
      STEP=1.0
  156 DO 158 I=1,NP
  158 TB(I)=P(I)*STEP/E(I)+TH(I)
      DO 162 I=1,NP
      IF(TH(I)*TB(I))166,166,162
  162 CONTINUE
      SUMB=0
      DO 165 NCASE=1,NC
      TB(9)=TB(9)*VEL(1)/VEL(NCASE)
      TB(6)=PEC(NCASE)
      TB(10)=PUL(NCASE)
      CALL MODEL(TB,F(1,NCASE),NOB(NCASE),X(1,NCASE),INDEX,MODE)
      DO 164 I=1,NOB(NCASE)
      R(I,NCASE)=Y(I,NCASE)-F(I,NCASE)
  164 SUMB=SUMB+R(I,NCASE)*R(I,NCASE)
      CSS(NCASE)=0.0
      IF(NCASE.EQ.1)THEN
      CSS(NCASE)=SUMB
      ELSE
      CSS(NCASE)=SUMB-CSS(NCASE-1)
      ENDIF
  165 CONTINUE
  166 SUM1=0.0
      SUM2=0.0
      SUM3=0.0
      DO 168 I=1,NP
      SUM1=SUM1+P(I)*PHI(I)
      SUM2=SUM2+P(I)*P(I)
  168 SUM3=SUM3+PHI(I)*PHI(I)
      ARG1=0.
      IF(NP.GT.1) ARG1=DSQRT(1.-ARG*ARG)
      ANGLE=57.29578*DATAN2(ARG1,ARG)
C
      DO 172 I=1,NP
      IF(TH(I)*TB(I))174,174,172
  172 CONTINUE
      WRITE(*,*)SUMB,SSQ
      IF((SUMB-SSQ).LT.1.D-07)GOTO 180
  174 IF(ANGLE-30.0)176,176,178
  176 STEP=0.5*STEP
      GOTO 156
  178 GA=10.*GA
      GOTO 150
C     ----- PRINT COEFFICIENTS AFTER EACH ITERATION -----
  180 CONTINUE
      DO 182 I=1,NP
  182 TH(I)=TB(I)
      WRITE(KP,1012) NIT,SUMB,(TH(I),I=1,NP)
      DO 186 I=1,NP
      IF(DABS(P(I)*STEP/E(I))/(1.D-20+DABS(TH(I)))-STOPCR)186,186,194
  186 CONTINUE
      GOTO 196
  194 SSQ=SUMB
      IF(NIT.LE.MIT)GOTO 134
C     ----- END OF ITERATION LOOP -----
  196 CONTINUE
      CALL MATINV(D,NP,P)
C     ----- WRITE CORRELATION MATRIX -----
```

```
      DO 138 I=1,NP
  138 E(I)=DSQRT(DMAX1(D(I,I),1.D-20))
      WRITE(KP,1013) (I,I=1,NP)
      DO 202 I=1,NP
      DO 200 J=1,I
  200 A(J,I)=D(J,I)/(E(I)*E(J))
  202 WRITE(KP,1014) I,(A(J,I),J=1,I)
C     ----- CALCULATE 95% CONFIDENCE INTERVAL -----
      Z=1./FLOAT(NOB(1)-NP)
      SDEV=DSQRT(Z*SUMB)
      TVAR=1.96+Z*(2.3773+Z*(2.7135+Z*(3.187936+2.4666666*Z**2)))
      WRITE(KP,1015)
      WRITE(KP,2002)
      DO 208 I=1,NP
      SECDEF=E(I)*SDEV
      TVALUE=TH(I)/SECDEF
      TSEC=TVAR*SECDEF
      TMCDE=TH(I)-TSEC
      TPCDE=TH(I)+TSEC
      J=2*I-1
  208 WRITE(KP,1016)I,BI(J),BI(J+1),TH(I),SECDEF,TVALUE,TMCDE,TPCDE
C     ----- PREPARE FINAL OUTPUT -----
      WRITE(KP,2003)
      DO 211 NCASE=1,NC
      AOMEGA=TH(9)*VEL(1)/VEL(NCASE)
      WRITE(KP,2008)NCASE,AOMEGA,CSS(NCASE)
      WRITE(7,2008)NCASE,AOMEGA,CSS(NCASE)
      DO 210 I=1,NOB(NCASE)
  210 WRITE(7,2001)X(I,NCASE),F(I,NCASE)
  211 CONTINUE
      AKP=(TH(7)-1.)*TPORO/BULK
      WRITE(KP,2004)AKP
      IF(MODE.GT.4)THEN
      AKB=TH(9)*TPORO*VEL(1)/(AKP*BULK*XLEN)
      WRITE(KP,2005)AKB
      ELSE
      AAE=TH(3)*EPORO*VEL(1)/XLEN
      WRITE(KP,2006)AAE
      AF=(TH(2)*(TPORO+BULK*AKP)-EPORO)/(BULK*AKP)
      WRITE(KP,2007)AF
      ENDIF
C     ----- END OF PROBLEM -----
 1000 FORMAT(//5X,67(1H*),/5X,1H*,65X,1H*/5X,1H*,5X,'NONLINEAR LEAST SQU
     1ARES ANALYSIS',28X,1H*/5X,1H*65X,1H*)
 1001 FORMAT(A60)
 1002 FORMAT(5X,1H*,A60,5X,1H*/5X,1H*,65X,1H*/5X,67(1H*))
 1004 FORMAT(5(2A3,4X))
 1005 FORMAT(5F10.0)
 1006 FORMAT(5I5)
 1007 FORMAT(//5X,'INITIAL VALUES OF COEFFICIENTS'/5X,30(1H=)/5X,'NO',
     16X,'NAME',7X,'INITIAL VALUE')
 1008 FORMAT(4X,I3,5X,2A3,4X,F12.3)
 1009 FORMAT(//5X,'OBSERVED DATA'/5X,13(1H=)/5X,'OBS. NO.',5X,'PORE VOLU
     1ME',5X,'CONCENTRATION')
 1010 FORMAT(5X,I5,5X,F12.4,4X,F12.4)
 1011 FORMAT(//5X,'ITERATION',5X,'SSQ',2X,5(4X,2A3))
 1012 FORMAT(5X,I5,6X,F9.7,2X,3F10.4,3(1X,E10.3))
 1013 FORMAT(//5X,'CORRELATION MATRIX'/5X,18(1H=)/8X,10(2X,I2,7X))
 1014 FORMAT(3X,I3,10(2X,F7.4,2X))
 1015 FORMAT(///5X,'NON-LINEAR LEAST SQUARES ANALYSIS, FINAL RESULTS'
     1/5X,48(1H=)//5AX,'95% CONFIDENCE LIMITS'/5X,'VAR',2X,'NAME'
     2,6X,'VALUE',6X,'S.E.COEFF.',3X,'T-VALUE',5X,'LOWER',8X,'UPPER')
 1016 FORMAT(5X,I2,2X,2A3,F12.5,3X,F9.4,4X,F8.2,2X,F9.4,4X,F9.4)
 1017 FORMAT(//5X,4(1H-),'ORDERED BY COMPUTER INPUT',5(1H-), 3X,8(1H-
     1),'ORDERED BY RESIDUALS',6(1H-)/11X,'PORE',3X,'CONCENTRATION',
     23X,'RESI-',9X,'PORE',3X,'CONCENTRATION',3X,'RESI-'/5X,'NO',2X,
     3'VOLUME',4X,'OBS.',2X,'FITTED',4X,'DUAL',3X,'NO',3X,'VOLUME',4X,
     4'OBS.',2X,'FITTED',4X,'DUAL')
 1018 FORMAT(5X,I2,4F8.3,3X,I2,4F8.3)
 1020 FORMAT(///5X,'END OF PROBLEM FOR CASE = ',I2)
 1021 FORMAT(5X,1H*,5X,'EQUILIBRIUM TRANSPORT (MODEL A)',22X,1H*)
 1022 FORMAT(5X,1H*,5X,'NON-EQUILIBRIUM TRANSPORT (MODEL B)',25X,1H*)
 1023 FORMAT(5X,1H*,5X,'ONE-SITE KINETIC ADSORPTION (MODEL D)',23X,1H*)
 1024 FORMAT(5X,1H*,5X,'FIRST-TYPE BOUNDARY CONDITION',31X,1H*)
 1025 FORMAT(5X,1H*,5X,'THIRD-TYPE BOUNDARY CONDITION',31X,1H*)
 1026 FORMAT(5X,'VELOCITY = ',F10.6,3X,', Pb = ',F4.3,', L = ',F6.2,
     1', D = ',F4.3,', De = ',F4.3)
 1027 FORMAT(//5X,'ITERATION',5X,'S.SSQ',2X,5(4X,2A3))
 2001 FORMAT(2X,F8.3,2X,F8.3)
 2002 FORMAT(2X,'OMEGA USES VELOCITY FROM FIRST CASE')
 2003 FORMAT(//5X,'FINAL MULTIPARAMETER RESULTS')
 2004 FORMAT(/5X,'AVERAGE Kp = ',E10.4)
 2005 FORMAT(5X,'AVERAGE kb = ',E10.4)
 2006 FORMAT(5X,'AVERAGE ALPHA(E) = ',E10.4)
 2007 FORMAT(5X,'AVERAGE F = ',E10.4)
 2008 FORMAT(5X,'DATASET = ',I2,',  OMEGA = ',E10.4,',  SSQ = ',F9.7)
C
C     ----- CLOSE FILES -----
      CLOSE(5)
      CLOSE(6)
      CLOSE(7)
      STOP
      END
C
C     ------------------------------------------------------------
      SUBROUTINE MATINV(A,NP,B)
      IMPLICIT REAL*8(A-H,O-Z)
      DIMENSION A(5,5),B(10),INDEX(5,2)
      DO 2 J=1,5
    2 INDEX(J,1)=0
      I=0
    4 AMAX=-1.0
      DO 11 J=1,NP
      IF(INDEX(J,1)) 11,6,11
    6 DO 10 K=1,NP
      IF(INDEX(K,1)) 10,8,10
    8 P=DABS(A(J,K))
      IF(P.LE.AMAX) GO TO 10
      IR=J
      IC=K
      AMAX=P
   10 CONTINUE
   11 CONTINUE
      IF(AMAX) 30,30,14
   14 INDEX(IC,1)=IR
      IF(IR.EQ.IC) GO TO 18
      DO 16 L=1,NP
      P=A(IR,L)
      A(IR,L)=A(IC,L)
   16 A(IC,L)=P
      P=B(IR)
      B(IR)=B(IC)
      B(IC)=P
      I=I+1
      INDEX(I,2)=IC
   18 P=1./A(IC,IC)
      A(IC,IC)=1.0
      DO 20 L=1,NP
   20 A(IC,L)=A(IC,L)*P
      B(IC)=B(IC)*P
      DO 24 K=1,NP
      IF(K.EQ.IC) GO TO 24
```

```
      P=A(K,IC)
      A(K,IC)=0.0
      DO 22 L=1,NP
   22 A(K,L)=A(K,L)-A(IC,L)*P
      B(K)=B(K)-B(IC)*P
   24 CONTINUE
      GO TO 4
   26 IC=INDEX(I,2)
      IR=INDEX(IC,1)
      DO 28 K=1,NP
      P=A(K,IR)
      A(K,IR)=A(K,IC)
   28 A(K,IC)=P
      I=I-1
   30 IF(I) 26,32,26
   32 RETURN
      END
C
C     ------------------------------------------------------------
      SUBROUTINE MODEL(B,Y,NOB,X,INDEX,MODE)
C
C     PURPOSE: TO CALCULATE CONCENTRATIONS FOR GIVEN PORE VOLUME
C
      IMPLICIT REAL*8(A-H,O-Z)
      DIMENSION B(10),Y(30),X(30),INDEX(5),XG(20),W(20)
      DATA XG/.03877242,.1160841,.1926376,.2681522,.3419941,.4137792,
     1.4830758,.5494671,.6125539,.6719567,.7273183,.7783057,.8246122,
     2.8659595,.9020988,.9328128,.9579168,.9772599,.9907262,.9982377/
      DATA W/.07750595,.07703982,.07611037,.07472317,.07288658,.07061165
     1,.06791204,.06480401,.06130624,.05743977,.05322785,.04863581,.0438
     227091,.03878217,.03346019,.02793701,.02224585,.01642106,.01049828,.
     300452128/
      K=0
      IF(MODE.LE.2) GO TO 12
C
C     ----- SOLUTION FOR NON-EQUILIBRIUM TRANSPORT (MODEL B) -----
      DO 2 I=6,10
      IF(INDEX(I-5).EQ.0) GO TO 2
      K=K+1
      B(I)=B(K)
    2 CONTINUE
      P=B(6)
      R=B(7)
      IF(MODE.GE.5) B(8)=1./R
      BETA=DMIN1(B(8),.9999D00)
      OMEGA=B(9)
      DO 10 J=1,NOB
      DO 9 M=1,2
      C=0.0
      T=X(J)+(1-M)*B(10)
      IF(T.LE.0.) GO TO 6
      A=DSQRT(1.+.05*P)
      T2=DMIN1(T,BETA*R*(1.+40.*(1.+A)/P))
      T1=DMAX1(0.000,BETA*R*(1.+40.*(1.-A)/P))
      IF(T2.LE.T1) GO TO 6
      DO 4 I=1,20
      TAU=0.5*(T1+T2+(T2-T1)*XG(I))
      C=C+W(I)*CCO(P,R,BETA,OMEGA,T,TAU,MODE)
      TAU=0.5*(T1+T2+(T1-T2)*XG(I))
    4 C=C+W(I)*CCO(P,R,BETA,OMEGA,T,TAU,MODE)
      C=0.5*(T2-T1)*C
    6 IF(M.EQ.2) GO TO 8
      Y(J)=C
    8 CONTINUE
   10 Y(J)=Y(J)-C
      RETURN
C
C     ----- SOLUTION FOR EQUILIBRIUM TRANSPORT (MODEL A) -----
   12 DO 14 I=4,6
      IF(INDEX(I-3).EQ.0) GO TO 14
      K=K+1
      B(I)=B(K)
   14 CONTINUE
      E=0.0
      P=B(4)
      R=B(5)
      DO 18 J=1,NOB
      DO 16 M=1,2
      C=0.0
      T=X(J)+(1-M)*B(6)
      IF(T.LE.0.) GO TO 18
      CM=0.5*(R-T)*DSQRT(P/(R*T))
      CP=0.5*(R+T)*DSQRT(P/(R*T))
      C=0.5*EXF(E,CM)+0.5*EXF(P,CP)
      IF(MODE.EQ.2) C=C+DSQRT(.3183099*P*T/R)*EXF(-CM*CM,E)-0.5*(2.*P+P*
     1T/R)*EXF(P,CP)
      IF(M.EQ.2) GO TO 18
      Y(J)=C
   16 CONTINUE
   18 Y(J)=Y(J)-C
      RETURN
      END
C
C     ------------------------------------------------------------
      FUNCTION CCO(P,R,BETA,OMEGA,T,TAU,MODE)
C
C     PURPOSE: TO CALCULATE THE ARGUMENT UNDER THE INTEGRAL SIGN -----
C
      IMPLICIT REAL*8 (A-H,O-Z)
      CCO=0.0
      BER=BETA*R
      CM=P*(BER-TAU)**2/(4.*BER*TAU)
      C=.282094B*DSQRT(P*BER/TAU**3)*DEXP(-CM)
      IF((MODE.EQ.3).OR.(MODE.EQ.5)) GO TO 2
      CP=(BER+TAU)*DSQRT(P/(4.*BER*TAU))
      C=2.*C*TAU/BER-0.5*P*EXF(P,CP)/BER
    2 IF(C.LT.1.D-07) RETURN
      EPSI=OMEGA*TAU/BER
      ETHA=OMEGA*(T-TAU)/(R-BER)
      CCO=C*GOLD(EPSI,ETHA)
      RETURN
      END
C
C     ------------------------------------------------------------
      FUNCTION GOLD(X,Y)
C
C     PURPOSE: TO CALCULATE J(X,Y)
C
      IMPLICIT REAL*8(A-H,O-Z)
      GOLD=0.0
      BF=0.0
      E=2.*DSQRT(X*Y)
      Z=X+Y-E
      IF(Z.GT.17.) GO TO 8
      IF(E.NE.0.) GO TO 2
      GOLD=DEXP(-X)
      RETURN
    2 A=DMAX1(X,Y)
      B=DMIN1(X,Y)
      NT=11.+2.*B+0.3*A
      IF(NT.GT.25) GO TO 6
      I=0
```

```
      IF(X.LT.Y) I=1
      GXY=1.+I*(B-1.)
      GX=1.0
      GY=GXY
      GZ=1.0
      DO 4 K=1,NT
      GX=GX*A/K
      GY=GY*B/(K+I)
      GZ=GZ+GX
    4 GXY=GXY+GY+GZ
      GOLD=GXY*DEXP(-X-Y)
      GO TO 8
    6 DA=DSQRT(A)
      DB=DSQRT(B)
      P=3.75/E
      BO=(.3989423+P*(.01328592+P*(.00225319-P*(.00157565-P*(.00916281-P
     1*(.02057706-P*(.02635537-P*(.01647633-.00392377*P)))))))/DSQRT(E)
      BF=BO*DEXP(-Z)
      P=1./(1.+.3275911*(DA-DB))
      ERF=P*(.2548296-P*(.2844967-P*(1.421414-P*(1.453152-P*1.061405))))
      P=0.25/E
      CO=1.-1.772454*(DA-DB)*ERF
      C1=0.5-Z*CO
      C2=0.75-Z*C1
      C3=1.875-Z*C2
      C4=6.5625-Z*C3
      SUM=.1994711*(A-B)*P*(CO+1.5*P*(C1+1.666667*P*(C2+1.75*P*(C3+P*(C4
     1*(1.8-3.3*P*Z)+97.45313*P)))))
      GOLD=0.5*BF+(.3535534*(DA+DB)*ERF+SUM)*BF/(BO*DSQRT(E))
    8 IF(X.LT.Y) GOLD=1.+BF-GOLD
      RETURN
      END
C
C     ------------------------------------------------------------------
      FUNCTION EXF(A,B)
C
C     PURPOSE: TO CALCULATE EXP(A) ERFC(B)
C
      IMPLICIT REAL*8 (A-H,O-Z)
      EXF=0.0
      IF((DABS(A).GT.170.).AND.(B.LE.0.)) RETURN
      IF(B.NE.0.0) GO TO 1
      EXF=DEXP(A)
      RETURN
    1 C=A+B
      IF((DABS(C).GT.170.).AND.(B.GT.0.)) RETURN
      IF(C.LT.-170.) GO TO 4
      X=DABS(B)
      IF(X.GT.3.0) GO TO 2
      T=1./(1.+.3275911*X)
      Y=T*(.2548296-T*(.2844967-T*(1.421414-T*(1.453152-1.061405*T))))
      GO TO 3
    2 Y=.5641896/(X+.5/(X+1./(X+1.5/(X+2./(X+2.5/(X+1.))))))
    3 EXF=Y*DEXP(C)
    4 IF(B.LT.0.0) EXF=2.*DEXP(A)-EXF
      RETURN
      END
```

E. Example Input for MFITIM

```
   2  . 6
   4    1   12   88
RF: DCB on 425 um phenyl polymer (PQ-L) 6-15-87
peclet     retard     beta       omega      pulse
    86.60      11.00      0.45      0.955      42.04
   0    1    1    1    0
   0.039 (V)   0.418 (Ab)   14.0 (L)   0.823 (θ)   0.42 (θe)
0.338      0.012
1.013      0.009
1.857      0.007
2.701      0.004
3.377      0.005
4.390      0.008      ETC.
```

F. Example Output from MFITIM

ITERATION	S.SSQ	R	B	O
0	1.9212210	9.9540	0.4122	0.430E+00
1	1.7468468	10.0467	0.4202	0.443E+00
2	1.5172770	10.0250	0.4260	0.479E+00
3	1.3223214	10.0259	0.4317	0.514E+00
4	1.1647480	10.0408	0.4375	0.548E+00
5	1.0415122	10.0620	0.4431	0.581E+00
6	0.9498723	10.0833	0.4485	0.611E+00
7	0.8850507	10.1012	0.4537	0.639E+00
8	0.8417236	10.1137	0.4585	0.665E+00
9	0.8147870	10.1206	0.4628	0.689E+00
10	0.7998219	10.1225	0.4667	0.711E+00
11	0.7932676	10.1203	0.4701	0.732E+00
12	0.7924009	10.1148	0.4730	0.751E+00
13	0.7902575	10.2004	0.4776	0.769E+00

CORRELATION MATRIX

	1	2	3
1	1.0000		
2	-0.3191	1.0000	
3	-0.1804	-0.8513	1.0000

NON-LINEAR LEAST SQUARES ANALYSIS, FINAL RESULTS

VAR	NAME	VALUE	S.E.COEFF.	T-VALUE	95% CONFIDENCE LIMITS LOWER	UPPER
OMEGA USES VELOCITY FROM FIRST CASE						
1	omega	10.20041	0.3875	26.32	9.4293	10.9709
2	omega	0.47756	0.0235	20.36	0.4309	0.5242
3	omega	0.75951	0.0386	19.69	0.6828	0.8362

FINAL MULTIPARAMETER RESULTS
DATASET = 1, OMEGA = 0.7658E+00, SSQ = 0.3128595
DATASET = 2, OMEGA = 0.7467E+00, SSQ = 0.4773980

AVERAGE Kp = 0.1828E+02
AVERAGE ALPHA(E) = 0.8886E-03
AVERAGE F = 0.4744E+00

REFERENCES

Akratanakul, S., L. Boersma, and G. Klock, Sorption processes in soils as influenced by pore water velocity; 1. Theory, *Soil Science*, *135*, 267-274, 1983.

Andersson, J. and A. Shapiro, Stochastic Analysis of one dimensional Steady state unsaturated flow, *Water Resources Research*, *19(1)*, 121-133, 1983.

Andersson, J. Y., H. Bjurstrom, M. Azoulay, and B. Carlsson, Experimental and theoretical investigation of the kinetics of the sorption of water vapour by silica gel, *Journal of Chemistry Society, Faraday Trans. I.*, *81*, 1985.

Antle, P. E., A. P. Goldberg, and R. L. Snyder, Characterization of silica based reversed-phase columns with respect to retention selectivity, *Journal of Chromatography*, *321*, 1-32, 1985.

Avnir, D., Fractal aspects of surface science - an interim report, *Material Research Society Symposium Proceedings*, *73*, 321-329, 1986.

Baehr, A., Selective Transport of Hydrocarbons in the unsaturated zone due to aqueous and vapor phase partitioning, *Water Resources Research*, *23(10)*, 1926-1938, 1987.

Bahr, J. and J. Rubin, Direct comparison of kinetic and local equilibrium formulations for solute transport affected by surface reactions, *Water Resources Research*, *23*, 438-452, 1987.

Ball, W. and P. Roberts, Desorption kinetics of trichloroethylene, *EOS*, *66*, 1985.

Barrer, R. M., Permeation, diffusion and solution of gases in organic polymers , *Transactions of the Faraday Society*, *35*, 628-656 , 1939.

Bear, J., in *Hydraulics of Groundwater*, p. 569, McGraw-Hill Inc., New York, 1979.

Beaufils, J., M. Hennion, and R. Rossett, Neutron scattering study of alkyl chain motion on reversed-phase liquid chromatographic packings, *Analytical Chemistry*, *57*, 2593-2596, 1985.

Bein-Vogelsang, U., A. Deege, H. Figge, J. Kohler, and G. Schomburg, Syntheses of stationary phases for reversed-phase LC using silanization and polymer coating, *Chromatographia, 19*, 1984.

Bird, R., W. Stewart, and E. Lightfoot, in *Transport Phenomena*, p. 780, John Wiley and Sons, New York, 1960.

Blevins, D. D., *Synthesis and characterization of bonded phase chromatographic absorbents,* Dept. of Chemistry, University of Arizona, Tucson, Arizona, 1982. Ph.D. Dissertation

Boast, C. W., Modeling the movement of chemicals in soils by water, *Soil Science, 115(3)*, 224-230, 1973.

Bondi, A., Van der Waals volumes and radii, *Journal of Physical Chemistry, 68(3)*, 441-451, 1964.

Cameron, D. and A. Klute, Convective-Dispersive solute transport with combined equilibrium and kinetic adsorption model, *Water Resources Research, 13*, 183-188, 1977.

Capel, P. and S. Eisenreich, Binding of organochlorines by lake sediment pore water colloids, *ACS Division of Environmental Chemistry, Annual Meeting*, 430-433, 1987.

Carslaw, H. S. and J. C. Jaeger, in *Conduction of Heat in Solids*, p. 510, Oxford at the Clarendon Press, 1959.

Carter, C. and I. Suffet, Binding of DDT to dissolved humic materials, *Environmental Science and Technology, 16(11)*, 735-740, 1982.

Chen, J., B. Shi, and Z. Du, Synthesis of phenylethynyl organosilane and polyphenylphenyl organosilane, *Gaodeng Xuexiao Huaxue Xuebao, 7(9)*, 807-810, 1986.

Chiou, C., D. Schmedding, and M. Manes, Partitioning of organic compounds in octanol-water systems, *Environmental Science and Technology, 16* , 4-10, 1982.

Chu, A. and S. Langer, Characterization of a chemically bonded stationary phase with kinetics in a liquid chromotographic reactor, *Analytical Chemistry, 57*, 2197-2204, 1985.

Coates, J. and A. Elzerman, Desorption kinetics for selected PCB congers from river sediments, *Journal of Contaminant Hydrology*, *1*, 191-210, 1986.

Coates, K. and B. Smith, Dead end pore volume and dispersion in porous media, *Journal of the Society of Petroleum Engineers*, *4*, 73-84, 1964.

Conder, J. and C. Young, in *Physicochemical Measurement by Gas Chromatography*, p. 621, J. Wiley and Sons, New York, NY, 1979.

Crank, J., in *The Mathematics of Diffusion*, p. 414, Clarendon Press, Oxford, 1985.

Daus, A., E. Frind, and E. Sudicky, Comparative error analysis in finite element formulations of the advection-dispersion equation, *Advanced Water Research*, *8*, 23-32, 1985.

Davidson, J., P. Rao, and P. Nkedi-Kizza, Physical processes influencing water and solute transport in soils: chemical mobility and reactivity in soils systems, *American Society of Agronomics Annual Meeting*, 35-47, Dec. 1981.

Den, T. S. and A. A. Kettrup, Synthesis of phenylalkyl bonded stationary phases and their application in the HPLC of aromatic hydrocarbons, *Chromatographia*, *19*, 231-235, 1985.

DiToro, D. and L. Horzempa, Reversible and resistant components of PCB adsorption-desorption: isotherms, *Environmental Science and Technology*, *16*, 594-602, 1982.

Drake, J. M., P. Levitz, and S. Sinha, General scaling phenomena in porous silica gels as probed by saxs and molecular adsorption (tiling), *Material Research Society Symposium*, *73*, 305-319, 1986.

El-Hassan, D. Blevins, and M. Burke, *A UV spectroscopic study of some variable chain length silica-immobilized alkyl-benzenes*, p. 29, 1986. unpublished manuscript, Univ. of Ariz., Dept. of Chem.

Fleming, B. A., Kinetics of reactions between silicic acid and amorphous silica surfaces in NaCl solutions, *Journal of Colloid and Interface Science*, *110*, 256-267, 1986.

Frank, H. and M. Evans, Free volume and entropy in condensed systems III. Entropy in binary liquid mixtures; partial molal entropy in dilute solutions; structure and thermodynamics in aqueous electrolytes, *Journal of Physical Chemistry*, *13*, 507-32, 1945.

Freeze, R. and J. Cherry, in *Groundwater*, p. 604, Prentice Hall, Inc., Englewood Cliffs, New Jersey, 1979.

Fressenden, R. and J. Fressenden, in *Organic Chemistry*, p. 1069p, Willard Grant Press, Boston, 1982.

Fyfe, C., G. Gobbi, and G. Kennedy, Quanitatively reliable silicon-29 magic-angle spinning nuclear magnetic resonance spectra of surfaces and surface-immobilized species at high field using a conventional high-resonution spectrometer, *Journal of Physical Chemistry*, *89*, 1985.

Giddings, J. C., in *Dynamics of Chromatography, Part 1, Principals and Theory*, p. 323, New York, 1965.

Gilpin, R., D. Camillo, and C. Janicki, Preparation and use of in situ chemically bonded small particle silica as packings in high pressure liquid chromatography, *Journal of Chromatography*, *121*, 1976.

Gleuckauf, E., Theory of chromatography, Part II-V, *Journal of Chemistry Society*, *26*, 1302-1329, 1947.

Graham-Bryce, I., The behaviour of pesticides in soil, in *The Chemistry of Soil Process*, edited by M. Hayes, pp. 621-671, J. Wiley & Sons, 1981.

Gschwend, P. M. and S. Wu, On the constancy of sediment-water partition coefficient of hydrophobic organic pollutants, *Environmental Science and Technology*, *19*, 90-96, 1985.

Halicioglu, T. and O. Sinanoglu, Solvent effects of cis trans azobenzene isomerization: A detailed application of a theory of solvent effects on molecular association, *NY Academy of Science Annual*, *158(1)*, 1969.

Hanai, T. and J. Hubert, Selectivity of a phenyl-bonded silica gel, *Journal of Chromatography, 291*, 81-89, 1984.

Hansch, C., J. Quinlan, and E. Lawrence, The linear free-energy relationship between partition coefficients and the aqueous solubility of organic liquids, *Journal of Organic Chemistry, 33(1)*, 347-351, 1968.

Hassett, J., W. Banwart, S. Wood, and J. Means, Sorption of naphthol: Implications concerning the limits of hydrophobic sorption, *Soil Science Society of America Journal, 45*, 38-42, 1981.

Hearn, M. T. W., Preparative and analytical applications of CDI-mediated affinity chromatography, in *Affinity Chromatography and Biological Recognition*, pp. 191-196, Academic Press, New York, 1983.

Horvath, C. and H. Lin, Movement and band spreading of unsorbed solutes in liquid chromatography, *Journal of Chromatography, 126*, 401-420, 1976.

Horvath, C. and H. Lin, Band Spreading in Liquid Chromatography, *Journal of Chromatography, 149*, 43-70 , 1978.

Horvath, C. and W. Melander, Liquid chromatography with bonded phases; theory and practice of reversed phase chromatography, *Journal of Chromatography Science, 15*, 393-404, 1977.

Horvath, C. and W. Melander, Reverse-phase chromatography and the hydrophobic effect, *American Laboratory, 9*, 17-36, 1978.

Horvath, C., W. Melander, and I. Molnar, Solvophobic interactions in liquid chromatography with nonpolar stationary phases, *Journal of Chromatography, 125*, 129-156, 1976.

Horvath, C., W. Melander, I. Molnar, and P. Molnar, Enhancement of retention by ion-pair formation in liquid chromatography with nonpolar stationary phase, *Analytical Chemistry, 49*, 2295-2305, 1977.

Hunnicutt, M. L. and J. M. Harris, Reactivity of organosilane reagents on microparticulate silica, *Analytical Chemistry*, *58*, 748-752, 1986.

Iler, K. L., in *The Chemistry of Silica*, John Wiley and Sons, Inc., New York, 1979.

Isaacson, P. and C. Frink, Nonreversible sorption of phenolic compounds by sediment fractions: The role of sediment organic matter, *Environmental Science and Technology*, *18*, 43-48, 1984.

Jackman, A. and K. Ng, The kinetics of ion exchange on natural sediments, *Water Resources Research*, *22*, 1664-1674, 1986.

Jacobson, J., J. Frenz, and C. Horvath, Measurement of adsorption isotherms by liquid chromatography, *Journal of Chromatography*, *316*, 53-68, 1984.

Jennings, A., Critical chemical reaction rates for multi-component groundwater contamination models, *Water Resources Research*, *23(9)*, 1775-1794, 1987.

Jennings, E. C. and R. G. Brownlee, Silica surface activity before and after bonding with silanes, *Analytical Chemistry*, *58* , 2895-6, 1986 .

Jinno, K. and M. Okamoto, The influence of the pore size of bonded phases containing phenyl groups on the retention of polycyclic aromatic hydrocarbons in reversed phase liquid chromatography, *Chromatographia*, *20*, 242-248, 1985.

Jones, K., Optimisation procedure for the silanisation of silicas reversed-phase high-performance liquid chromatography; I. Elimination of non-significant variables, *Journal of Chromatography*, *392*, 1-10, 1987.

Kahn, A., J. Hassett, W. Banwart, J. Means, and S. Wood, Sorption of acetophenone by sediments and soils, *Soil Science*, *128(5)*, 297-302, 1979.

Karch, K., I. Sebestian, and J. Halesz, Preparation and properties of reverse phases, *Journal of Chromatography*, *122*, 3-16, 1976.

Karickhoff, S., Organic pollutant sorption in aquatic systems, *Journal of Hydraulic Engineering*, *110*, 707-733, 1984.

Karickhoff, S., D. Brown, and T. Scott, Sorption of hydrophobic pollutants on natural sediments, *Water Resources Research*, *13* , 241-248, 1979.

Karickhoff, S. W., Sorption kinetics of hydrophobic pollutants in natural sediments, in *Contaminants and Sediments*, edited by R. A. Baker, vol. 2, pp. 193-205, Ann Arbor Science, Ann Arbor, MI, 1980.

Karickhoff, S. W. and K. R. Morris, Sorption dynamics of hydrophobic pollutants in sediment suspensions, *Environmental Toxicology and Chemistry*, *4*, 469-476, 1985.

Keefer, K. D., Growth and structure of fractally rough silica colloids, *Material Research Society Symposium Proceedings*, *73*, 295-304, 1986.

Keith, L. H. and W. A. Telliard, Priority pollutants - I. A perspective view, *Environmental Science & Technology*, *13(4)*, 416-423, 1979.

Kier, L. B. and L. H. Hall, in *Quantative Structure-Activity Analysis in the Biological Sciences*, p. 341p, J. Wiley and Sons, Inc., 1976.

Kier, L. B. and L. H. Hall, in *Molecular Connectivity in Structure-Activity Analysis*, p. 262 p, J. Wiley & Sons, Inc., New York, 1986.

Kingston, D. and B. B. Gerhart, Preparation of octadecyl porosil for reversed-phase liquid chromatography, *Journal of Chromatography*, *116*, 182-183, 1976.

Kinniburgh, D., General purpose adsorption isotherms, *Environmental Science and Technology* , *20*, 895-904, 1986 .

Kirkham, D. and W. Powers, in *Advanced Soil Physics*, p. 534, Wiley Interscience, New York, 1971.

Kobayashi, H. and B. E. Rittmann, Microbial removal of hazardous organic compounds, *Environmental Science and Technology*, *16*, 170-183, 1982.

Krupp, H., J. Biggar, and D. Nielson, Relative flow rates of salt and water in soil, *Soil Science Society of America, Proceedings*, *36*, 412-417, 1972.

Lapidus, L. and N. Amundson, Mathematics of adsorption in beds VI. The effect of longitudinal diffusion in ion exchange and chromatographic columns, *Journal of Physical Chemistry*, *56*, 984-8, 1952.

Larsson, P., M. Glad, L. Hansson, and M. Mansson, High performance liquid affinity chromatography, in *Affinity Chromatography*, edited by P. Dean, pp. 41-85, J. Wiley and Sons, New York, 1982.

Leenheer, J. and J. Ahlrichs, A kinetic and equilibrium study of the adsorption of carbaryl and parathion upon soil organic matter, *Soil Science Society of America Proceedings*, *35*, 700-705, 1971.

MacKay, D., W. Ball, and M. Durant, Variability of aquifer sorption properties in a field experiment on groundwater transport of organic solutes, *Journal of Contaminant Hydrology*, *1*, 119-132, 1986.

Macherey-Nagel, *Nucleosil and polygosil HPLC silica packing,* 86 pp., Macherey-Nagel, Duren, West Germany, 1987. HPLC Catalog

Marshall, T. and J. Homes, in *Soil Physics*, p. 345 p, Cambridge University Press, New York, 1979.

Matsuda, K. and M. Schnitzer, Reactions between fulvic acid, a soil humic material, and dialkyl phthalates, *Bulletin of Environmental Contaminant Toxicology*, *6(3)*, 200-204, 1971.

McBath, P. and J. Hassett, Practical field sampling methods for determining free versys bound concentrations fo hydrophobic compounds in natural water systems, *ACS Division of Environmental Chemistry, Annual Meeting*, 424, 1987.

McCarty, P., M. Reinhard, and B. Rittmann, Trace organics in groundwater, *Environmental Science and Technology*, *15(1)*, 40-51, 1981.

McGuire, M. and I. Suffet, The calculated net adsorption energy concept, in *Activated Carbon Adsorption - Volume 1*, pp. 91-115, 1979.

Means, J. and R. Wijayaratne, *Sorption of benzidine, tolidine, and azobenzene to colloidal organic matter*, pp. 417-419, 1987. ACS Division of Chemistry Annual Meeting

Melander, W., D. Campbell, and C. Horvath, Enthalpy-entropy compensation in reversed-phase chromatography, *Journal of Chromatography, 158*, 215-225, 1978.

Miller, C. and W. Weber, Jr., Modeling organic contaminant partitioning in groundwater systems, *Ground Water, 22(5)*, 584-92, 1984.

Miller, C. and W. Weber, Jr., Modeling the sorption of hydrophobic compounds by aquifer materials - I. Rates and equilibria, *Water Research*, 22, in press, 1987.

Miller, M., R. Linton, G. Macel, and B. Hawkins, Characterization of silanol reactivity and acidity on octadecyl-bonded chromatographic supporty by 29Si solid state NMR and Surface Titration, *Journal of Chromatography, 319*, 9-21, 1985.

Nkedi-Kizza, P., P. Rao, and A. Hornsby, Influence of organic cosolvents on leaching of hydrophobic organic chemicals through soils, *Environmental Science and Technology, 21*, 1107-1111, 1987.

Oliver, B., Desorption of chlorinated hydrocarbons from spiked and anthropogenically contaminated sediments, *Chemosphere, 14(8)*, 1087-1106, 1985.

Opperhulzen, A., P. Serne, and J. VanderSteen, Thermodynamics of fish/water and octanol/water partitioning of some chlorinated benzenes, *Environmental Science and Technology, 22(3)*, 286-291, 1988.

Parker, J. and M. Th. VanGenuchten , Determining Transport Parameters from Laboratory and Field Tracer Experiments, *Virginia Agricultural Experiment Station Bulletin 84-3*, 94 pp., 1984.

Parker, J. and A. Valocchi, Constraints on the validity of equilibrium and first-order kinetic transport models in structured soils, *Water Resources Research, 22*, 399-407, 1986.

Pfeffer, R., Effect of interstitial stagnant fluid on band spreading, *Industrial Engineering Chemical Fundamentals*, *3*, 380, 1964.

Porterfield, W., in *Inorganic Chemistry*, pp. 62-68, Addison-Wesley Publishing Co., Reading, Mass., 1984.

Rao, P. S. C., J. Davidson, R. Jessup, and H. Selim, Evaluation of conceptual models for describing nonequilibrium adsorption-desorption of pesticides during steady flow in soils, *Soil Science Society of America, Journal*, *43*, 22-28, 1979.

Rao, P. S. C. and R. E. Jessup, Development and verification of simulation models for describing pesticide dynamics in soils, *Ecological Modelling*, *16*, 67-75, 1982.

Roberts, P. V., M. Goltz, R. Summers, J. C. Crittenden, and P. Nkedi-Kizza, The influence of mass transfer on solute transport in column experiments with an aggregate soil, *Journal of Contaminant Hydrology*, *1*, 375-393, 1987.

Rogers, R. D., J. C. McFarlane, and A. J. Cross, Adsorption and desorption of benzene in two soils and montmorillonite clay, *Environmental Science & Technology*, *14*, 457-460, 1980.

Rose, D., Hydrodynamic dispersion in porous materials, *Soil Science*, *123*, 277-283, 1977.

Rubin, J., Transport of reacting solutes in porous media: relation between mathematical nature of problem formulation and chemical nature of reactions, *Water Resources Research*, *19*, 1231-1252, 1983.

Sabljic, A., Calculation of retention indices by molecular topology, *Journal of Chromatography*, *319*, 1-8, 1985.

Schabron, J., R. Hurtubise, and H. Silver, Separation of hydroaromatics and polycyclic aromatic hydrocarbons and determination of tetralin and naphthalene in coal derived solvents, *Analytical Chemistry*, *49(14)*, 2253-2260, 1977.

Schwarzenbach, R. and J. Westall, Transport of nonpolar organic compounds from surface water to groundwater, *Environmental Science and Technology*, *15*, 1360-1366, 1981.

Sears, G., Determination of specific surface area of colloidal silica by titration with sodium hydroxide, *Analytical Chemistry*, *28*, 1981-1983, 1956.

Sinanoglu, O., An intermolecular potential for use in liquids, *Chemical Physics Letters*, *1*, 340-342, 1967.

Sinanoglu, O., Solvent effects on molecular associations in molecular associations in biology, in *Molecular Connectivity in Biological Sciences*, pp. 427-445, Academic Press, New York, 1968.

Snyder, L. and J. Kirkland, in *Introduction to Modern Liquid Chromatography*, J. Wiley and Sons, New York, 1979.

Sposito, G., in *The Surface Chemistry of Soils*, Oxford University Press, New York, 1984.

Sposito, G. and D. Barry, On the Dagan Model of solute transport in groundwater; fundamental aspects, *Water Resources Research*, *23(10)*, 1987.

Streuli, C. and M. Orloff, Chromatographic adsorption constants and pi electron delocalization energies, *Journal of Chromatography*, *62*, 1971.

Stumm, W. and J. J. Morgan, in *Aquatic Chemistry*, p. 780 , J. Wiley and Sons, New York, 1981.

Stumm, W., R. Schwartzenbach, and L. Sigg, A plea for more concepts and less monitoring and testing, *Angewandte Chemie*, *22*, 380-389, 1983. Environmental Analytical Chemistry to Ecotoxicology

Thurman, E. M., *Organic Geochemistry of Natural Waters,* Martinus Nijhoff, Dordrecht, Netherlands, 1985.

Thus, J. L. and J. C. Kraak, Comparison of phenyl- and octadecyl-modified silica gel as stationary phase for the prediction of n-octanol-water partition coefficients by high-performance liquid chromatography, *Journal of Chromatography*, *320*, 271-9, 1985.

Tomlinson, E., Chromatographic hydrophobic parameters in correlation analysis of structure-activity relationships, *Journal of Chromatography, 113*, 1-45, 1975.

Toyohide, T. and D. Ishii, High back pressure liquid chromatography: Studies on the retention behaviour of aromatic compounds, *Journal of Chromatography, 244*, 23-32, 1982.

Urban, M. W. and J. L. Koenig, Enhancement of the surface modes in photoacoustic FTIR spectroscopy using a highly polarizable inert gas, *Applied Spectroscopy, 39(6)*, 1051-6, 1985.

Valocchi, A., Validity of the local equilibrium assumption for modeling solute transport through homogeneous soils, *Water Resources Research, 21*, 808-820, 1985.

Valocchi, A., Effect of radial flow on deviations from local equilibrium during sorbing solute transport through homogeneous soils, *Water Resources Research, 22*, 1693-1701, 1986.

VanDeemter, J., F. Zuiderweg, and A. Klinkenberg, Band Spreading in Chromatographic Systems, *Chemical Engineering Science, 5*, 271, 1956.

VanGenuchten, M., A general approach for modeling solute transport in structured soils: IAH Memoires, *Hydrogeology of Rocks of Low Permeability, 17(2)*, 513-526, 1985.

VanGenuchten, M. and W. Alves, *Analytical solutions of the 1D convective/dispersion solute transport equations*, p. 151, 1982. USDA Technology Bulletin

VanGenuchten, M. and R. Cleary, Movement of solutes in soil; computer simulated and laboratory results in soil chemistry, in *Physico-Chemical Models*, pp. 349-86, Elsevier Science, New York, 1979.

VanGenuchten, M., J. Davidson, and P. Wierenga, An evaluation of kinetic and equilibrium equations for the prediction of pesticide movement through porous media, *Soil Science Society of America Proceedings, 38*, 29-35, 1974.

VanGenuchten, M. Th., Non-equilibrium transport parameters from miscible displacement experiments, *Research Report 119*, 88 pp., U. S. Salinity Lab, Riverside, CA, 1981.

VanGenuchten, M. Th. and R. W. Cleary, Movement of solutes in soil: computer simulated and laboratory results, in *Soil Chemistry, Physico-Chemical Models*, edited by G. H. Bolt, pp. 349-386, Elsevier, Amsterdam, 1982.

VanGenuchten, M. Th. and F. N. Dalton, Models for simulating salt movement in aggregated field soils, *Geoderma , 38*, 165-183, 1986.

VanGenuchten, M. Th. and P. J. Wierenga, Mass transfer studies in sorbing porous media I. analytical solutions, *Journal of the Soil Science Society of America, 40*, 473-480, 1976.

Weber, W., Evolution of a technology, *Journal of Environmental Engineering, 110(5)*, 899-917, 1984.

Weber, W. and C. Wang, A microscale system for estimation of model parameters for fixed bed absorbers, *Environmental Science and Technology, 21(11)*, 1096-1102, 1987.

Welty, J., C. Wicks, and R. Wilson, in *Fundamentals of momentum, heat, and mass transfer*, p. 629, J. Wiley and Sons, New York, 1976.

Whitehead, T. W. and R. C. Bales, Sorption kinetics of alkyl halides on desert alluvial sediments, *in preparation*, 1987.

Wilson, J., G. Smith, J. Cochran, J. Barker, and P. Roberts, Field evaluations of a simple microcosm simulating the behavior of volatile organic compounds in subsurface materials, *Water Resources Research, 23(8)*, 1547-1553, 1987.

Wu, S. and P. Gschwend, Sorption kinetics of hydrophobic organic compounds to natural sediments and soils, *Environmental Science and Technology, 20*, 717-725, 1986.

Yalkowski, S., R. Orr, and S. Valvani, Solubility and partitioning; 3. The solubility of halobenzenes in water, *Industrial Engineering Chemistry Fundamentals, 18(4)*,

351-353, 1979.

Yalkowsky, S., S. Valvani, and D. MacKay, Estimation of the aqueous solubility of some aromatic compounds, *Residue Reviews*, *85* , 43-55, 1983.

Yang, S. S. and R. K. Gilpin, Reordering/resolution of silica immobilized non-hydrogen bonding ligands used as stationary phases in high performance liquid chromatography, *Journal of Chromatography*, *394*, 295-303, 1987.

Yeroshenkova, G. V., S. A. Volkov, and K. I. Sakodynskii, Effect of packing irregularities along the bed length, *Journal of Chromatography*, *262*, 19-32, 1983.

Zerda, K. S., C. P. Gerba, K. C. Hou, and S. M. Goyal, Adsorption of viruses to change-modified silica, *Applied and Environmentall Microbiology*, *49*, 91-95, 1985.

Zierath, D., J. Hassett, W. Banwart, and S. Wood, Sorption of benzidine by sediments and soils, *Soil Science*, *129(5)*, 277-81, 1980.